NASA CR-134604
R73-AEG-417

TF34 QUIET NACELLE

NEARFIELD ACOUSTIC TEST RESULTS

by

W.E. COWARD, E.B. SMITH, and H.D. SOWERS

GENERAL ELECTRIC COMPANY

prepared for

NATIONAL AERONAUTICS AND SPACE ADMINISTRATION

NASA-Lewis Research Center

CONTRACT NAS3-17845

1. Report No. NAS CR-134604	2. Government Accession No.	3. Recipient's Catalog No.
4. Title and Subtitle TF-34 Quiet Nacelle Nearfield Acoustic Test Results		5. Report Date March 1974 6. Performing Organization Code
7. Author(s) Coward, W. E., Smith, E. B., and Sowers, H. D.		8. Performing Organization Report No. R73-AEG-417 10. Work Unit No. Y0F6276
9. Performing Organization Name and Address General Electric Company 1 Jimson Road Cincinnati, OH 45215		11. Contract or Grant No. NAS3-17845 13. Type of Report and Period Covered Contractor Report
12. Sponsoring Agency Name and Address NASA-Lewis Research Center 21000 Brookpark Road Cleveland, OH 44135		14. Sponsoring Agency Code

15. Supplementary Notes

Project Manager, Richard G. Goldman
V/STOL and Noise Division, NASA-Lewis Research Center
21000, Brookpark, Road, Cleveland, Ohio 44135

16. Abstract

This report presents the results of the nearfield acoustic tests conducted on the TF34 Quiet Nacelle at Edwards Flight Test Center. The high fan noise suppression levels being sought (26 PNdB reduction in aft fan noise) necessitated the use of an extensive system of special nearfield acoustic instrumentation to properly evaluate the suppression achieved. The design, operation, and test results from each of these nearfield acoustic instrumentation systems are presented.

17. Key Words (Suggested by Author(s))	18. Distribution Statement
TF34 Acoustic Nacelle Nearfield Acoustic Tests	Unclassified - unlimited

19. Security Classif. (of this report)	20. Security Classif. (of this page)	21. No. of Pages	22. Price*
Unclassified	Unclassified	185	$12.25

* For sale by the National Technical Information Service, Springfield, Virginia 22151

TABLE OF CONTENTS

I. INTRODUCTION

The TF34 Quiet Nacelle acoustic test program was conducted by the NASA Lewis Research Center and the General Electric Company during the time period from March to November, 1972. The test site was located at the Edwards Flight Test Center in California.

A basic goal of the program was to demonstrate a reduction of 26 PNdB in the aft fan noise radiated to the 500 ft sideline, through the application of acoustic treatment. However, pre-test predictions indicated that at design speed, only 16.5 PNdB reduction would be measurable at the max aft sideline angle, due to the masking effect of jet noise. It was also a possibility that high-frequency fan noise might "bypass" the acoustic treatment by leaking through the flexible seals in the fan flowpath, and exiting out through the bay cooling annulus. A secondary objective thus arose, namely that of isolating the constituent noise sources on a component-by-component basis; this would allow a true determination of fan noise suppression achieved, and hopefully make possible the identification of any extraneous noise sources that might arise to interfere with the achievement of the basic suppression goals.

It was with this later objective in mind that an extensive system of special nearfield acoustic instrumentation was proposed for use during the testing. This system included acoustic probes, the directional acoustic array, nearfield microphones, and flush-mounted Kulite pressure transducers. The design, operation, and test results from each of these items are the subject of this report.

II. DESCRIPTION OF TEST SET-UP AND INSTRUMENTATION

A. Test Program

The overall TF34 Quiet Nacelle Acoustic Test Program consisted of a series of 26 separate configurations, based on the TF34 engine with acoustic suppression.[1] There were four basic objectives to the program; these were:

(1) The determination of the baseline unsuppressed noise signature of the TF34-GE2 engine.

(2) The investigation of massive fan and core noise acoustic suppression, including the effect of acoustic treatment on fan source noise generation. A specific goal was to obtain a 26 PNdB reduction in aft fan noise measured on a 500 ft. sideline.

(3) The determination of the overall noise signature of the acoustically suppressed TF34 engine, employing various fan and core nozzle exhaust systems; to be used as a baseline for powered-lift system tests.

(4) The investigation of the noise inherent in the various powered lift wing/engine systems, such as external blown flaps, and the determination of means to reduce this noise.

The last two objectives could be obtained adequately with the use of farfield acoustic instrumentation; the first two, however, required an instrumentation system that would allow a detailed, component by component study of the noise generation and suppression. There were five basic test configurations run to obtain these first two objectives:

(1) Baseline unsuppressed engine test — to establish the baseline noise signature of the untreated TF34 engine.

(2) Fully suppressed engine test (inlet splitters forward) - to demonstrate massive fan noise suppression, and to determine possible effects of treated splitters on fan source noise.

(3) Fully suppressed engine test (inlet splitters moved aft) - to determine effects of closer fan-splitter spacing on fan source noise generation and fan inlet noise suppression.

(4) Fully suppressed engine test - as a baseline for the unsuppressed core testing.

(5) Suppressed engine test with core acoustic suppressor removed - to establish the unsuppressed core noise signature, and investigate core noise suppression.

B. Engine and Instrumentation Configuration

The baseline unsuppressed TF34 engine[2] (Figure II B-1) is a 9000-pound thrust class high bypass (6:1) turbofan engine, with a fan tip diameter of 44 inches. The rotor-exit guide vane spacing is extremely close (~1/4 blade chord).

The TF34 suppressed nacelle[1,3] (Figure II B-2) consists of massive acoustic suppression in the inlet and fan and core exhausts. The inlet suppressor is an aluminum honeycomb resonator configuration, employing three treated splitters. The fan and core exhaust suppressors are bulk absorber configurations, composed of varying thicknesses in order to "tune" the suppression over a wide range of frequencies. Two treated splitters are employed in the fan exhaust.

The predicted noise reductions for the inlet suppressor were as high as 32 dB SPL; those for the fan exhaust were up to 37 dB SPL. However, as was pointed out in the introduction, the resulting suppressed fan noise levels would be well below those from other components such as the jet, making it impossible to measure the full noise suppression on farfield microphones. The possibility also arose that the suppression goals might not be met. This contingency would require the ability to "sort out" the various noise component levels, in order to determine whether the failure was due to inadequate acoustic suppression performance, or to possible contamination by some extraneous noise source, such as fan noise bypassing the treatment. A third problem area was the determination of the effect of the inlet and fan exhaust splitters on fan source noise generation. This would of course require acoustic measurements to be made directly in the flow ducts.

The nearfield acoustic instrumentation system was designed in order to resolve the above problems. The instrumentation sytem consisted of the following components:

(1) Traversing Acoustic Probes and Core Rakes - Two probes and the core rake were employed on the baseline engine test; four probes and the core rake on the fully suppressed engine. The purpose of these probes was to determine the source noise power levels upstream and downstream of the fan, and in the core engine exhaust. The two "extra" probes in the suppressed nacelle provided a measure of the total noise reduction over the acoustic treatment. The traversing probes also provided a means to determine the radial distribution of the source noise in the duct, the key item in the radial positioning of acoustically treated splitters.

(2) Flush Mounted "Kulite" Pressure Transducers - The suppressed engine contained ten Kulites axially spaced along the outer wall of the treated fan exhaust duct. Seven Kulites were also placed along the outer wall of the treated fan inlet duct. These transducers were used to determine the "decay rate" of fan noise as a function of acoustic treatment length.

(3) Directional Acoustic Array - Use of this apparatus made possible the determination of the noise signature radiated to the farfield from specific noise source locations on the engine (fan inlet, fan nozzle, core nozzle, etc.) Knowledge of the directivity patterns of the various sources allows a more exacting determination of the effects of specific treatment on farfield noise.

(4) Nearfield Microphones - Ten microphones, placed along an eight-foot sideline, were used in conjunction with the directional array to aid in the determination of constituent noise signatures.

Figure II B-1 indicates the general locations of the nearfield instrumentation employed on the baseline unsuppressed engine. Figures II B-2 and II B-3 are similar sketches for the suppressed nacelle.

Tables II B-1 and II B-2 are a summary of the five basic test configurations which employed the nearfield instrumentation, listing the run numbers, test dates, etc. Each configuration has been assigned a reference number. The legends of all the acoustic data plots are keyed to this reference number, as an aid in determining the exact configurations being compared.

TABLE II B-1

SUMMARY OF TF34 NEARFIELD ACOUSTIC TESTS

REF. TEST NO	CONFIGURATION	FAN INLET PROBES	FAN EXHAUST PROBES	CORE EXHAUST RAKE	INLET KULITE TRANSDUCERS	FAN EXHAUST KULITE TRANSDUCERS	ACOUSTIC DIRECTIVITY ARRAY	NEARFIELD MICROPHONES	NOTES AND COMMENTS
1	BASELINE UNTREATED ENGINE, S-3A WAIST COWL + INLET BELLMOUTH								(1) ONE INLET PROBE, ONE FAN EXHAUST PROBE ON THIS CONFIGURATION
	RUN NUMBER	4(1)	4(1)	1					
	TEST DATE	3/30/72	3/30/72	3/29/72					
	DATA POINT NOS.	35 - 38	35 - 38	17 - 19					
	TYPE OF DATA RED.								
	1/3 OCTAVE BAND	X	X	X					
	NARROWBANDS	X	X	X					
	FAN PHYSICAL SPEED PTS.	3 5100-6910	3 5100-6910	3 5100-6830					
2	FULLY SUPPRESSED (BULK FAN EXHAUST AND CORE EXHAUST) SEPARATE FLOW, A_{28}=790 $in.^2$, A_{8}=280 $in.^2$ INLET SPLITTERS FORWARD								(1) TWO INLET PROBES, TWO FAN EXHAUST PROBES (2) DIRECTIVITY ARRAY MEASUREMENTS AT 7 FARFIELD ANGLES, POINTED AT 9 ENGINE STATIONS FOR EACH ANGLE (3) 7 KULITES IN INLET, 10 KULITES IN FAN EXHAUST DUCT
	RUN NUMBER	7(1)	7	7	8(3)	5,7(3)	6(2)	6	
	TEST DATE	6/2/72	6/2/72	6/2/72	6/6/72	5/23, 6/3/72	5/26 5/30	5/26/72	
	DATA POINT NOS.	119 125-127	124 126-130	116-118	153-156 158-161 162	71,72 136-138 143	77-113	77,78,80	
	TYPE OF DATA RED.								
	1/3 OCTAVE BAND	X	X	X			X	X	
	NARROWBAND	X	X	X	X	X	X	X	
	FAN PHYSICAL SPEED PTS.	3 5100-6910	3 5100-6880	3 5100-6950	5 5100-max	4 5100-7140	3 5100-max	3 5100-max	
3	FULLY SUPPRESSED (BULK FAN EXHAUST AND CORE EXHAUST) SEPARATE FLOW, FULL BLANKET, INLET SPLITTERS AFT								(1) 7 KULITES IN INLET, 4 KULITES IN FAN EXHAUST DUCT (2) DIRECTIVITY ARRAY MEASUREMENTS AT 5 FARFIELD ANGLES, POINTED AT 5 ENGINE STATIONS FOR EACH ANGLE
	RUN NUMBER	9	9		10(3)	10(1)	11(2)	11	
	TEST DATE	6/10/72	6/10/72		6/15/72	6/15/72	6/16/72	6/16/72	
	DATA POINT NOS.	167-173 175	172 174-180		198-202	198-202	210-227	210,211 213	
	TYPE OF DATA RED.								
	1/3 OCTAVE BAND	X	X				X	X	
	NARROWBAND	X	X		X	X	X	X	
	FAN PHYSICAL SPEED PTS	3 5100-7080	3 5100-7080		5 5100-max	5 5100-max	3 5120-7030	3 5130-7000	

TABLE II B-2

SUMMARY OF TF34 NEARFIELD ACOUSTIC TESTS

REF. TEST NO	CONFIGURATION	FAN INLET PROBES	FAN EXHAUST PROBES	CORE EXHAUST RAKE	INLET KULITE TRANSDUCERS	FAN EXHAUST KULITE TRANSDUCERS	ACOUSTIC DIRECTIVITY ARRAY	NEARFIELD MICROPHONES	NOTES AND COMMENTS
4	SEPARATE FLOW, FULLY SUPPRESSED BASELINE FOR CORE NOISE TESTS RUN NUMBER TEST DATE DATA POINT NOS. TYPE OF DATA RED. 1/3 OCTAVE BAND NARROWBAND FAN PHYSICAL SPEED PTS.			36,37(1) 11/9, 10/72 676-683 692-699 X X 8 1948-6910					(1) DUE TO PROBLEMS WITH THE CORE RAKE MICROPHONES A REPEAT RUN WAS NECESSARY
5	AS ABOVE, BUT WITH CORE EXHAUST ACOUSTIC TREATMENT REMOVED RUN NUMBER TEST DATE DATA POINT NOS. TYPE OF DATA RED. 1/3 OCTAVE BAND NARROWBAND FAN PHYSICAL SPEED PTS.			40 11/18/72 710-717 X X 8 1968-6895					(1) RUN 38 ABORTED DUE TO RAIN, AFTER ONE SPEED POINT WAS RUN

FIGURE II B-1

TF34 BASELINE UNSUPPRESSED ENGINE

NEARFIELD ACOUSTIC INSTRUMENTATION LOCATIONS

(TEST 1)

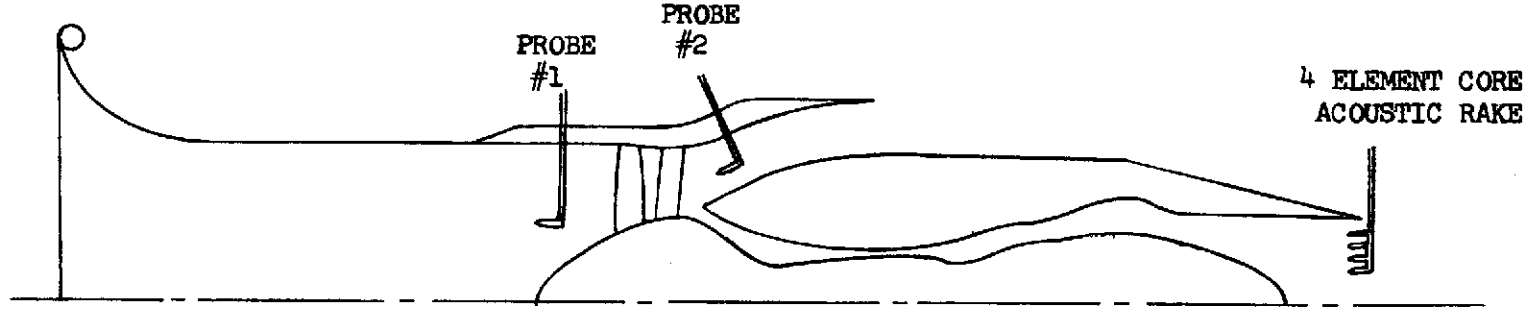

FIGURE II B-2

TF34 SUPPRESSED NACELLE

NEARFIELD ACOUSTIC INSTRUMENTATION

INTERNAL TO ENGINE

(TESTS 2 - 5)

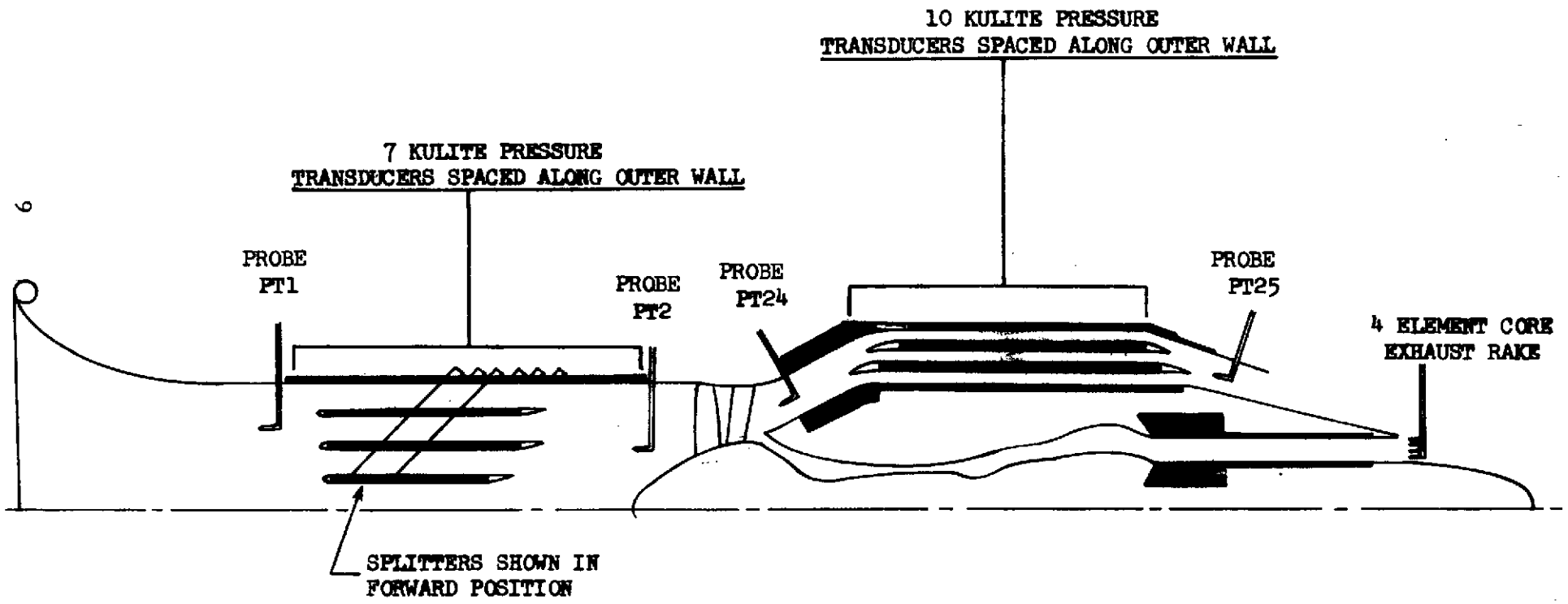

FIGURE II B-3

TF34 SUPPRESSED NACELLE

NEARFIELD ACOUSTIC INSTRUMENTATION

EXTERNAL TO ENGINE

(TESTS 2 & 3)

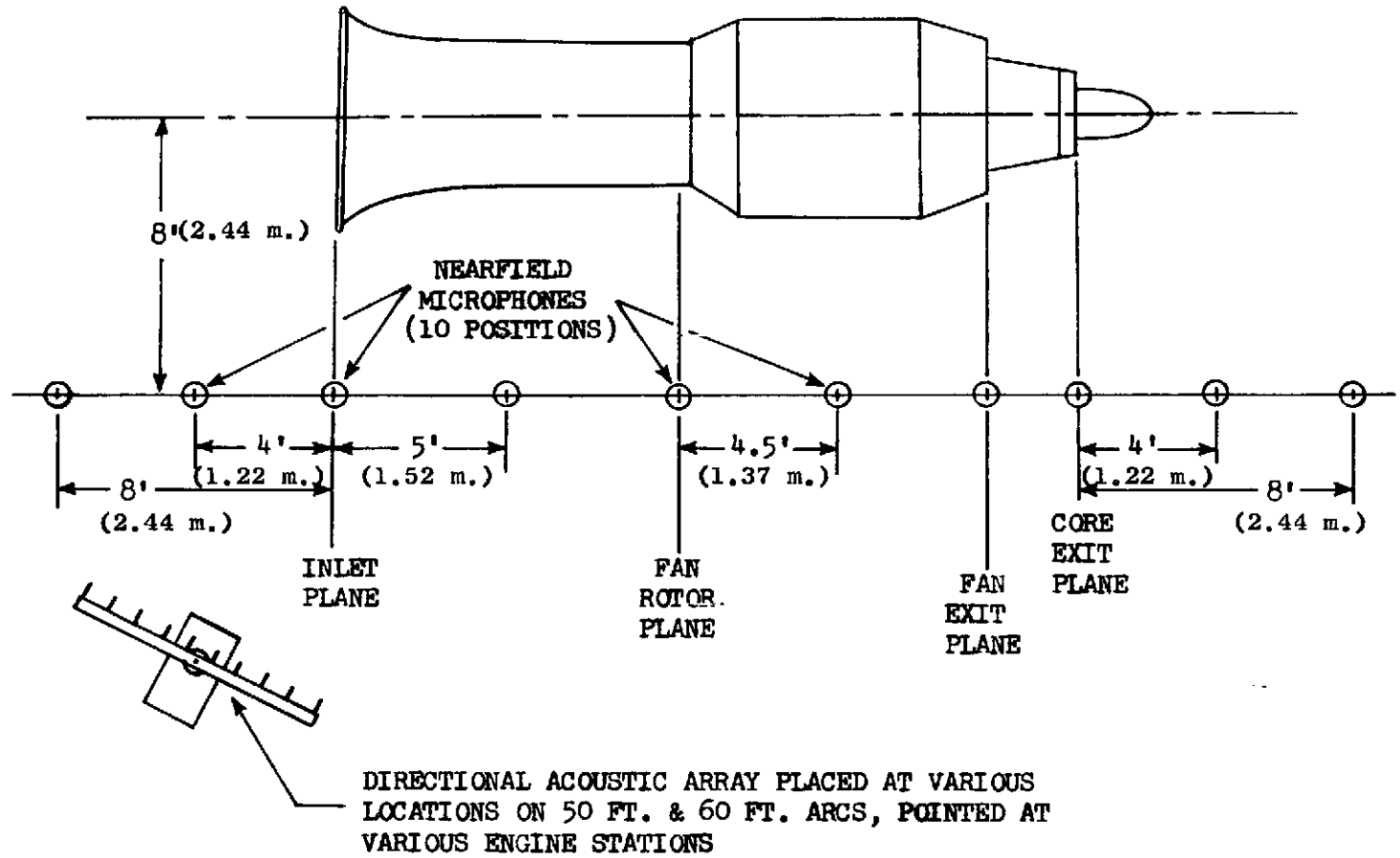

III. NEARFIELD ACOUSTIC INSTRUMENTATION

A. Acoustic Probes

1. Design

The acoustic probes (shown schematically in Figure III A-1) basically consist of a stainless steel waveguide with a streamlined tip containing rows of small holes which allowed the sound pressure to enter. A microphone was located at the opposite end of each probe, which was also attached to an "infinite length" termination coil designed to prevent internal reflections. An actuator system was employed on all the fan probes, in order to allow the sensing element to be traversed radially in and out of the duct, so that measurements could be taken at any radial immersion desired. The core acoustic rake consisted of four stationary probe elements, symmetrically spaced across the duct, each element leading to its own microphone. All probes and rakes were previously calibrated in a laboratory test duct, using a known acoustic input signal. The resulting correction factors for each probe and the rake are listed in Tables III A-1 and III A-2.

2. Data Acquisition

Two fan duct acoustic probes and the core rake were employed on the unsuppressed baseline configuration. The probe locations were in the inlet just ahead of the fan, and in the fan exhaust duct just downstream of the fan; Figure III A-2 is a detailed sketch of these probe locations. The core exhaust rake was set up in the core exhaust duct plane (Figure III A-3). Even though the rake was not designed for the unsuppressed core duct (the span of the

elements was not great enough to sample the entire duct) it was used in an attempt to get a preliminary estimate of the unsuppressed core noise levels.

Four fan duct acoustic probes were used on the fully suppressed nacelle, for both the inlet splitters forward and inlet splitters aft testing. One probe was employed in the inlet upstream of the inlet splitters, the second just downstream of the inlet splitters and ahead of the fan rotor, the third just downstream of the fan rotor at the beginning of the fan exhaust treatment, and the fourth just downstream of the fan exhaust splitters. The two inlet probe locations are detailed in Figure III A-4, the fan exhaust probe locations in Figure III A-5. The core exhaust probe was located in the core exhaust duct plane (Figure III A-6), and was employed only on the splitters forward test.

For all three tests, probe and rake data was recorded at three speed points; 5100 rpm, 6200 rpm, and max power ($\sim$7000 rpm). For each speed, the probes were traversed in and out, and data were recorded at each of a pre-selected set of radial immersion depths, tabulated in Table III A-3. Due to constraints imposed by the probe structural critical frequencies, certain immersion depths were not used during the runs with the inlet probes, in order to prevent possible damage to the fan rotor.

A special set of tests employing the core rake was run later in the program, to investigate core noise. A range of eight speed points, from max power down to approximately 2000 rpm, was used in an attempt to allow the separation of true core noise from the jet noise background.

3. Data Reduction

The data from each probe at each immersion, and from each rake element, was analyzed on both a 20 Hz narrowband and one-third octave band basis, from 50 Hz to 10 KHz. The probe correction factors were applied to the one-third octave data, and the acoustic power levels in the duct at each probe measuring plane were calculated by logarithmically summing the levels at each immersion (applying a power factor correction based on the duct area).

B. Flush Mounted Kulite Pressure Transducers

1. Design

The Kulite pressure-sensitive transducer consists basically of a small diaphragm on which are etched four semi-conductor strain gages, arranged in the form of a Wheatstone bridge. There are two leads in for the D.C. input to balance the bridge. Pressure signals sensed by the diaphragm cause distortion of the strain gages and changes in their resistance, which results in an output electrical signal which is then carried out on two leads to the signal conditioning equipment. The Kulites are calibrated before use by means of a known pressure signal input.

2. Data Acquisition

Kulite transducers were employed only on the fully suppressed nacelle testing. For the inlet splitters forward configuration, seven Kulites were flush mounted along the inlet outer wall, at the locations detailed in Figure III A-4 of the preceeding section. Ten Kulites were flush mounted along the

outer wall of the fan exhaust duct, at the locations detailed in Figure III A-5 of the preceeding section. Only twelve Kulites were available for use, so the inlet and aft data were acquired on two separate runs. For the inlet splitters aft configuration, both inlet and aft Kulites were recorded on the same run. Seven Kulites were employed in the inlet, exactly as before, but only four were emplaced in the fan exhaust; these were numbers K1, K2, K7 and K8 (Figure III A-5). It was throught that four fan exhaust duct Kulites would be enough to monitor any possible changes in aft fan noise due to closer inlet splitter spacing.

3. Data Reduction

The data recorded on each Kulite transducer was analyzed on a 20 Hz narrowband basis, from 50 Hz to 10 KHz.

C. Directional Acoustic Array

1. Design

The directional acoustic microphone array (Figure III C-1) consists of a rigid beam containing fourteen equally spaced microphones, and associated shading and summing electronics. This shading of the individual microphones results in the entire system having a "focal" point, similar to a parabolic reflector; thus, the array may be aimed at a point source, and record the noise from that particular source. An omni-directional microphone is also mounted on the array, to record the total noise signal for all sources. The on-axis gain of the total system is 19 dB, relative to the output of a single microphone element. The design of the array encompasses a frequency range from 1.25 KHz to 6.3 KHz. The array "sensitivity characteristics" over this

frequency range are shown in Figure III C-2. The peak at zero degrees represents the on-axis sensitivity of the array; this falls to the horizontal line representing the effective side lobe suppression. Additional peaks represent off-axis major lobe sensitivity, an undesirable side-effect inherent in an array design exhibiting narrow "sensitivity beam" patterns. Given two side-by-side noise sources of equal amplitude, when the array is "focused" on source 1, source 2 must be suppressed by at least 6 dB by the side-lobe suppression to insure minimum interference with source 1. Examination of the array sensitivity characteristics in Figure III C-2 shows that this "6 dB down" point occurs at 2.5° angle for 1.25 KHz, and at 1° angle for 6.3 KHz; thus at 1.25 KHz, the array can resolve equal amplitude sources that subtend an angle of 2.5° with the axis; at 6.3 KHz, the resolution capability narrows to 1°). Figure III C-3 is a schematic representation of these resolution limits. At a measurement radius of 50 ft., a 2.5° angle intersects a linear distance of 2.2 ft. on the engine; this is less than the separation distance of the major sources on both the suppressed and unsuppressed nacelles.

The array side lobe sensitivity actually achieved is greater than the design goal of -40 dB relative to the on-axis sensitivity. This difference arises from atmospheric conditions which cause the acoustic signal to arrive at each microphone element at a less than optimum phase relationship. The side lobes, off axis major lobes, atmospheric disturbances, ground reflection, large source size (as opposed to the optimum point source), the tolerance involved in placing the microphone elements on the proper radius of curvature, and the tolerance of each microphone sensitivity, are all potential contributors to system inaccuracy.

2. Data Acquisition

For the suppressed nacelle testing, the array was located in the sound field at angles of 30°, 50°, 70°, 90°, 100°, 110°, and 130° (relative to the inlet), at varying radii of 50 ft. to 72 ft. At each measurement angle, the array was pointed at each of 9 different engine positions (See Figure III C-4); acoustic data was recorded from each combination of angle and pointing position for three speed points; 5100 rpm, 6200 rpm, and max power (∿7100 rpm).

Previous acoustic tests employing the array had been run on an unsuppressed TF34 engine (on the same test site) which was almost identical to the baseline unsuppressed engine for these tests.[2] The data from those tests was employed as a baseline for the array testing on the fully suppressed nacelle; Figure III C-5 is a sketch showing the measuring positions employed for the unsuppressed engine.

The array was also used on the fully suppressed nacelle test with the inlet splitters moved aft. On this configuration, the same positions shown in Figure III C-4 were employed, with the exceptions that the 70° and 90° measurement angles and the two fan casing and two core exhaust engine measuring stations were eliminated.

The measuring radius used for the array was chosen based on the array characteristics and the spacing between the anticipated engine noise sources. As an example, for the unsuppressed engine; with the array pointed at the fan exhaust, the inlet subtends an angle of 2.9° with the array axis when the array

is located at the 90° measurement angle on a 50 ft radius (Figure III C-6). For measurement angles of 50° and 130° on a 50 ft. radius, this angle decreases to 2.0° (less than the 2.5° minimum resolution at 1.25 KHz), but it was anticipated that fan exhaust noise would not be a problem at 50°, and conversely that inlet noise would be relatively low at 130°. A measurement arc of 50 ft. would therefore permit noise source resolution down to 1.25 KHz. The off-axis major lobes (See Figure III C-2) fall at 10.5° at 6.3 KHz, and above 50° at 1.25 KHz. At 50 ft. distance, these off-axis lobes do not intersect the engine for the measurements indicated on the drawing; however, it is apparent that when the array is pointed at measuring stations either forward or aft of the fan exhaust, the off-axis major lobes for 6.3 KHz will begin to intersect the engine at other noise source locations, and corrections will have to be applied. As the array is pointed more and more to either side of the fan exhaust, the off-axis major lobes for the lower frequencies will also begin to intersect the engine source locations.

The selection of the measurement arc distance for the array thus becomes a trade-off between using small distances to increase the resolution, and large distances to spread the off-axis major lobes further away from the engine measuring stations. A third complication is the desire to maintain, as nearly as is possible, a constant distance between the array and the source being measured to allow a direct comparison of relative source strengths. This is particularly important for the long suppressed nacelle. The array measurement arc was centered on the core exhaust, and when the array was placed at the forward angles (30° and 50°), the distance from the inlet was considerablely less than

50 ft. The comparison of inlet to exhaust noise source strengths would thus be complicated by the distance factor, with different attenuations, ground reflection patterns, etc. It became necessary to place the inlet measurement positions at distances of 60 ft. and 72 ft. from the core exhaust.

3. Data Reduction

The array output was analyzed up to 10 KHz using a 20 Hz bandwidth filter. The results were tabulated for pure tones as well as broadband noise over the range from 1.25 KHz to 6.3 KHz and corrections for the array characteristics were applied.

D. Nearfield Microphones

1. Design

The microphones employed for the near field testing were standard B&K 4134 one-half inch condensor microphones, mounted vertically (grazing incidence).

2. Data Acquisition

Ten microphones were employed on the fully suppressed nacelle testing, for both the inlet splitters forward and inlet splitters aft configurations. The microphones were located along a line eight feet from the engine centerline, parallel to the engine axis. The microphone heads were at engine centerline height. The microphone locations for both configurations, and their identifying letters, were as follows (See Figure II B-3):

Mic A - 8 ft. forward of inlet plane

Mic B - 4 ft. forward of inlet plane

Mic C - In the plane of the inlet

Mic D - 5 ft. aft of the inlet plane

Mic E - In the plane of the fan rotor

Mic F - 4.5 ft. aft of the fan rotor plane

Mic G - In the plane of the fan exhaust

Mic H - In the plane of the core exhaust

Mic I - 4 ft. aft of the core exhaust plane

Mic J - 8 ft. aft of the core exhaust plane

3. Data Reduction

The data recorded on each microphone was analyzed on both a one-third octave band and 20 Hz narrowband basis, from 50 Hz to 10 KHz.

TABLE III A-1

TF34 ACOUSTIC PROBE SPL CORRECTIONS IN dB
(ONE THIRD OCTAVE BAND)
TO BE ADDED TO RAW PROBE SPL'S

1/3 O.B. Center Frequency		Unsuppressed Baseline			Suppressed Nacelle			
		Probe No. 1	Probe No. 2		PT1	PT2	PT24	PT25
50		0.4	0.6		0.4	0.4	0.6	0.5
63		0.5	0.6		0.5	0.4	0.6	0.6
80		0.6	0.7		0.6	0.5	0.7	0.7
100		0.8	0.7		0.8	0.5	0.7	0.8
125		1.0	0.8		1.0	0.7	0.8	0.8
160		1.2	0.8		1.2	0.8	0.8	0.9
200		1.4	0.9		1.4	1.3	0.9	0.9
250		1.6	1.0		1.6	1.5	1.0	1.0
315		1.8	1.1		1.8	1.7	1.1	1.2
400		2.0	1.3		2.0	2.1	1.3	1.5
500		2.2	1.4		2.2	2.5	1.4	1.7
630		2.5	1.5		2.5	2.8	1.5	1.9
800		2.7	1.7		2.7	3.2	1.7	2.3
1000		3.0	2.0		3.0	3.4	2.0	2.5
1250		3.2	2.2		3.2	3.7	2.2	2.7
1600		3.5	2.7		3.5	3.8	2.7	2.8
2000		3.8	3.0		3.8	4.5	3.0	3.0
2500		4.4	3.2		4.4	4.8	3.2	3.5
3150		5.0	3.7		5.0	5.5	3.7	4.0
4000		6.1	4.4		6.1	6.0	4.4	4.3
5000		6.4	5.0		6.4	6.9	5.0	4.7
6300		7.4	5.4		7.4	7.5	5.4	5.3
8000		8.5	6.7		8.5	8.5	6.5	5.9
10,000		9.5	7.0		9.5	9.5	7.0	6.5

Note: A random incidence correction factor of -2 dB is applied to each 1/3 octave band SPL, in addition to the corrections above.

TABLE III A-2

TF34 CORE EXHAUST RAKE CORRECTIONS
IN dB (ONCE THIRD OCTAVE BAND)
TO BE ADDED TO RAW SPL DATA FROM RAKE

1/3 O.B. Center Frequency	Element A			Element B			Element C			Element D		
	Probe Corr.	Elect Corr.	Total Corr.	Probe Corr.	Elect Corr.	Total Corr.	Probe Corr.	Elect Corr.	Total Corr.	Probe Corr.	Elect Corr.	Total Corr.
50	0.4	0.52	0.92	0.5	0.99	1.49	0.5	0.81	1.31	0.5	0.41	0.91
63	0.4	1.33	1.73	0.5	1.60	2.10	0.5	1.30	1.8	0.5	0.97	1.47
80	0.4	1.15	1.55	0.6	1.40	2.0	0.55	0.91	1.46	0.55	0.54	1.09
100	0.5	0.9	1.40	0.65	1.20	1.85	0.6	0.96	1.56	0.6	0.79	1.39
125	0.6	0.28	0.88	0.7	0.53	1.23	0.7	0.30	1.0	0.65	0.19	0.84
160	0.7	0.58	1.28	0.75	0.49	1.24	0.85	0.36	1.21	0.7	-0.04	0.66
200	0.8	0.45	1.25	0.85	0.79	1.59	1.1	0.23	1.33	0.75	0.08	0.83
250	0.9	-0.03	0.87	0.9	-0.05	0.85	1.2	-0.01	1.19	1.1	0.	1.1
315	1.1	0.45	1.55	1.0	0.45	1.45	1.3	0.5	1.8	1.2	0.05	1.25
400	1.2	0.38	1.58	1.2	0.16	1.36	1.4	0.38	1.78	1.35	0.5	1.85
500	1.3	0.29	1.59	1.5	0.29	1.79	1.5	0.14	1.64	1.5	-0.07	1.57
630	1.4	0.51	1.91	1.6	0.45	2.05	1.6	0.34	1.94	1.8	0.2	2.0
800	1.7	0.16	1.86	1.7	0.16	1.86	1.9	0.49	2.39	2.0	0.06	2.06
1000	1.8	0.42	2.22	1.9	0.57	2.47	2.0	0.37	2.37	2.2	0.17	2.37
1250	2.0	0.22	2.22	2.1	0.30	2.4	2.2	0.12	2.32	2.4	-0.06	2.34
1600	2.2	0.59	2.79	2.4	0.36	2.76	2.5	0.35	2.85	2.7	0.23	2.93
2000	2.6	0.8	3.40	2.7	0.54	3.24	2.9	0.41	3.31	3.0	0.02	3.02
2500	2.9	0.27	3.17	3.0	0.02	3.02	3.2	0.31	3.51	3.4	0.17	3.57
3150	3.2	0.44	3.64	3.4	0.69	4.09	3.5	1.02	4.52	3.7	0.59	4.29
4000	3.6	0.77	4.35	3.8	0.53	4.33	4.0	0.45	4.45	4.2	-0.12	4.08
5000	4.0	0.76	4.76	4.2	0.67	4.87	4.5	0.83	5.33	4.7	0.2	4.9
6300	4.5	0.98	5.48	4.7	0.74	5.44	5.0	0.79	5.79	5.4	0.69	6.09
8000	5.0	0.85	5.85	5.3	1.10	6.40	5.6	0.9	6.5	5.9	0.24	6.14
10,000	5.5	1.40	6.90	5.8	1.40	7.20	6.0	1.15	7.15	6.5	1.05	7.55

Note: A random incidence correction factor of -2 dB is applied to each 1/3 octave band SPL, in addition to the corrections above.

TABLE III A-3

TF34 QUIET NACELLE TESTING

ACOUSTIC PROBE IMMERSION DEPTHS

(MEASURED IN INCHES FROM OUTER WALL)

	UNSUPPRESSED BASELINE			FULLY SUPPRESSED BASELINE					
	PROBE #1		PROBE #2	PT 1		PT2		PT24	PT25
IMMERSION NUMBER	5100 RPM	6200 RPM & MAX POWER	ALL SPEEDS	5100 RPM	6200 RPM & MAX POWER	5100 RPM	6200 RPM & MAX POWER	ALL SPEEDS	ALL SPEEDS
1	2	2	1	2	2	2	2	1	1
2	4	4	2	4	4	4	4	2	2
3	6	6	3	6	6	6	6	3	3
4	8	8	4	8	8	8	8	4	4
5	10	10	5	10	10	10	10	5	5
6	12	11	6	12	14	12	14	6	5.5
7	12.5	14	7	16	16	15	15	--	--
8	--	--	--	18	18	--	--	--	--
9	--	--	--	20	20	--	--	--	--
10	--	--	--	22	22	--	--	--	--

FOUR ELEMENT CORE RAKE IMMERSION DEPTHS (MEASURED IN INCHES FROM OUTER WALL)

ELEMENT	BASELINE UNSUPPRESSED CORE	SUPPRESSED NACELLE CORE
A	1.40	0.55
B	2.38	1.53
C	3.48	2.63
D	4.64	3.79

FIGURE III A-1

SCHEMATIC OF ACOUSTIC PROBE SYSTEM

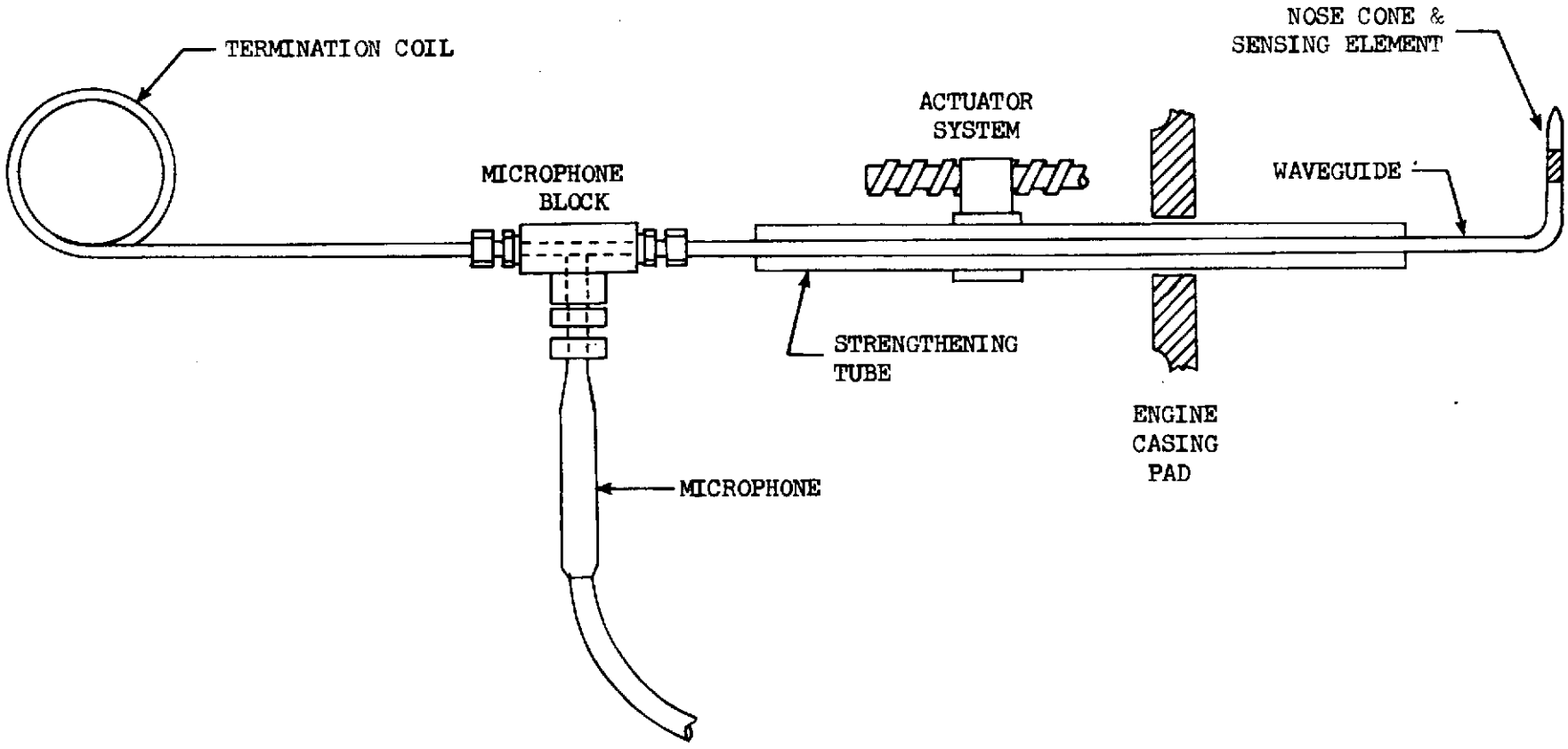

FIGURE III A-2

TF34 BASELINE UNSUPPRESSED ENGINE

FAN INLET & EXIT PROBE LOCATIONS

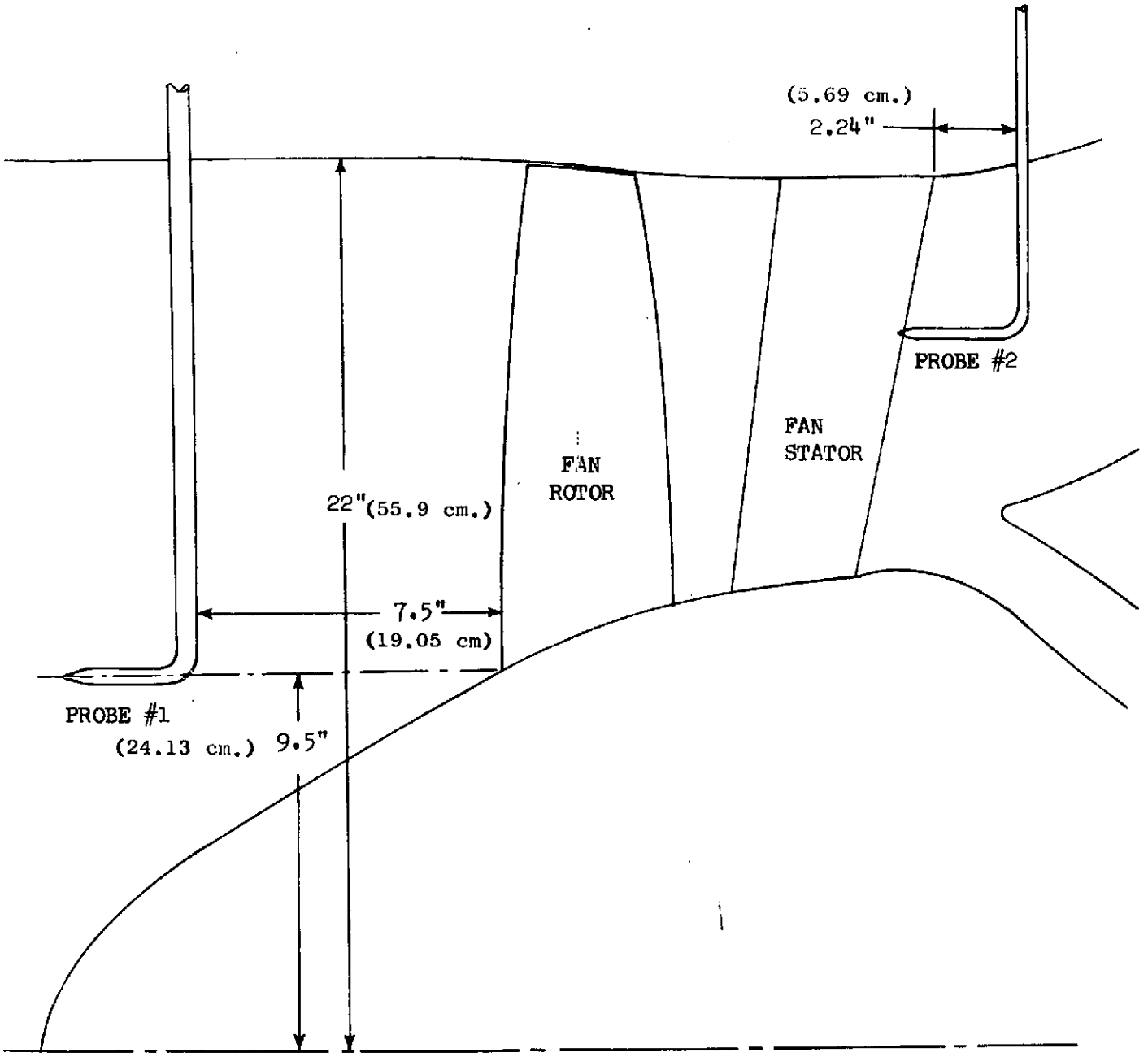

FIGURE III A-3

TF34 BASELINE UNSUPPRESSED ENGINE

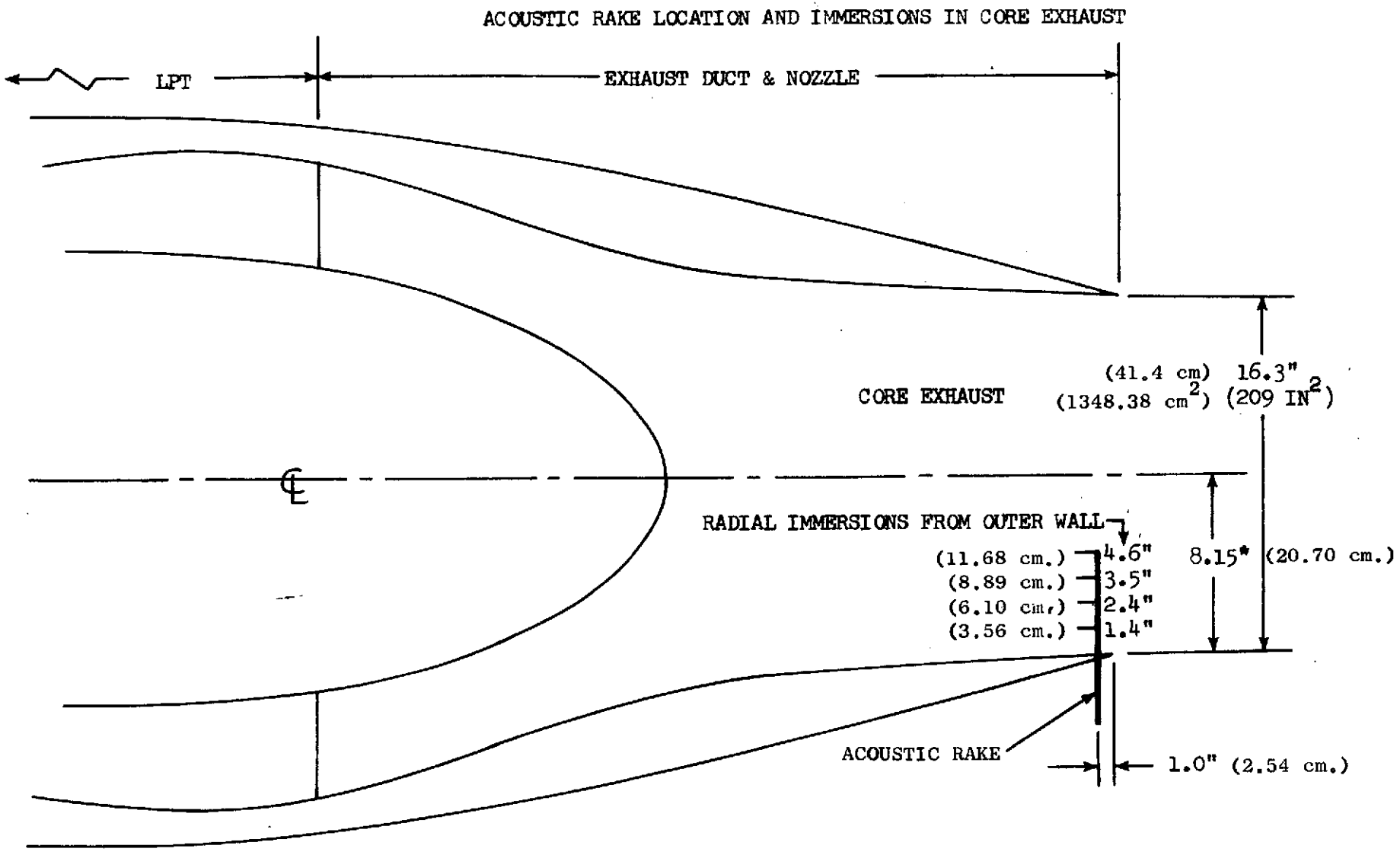

FIGURE III A-4

TF34 FULLY SUPPRESSED NACELLE

INLET ACOUSTIC INSTRUMENTATION LAYOUT

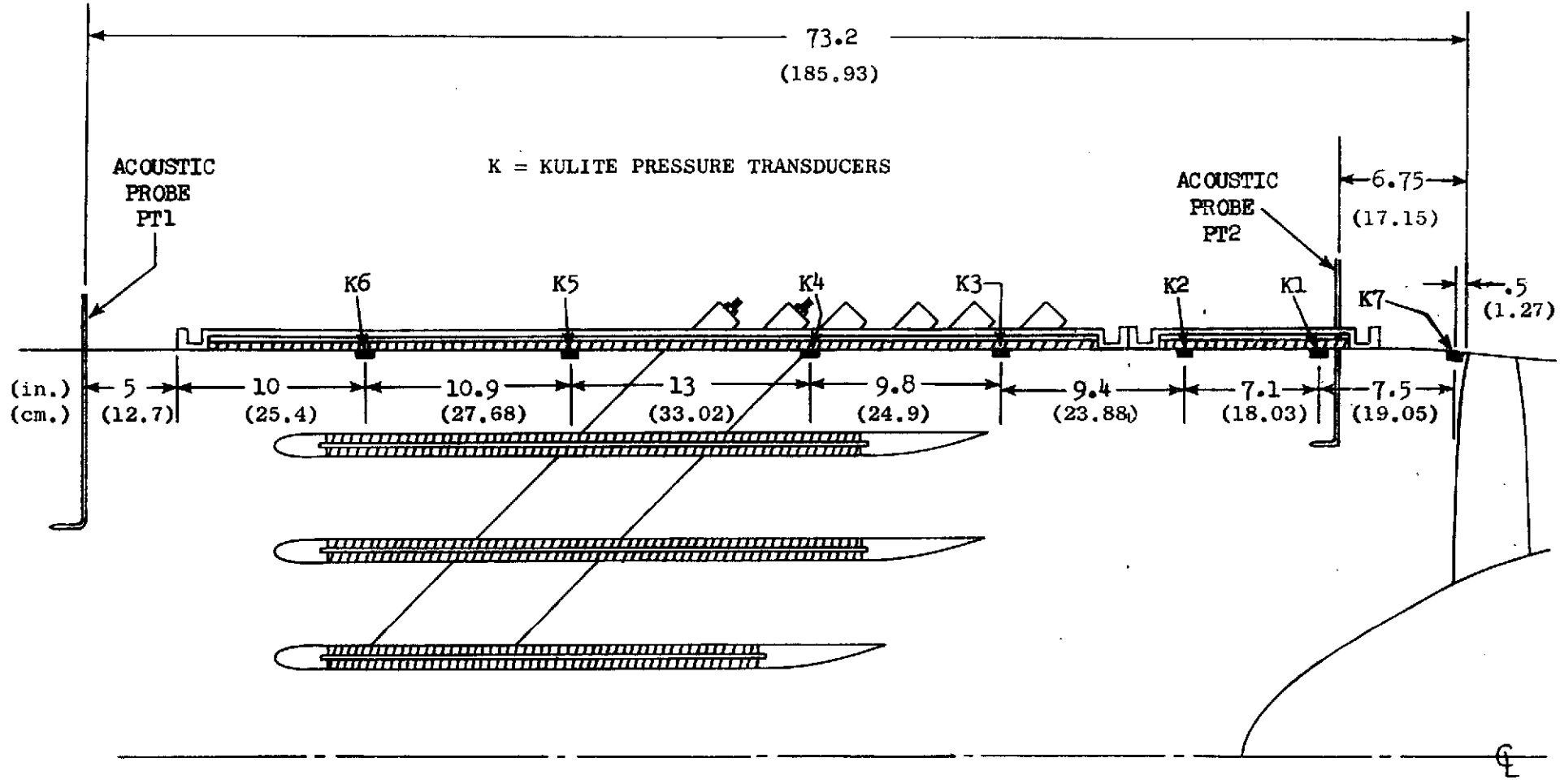

DIMENSIONS IN INCHES
(CENTIMETERS)

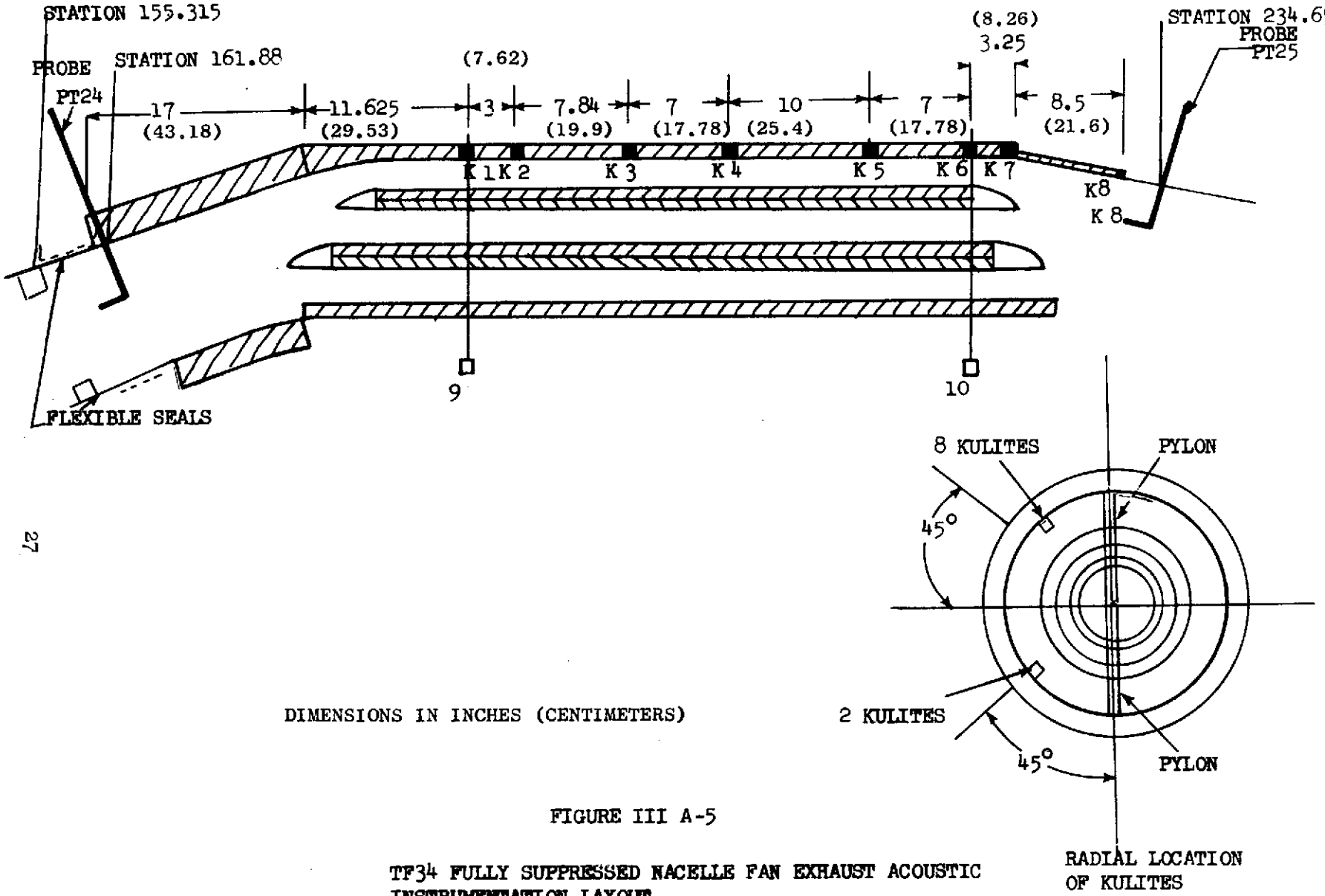

DIMENSIONS IN INCHES (CENTIMETERS)

FIGURE III A-5

TF34 FULLY SUPPRESSED NACELLE FAN EXHAUST ACOUSTIC INSTRUMENTATION LAYOUT

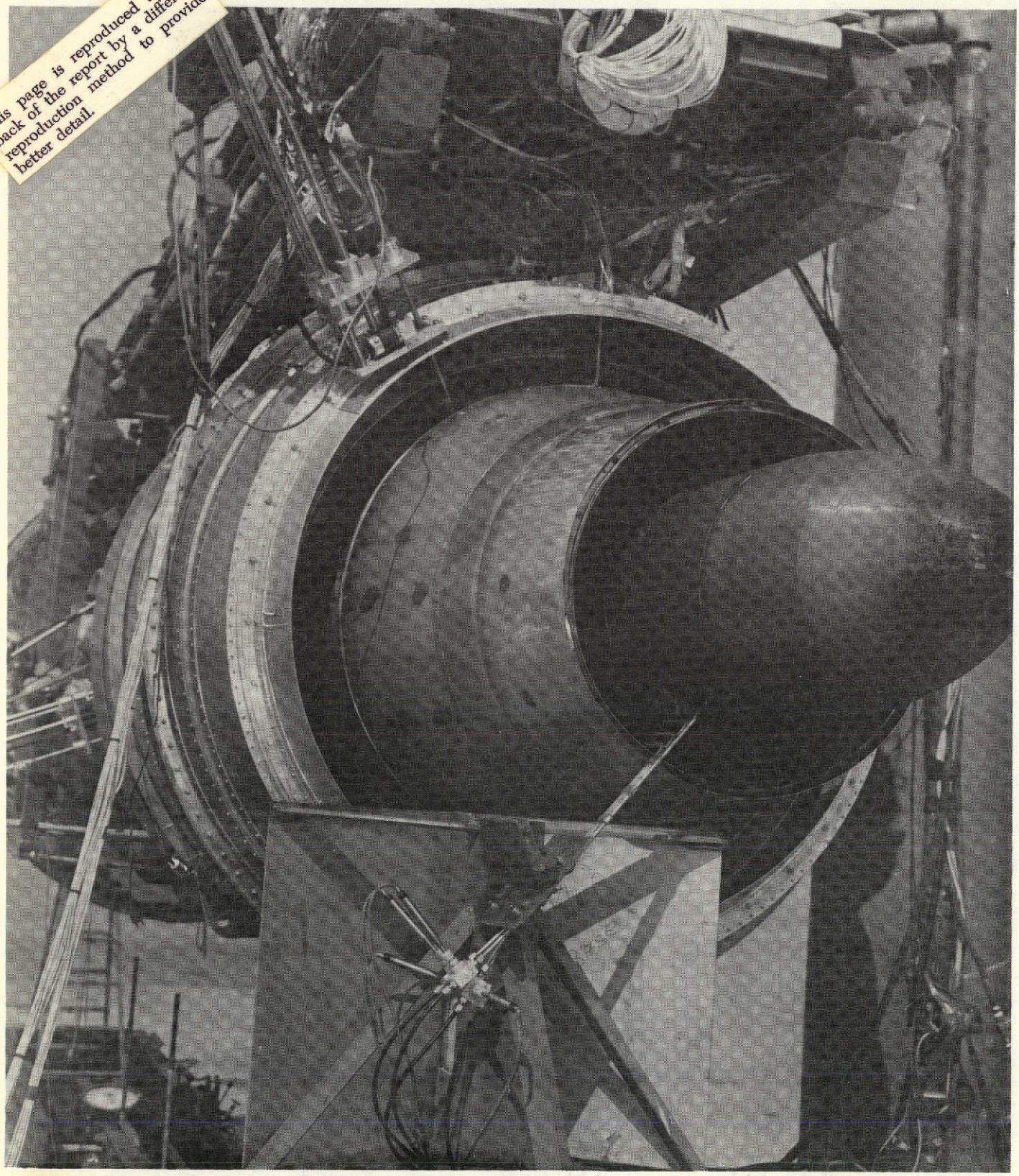

FIGURE III A-6 CORE EXHAUST RAKE IN PLACE ON TF34 QUIET NACELLE

This page is reproduced at the back of the report by a different reproduction method to provide better detail.

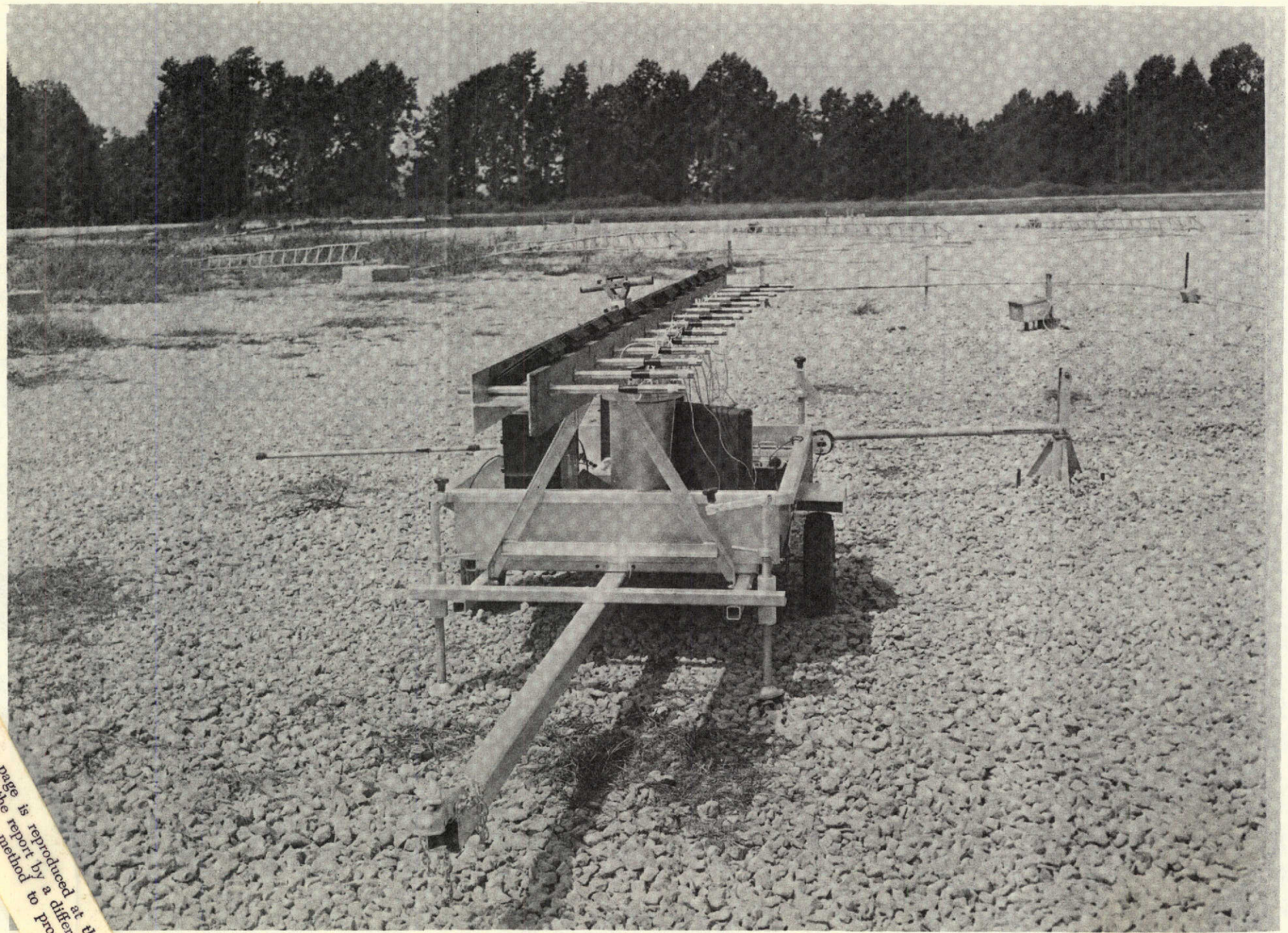

FIGURE III C-1 DIRECTIONAL MICROPHONE ARRAY

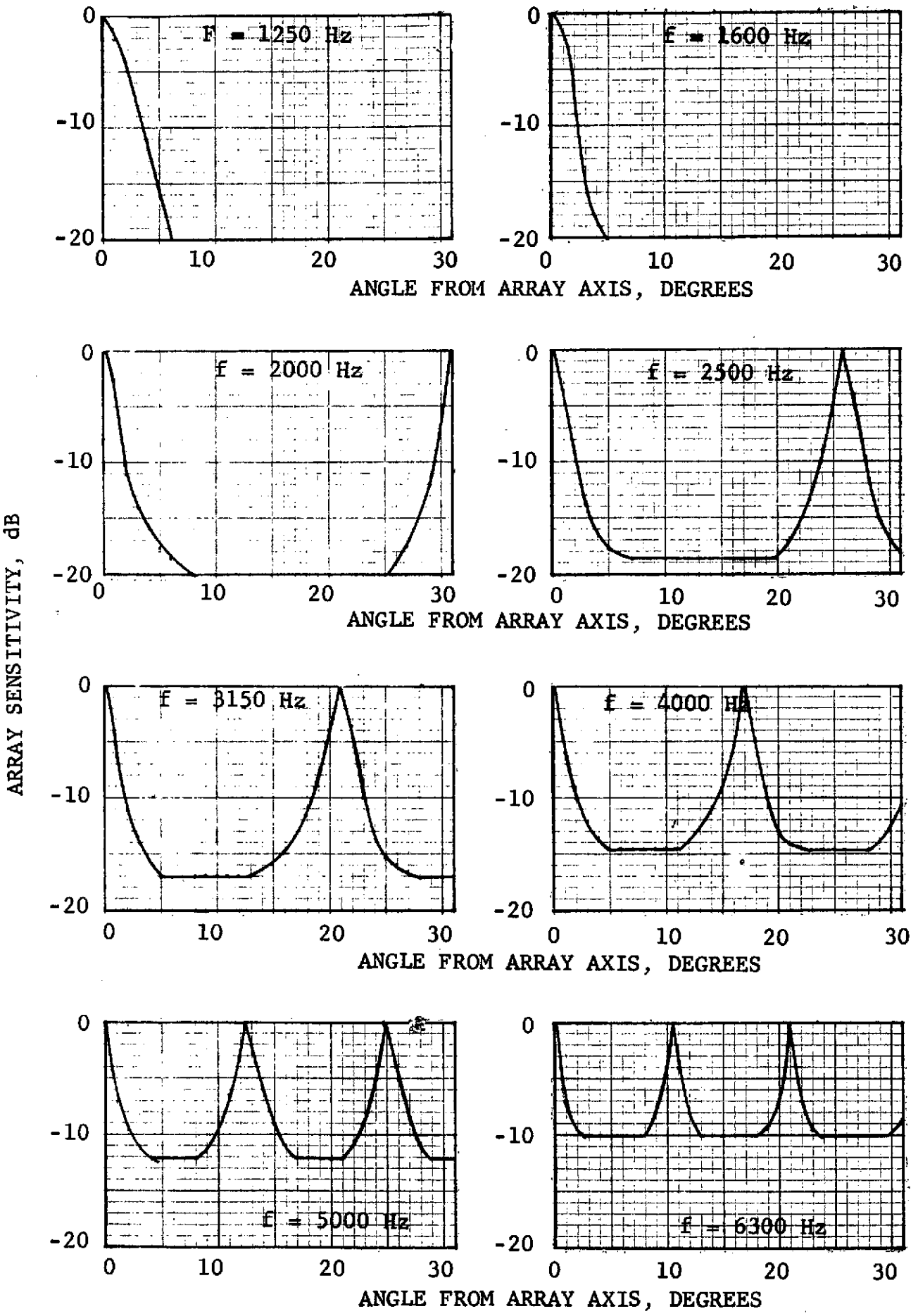

FIGURE III C-2

BEAM PATTERNS OF DIRECTIONAL ACOUSTIC ARRAY

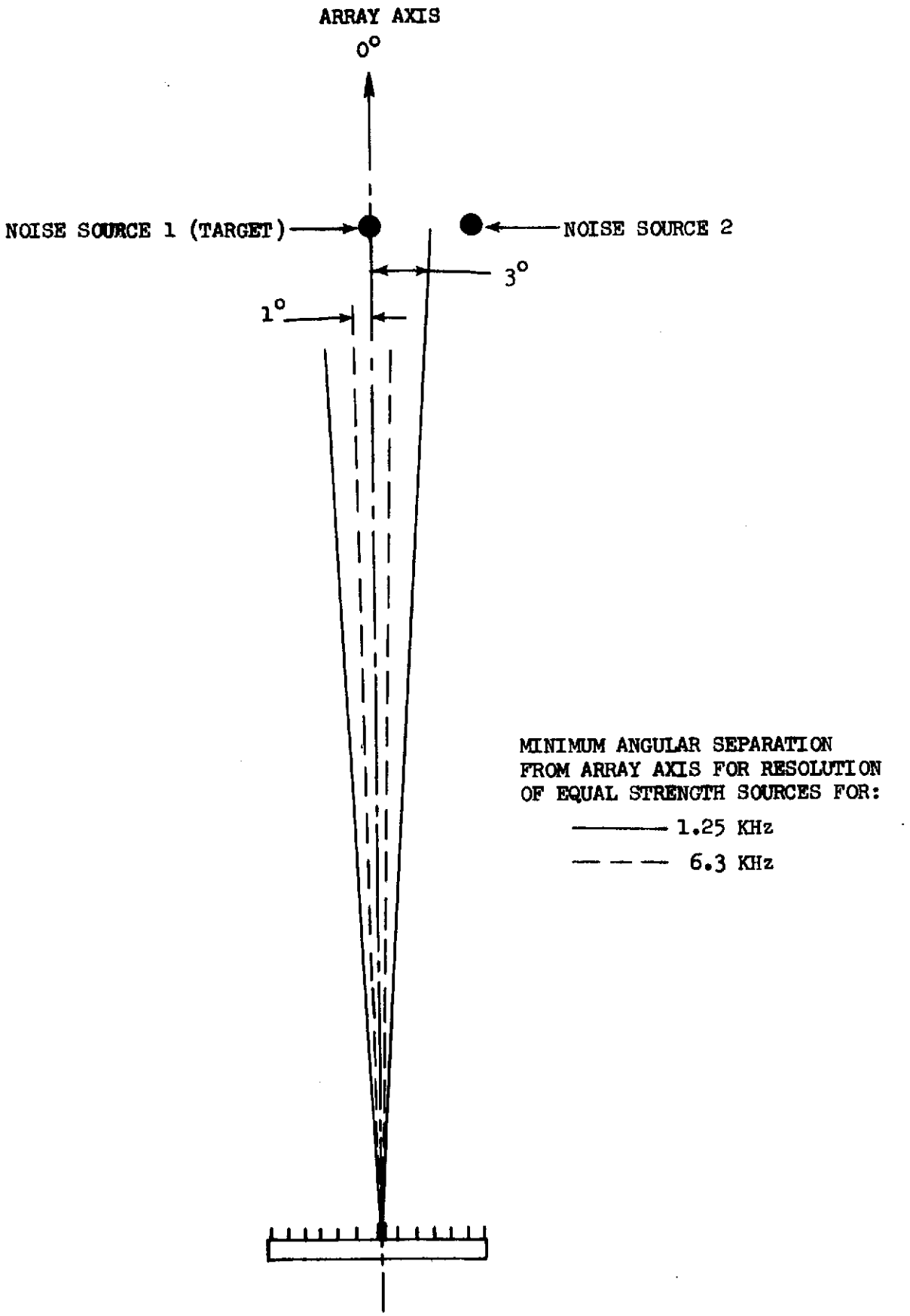

ACOUSTIC DIRECTIVITY ARRAY RESOLUTION CAPABILITY

FIGURE III C-3

FIGURE III C-4

DIRECTIONAL ACOUSTIC ARRAY POSITIONING ON TF34 FULLY SUPPRESSED, INLET SPLITTERS FORWARD

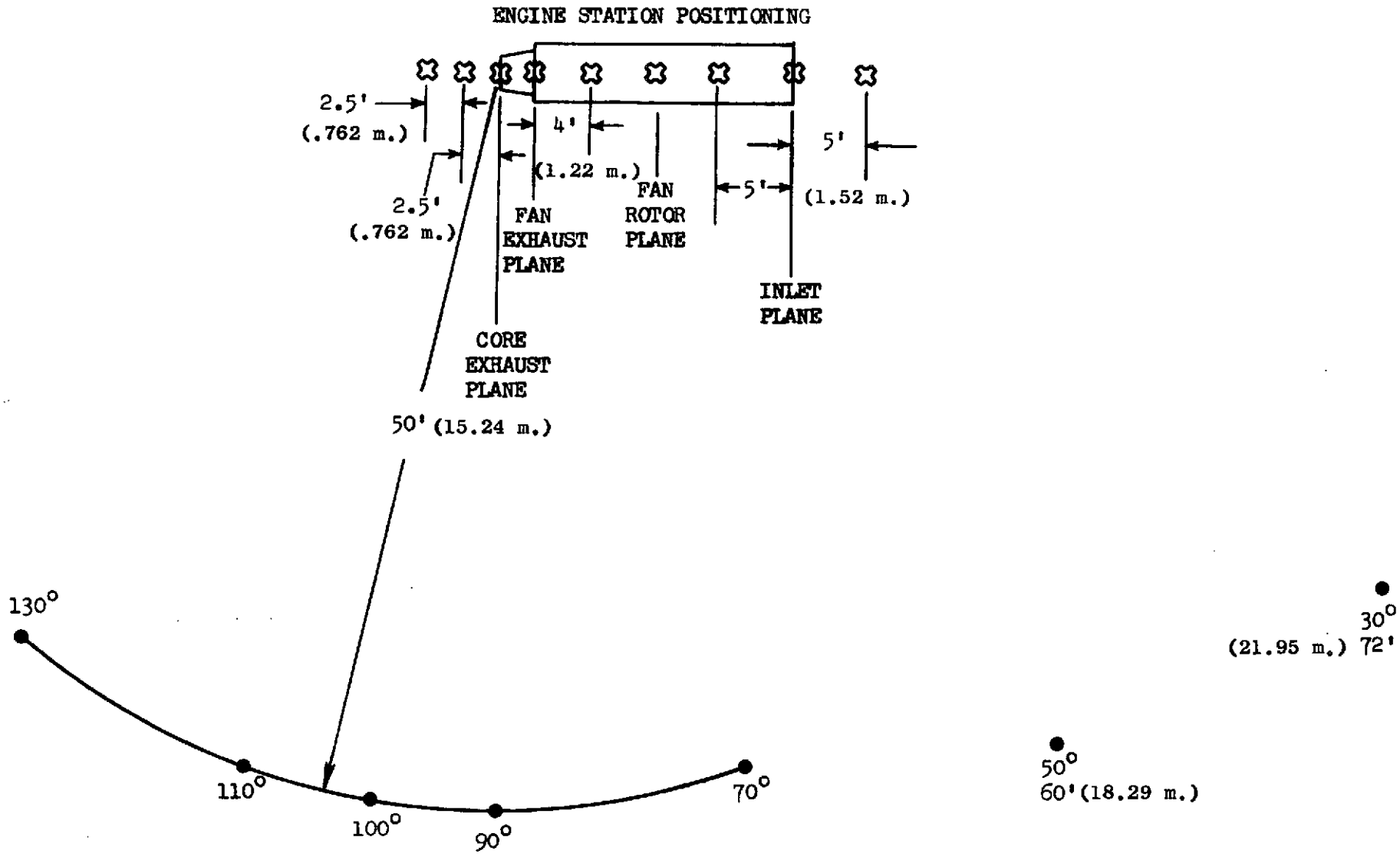

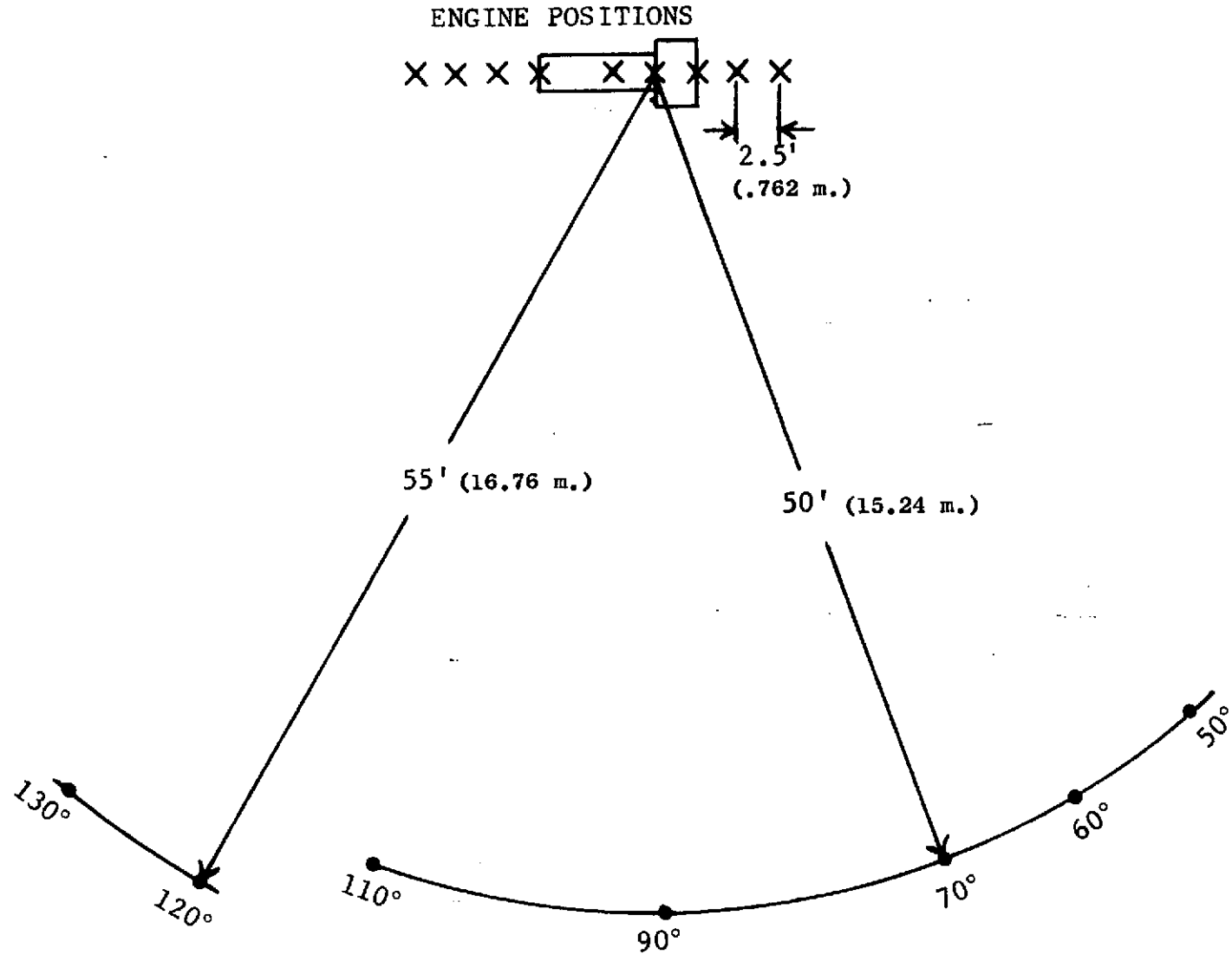

FIGURE III C-5

DIRECTIONAL ACOUSTIC ARRAY POSITIONING ON TF34
BASELINE CONFIGURATION

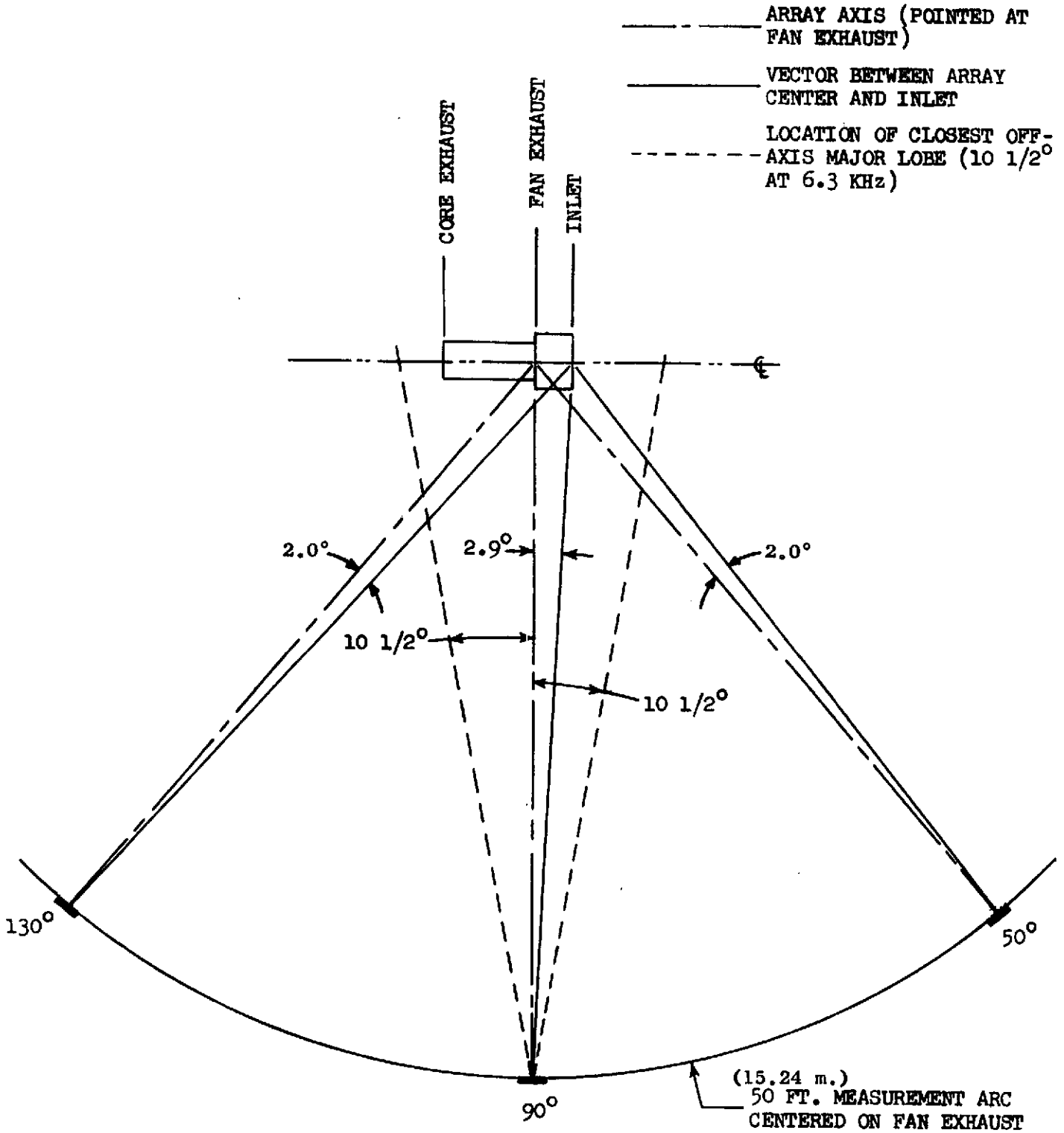

FIGURE III C-6

ACOUSTIC DIRECTIVITY ARRAY MEASUREMENTS ON TF34 UNSUPPRESSED BASELINE ENGINE, ARRAY POINTED AT FAN EXHAUST

IV. TEST RESULTS

A. Probes

One-third octave band PWL spectra were calculated for all acoustic probe runs, as outlined in Section III.A. These PWL spectra are compared in this section. It should be noted here that the probe-recorded broadband noise is subject to the high noise floors inherent in acoustic probe measurements. The probe records the "true noise" signal, local aerodynamic pressure fluctuations, and noise generated by flow over the probe. All of these sources are seen as broadband noise and are inseparable without knowing the individual levels. For these reasons, it is customary, when attempting to measure noise suppressions obtained, to only consider the pure tones. Nevertheless, it is felt that total spectral comparisons of probe data can be of some use, where systematic differences in broadband levels indicate the presence of a dominant fan noise signal, although not being an absolute measure of its magnitude.

Figures IV A-1 through IV A-3 are comparisons of the PWL spectra measured on the inlet probes for the baseline and the suppressed, splitters forward configurations for three power settings. Baseline nacelle probe No. 1 and suppressed nacelle probe PT2 are spaced almost an identical distance ahead of the fan rotor, and a direct comparison is thus possible (suppressed nacelle probe PT1 is placed immediately upstream of the inlet splitters). Comparison of the data (Probe 1 vs PT2) indicates that the presence of the splitters had no significant effect on the fan source noise as regards pure tones. The splitters do cause an apparent low frequency broadband noise increase, especially at 5100 RPM. The marked increase in spectral levels between 500 Hz to 2 KHz,

evidenced in the 6200 RPM and maximum power data is due to the onset of the generation of multiple pure tones. The PWL spectra recorded on probe PT1 are indicative of the massive pure tone and MPT suppressions achieved through the inlet treatment.

Figures IV A-4 through IV A-6 are corresponding PWL spectral plots from the fan exhaust duct acoustic probes on the baseline and suppressed, splitters forward configurations. Here the baseline nacelle probe No. 2 and the suppressed nacelle probe PT24 are in somewhat different locations in respect to the fan, probe No. 2 being closer to the rotor exit plane. The fan source noise will thus be somewhat more attenuated when it reaches probe PT24 than it would be at probe No. 2. Comparison of the PWL spectra at all three power settings shows that the levels recorded on probe No. 2 are systematically higher, especially at the higher frequencies. When the differences in measuring position are taken into account, it appears that the presence of the splitters has little effect on fan source noise in the exhaust. The spectra recorded on probe PT25, downstream of the fan exhaust splitters, show that all pure tones have been removed by the treatment. Comparison of the inlet and fan exhaust PWL spectra would indicate that the exhaust suppressions achieved were less dramatic than those in the inlet. It should be remembered, however, that the downstream exhaust probe PT25 is in a relatively high velocity flow near the fan nozzle exit. The levels recorded on this probe are "swamped" by extraneous broadband noise and pseudo-noise sources, with the true fan exhaust levels being considerably lower. Data from the acoustic directivity array (Section IV.C.) lends credence to this conclusion by showing much larger aft fan broadband suppression values.

Figures IV A-7 through IV A-12 are direct comparisons of the probe PWL spectra recorded from all fan acoustic probes in the suppressed nacelles, for the inlet splitters forward versus inlet splitters aft configurations. As regards the fan source noise levels (probes PT2 and PT24), there seems to be little or no systematic difference, in either the inlet or fan exhaust, between splitters forward and splitters aft data. The low frequency broadband noise increase indicated on the inlet probe PT2, for the splitters forward test, does not occur for the splitters aft configuration; also the second harmonic tone in the fan exhaust (PT24) seems to be somewhat stronger with splitters forward at 6200 RPM, but this situation is reversed at max power. Comparison of the suppressed fan noise levels (probes PT1 and PT25) indicates that the splitters forward data is consistently higher than the splitters aft data, for both inlet and fan exhaust. Part of this difference may be due to the fact that the test speed points were set on the basis of physical fan speed and the splitters forward probe testing was run on a colder day, thus resulting in higher power settings. However, even if this power setting difference is taken into account, the resulting shift in levels would still not collapse the two sets of data. In any case, this apparent difference is not measurable in the farfield, either on the farfield microphones or on the directivity array.

Figures IV A-13 through IV A-15 are comparisons of the baseline fan probe total power levels (inlet + fan exhaust) and the measured baseline farfield PWL spectra for the corresponding power setting. These comparisons show that at least for 800 Hz and above, where jet noise is not present, the unsuppressed baseline probes are measuring true fan noise, both for pure tones and broadband. They are also an indicator of the domination of the farfield noise signature by

unsuppressed fan noise. Figures IV A-16 through IV A-18 are similar comparisons of fan probe and farfield PWL spectra, for the fully suppressed nacelle with inlet splitters forward; here the total suppressed fan probe noise level is arrived at by summing the spectra recorded on probes PT1 and PT25. The fan probe levels above 800 Hz are seen to be higher than the total engine noise levels measured in the farfield. It is evident that the high frequency broadband noise recorded on these probes is not true fan noise and that, indeed the data from the probes is swamped by pseudo-noise which does not radiate to the farfield.

Figures IV A-19 through IV A-21 are comparisons of the core rake PWL spectra recorded on the unsuppressed baseline and fully suppressed nacelle. The core exhaust ducts for the two configuraitons are quite different, the suppressed duct being much longer and narrower than the baseline. The basic noise transmission characteristics through these ducts vary as well, so much so that a valid measure of the core suppression effectiveness is not obtainable from this data; it is presented here for purposes of general comparison only.

Figures IV A-22 through IV A-29 are core rake PWL comparisons from the core noise tests; here both runs were made on the suppressed nacelle, the only difference being that for one case the core exhaust suppression was replaced with a hardwall duct. The only observable differences between the treated and untreated core data are at the very lowest power settings. At 2000 RPM fan speed, the core suppression is worth 5-15 db PWL at all frequencies above 400 Hz; for 3000 RPM, 4000 RPM and 5100 RPM, the only significant differences are due to turbine pure tone suppression; above these speeds the differences are minimal or non-existant. The fact that measurable suppressions are achieved only at very low power settings, regardless of the presence of massive core

suppression, would again lead to the conclusion that an extaneous broadband noise source was present at least for the higher speed runs. The core rake (Figure III A-6) was mounted external to the engine, and incorporated a rather large rectangular shield to protect the instrument from the fan exhaust stream; it may be that the impingement of the fan stream upon this plate is generating noise which is recorded by the rake elements, masking the core noise at the higher speed points.

Figures IV A-30 through IV A-35 are radial profiles of the fan source PWL recorded in the inlet, for the baseline case and the two suppressed nacelle cases. This radial distribution of acoustic energy is of course important in achieving the optimum radial spacing of acoustic splitters. Two sets of distribution curves are included, one for the fan fundamental tone, the other for the second harmonic tone; within the limits of data scatter, all three configurations show the same trends. The fundamental tone energy distributions are skewed toward the rotor tip. For an immersion of 2 inches to an immersion of 6 inches the PWL decreases rapidly by approximately 10 dB for maximum power and 6200 RPM, and about 3 dB for 5100 RPM. For the area between immersions of 6 to 15 inches, the PWL reduction amounts to about 5 dB for maximum power and 6200 RPM, while virtually no reduction was seen at 5100 RPM. In the case of the second harmonic tone energy, a rapid drop was also noted from 2 inches to 6 inches immersion depth, but from that point on, the distribution became fairly flat for 5100 RPM and 6200 RPM. At maximum power, an irregular pattern was found from 6 inches depth to 15 inches depth, possibly due to certain higher modes set up in the inlet duct. It seems that a splitter placed to give an outer passage height of up to 6 inches would be ideal to reduce the source PWL by a significant amount. The outer splitter in the TF34 suppressed inlet was

very effectively placed with a passage height of 4.5 inches. No PWL distributions were plotted for the fan exhaust noise; due to the unfavorable ratio of duct height to the wavelength of the fan tone noise, no systematic energy distribution was noted.

Figures IV A-36 through IV A-41 are typical plots of the uncorrected 20 Hz narrowband SPL data recorded on the inlet and fan exhaust probes, comparing the probe SPL's ahead of and behind the acoustic treatment. The strong pure tone and MPT levels of the fan source noise are apparent, as are the dramatic reductions achieved through the acoustic treatment; tone suppressions of up to 35 dB are evident. Figures IV A-42 and IV A-43 are summaries of the space averaged pure tone and MPT suppressions measured by the inlet and exhaust acoustic probes at maximum power, for both splitters forward and splitters aft cases. These are compared to the predicted suppression spectra; and in every instance, the suppressions achieved were equal to or greater than predicted (MPT suppression values were not included in the inlet suppression prediction). Broadband fan suppressions were not compared, due to the extraneous noise masking the true broadband levels on probes PT1 and PT25.

Figure IV A-44 is a similar comparison of measured and predicted suppressions across the core exhaust treatment, from the 2000 RPM test point of the core noise tests. The comparisons here are for broadband as well as turbine pure tone noise suppressions; some "masking" may have occurred, as has been previously discussed, but the achieved reductions still compare favorably to the predicted values.

B. Kulite Transducers

Kulite pressure transducers were employed along the treated outer walls of the inlet duct and fan exhaust duct of the suppressed configuration, for both the inlet splitters forward and inlet splitters aft runs.

Figures IV B-1 through IV B-7 are plots of the fan pure tone noise signals (20 Hz bandwidth) measured on each of the inlet Kulites, for three speed points and for both inlet splitter positions. These plots provide a measure of the noise "decay" over the acoustic treatment length. Figure IV B-8 is a summary of the blade passing fundamental tone suppression per L/H achieved through the inlet splitter section for several fan speeds (L = treatment length, H = treated passage height). As can be seen tone noise decays of 40-75 dB were achieved through the total inlet, the decay through the splitter section being on the order of 20-40 dB. Tone noise decay rates of 3-6 dB per L/H were achieved in the splitter section. There seems to be no significant differences in the inlet treatment performance between the splitters forward and splitters aft configuration.

Figures IV B-9 through IV B-14 are plots of the fan pure tone noise decay measured on the fan exhaust Kulites, again for three speeds and for both inlet splitter positions. Here the pure tone SPL's transmitted along the fan exhaust duct wall were apparently already greatly attenuated by the treatment ahead of the fan exhaust splitters. The remaining tone reductions (down to the broadband floor) were accomplished in the first three inches of the exhaust splitters. The fundamental tone decay measured by the fan exhaust Kulites over this first three inches is approximately 5 dB per L/H at the maximum speed.

The fact that the fan tone noise hits an apparent "floor" after only three inches of splitter length and that no further reduction occurs over the rest of the splitter, would suggest the possibility that some extraneous broadband noise source was masking further noise reductions existed in the fan exhaust duct. Figure IV B-15 is a detailed plot of the noise levels, recorded on the exhaust Kulites, for the fan fundamental tone at maximum power, plotted as a function of treatment L/H; in this plot the floor is quite obvious. A prediction was made of the theoretical broadband noise level that would be generated by the airflow over the treatment; this prediction is a function of flow velocity, surface roughness, boundary layer thickness, etc., as is based on published work by Ffowcs-Williams.[4] This predicted self-noise for the 20 Hz band centered at the fan fundamental frequency is also indicated on Figure IV B-15. It should be pointed out that this prediction is only for the actual propagating acoustic signal from the flow; the Kulites will also measure the fluctuating aerodynamic pressure signals in the duct, but this latter component does not contribute to the noise radiated from the exhaust. By the use of correlation analysis techniques it is possible to separate out the overall acoustic and aerodynamic components. When cross-correlation coefficient between succeeding Kulites is plotted as a function of the time delay, γ, two peaks will be generated, one at the time delay corresponding to the acoustic velocity plus the flow velocity, the other at the time delay corresponding only to the flow velocity. The former peak of course represents the actual acoustic signal, and the latter the aerodynamic signal; the ratio between these peaks may then be used to determine the relative levels between the SPL and the fluctuating aerodynamic pressure. Figure IV B-16 is

a typical example of such an analysis for the TF34 fan exhaust duct Kulites. Figure IV B-17 is the resulting plot of "actual acoustic" OASPL in the exhaust duct, compared to the "total signal" OASPL measured by the Kulites. It is apparent that the "pseudo-noise" may make up a large proportion of the broadband noise floor that the Kulites are measuring. In this rough cut, no attempt was made to use filtration techniques to sort out the aero and acoustic components of the signal at the fan fundamental frequency. It is, however, intuitively obvious that the predicted noise floor in Figure IV B-15 could be "in the ballpark", and that the fan exhaust duct noise floor in the TF34 suppressed nacelle could be due to treatment generated flow noise.

C. Directional Acoustic Array

The directional array was used on the tests of the fully suppressed nacelle, both for inlet splitters forward and splitters aft.

The fully suppressed data with inlet splitters aft was seen to exhibit no significant differences when compared to the inlet splitters forward configuration. Figures IV C-1 through IV C-4 are comparisons of the uncorrected narrowband data for the two configurations, measured from the fan inlet and fan exhaust, for two power settings. The similarity is evident; all of the splitters aft data is with $\pm$ 2 dB of the corresponding splitters forward data, and this difference is within the limits of array repeatability.

Figures IV C-5 through IV C-7 show the SPL spectra measured from the major sources (fan exhaust core nozzle, core jet) at the maximum aft angle; also included, for reference, are the corresponding spectra from the unsuppressed engine test. (The measured angle differs between the suppressed and unsuppressed

configurations, to compensate for differences in the referenced center of measurement). The "core jet" data is the sum of the values measured at the two locations downstream of the core exhaust plane (See Section III.C.2). The data indicates that, for the unsuppressed configuration, the dominant aft noise source is the fan exhaust, followed by the core jet. In the case of the treated nacelle, the contribution from the fan exhaust is reduced to the level of the core components. The core component levels are lower than for the unsuppressed case, due to the combined effects of reducing the jet velocity (opened nozzle), and core acoustic treatment.

Figure IV C-8 shows the fully suppressed component spectra from the fan inlet, fan exhaust, and core, all measured at the maximum forward angle. In this and all remaining figures in this section, the "core" component refers to the sum of all three aftmost engine measuring positions. The "core" noise (core and core jet) is seen to be the dominant forward noise source at all speeds, being greater than even the suppressed fan inlet noise.

Figures IV C-9 and IV C-10 show the directivity of the dominant suppressed engine fan pure tones (within the frequency range measured by the array), at 5100 and 7100 (max) RPM. It can be seen that the major tone sources are the inlet and fan casing, even at the aft angles. It should be remembered, at this point, that these tones are highly suppressed, and are well below the other engine component noise levels; so they will have no effect on sideline noise.

Figures IV C-11 through IV C-19 are directivity plots for suppressed engine component broadband noise in the 1.25, 2.5, and 5.0 KHz third octave bands, for all three speed points. These show the dominance of core and core jet noise below 2.5 KHz, at all angles; above 2.5 KHz, there seems to be no consistently dominant source.

The measured inlet and fan exhaust suppressions achieved for both broadband noise and pure tones are shown in Figures IV C-20 through IV C-22. Pure tone suppressions on the order of 55 to 65 dB were recorded; the peak broadband suppression achieved was 38 dB (one-third octave measurements). Also indicated are the predicted suppression values; it is apparent that the broadband fan noise suppressions seen by the array are close to these predictions, especially for the low speed point. The fact that the measured broadband suppression performance is below predictions especially for the fan exhaust at the higher speed points is another indication of the possible presence of some sort of flow noise floor.

D. Nearfield Microphones

Figures IV D-1 through IV D-27 are plots of the one-third octave SPL spectra recorded on all the nearfield microphones at three power settings, comparing splitters forward to splitters aft data. (Microphone "G" was inoperative and is not included). Figures IV D-28 through IV D-36 are the corresponding 20 Hz narrowband SPL spectral comparisons from three representative microphones; "B" (forward of the inlet), "E" (plane of fan rotor), and "H" (downstream of the fan exhaust, at the core exit). AT 5100 and 6200 RPM, the splitters forward configuration seems to exhibit broad levels from the inlet and inlet casing area which are higher than the comparative splitters aft data. The data from the microphones aft of the fan plane indicate no significant differences between the two configurations; nor are any differences indicated at any microphone position for the maximum power setting.

A "leakage" of high frequency fan noise (fan harmonic tones) through the inlet treatment is apparent on the microphones forward of the inlet. This is of course especially true for the 5100 RPM setting, since the fan inlet treatment is "optimized" for the suppression of the fan tones at maximum power. To a lesser extent, fan harmonic tones are also present in the spectra for the inlet casing and fan exhaust areas, but these become indistinguishable at the higher power settings. Although the probe data shows the fan exhaust source noise to be higher than that for the inlet, the high frequency fan noise recorded on the nearfield microphones is greater for the inlet than for the fan exhaust area, at all power settings. On the farfield (100' arc) microphones, this leakage is apparent only at the most forward angles (0° to 30°); it would therefore have little effect on the noise projected to a sideline.

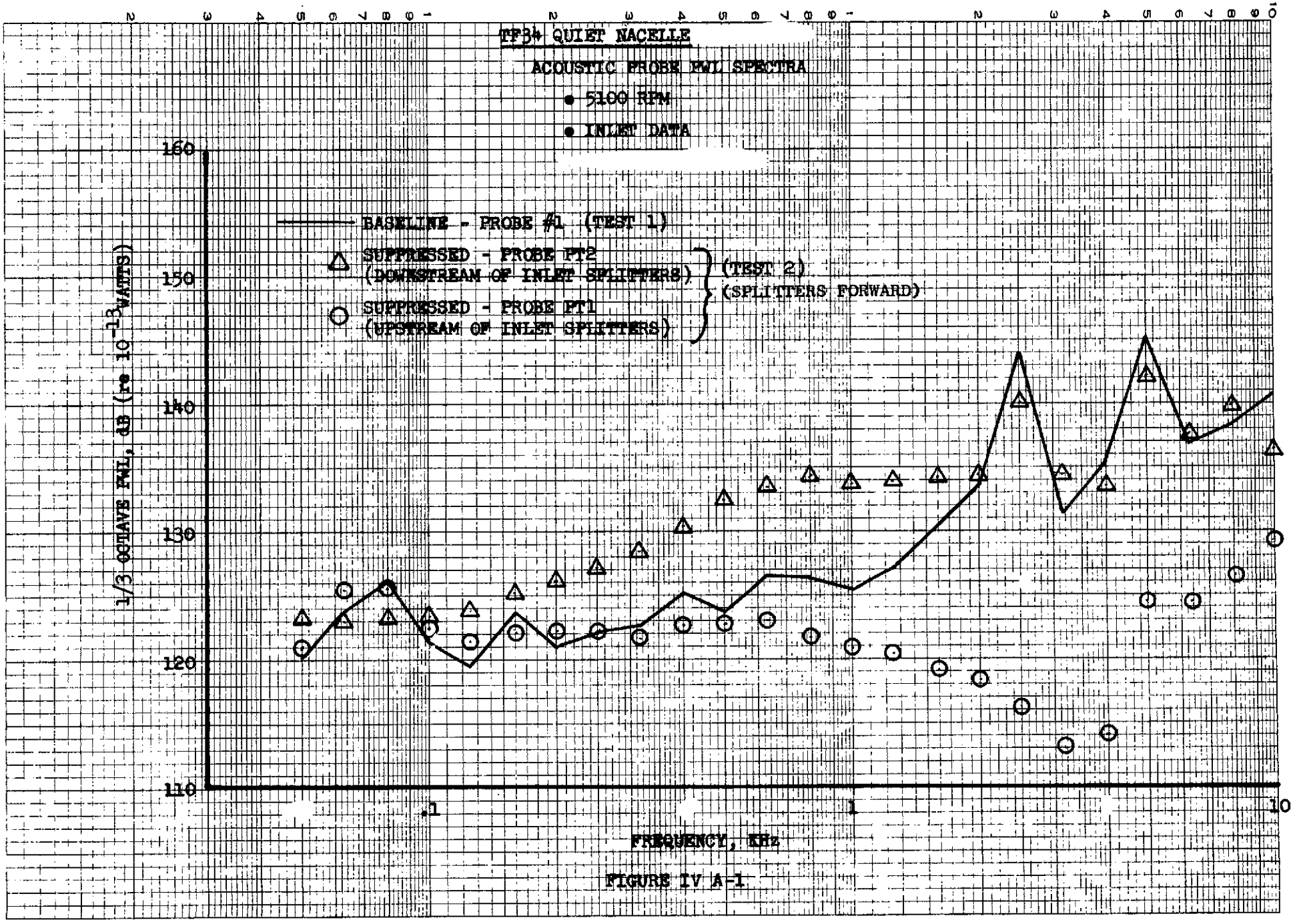

FIGURE IV A-1

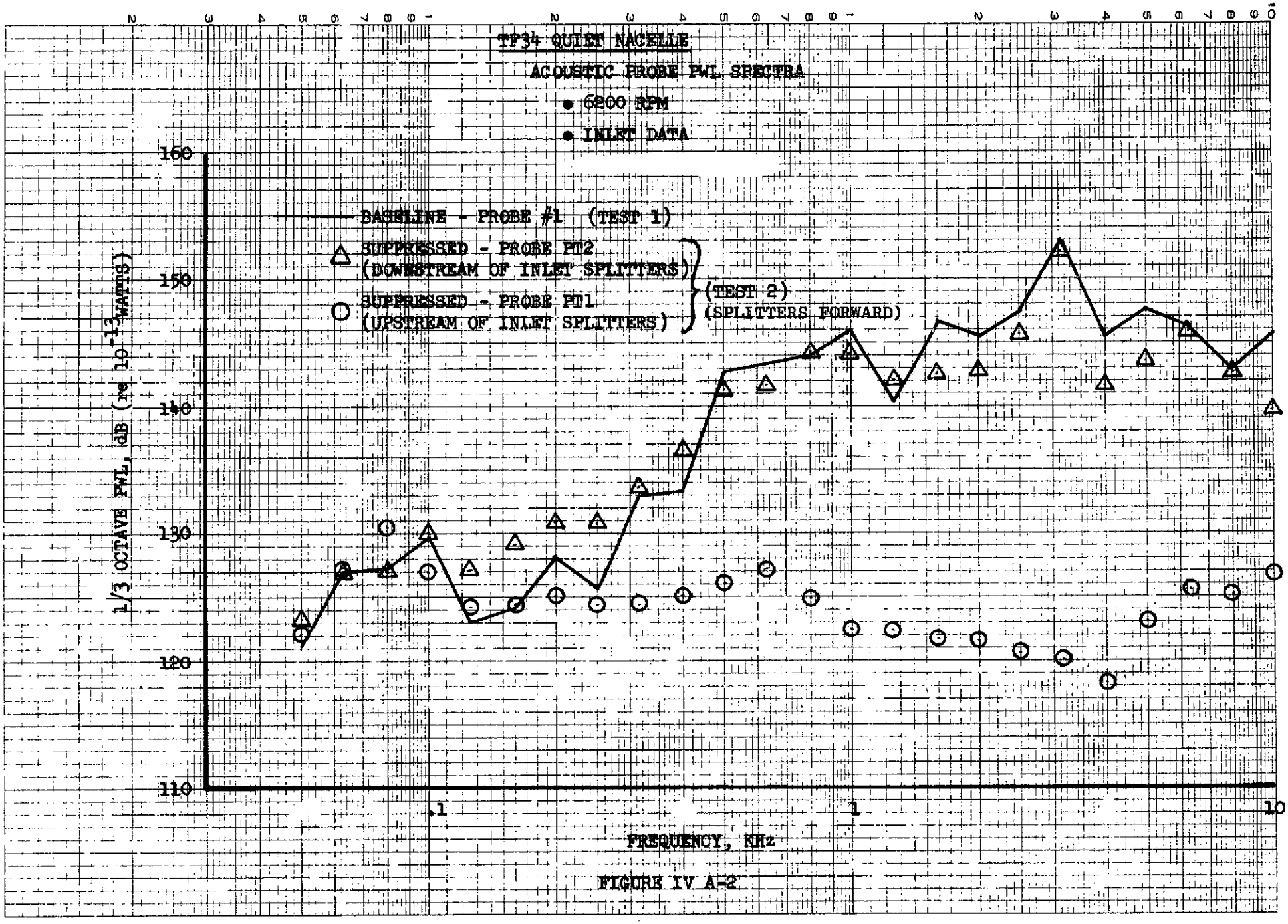

FIGURE IV A-2

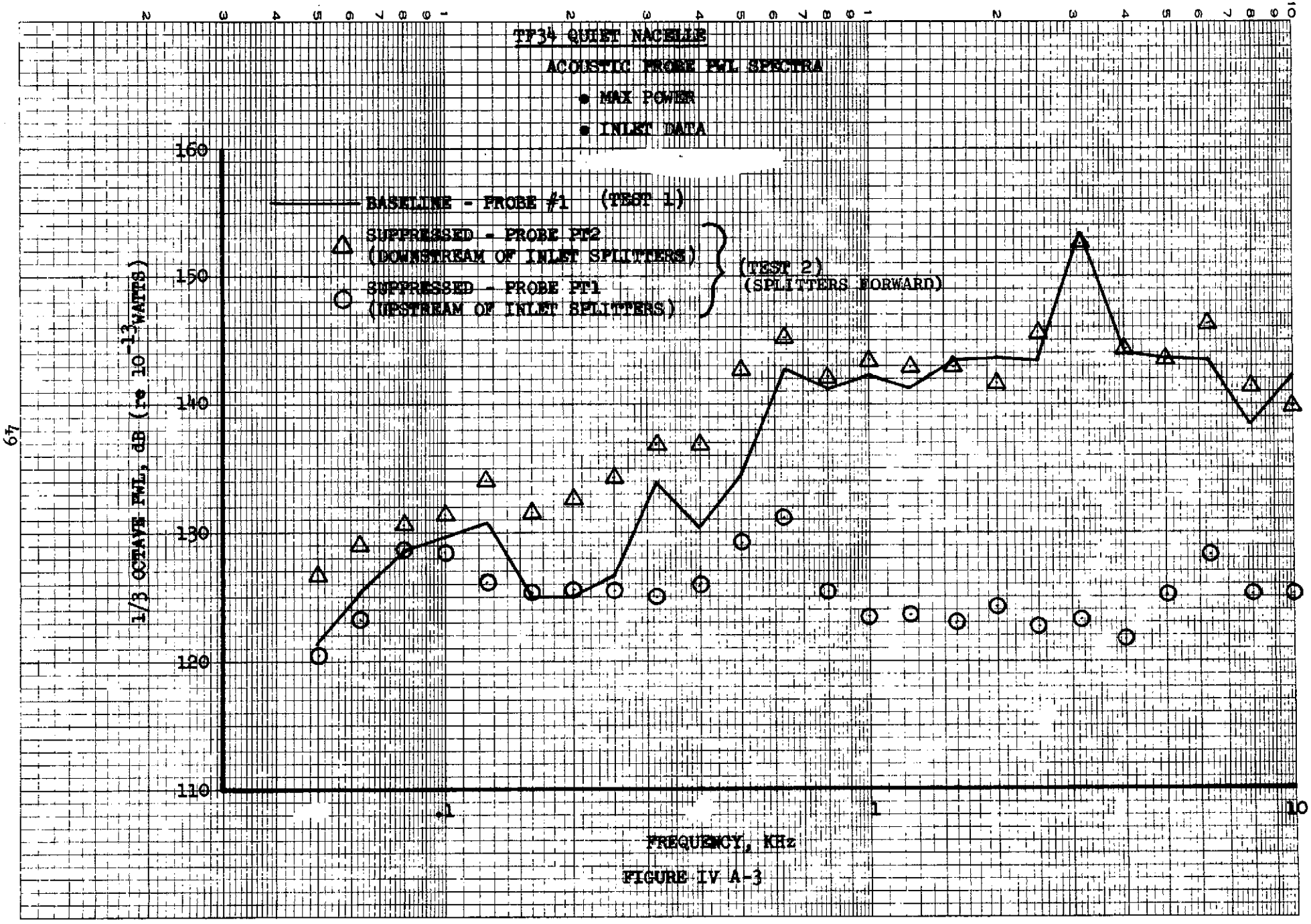

FIGURE IV A-3

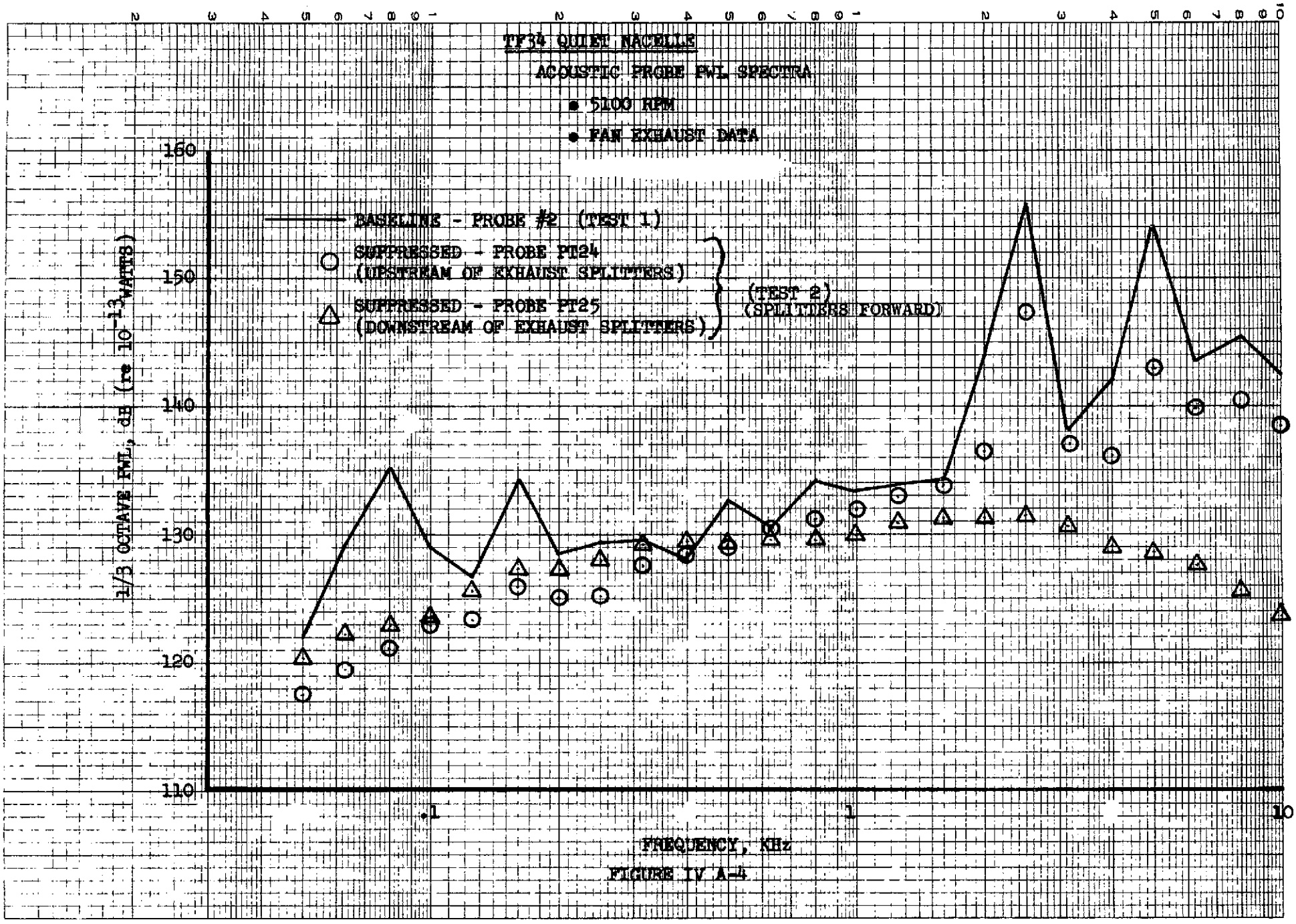

FIGURE IV A-4

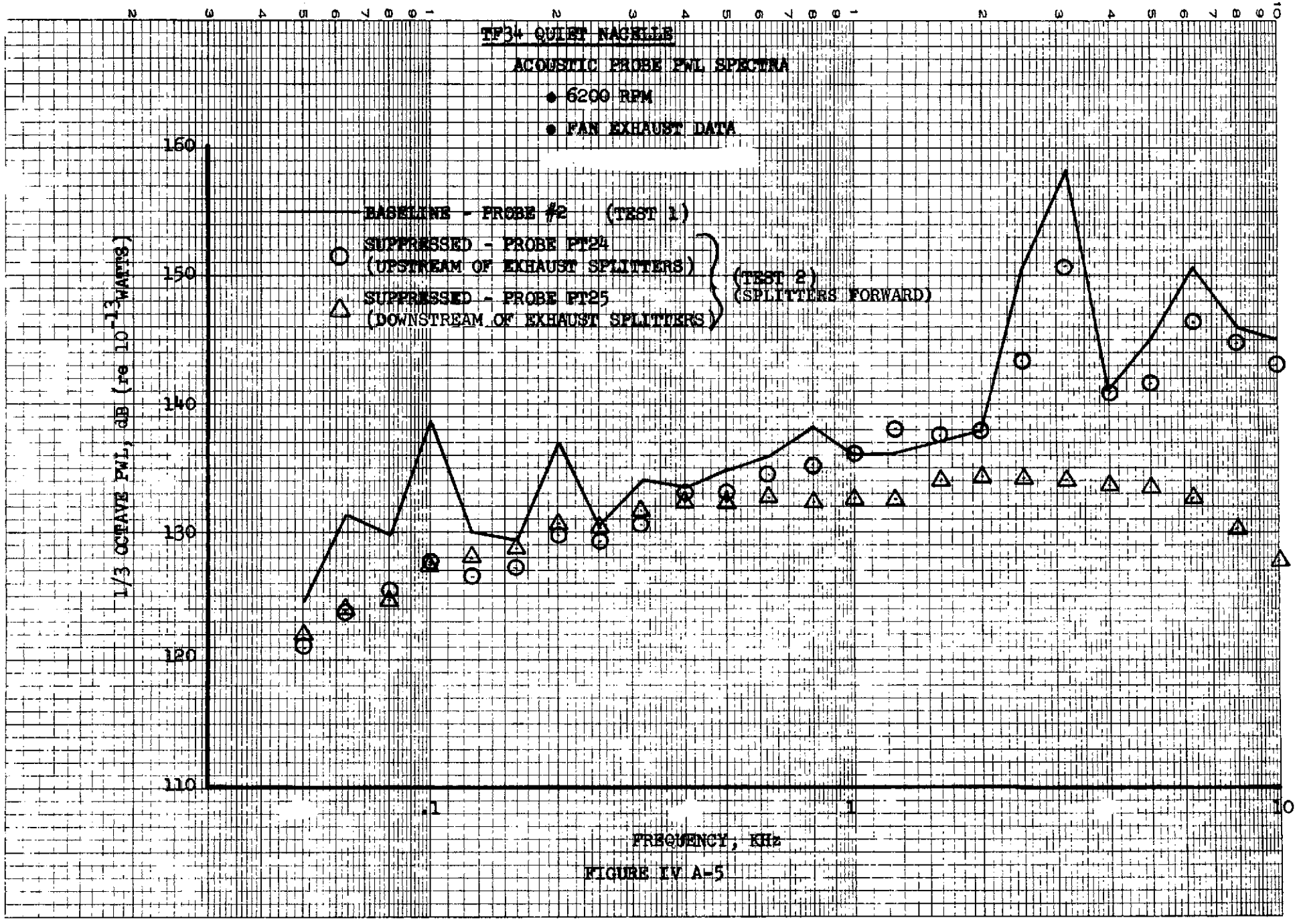

FIGURE IV A-5

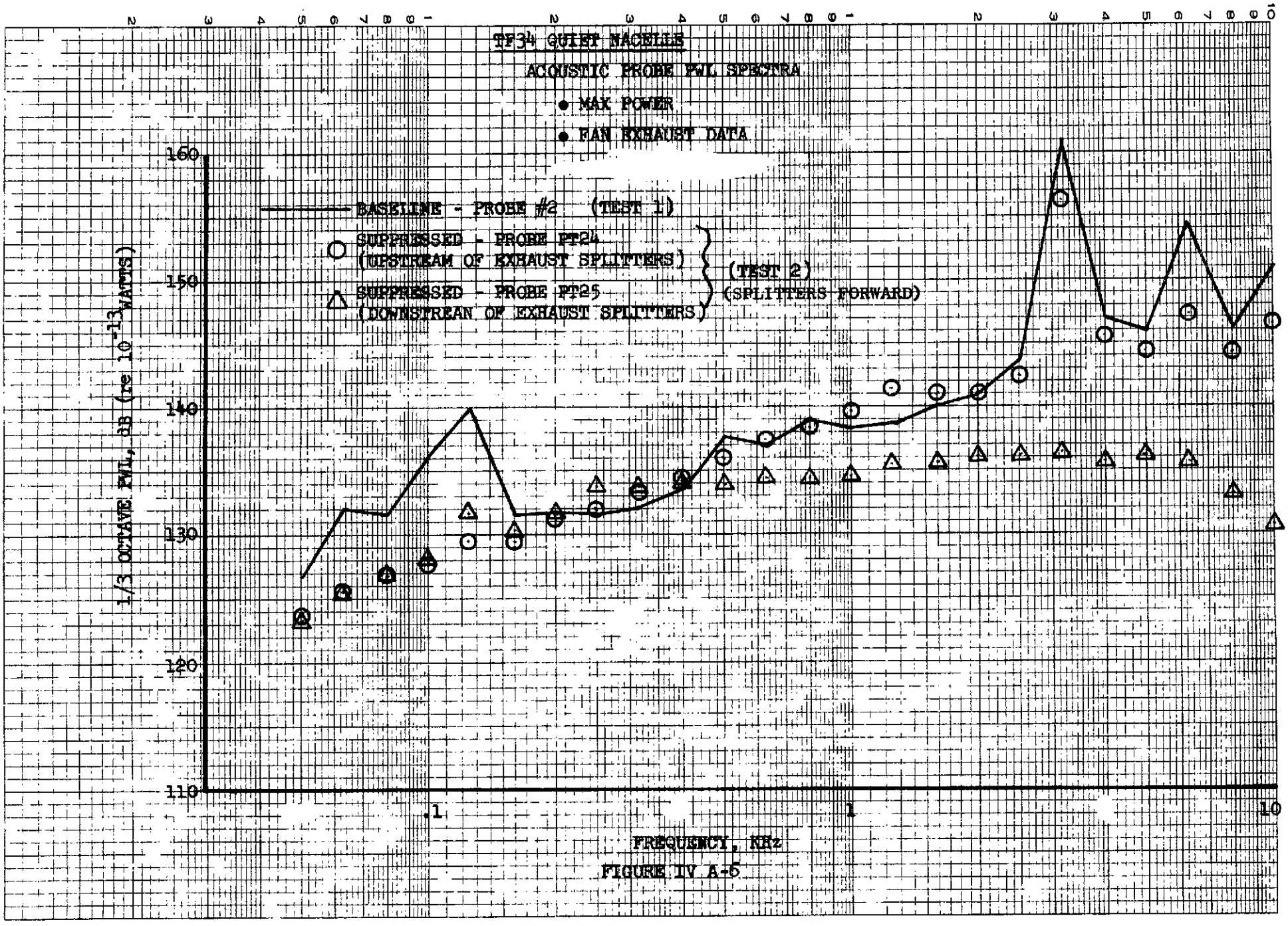

FIGURE IV A-5

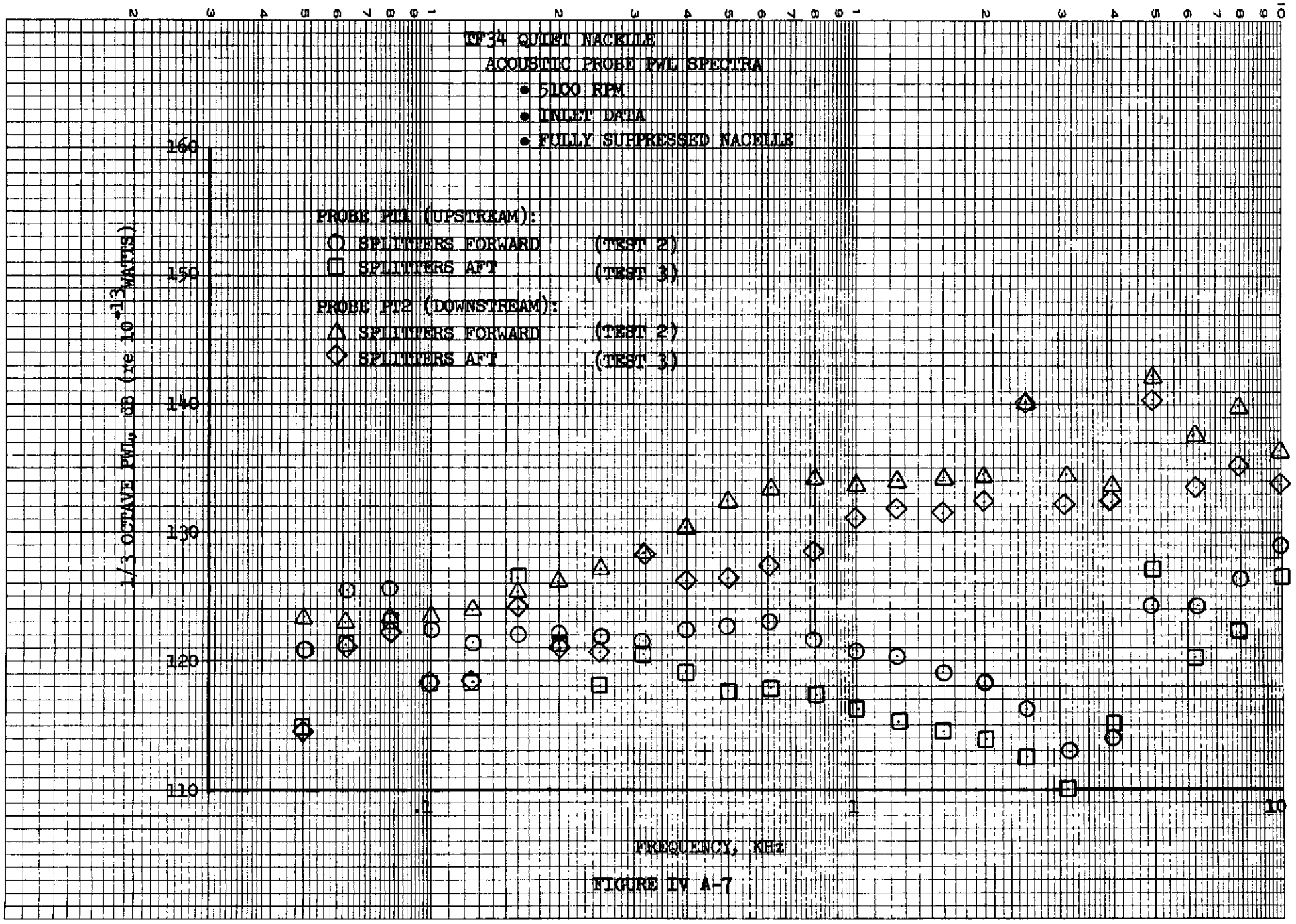

FIGURE IV A-7

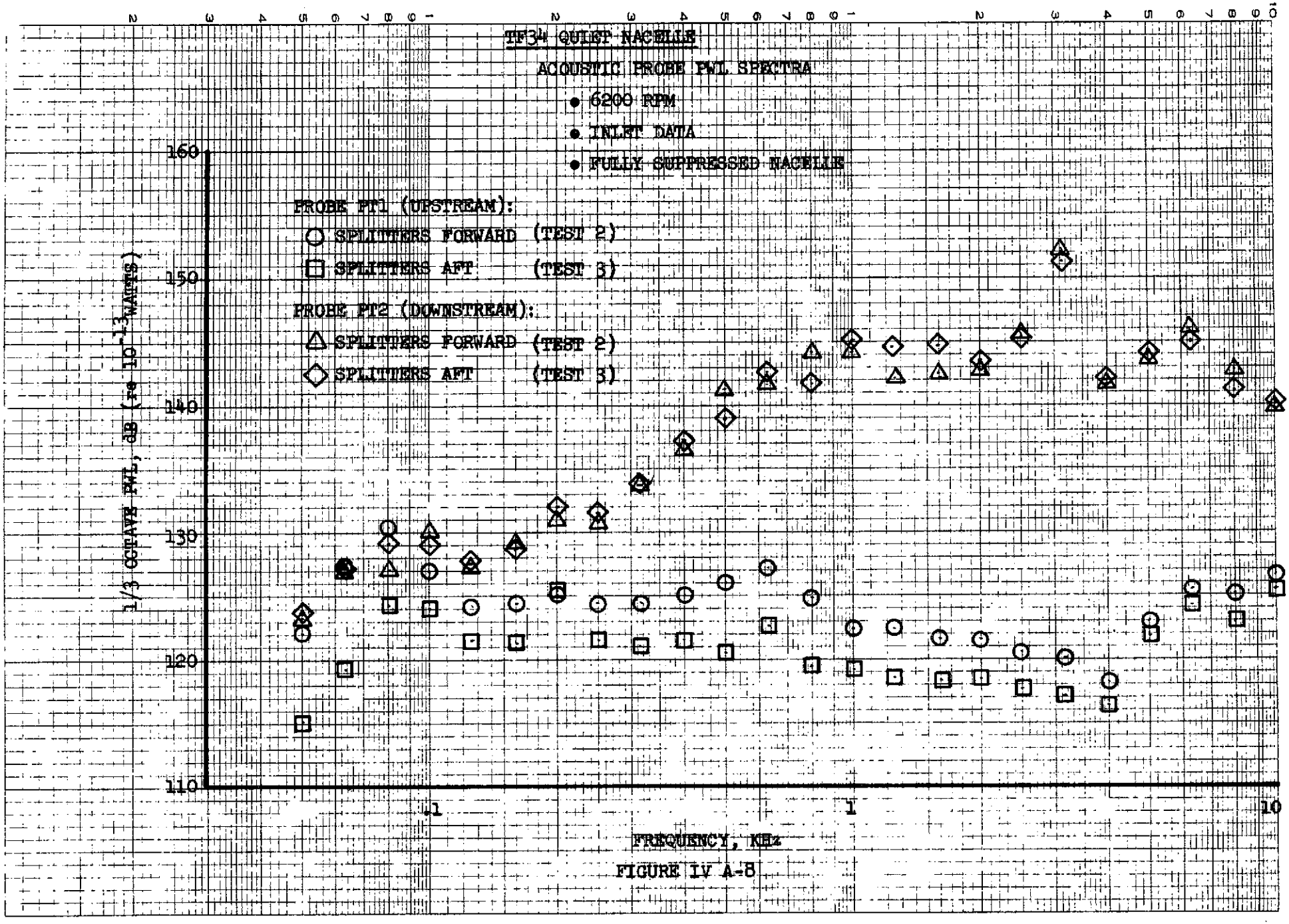

FIGURE IV A-8

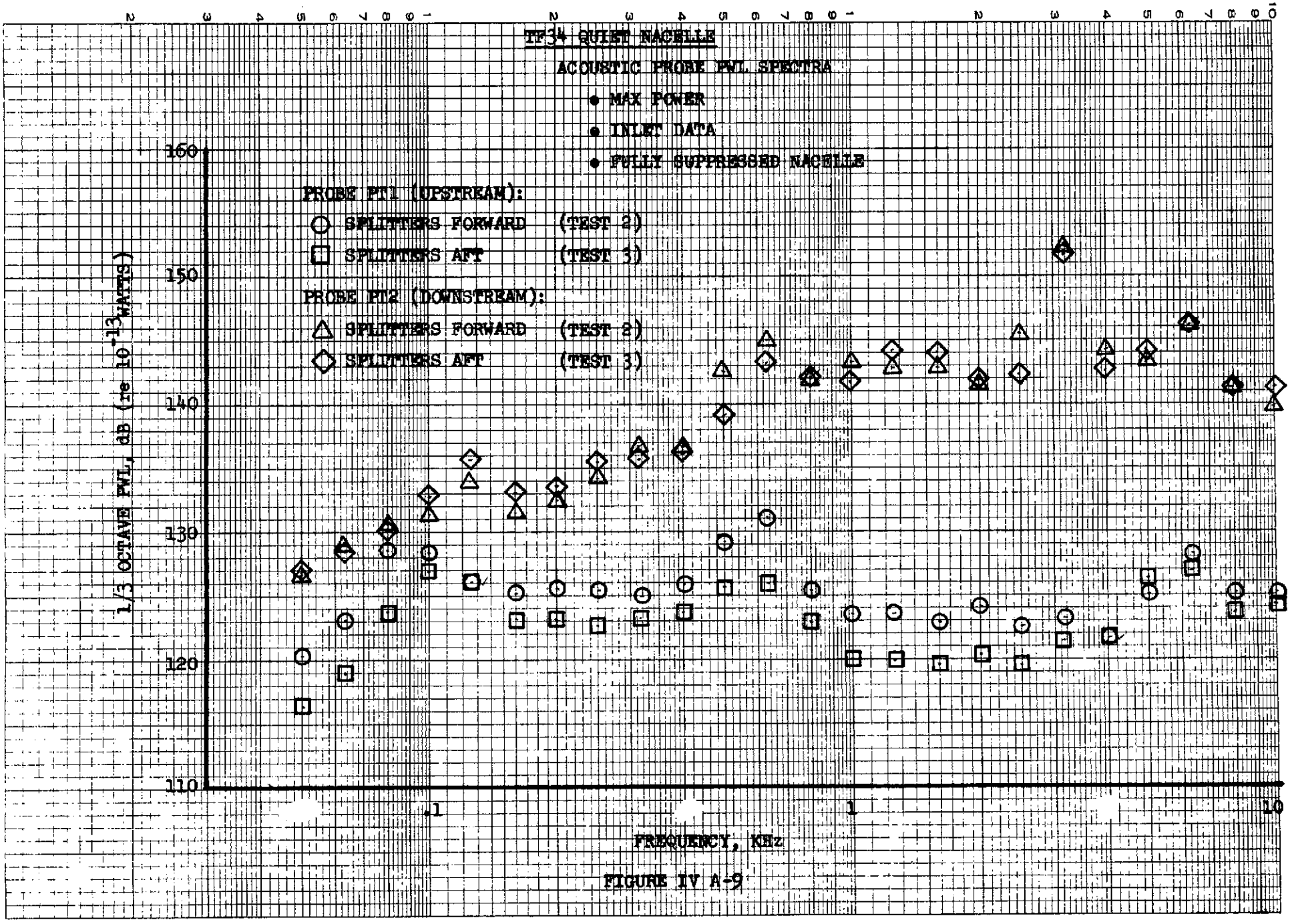

FIGURE IV A-9

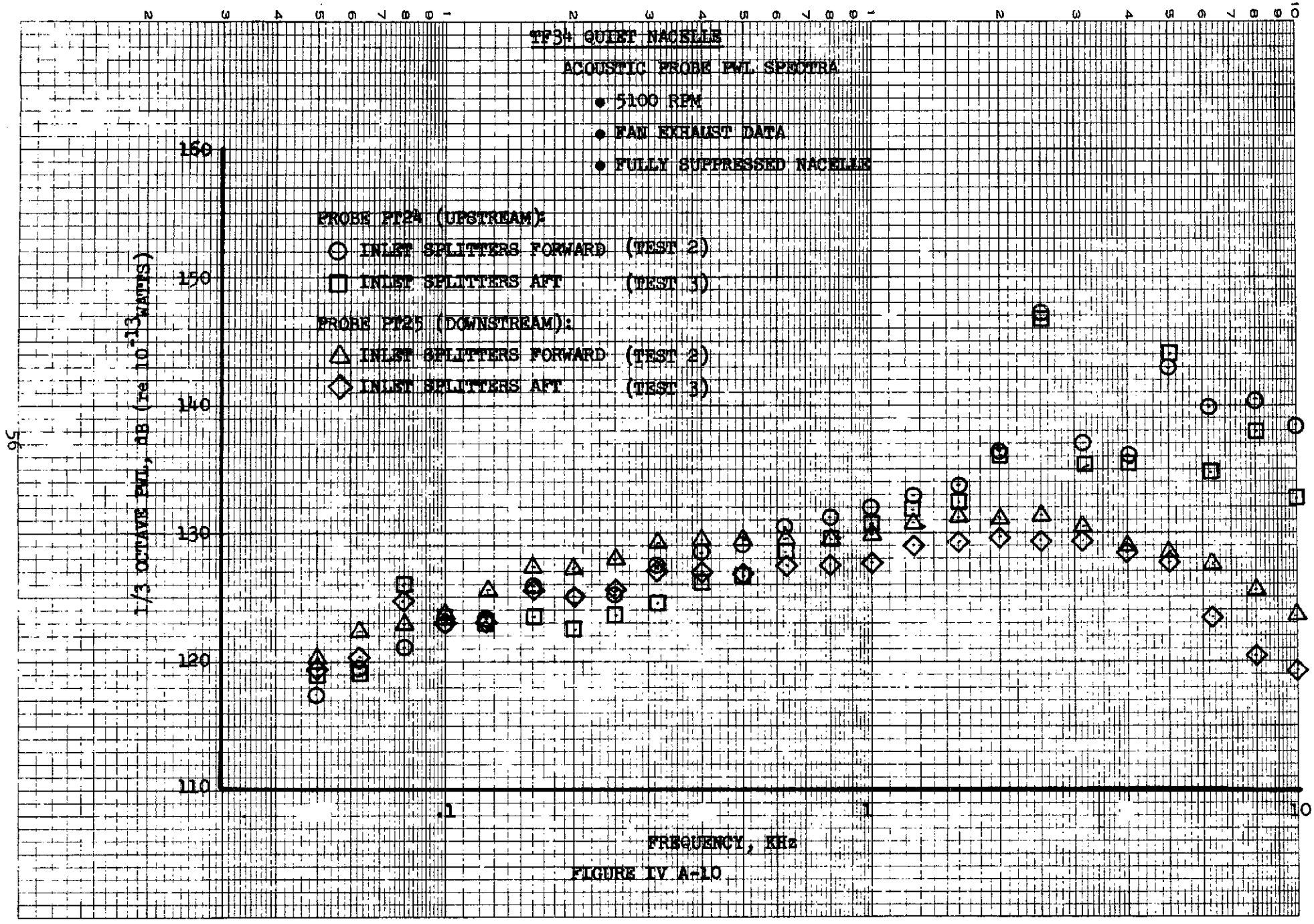

FIGURE IV A-10

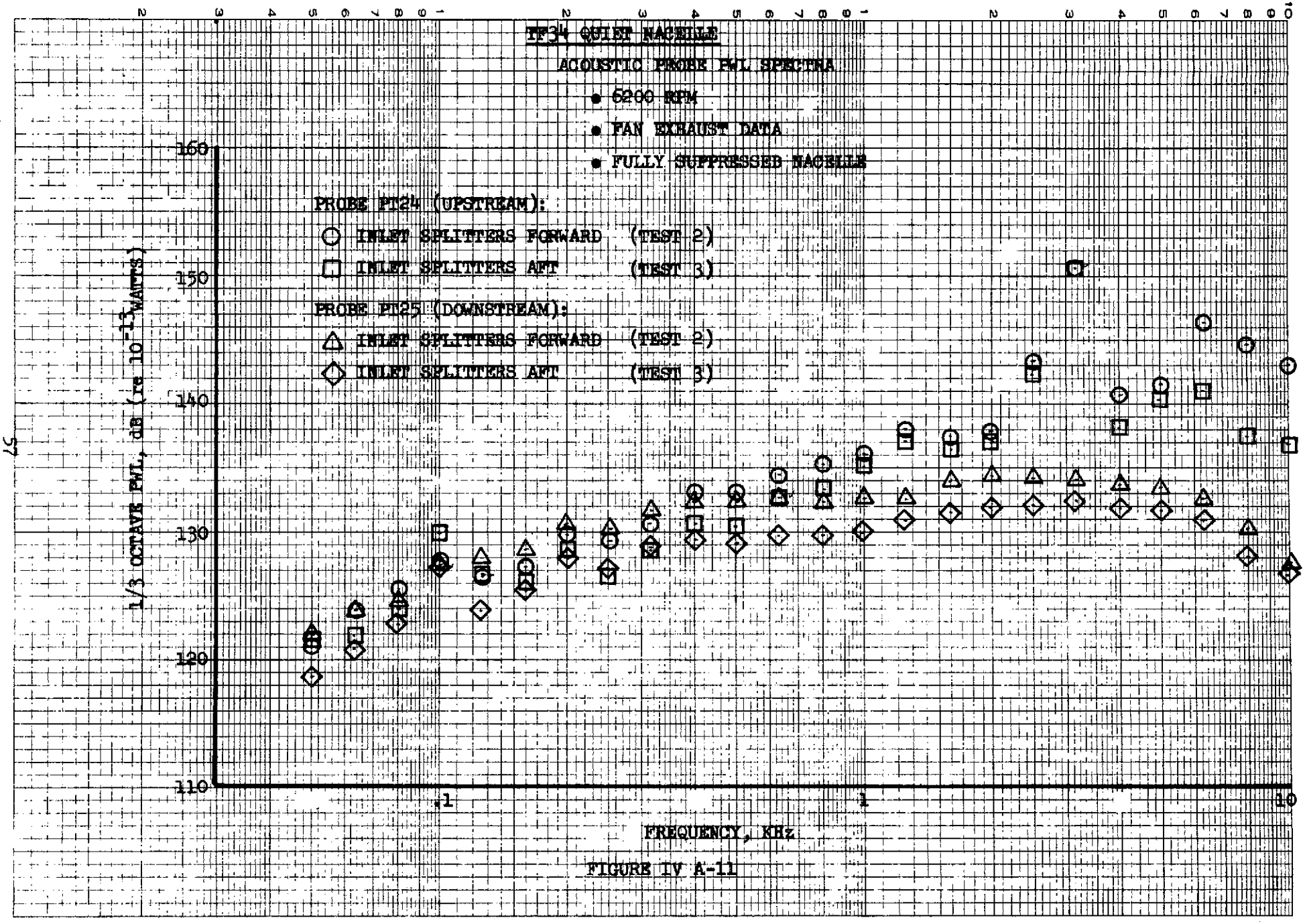

FIGURE IV A-11

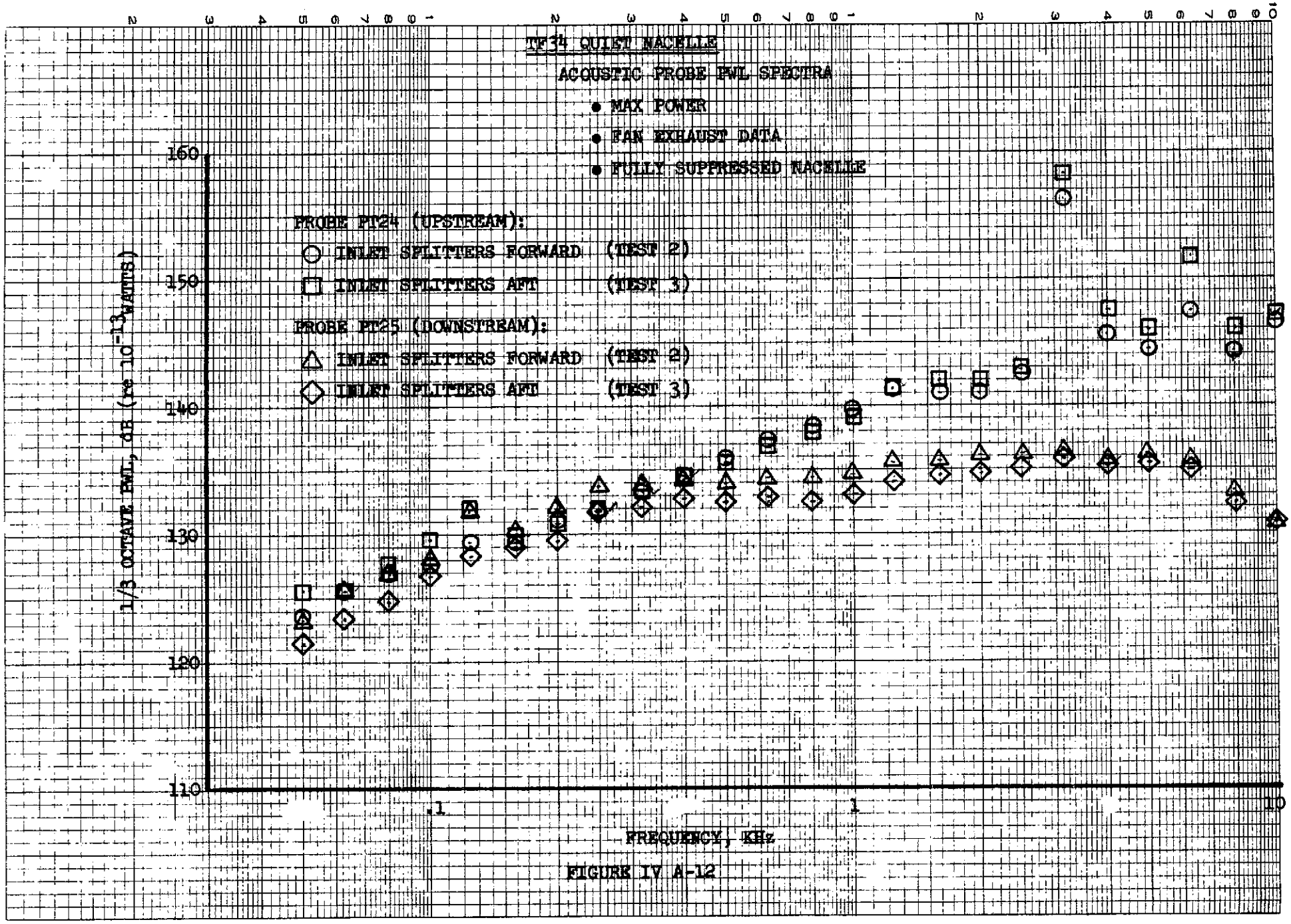

FIGURE IV A-12

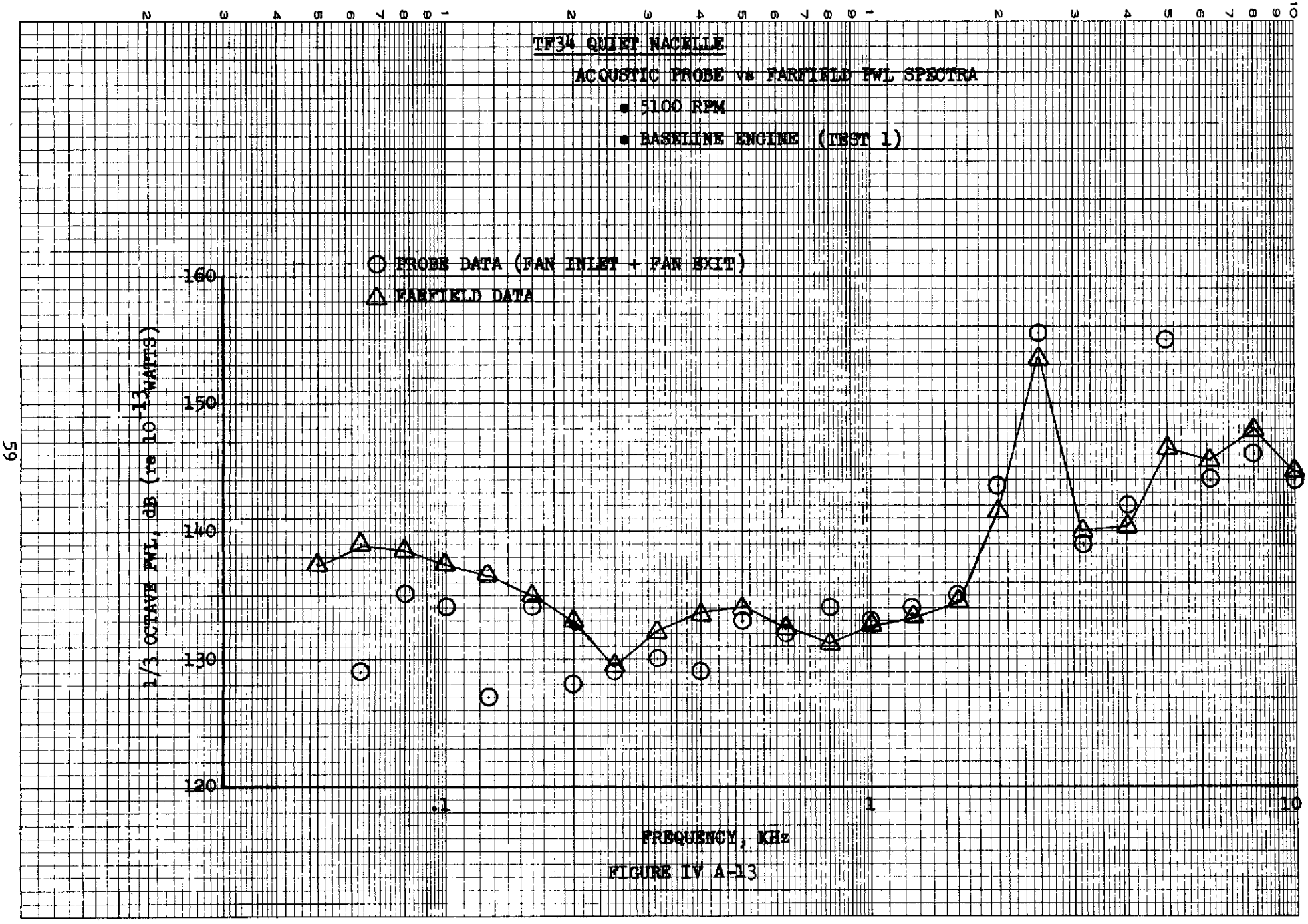

FIGURE IV A-13

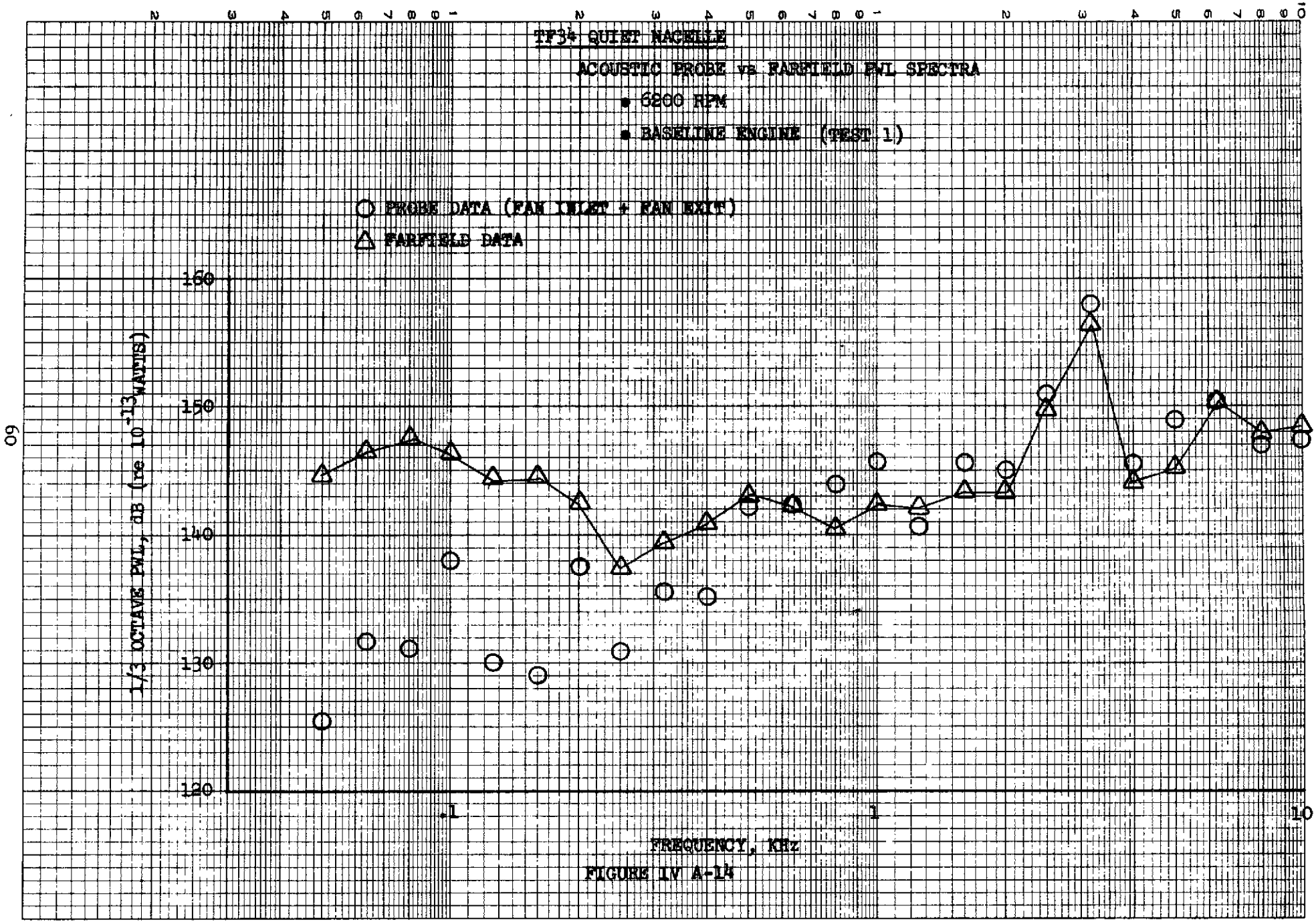

FIGURE IV A-14

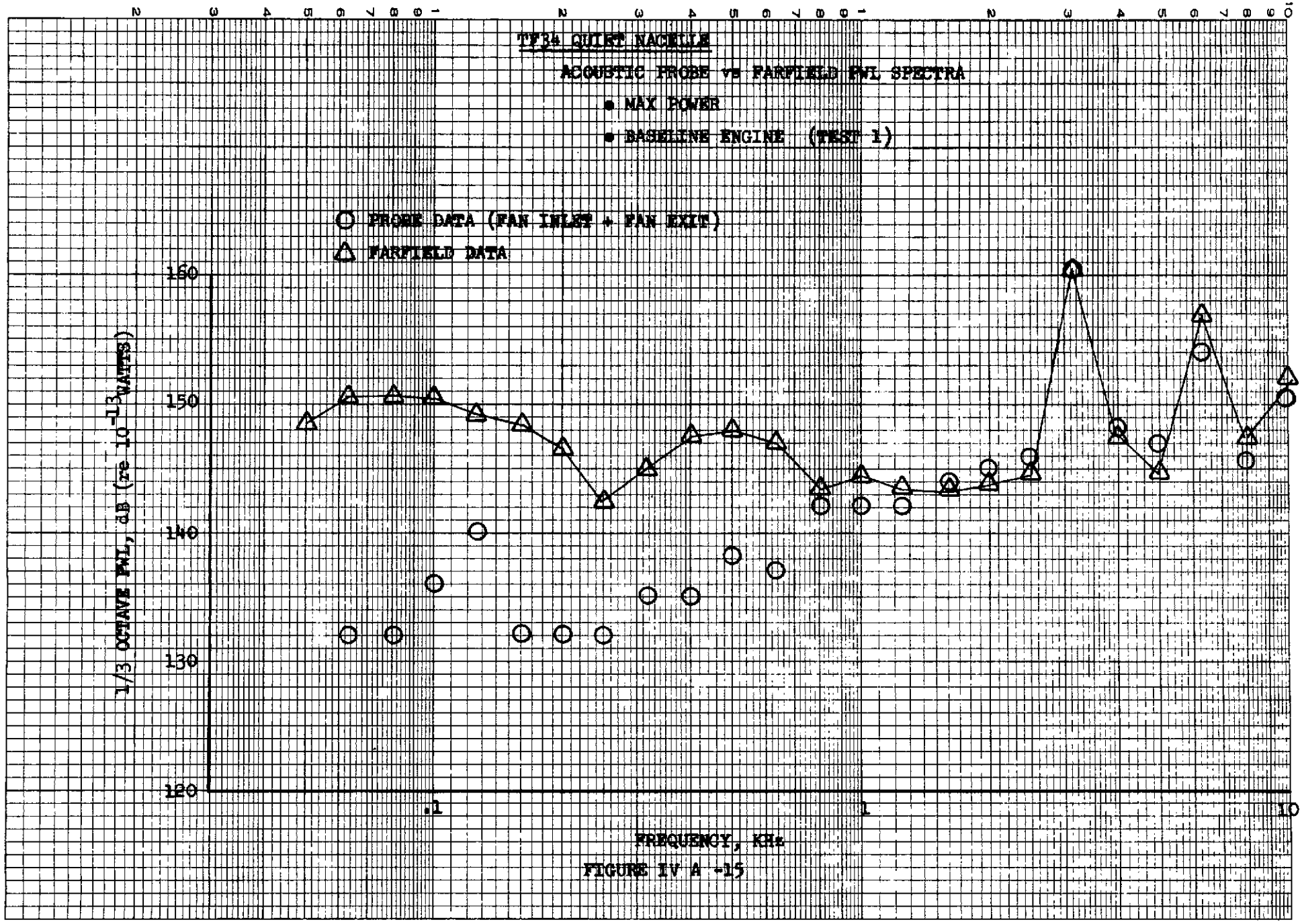

FIGURE IV A -15

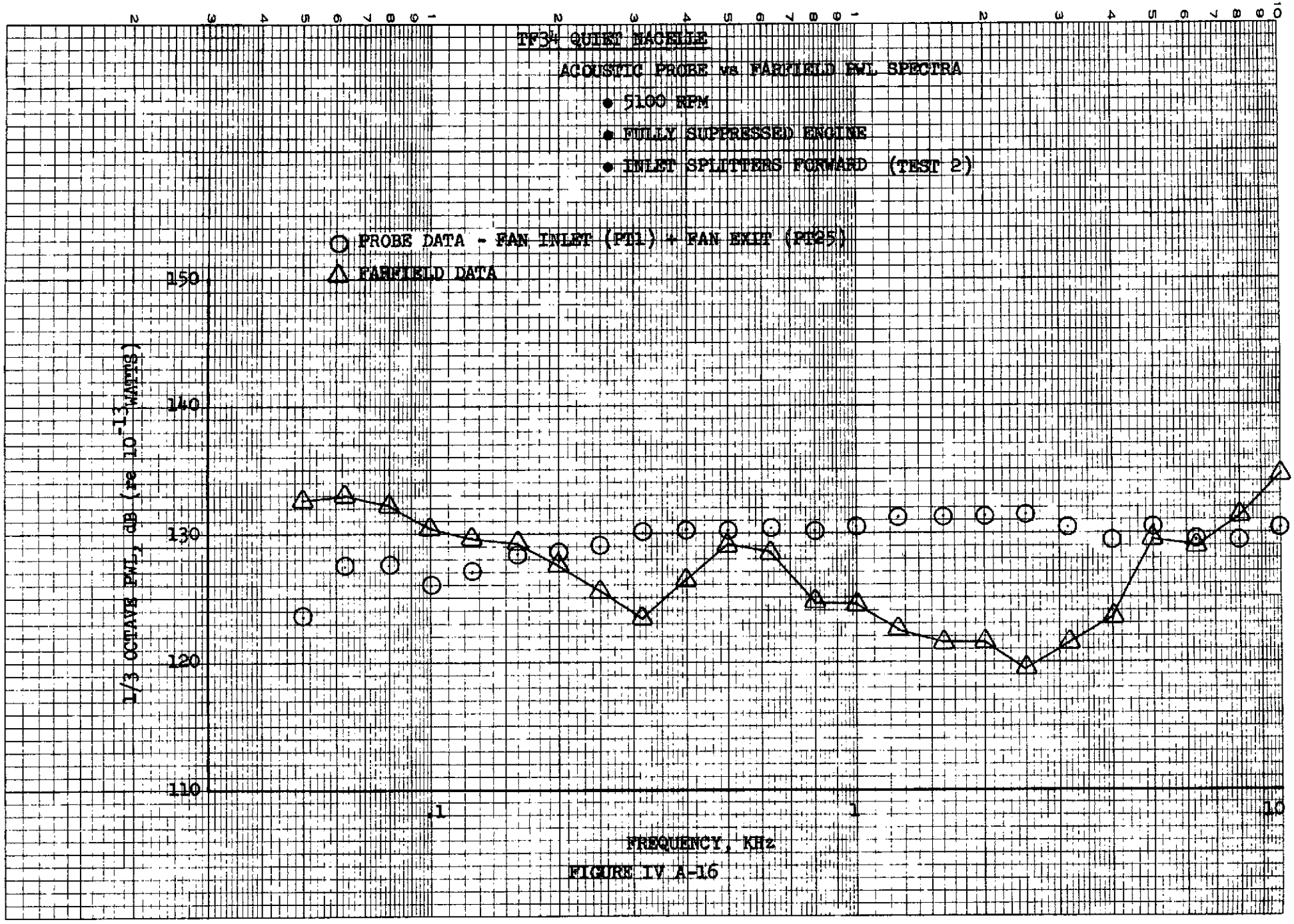

FIGURE IV A-16

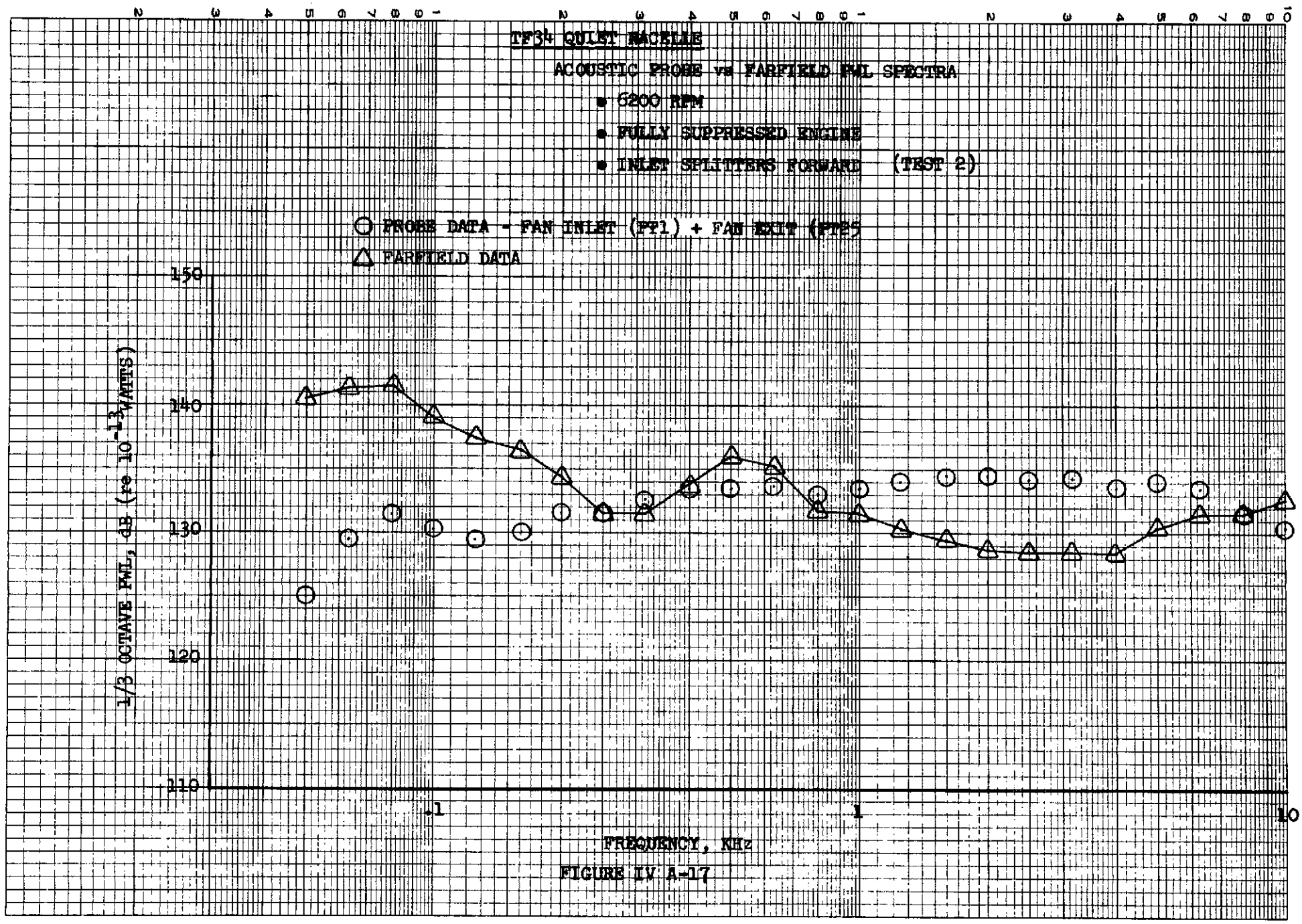

FIGURE IV A-17

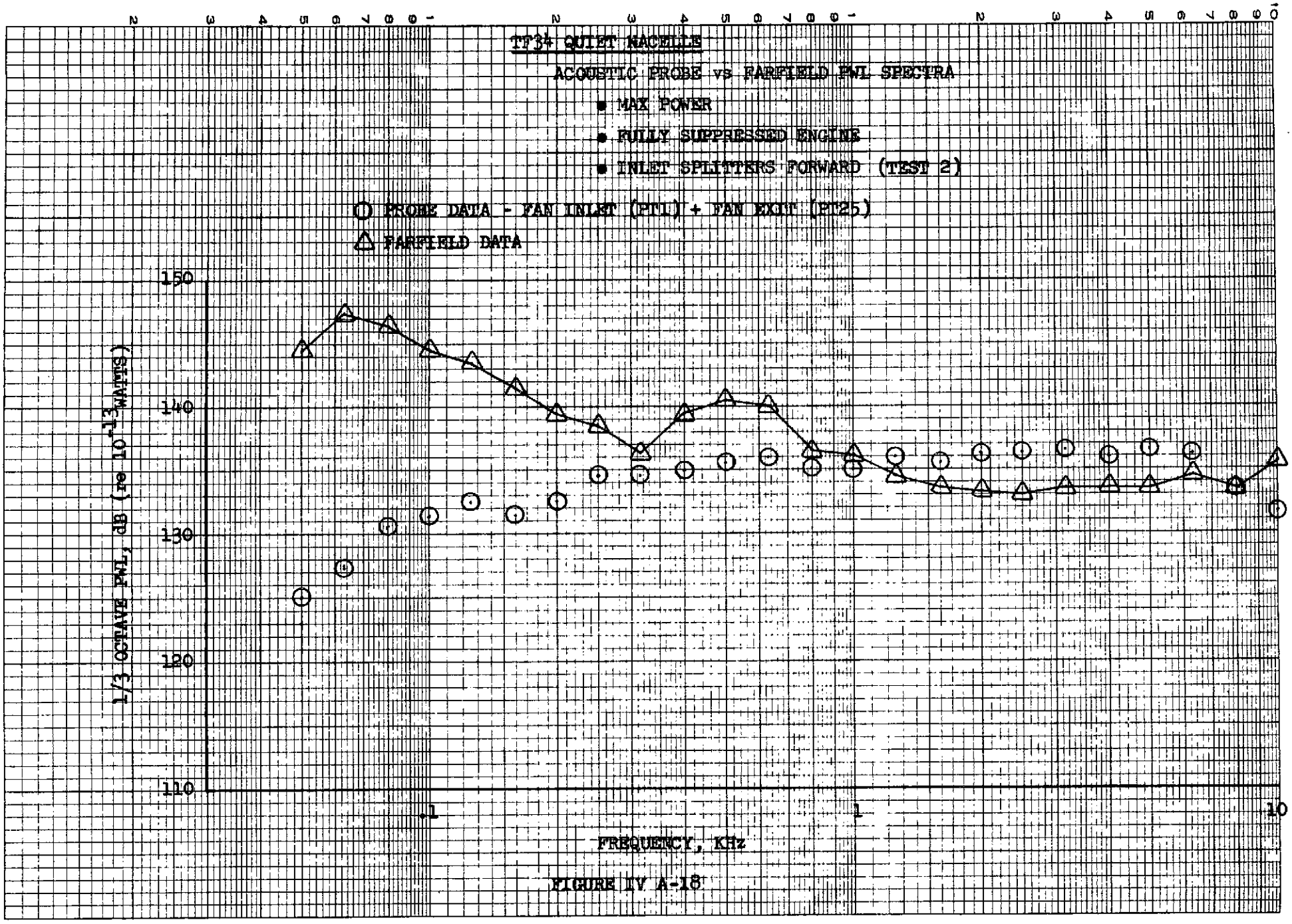

FIGURE IV A-18

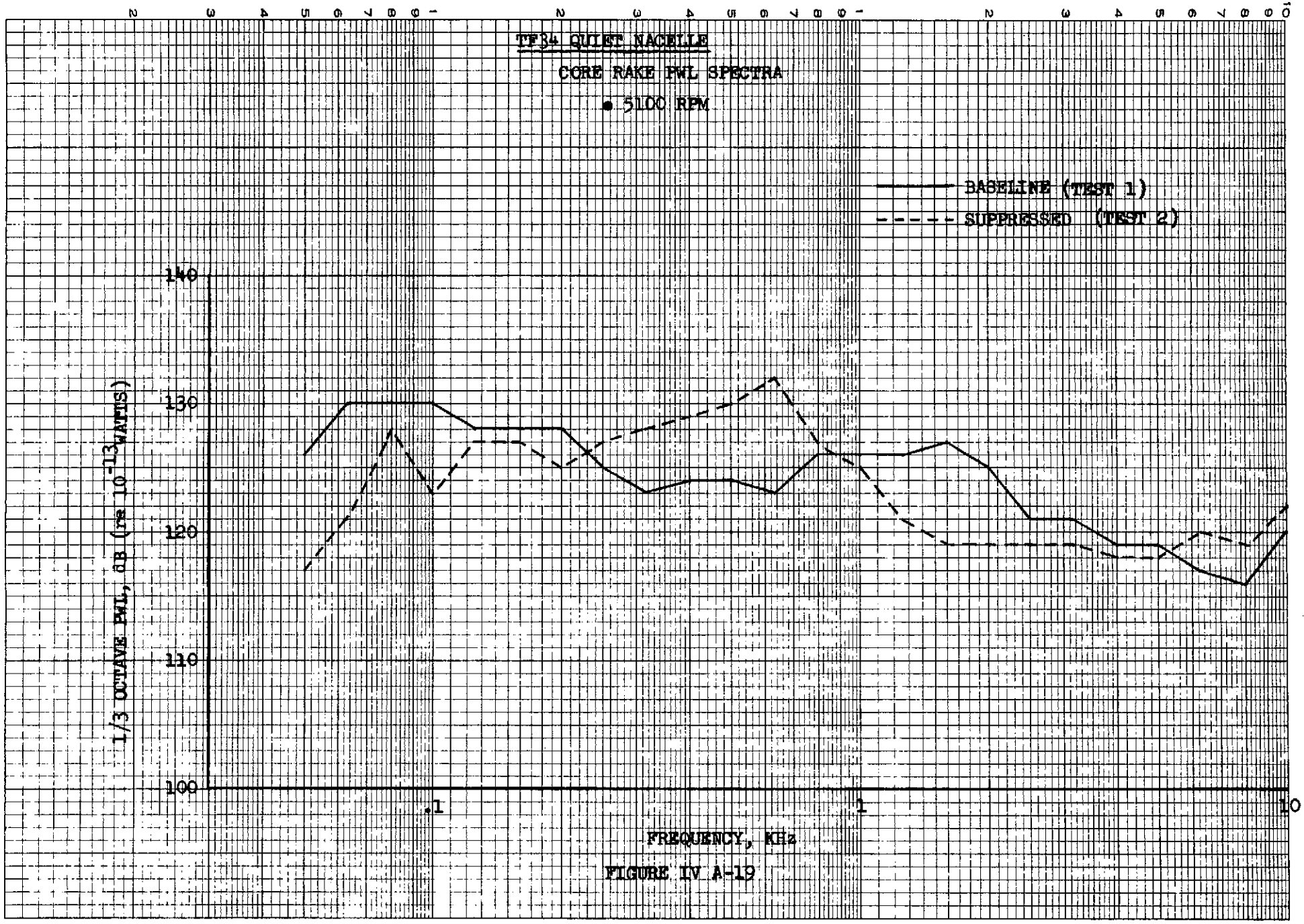

FIGURE IV A-19

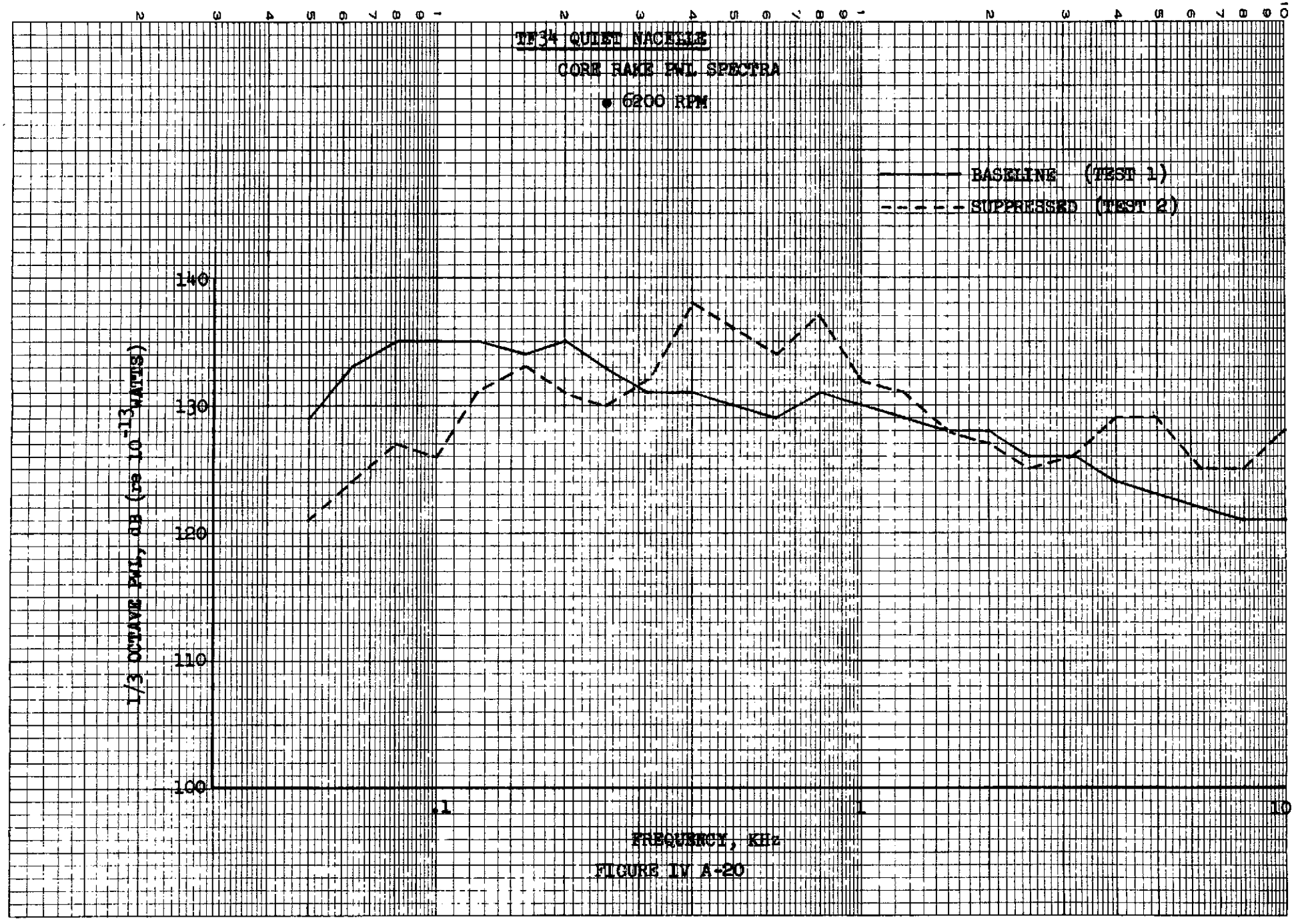

FIGURE IV A-20

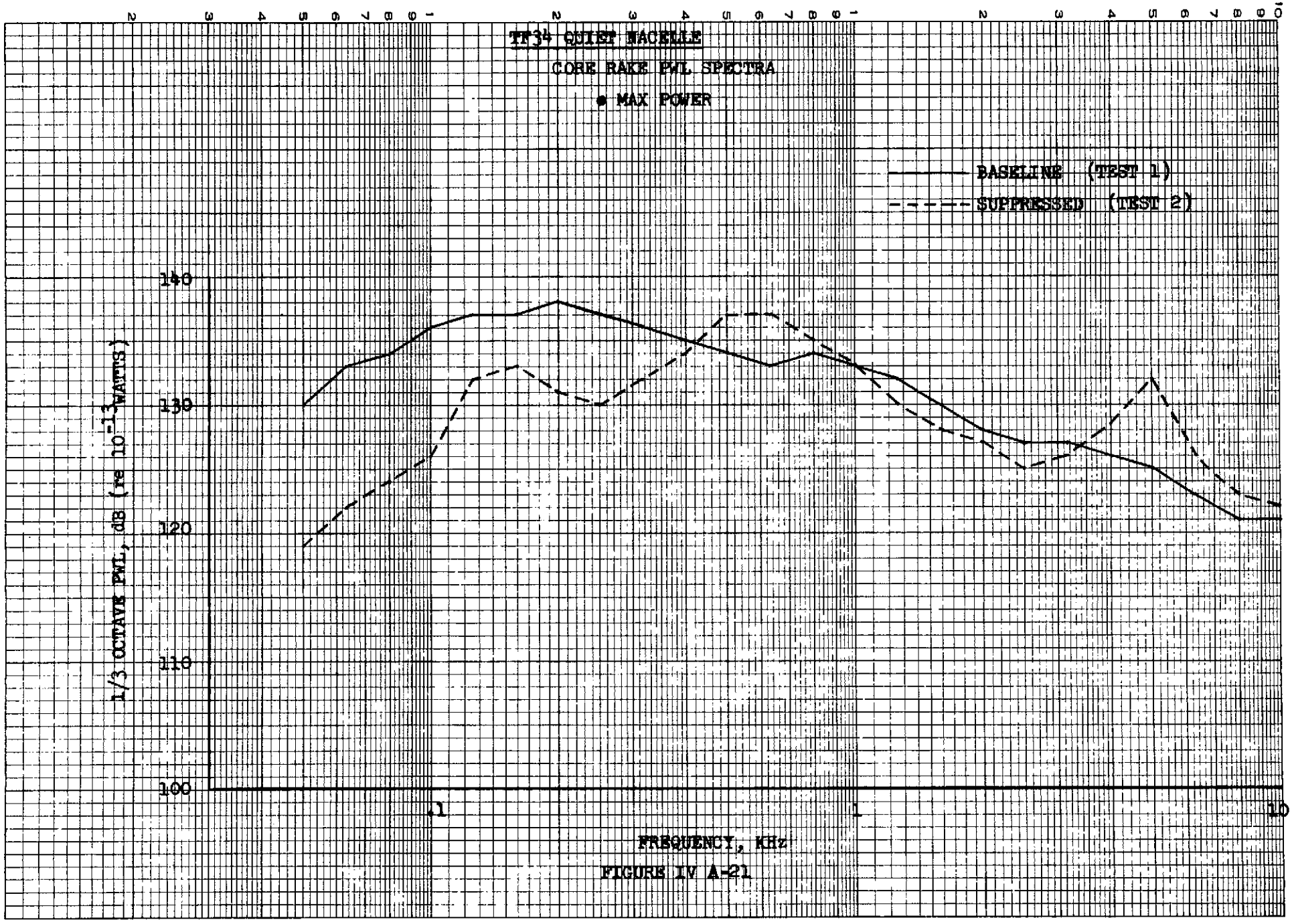

FIGURE IV A-21

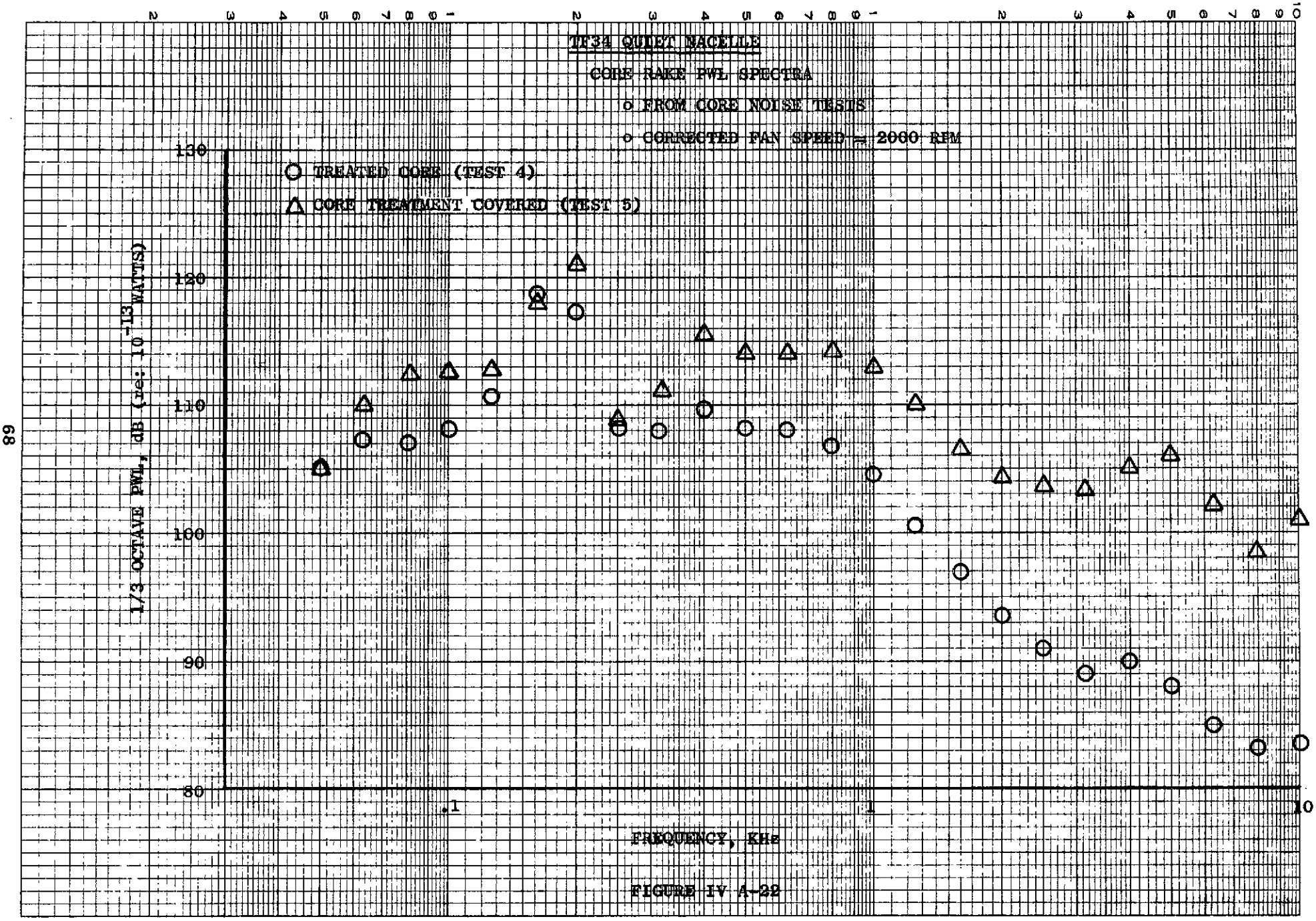

FIGURE IV A-22

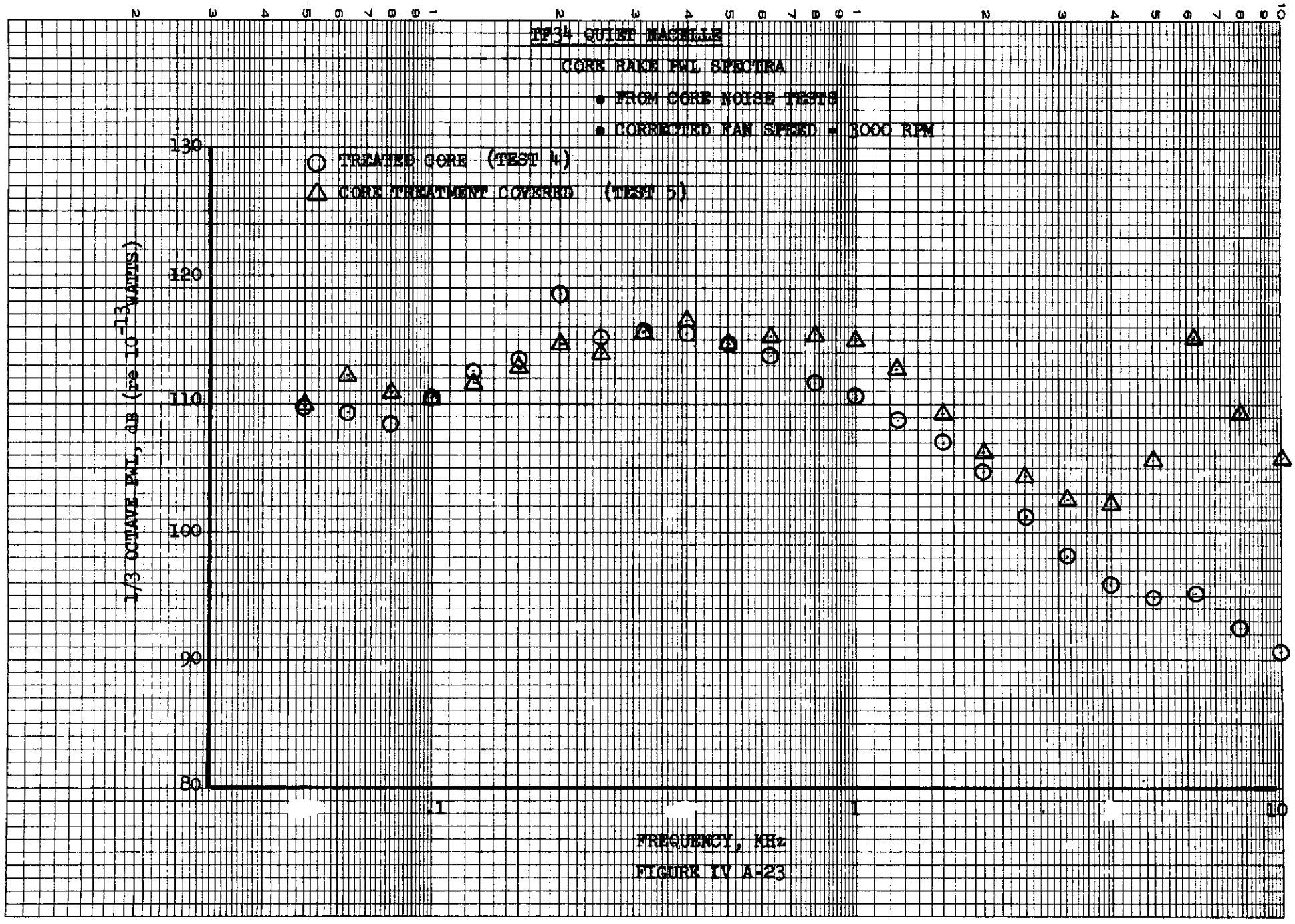

FIGURE IV A-23

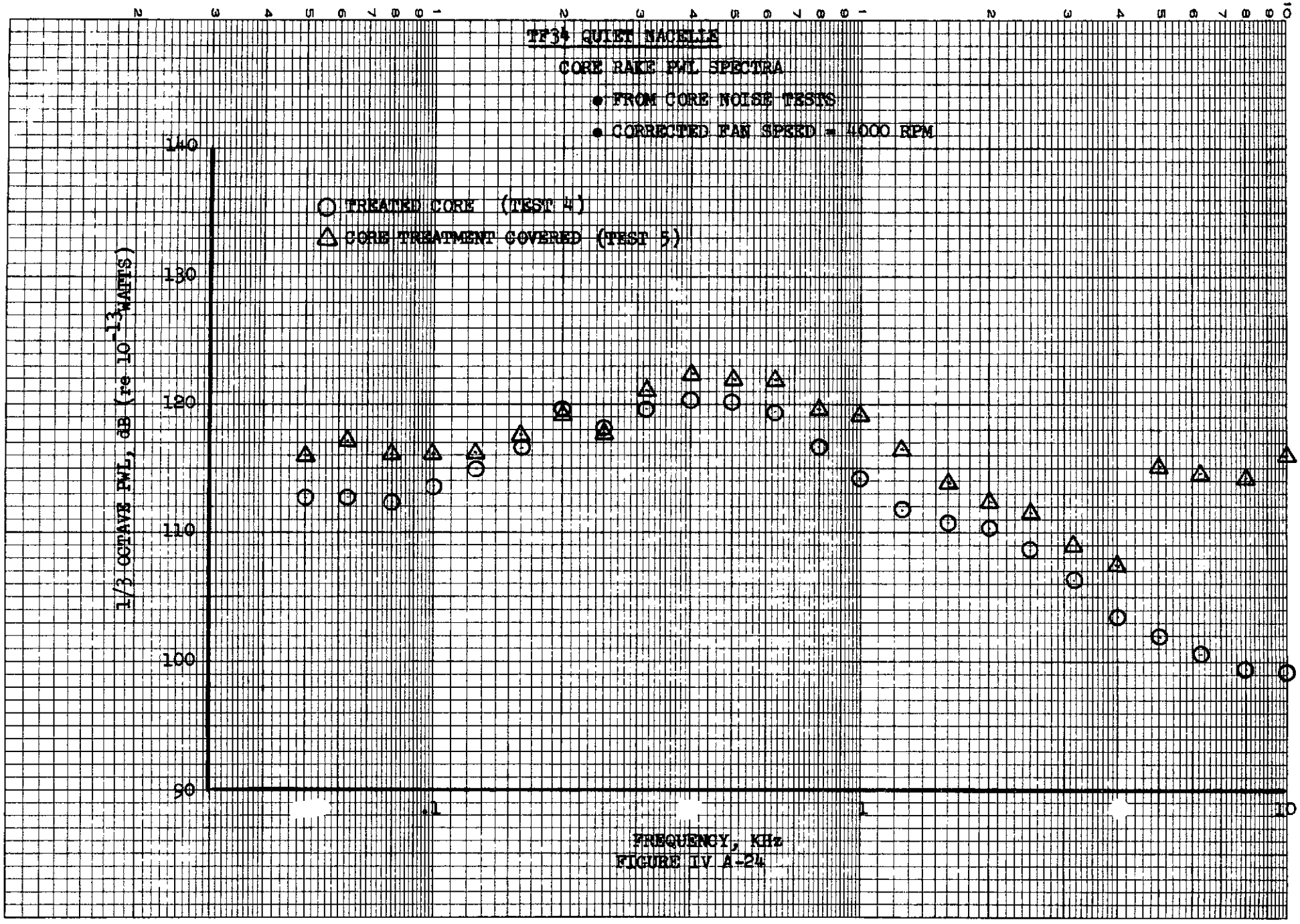

FIGURE IV A-24

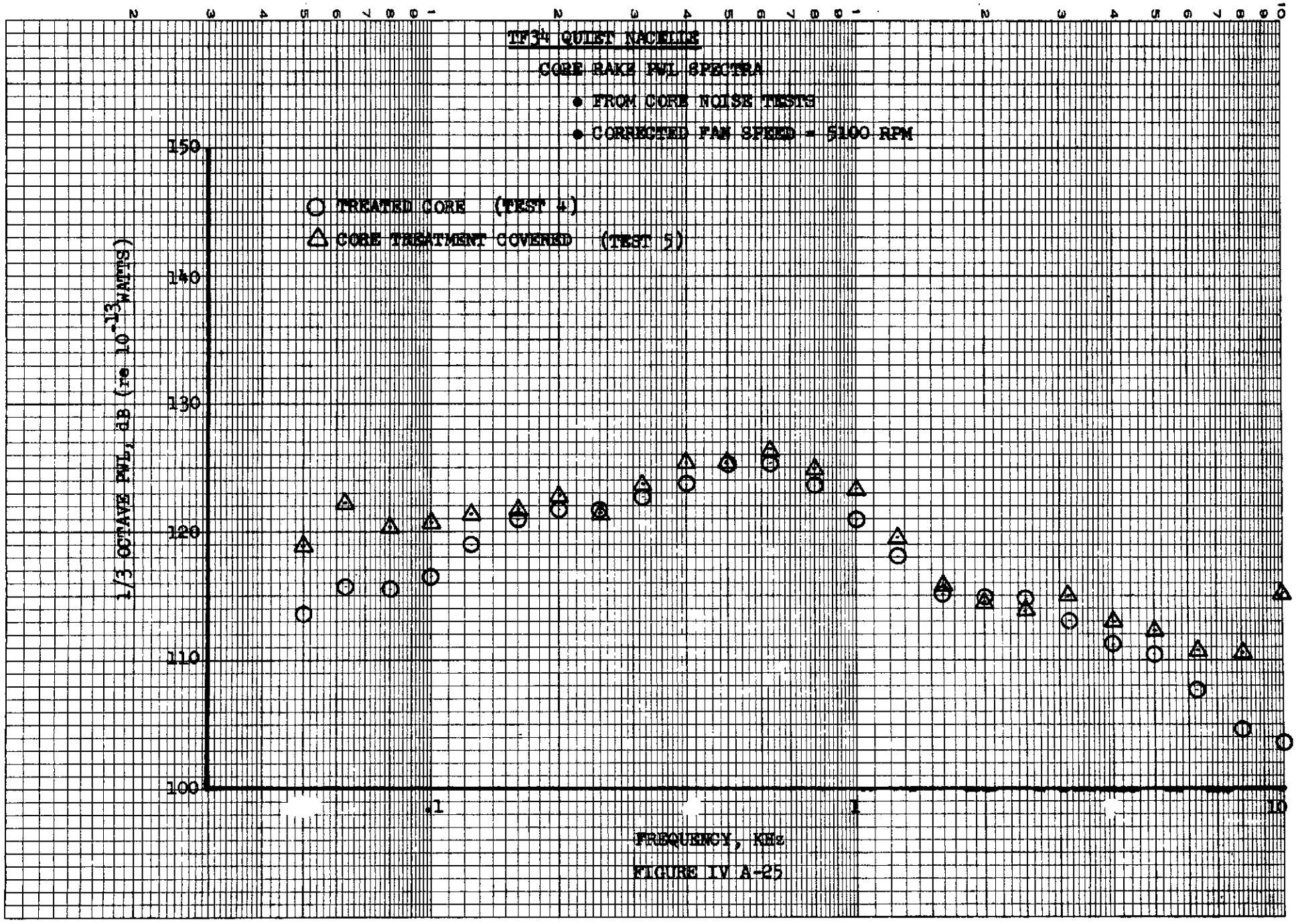

FIGURE IV A-25

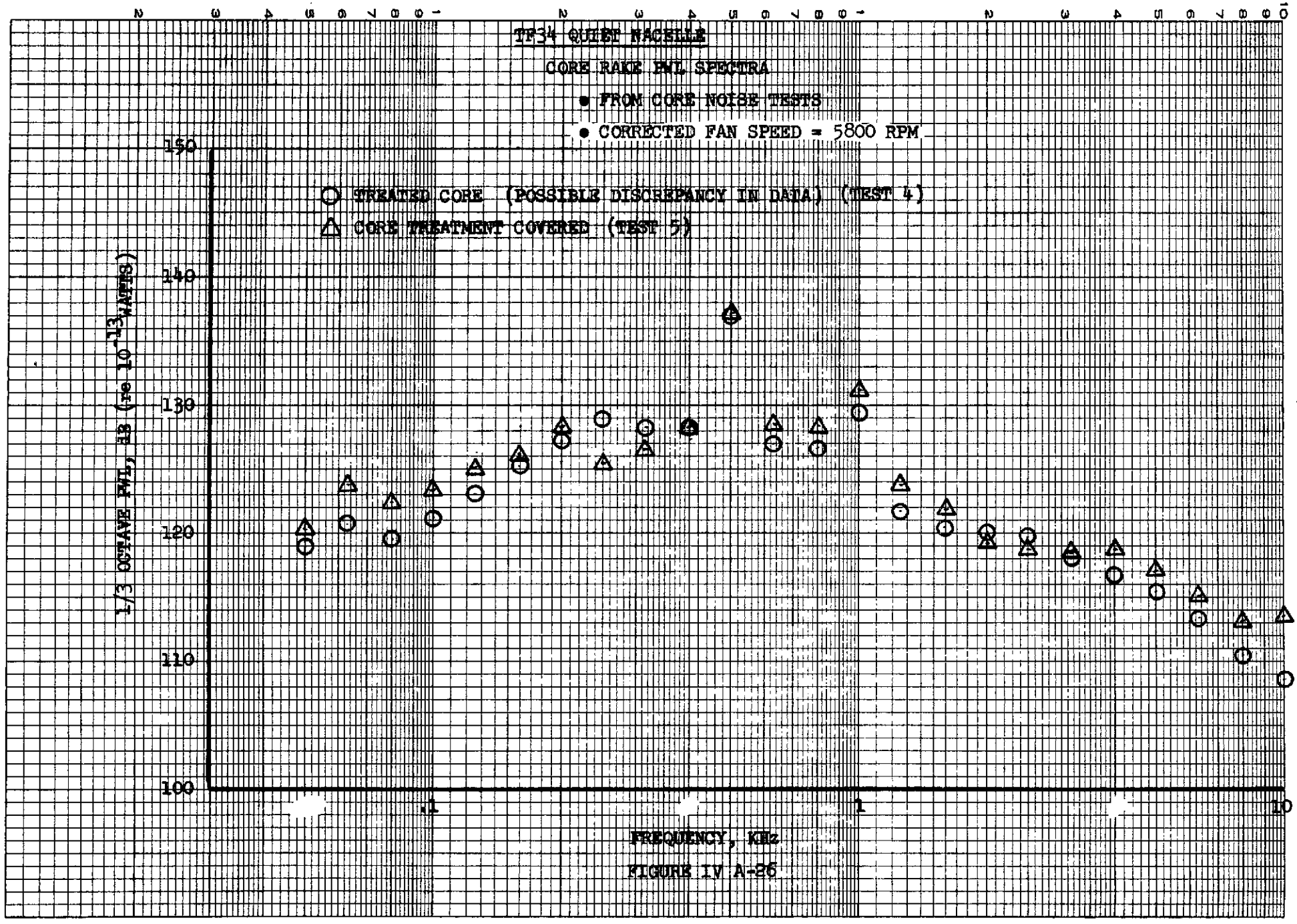

FIGURE IV A-26

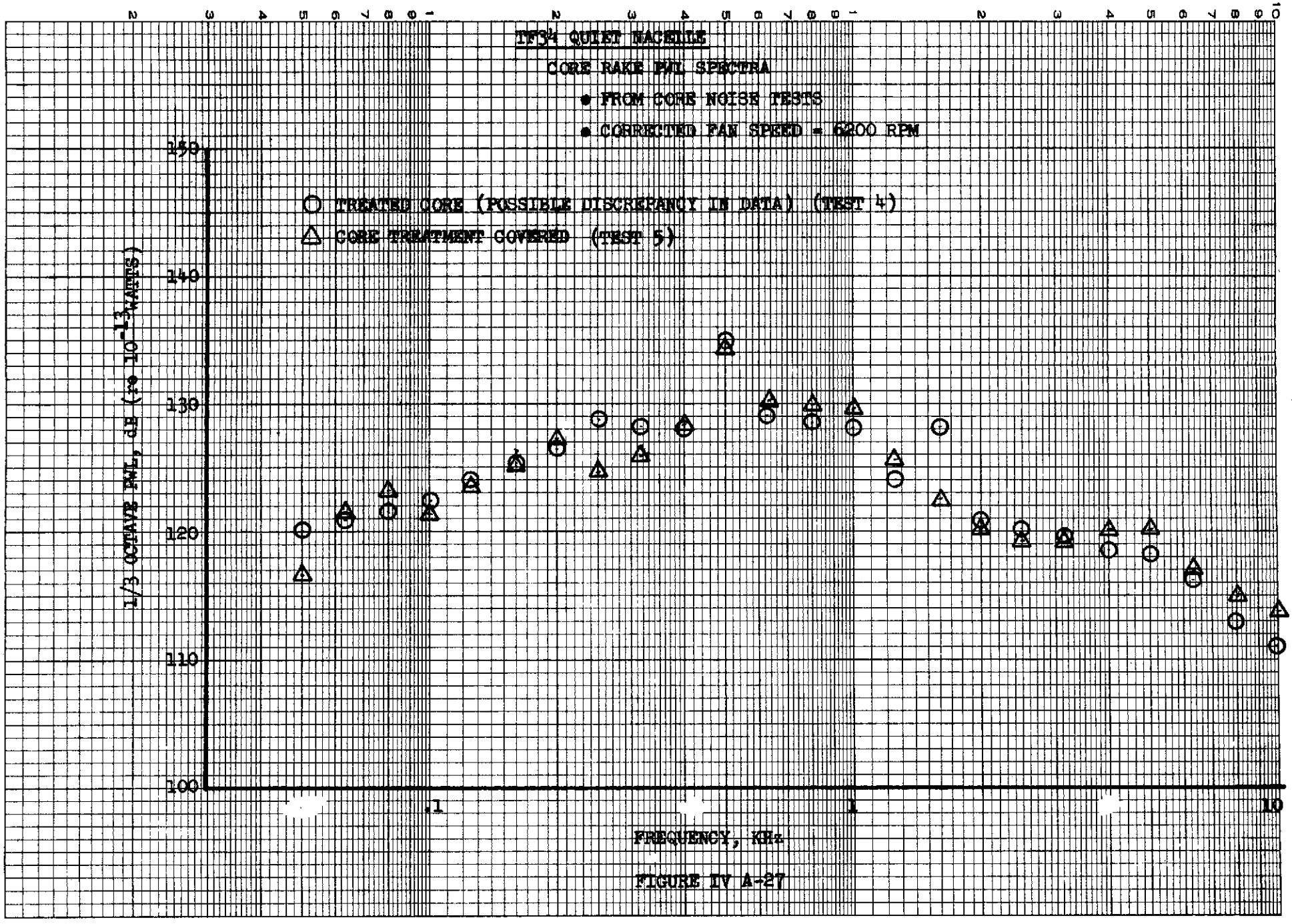

FIGURE IV A-27

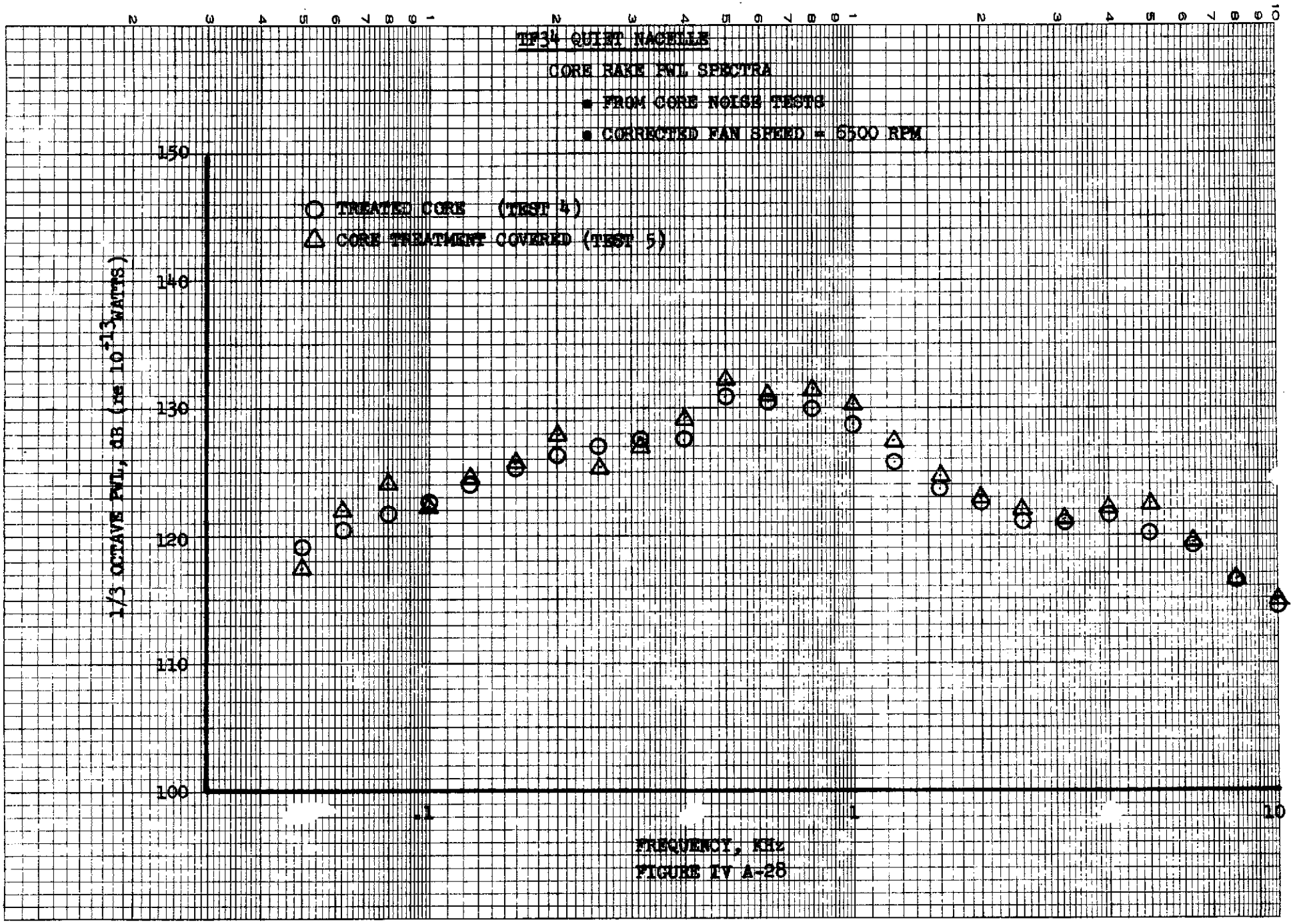

FIGURE IV A-28

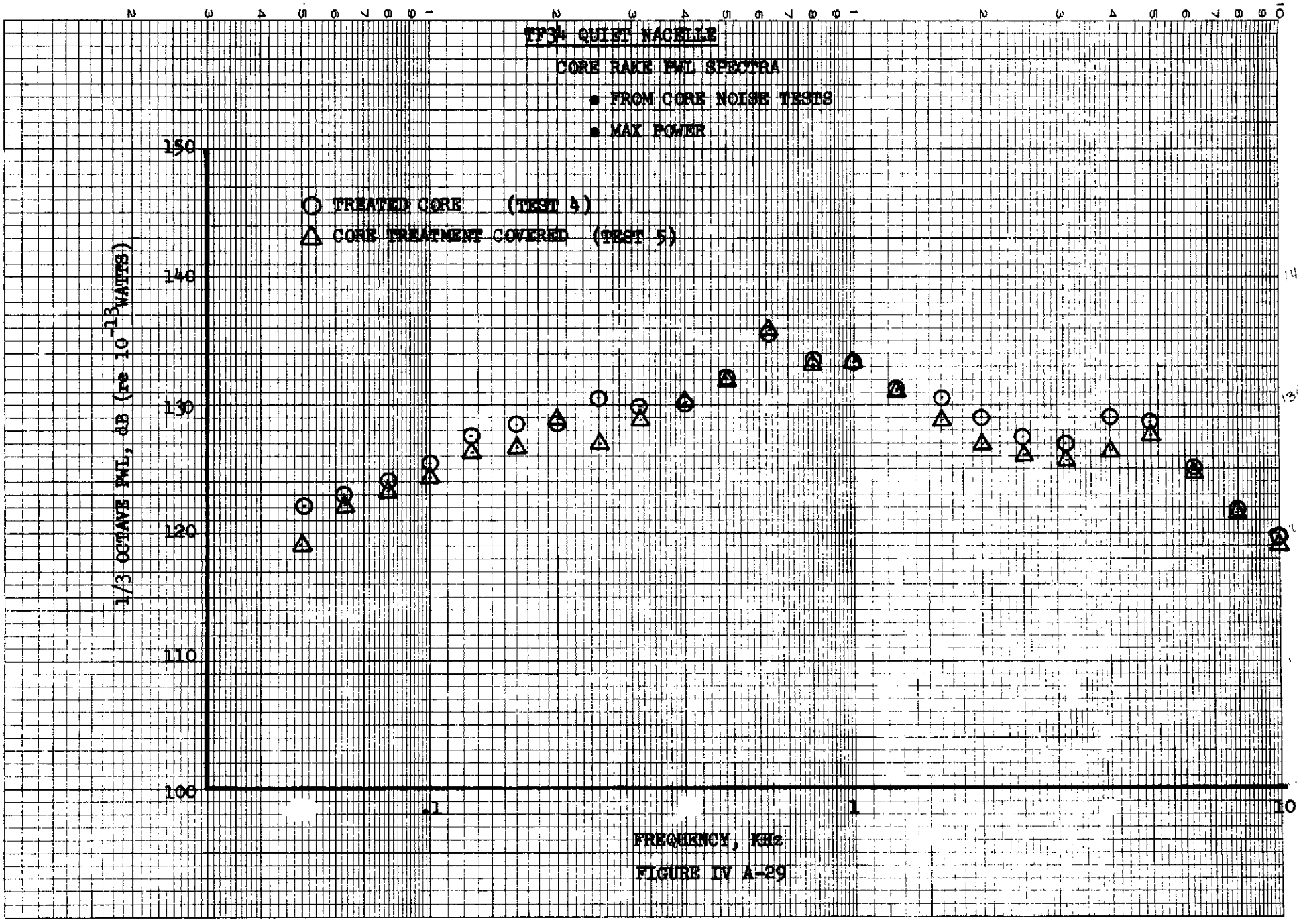

FIGURE IV A-29

FIGURE IV A-30

TF34 INLET SOUND POWER SOURCE PROFILE

- FAN FUNDAMENTAL FREQUENCY
- 5100 RPM

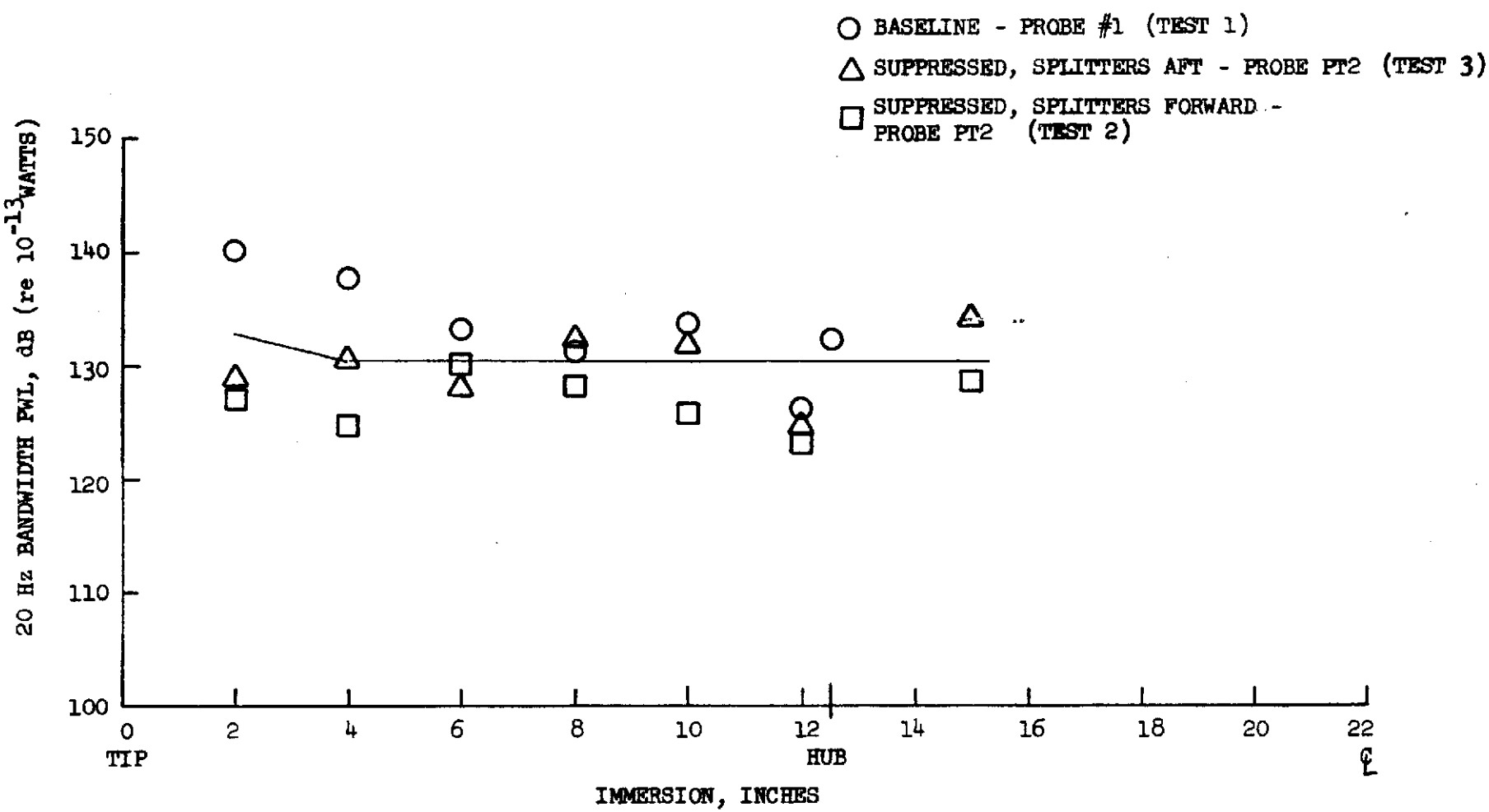

FIGURE IV A-31

TF34 INLET SOUND POWER SOURCE PROFILE

- FAN FUNDAMENTAL FREQUENCY
- 6200 RPM

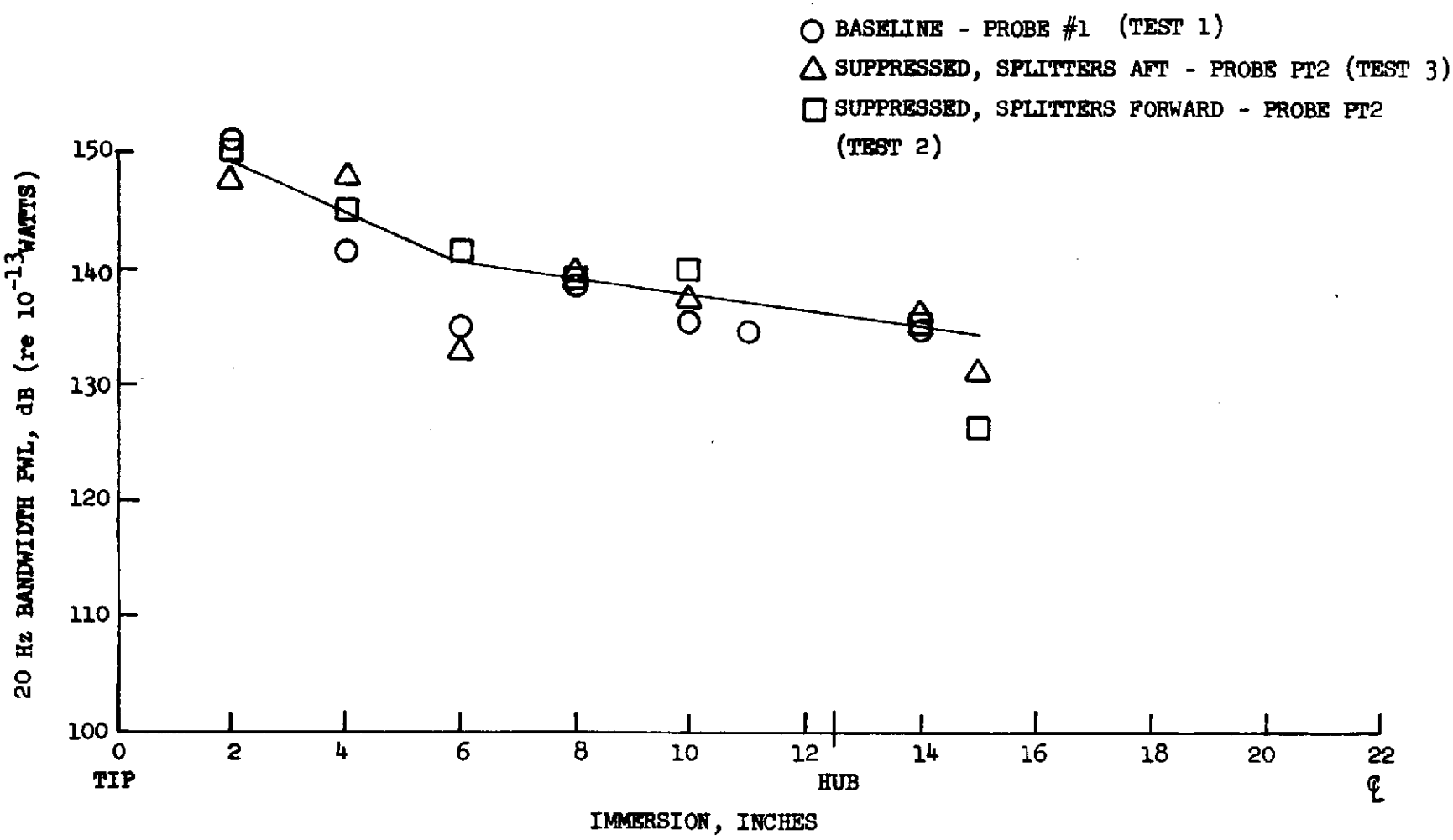

FIGURE IV A-32

TF34 INLET SOUND POWER SOURCE PROFILE

- FAN FUNDAMENTAL FREQUENCY
- MAX POWER

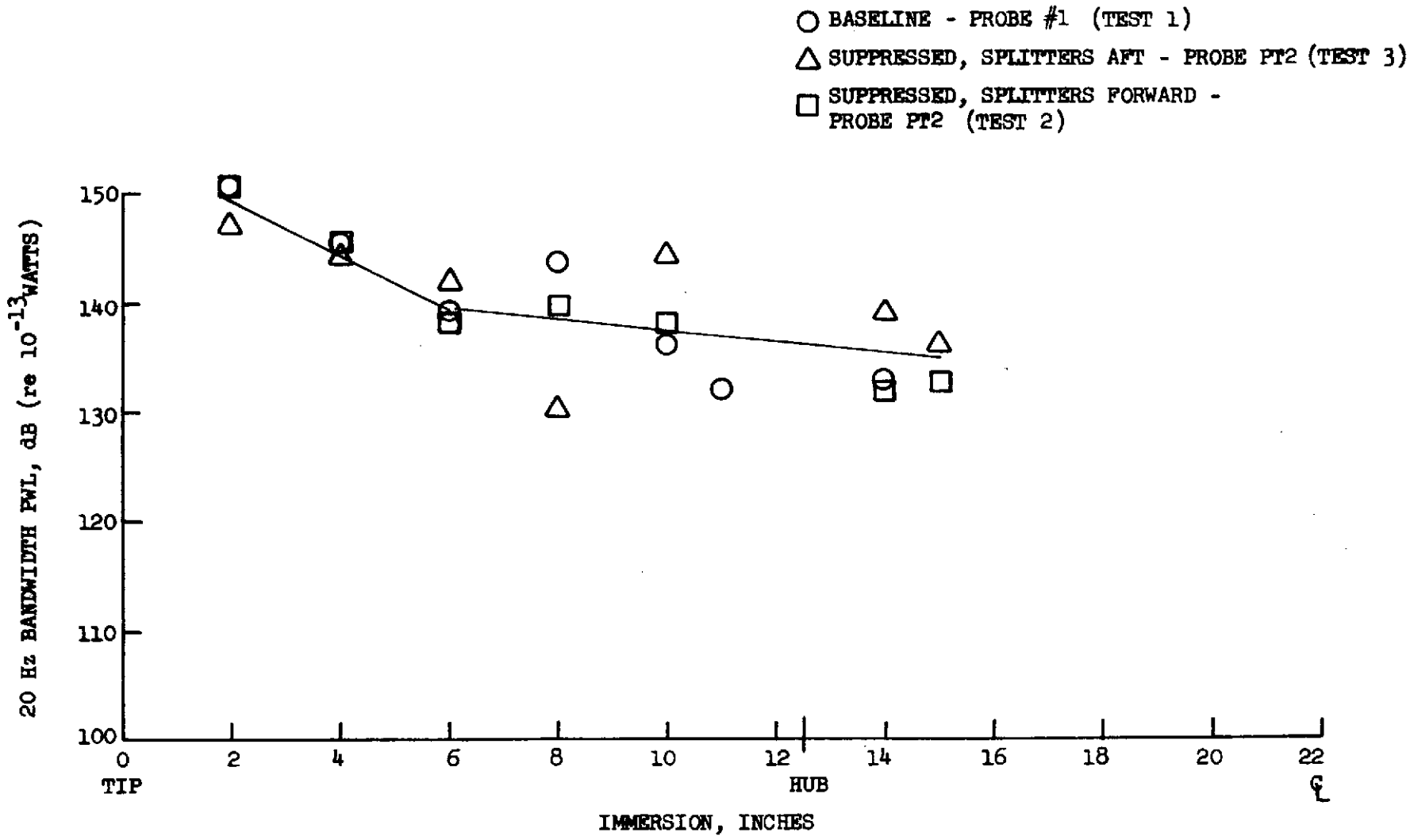

FIGURE IV A-33

TF34 INLET SOUND POWER SOURCE PROFILE

- FAN SECOND HARMONIC FREQUENCY
- 5100 RPM

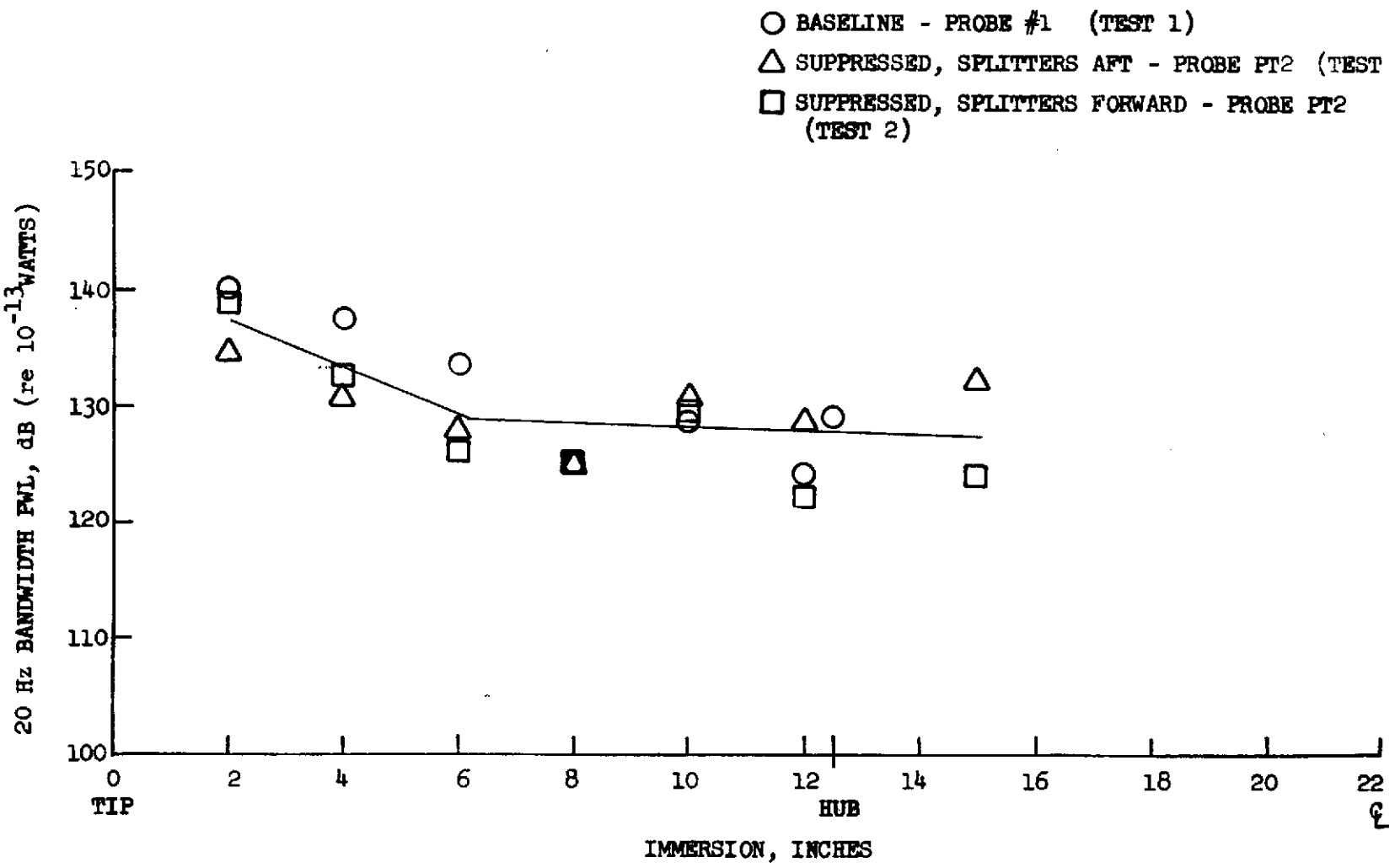

FIGURE IV A-34

TF34 INLET SOUND POWER SOURCE PROFILE

- FAN SECOND HARMONIC FREQUENCY
- 6200 RPM

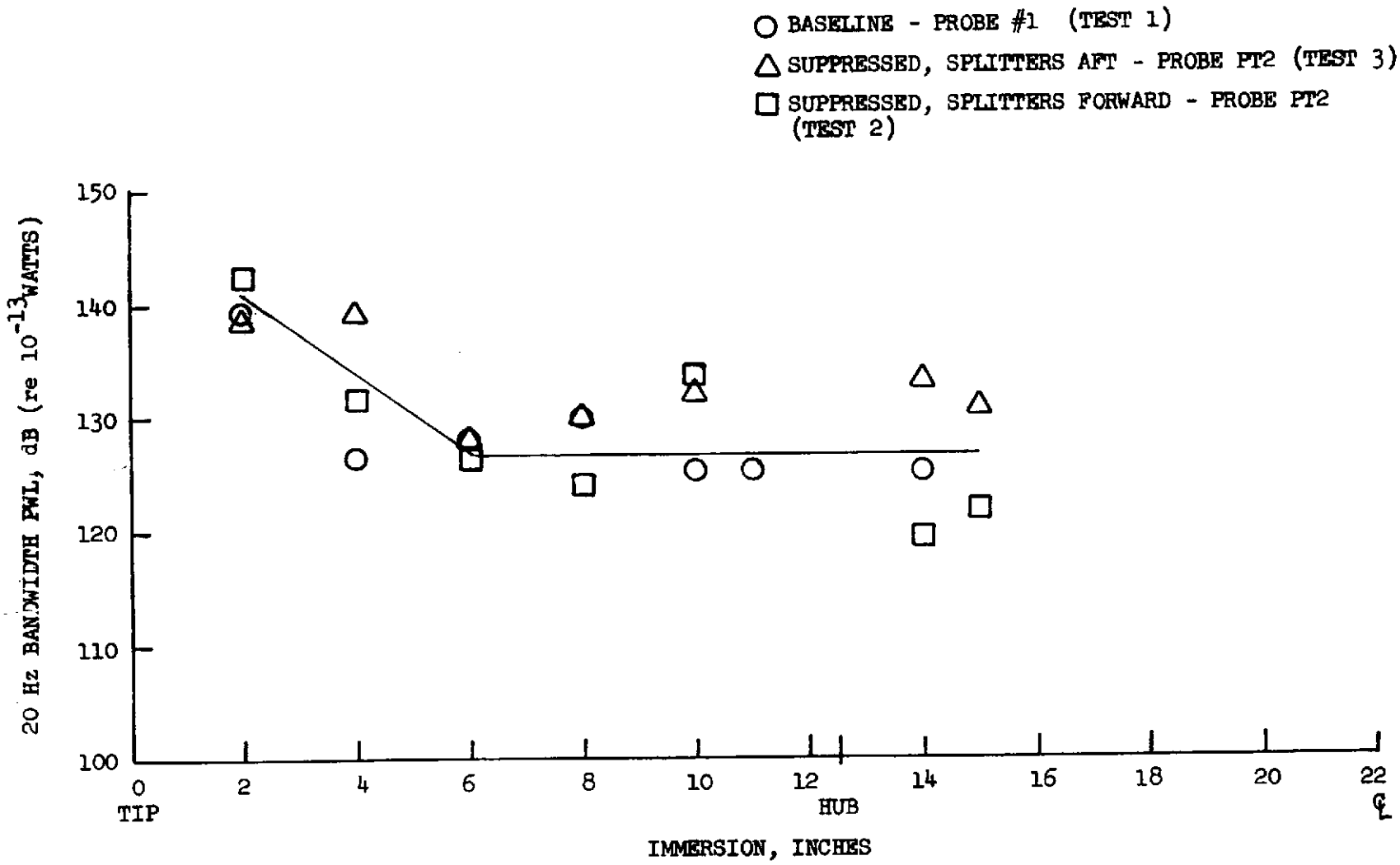

FIGURE IV A-35

TF34 INLET SOUND POWER SOURCE PROFILE

- FAN SECOND HARMONIC FREQUENCY
- MAX POWER

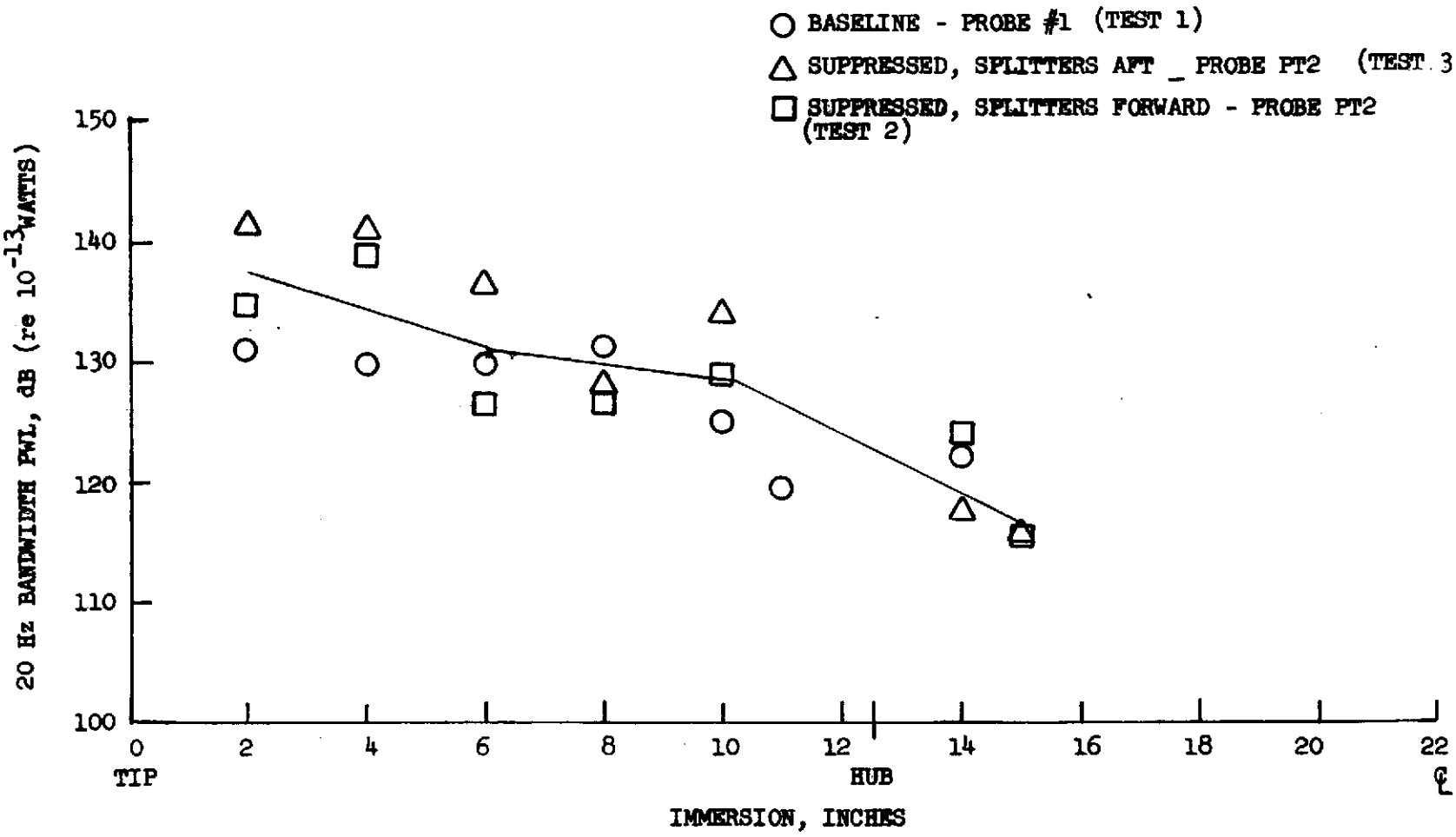

FIGURE IV A-36

TF34 FULLY SUPPRESSED NACELLE

ACOUSTIC PROBE SPECTRA (UNCORRECTED)

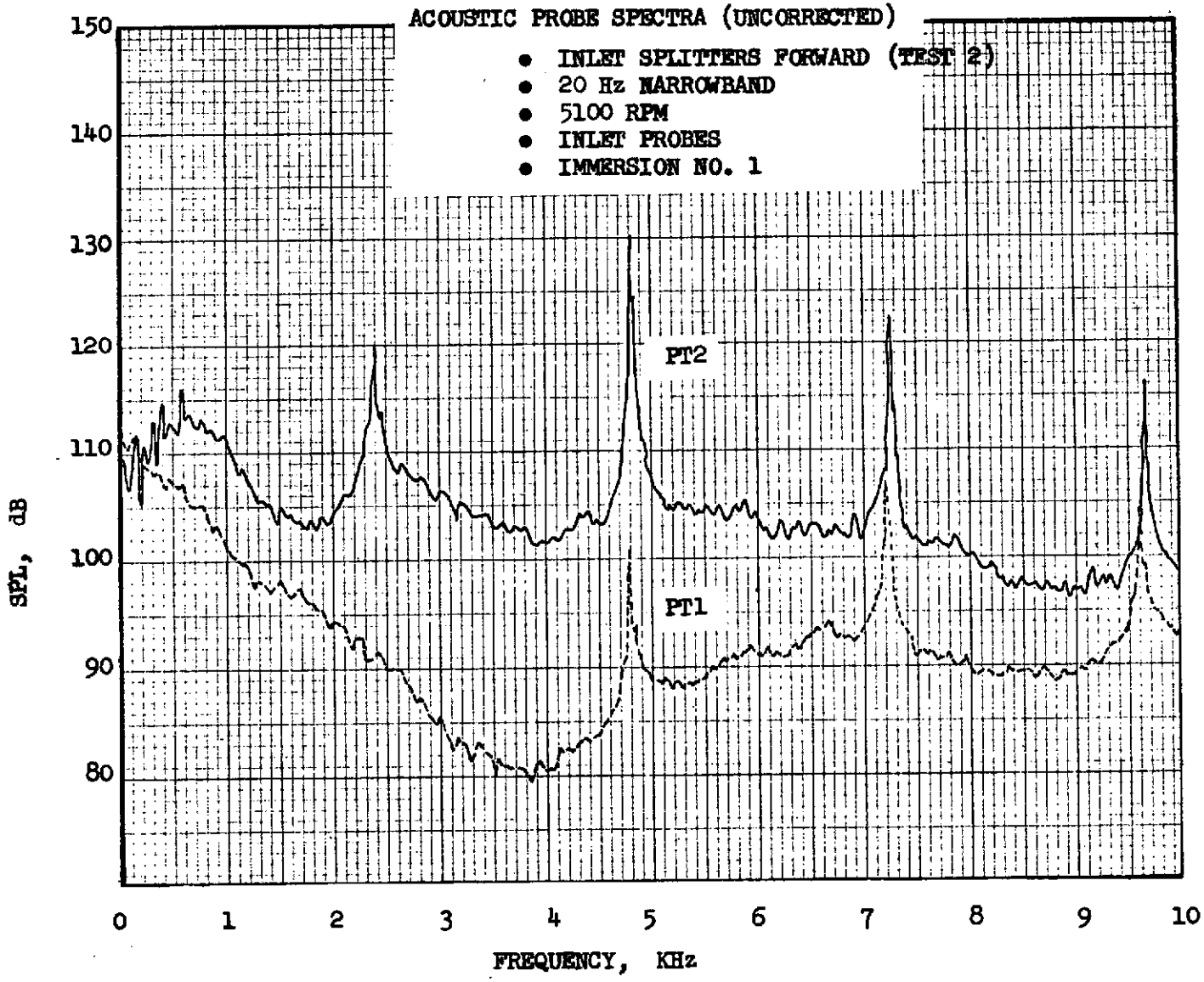

FIGURE IV A-37

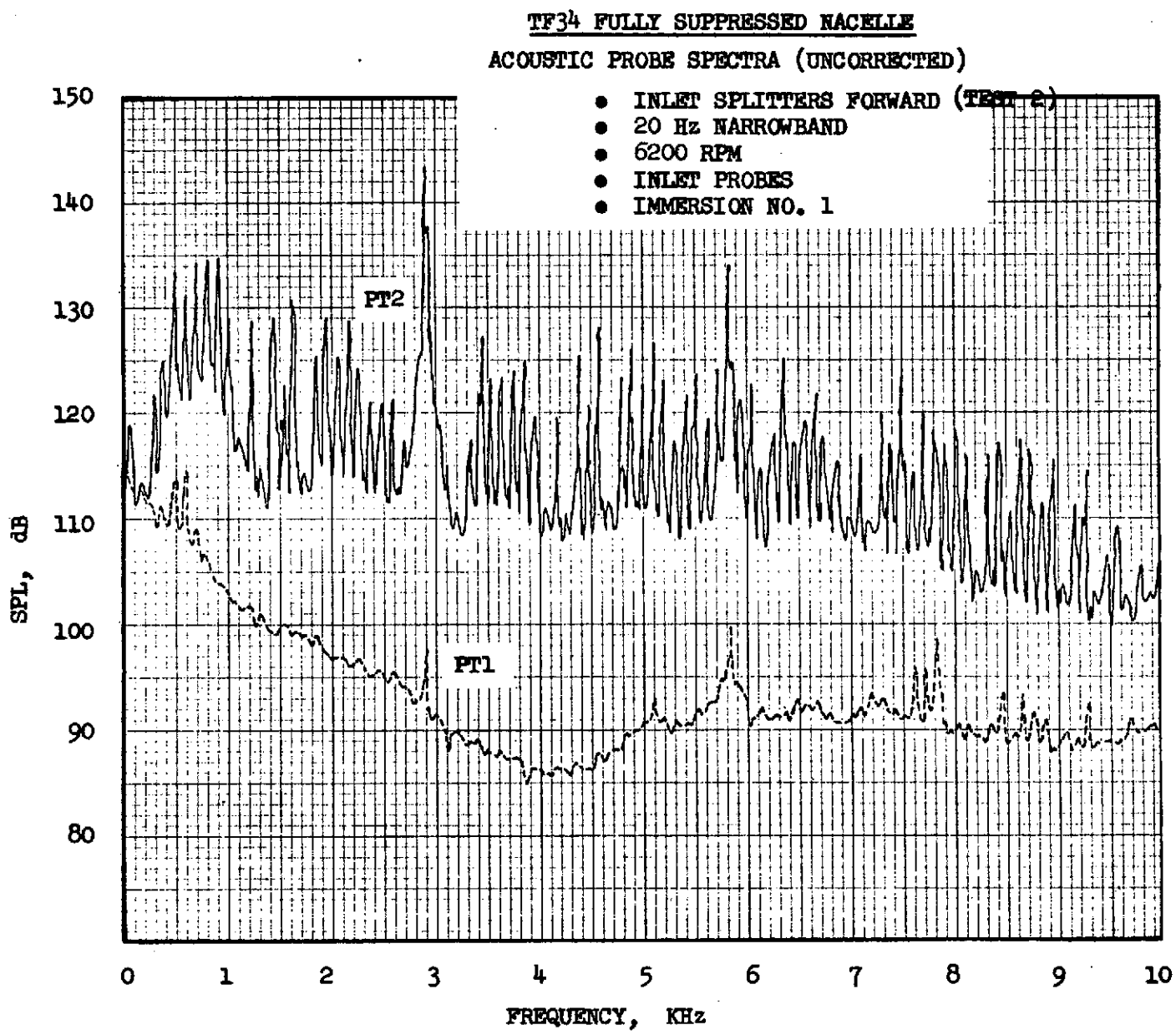

FIGURE IV A-38

TF34 FULLY SUPPRESSED NACELLE

ACOUSTIC PROBE SPECTRA (UNCORRECTED)

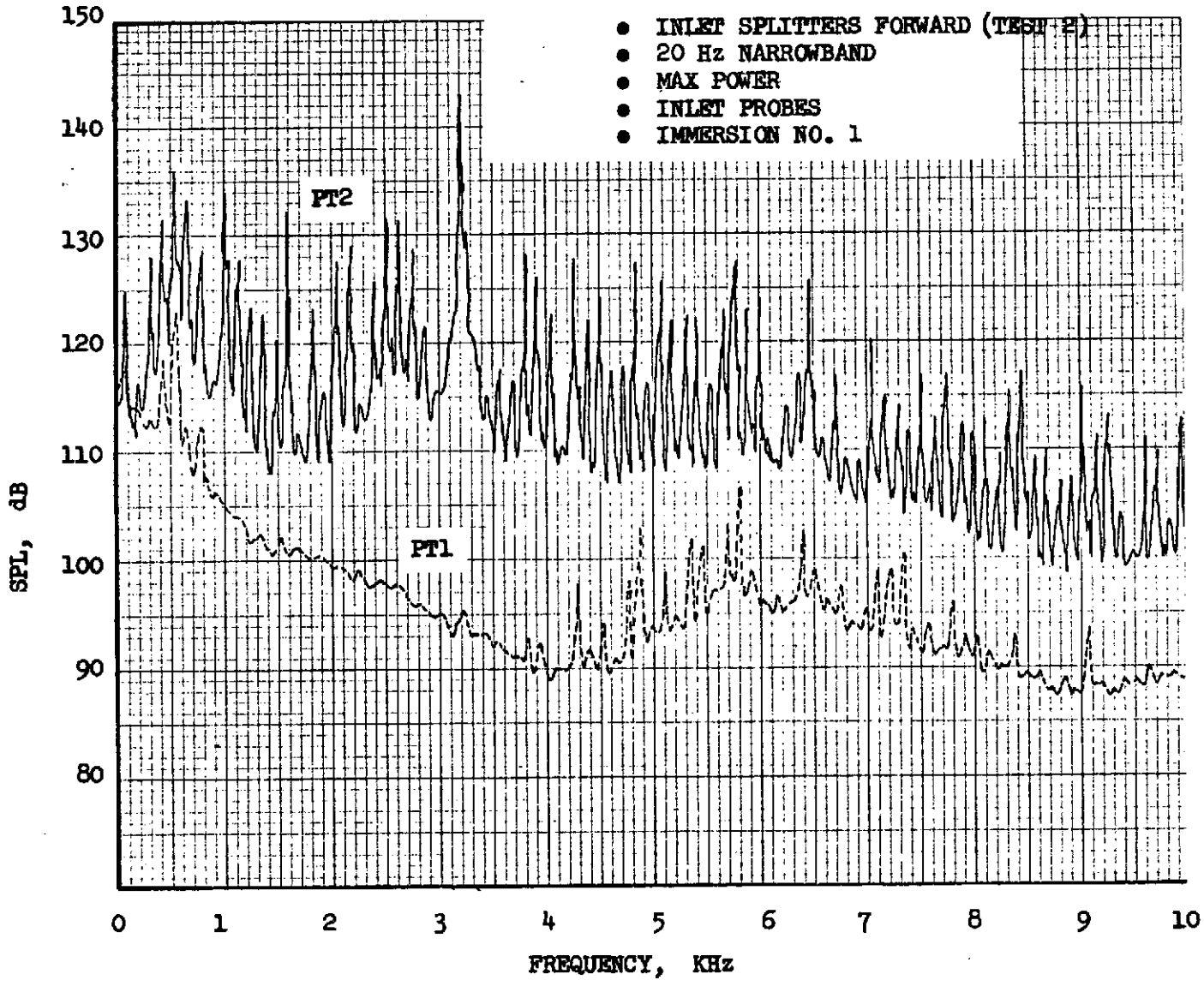

FIGURE IV A-39

TF34 FULLY SUPPRESSED NACELLE

ACOUSTIC PROBE SPECTRA (UNCORRECTED)

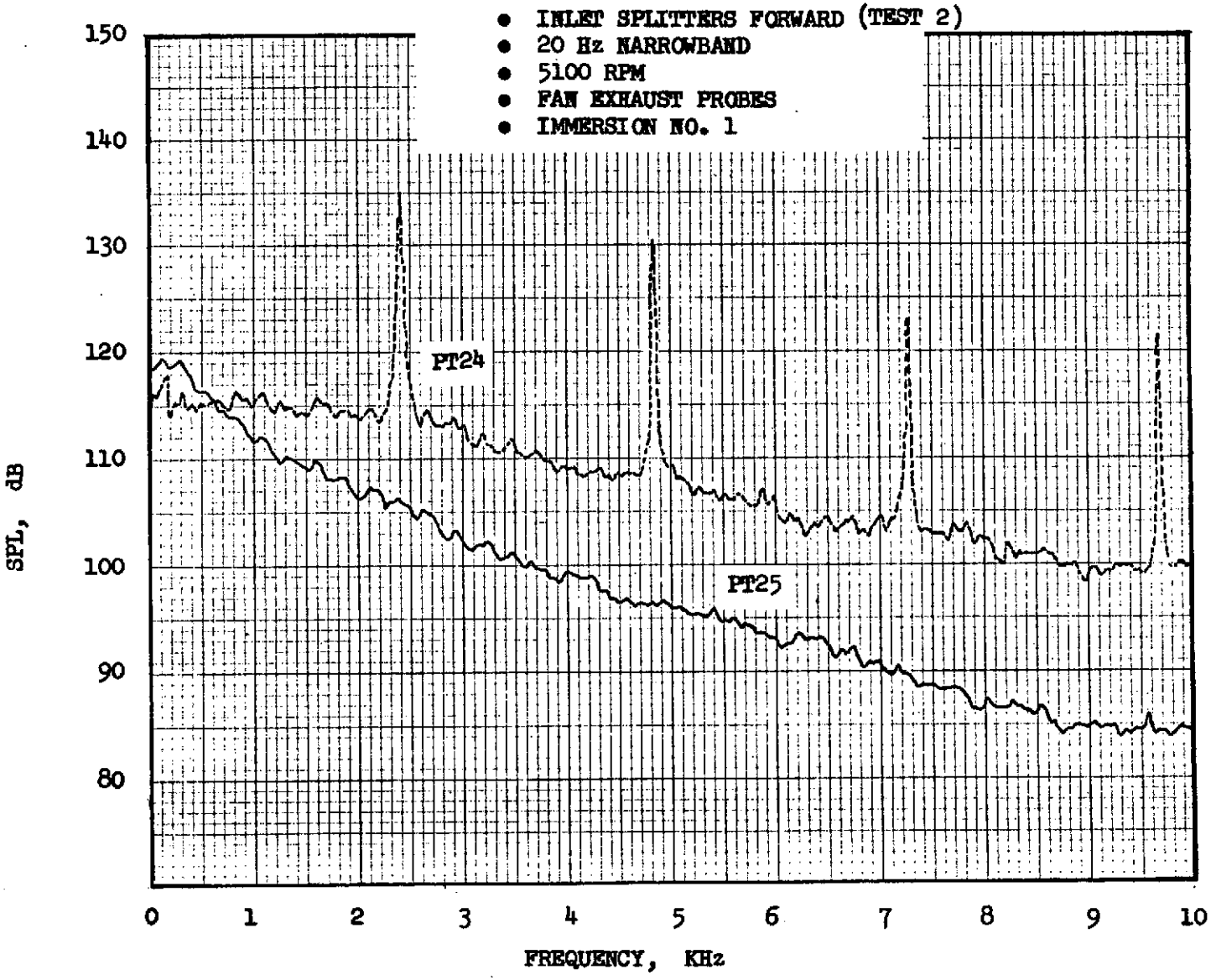

FIGURE IV A-40

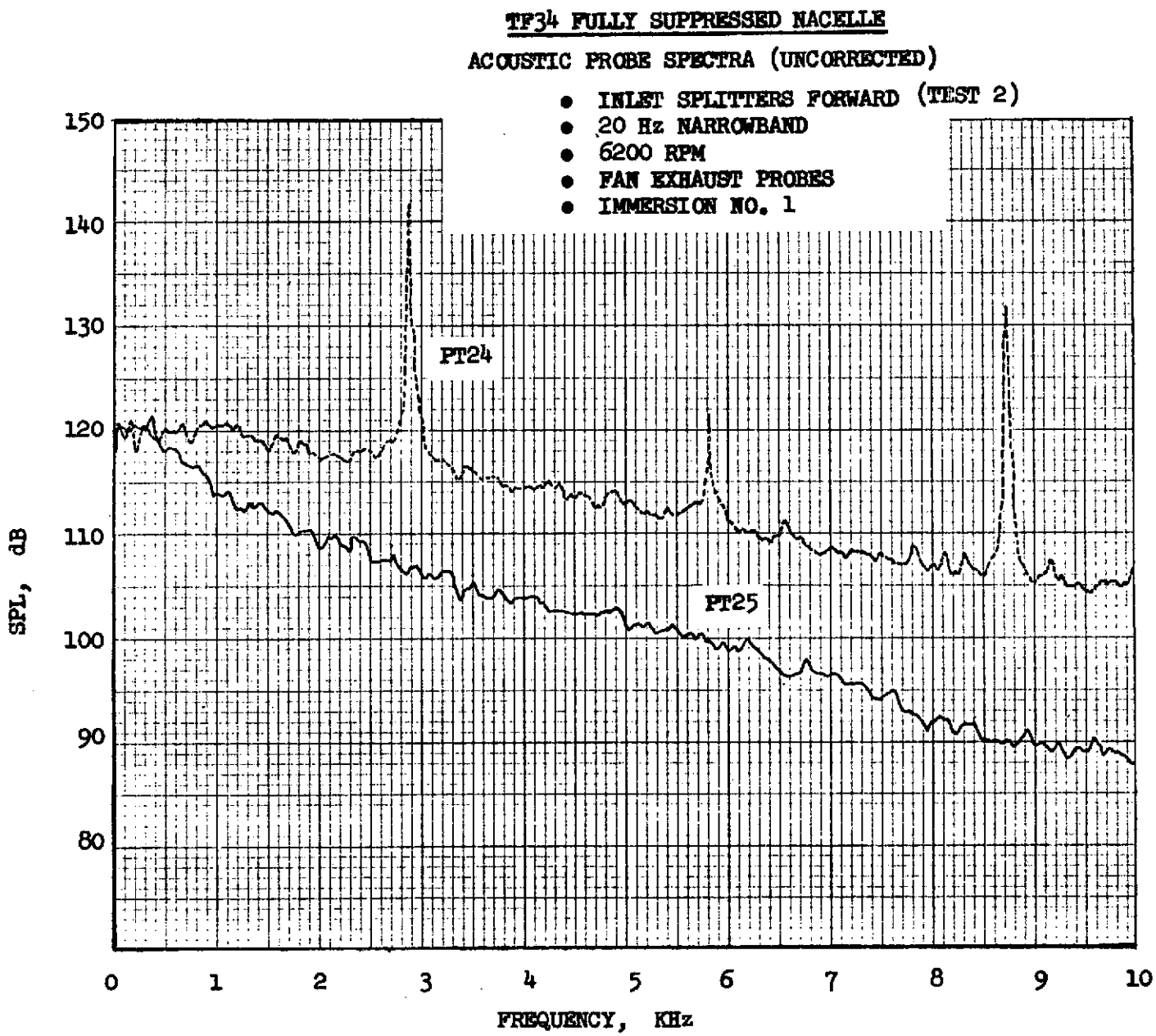

FIGURE IV A-41

TF34 FULLY SUPPRESSED NACELLE

ACOUSTIC PROBE SPECTRA (UNCORRECTED)

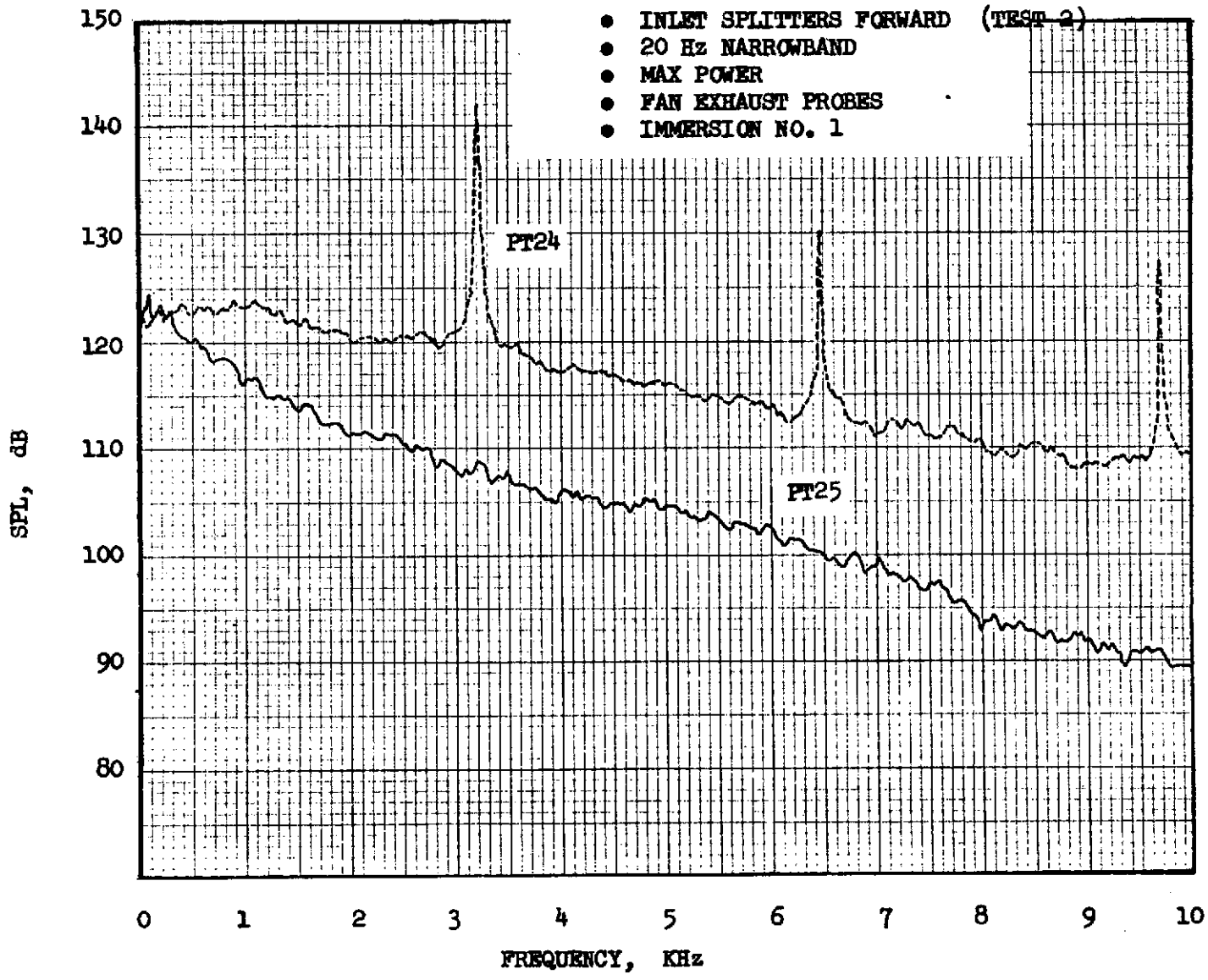

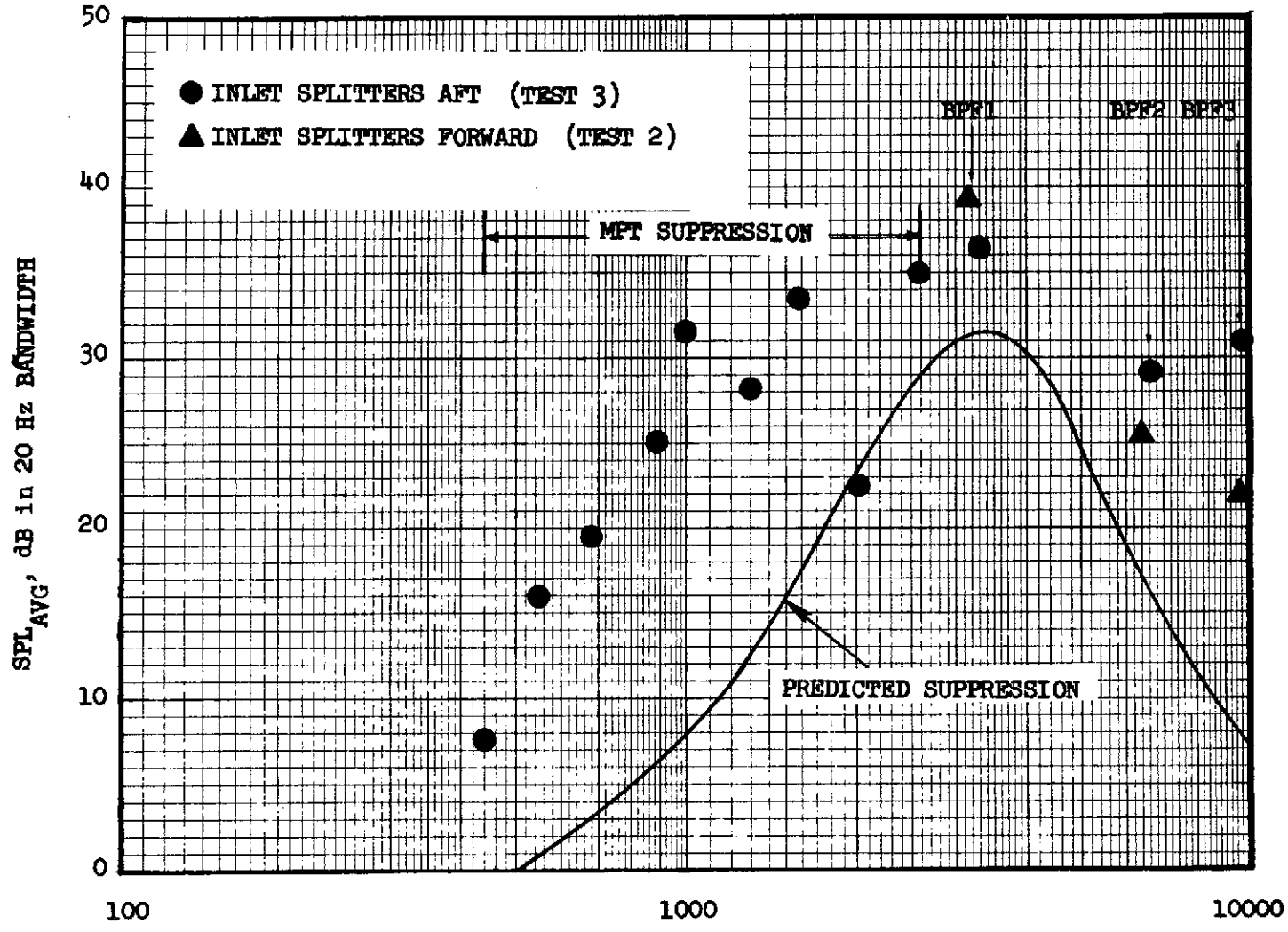

TF34 FULLY SUPPRESSED NACELLE

PREDICTED vs. MEASURED SUPPRESSION ACROSS TREATED INLET TREATMENT (TONES ONLY)

MAX POWER

FIGURE IV A-42

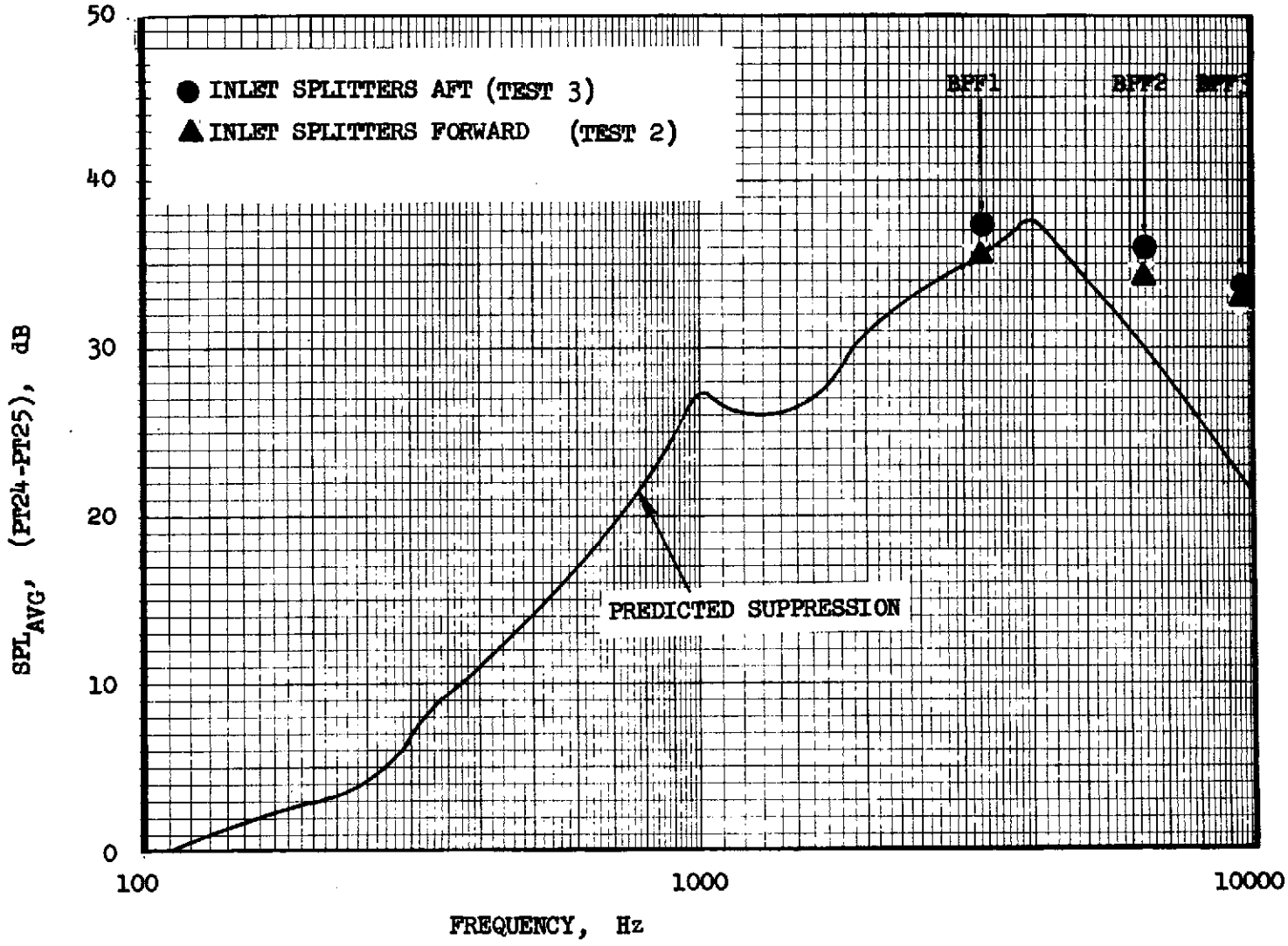

TF34 FULLY SUPPRESSED NACELLE

PREDICTED vs. MEASURED SUPPRESSION ACROSS TREATED FAN EXHAUST TREATMENT (TONES ONLY)

MAX POWER

FIGURE IV A-43

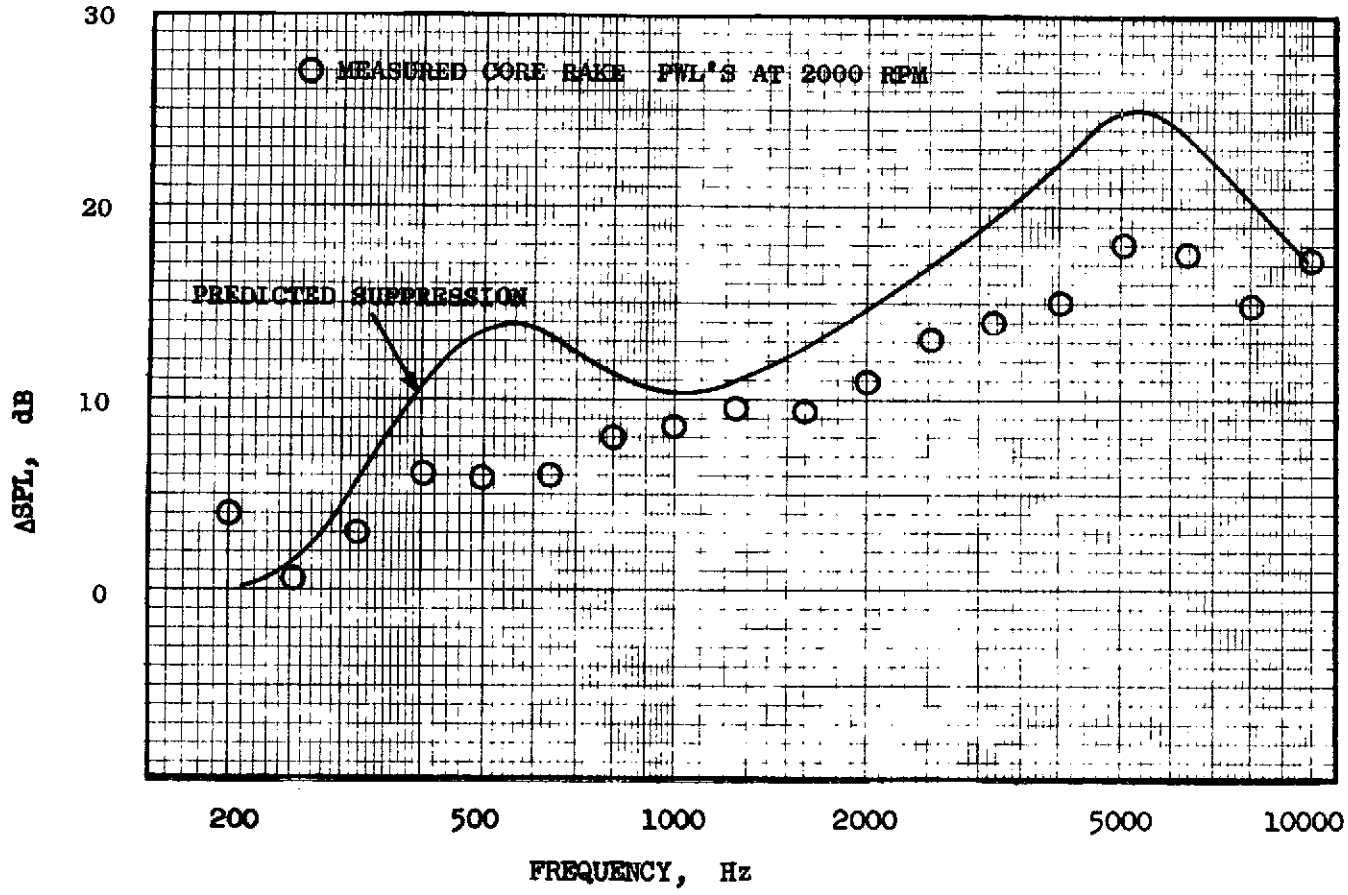

FIGURE IV A-44 TF34 FULLY SUPPRESSED NACELLE CORE NOISE TESTS
PREDICTED vs. MEASURED SUPPRESSION ACROSS CORE EXHAUST TREATMENT

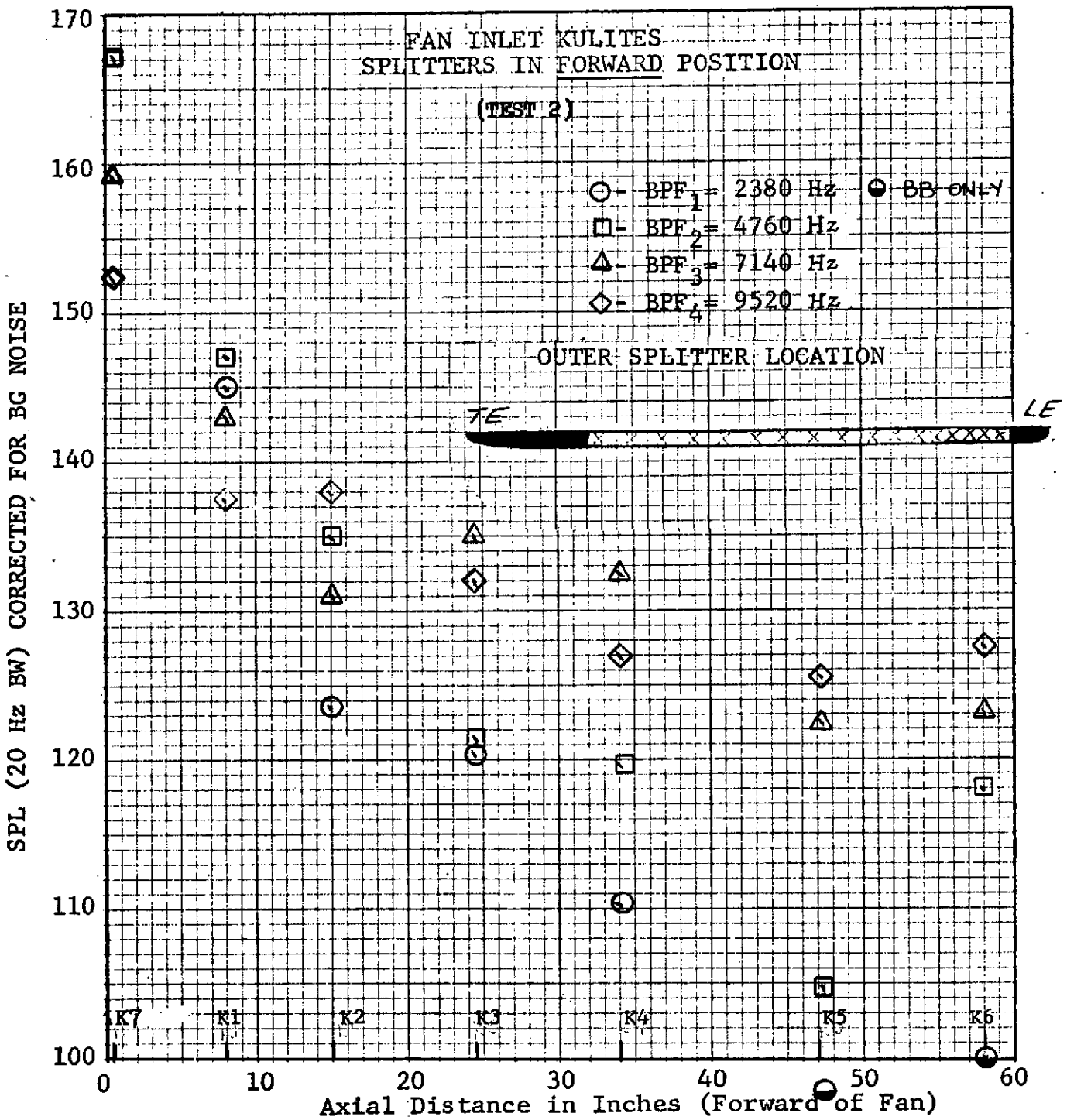

FIGURE IV B-1

FUNDAMENTAL, SECOND HARMONIC, AND THIRD HARMONIC DECAY IN THE FAN INLET WITH AXIAL DISTANCE

NF = 5100 RPM

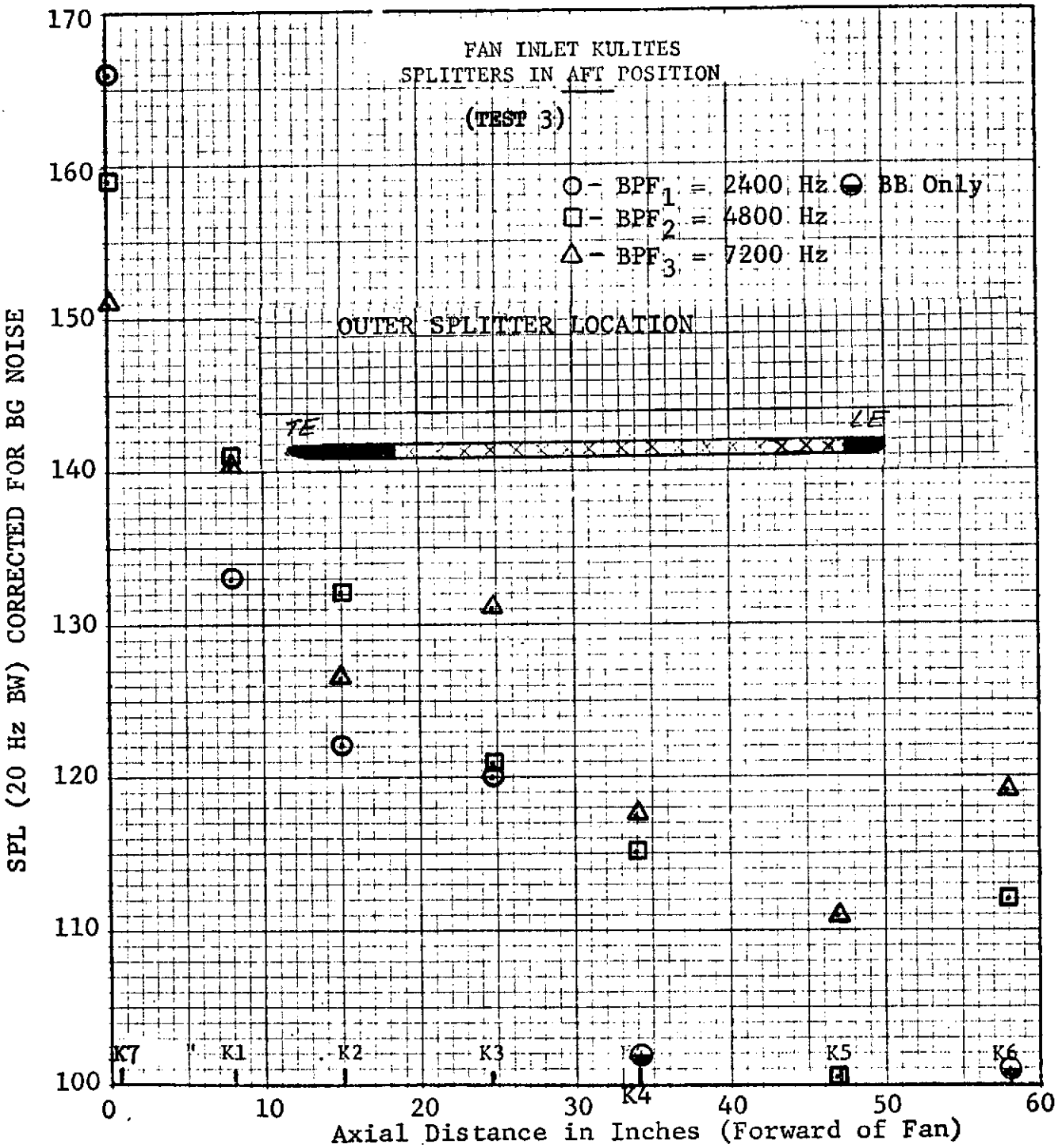

FIGURE IV B-2 ◒ 91

FUNDAMENTAL, SECOND HARMONIC, AND THIRD HARMONIC DECAY IN THE FAN INLET WITH AXIAL DISTANCE

NF = 5100 RPM

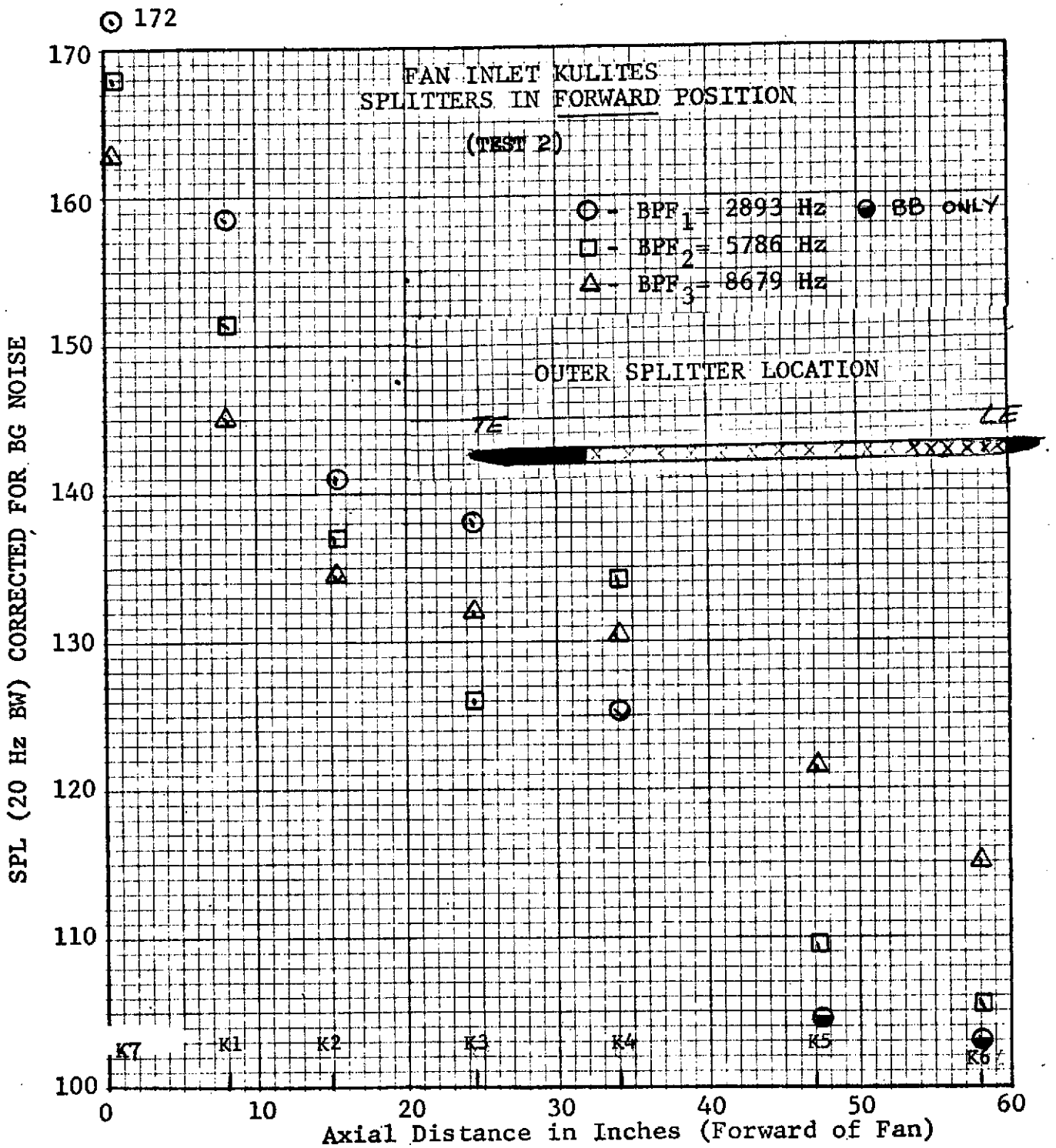

FIGURE IV B-3

FUNDAMENTAL, SECOND HARMONIC, AND THIRD HARMONIC DECAY IN THE FAN INLET WITH AXIAL DISTANCE

NF = 6200 RPM

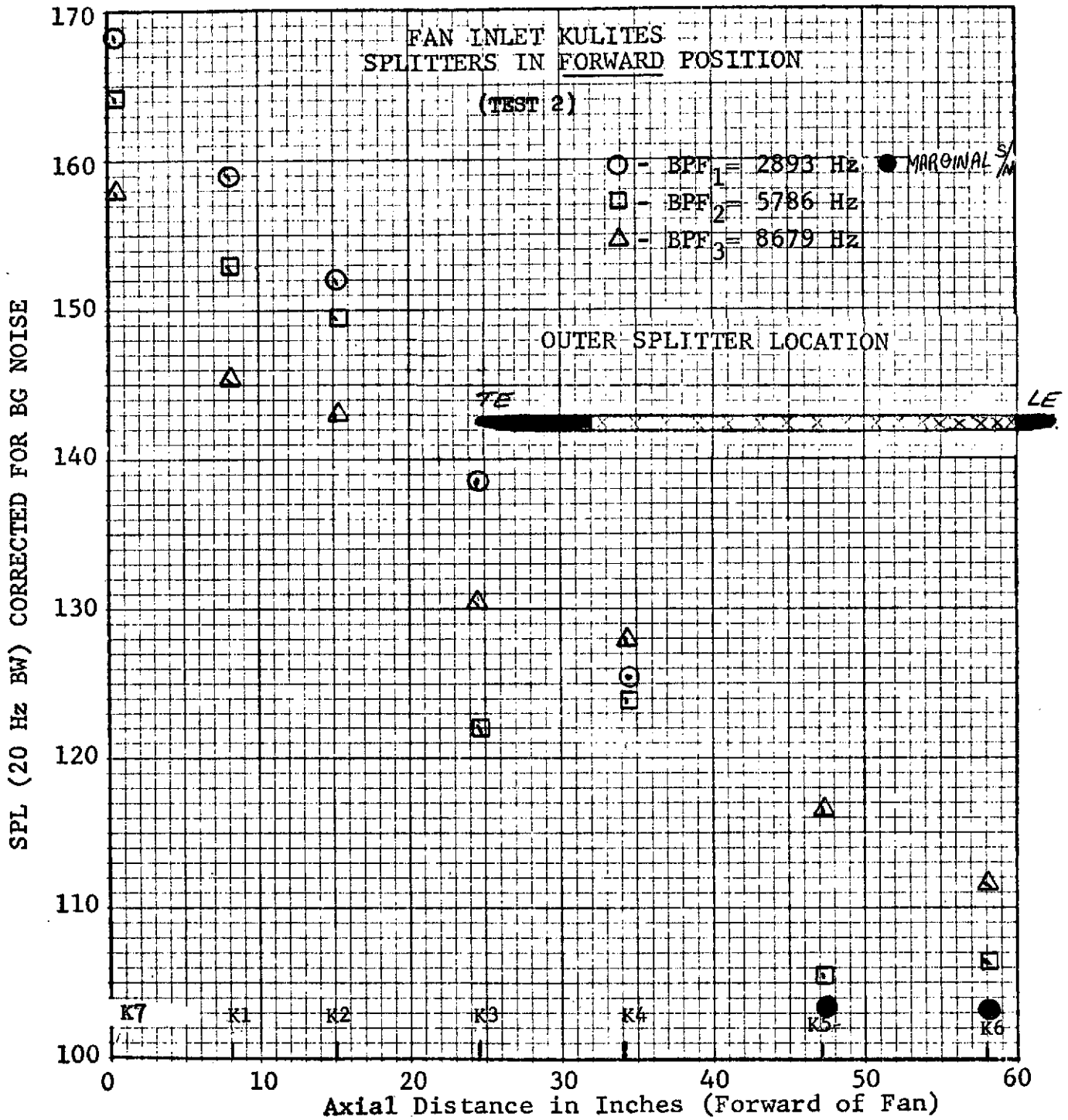

FIGURE IV B-4

FUNDAMENTAL, SECOND HARMONIC, AND THIRD HARMONIC DECAY IN THE FAN INLET WITH AXIAL DISTANCE

NF = 6200 RPM (REPEAT)

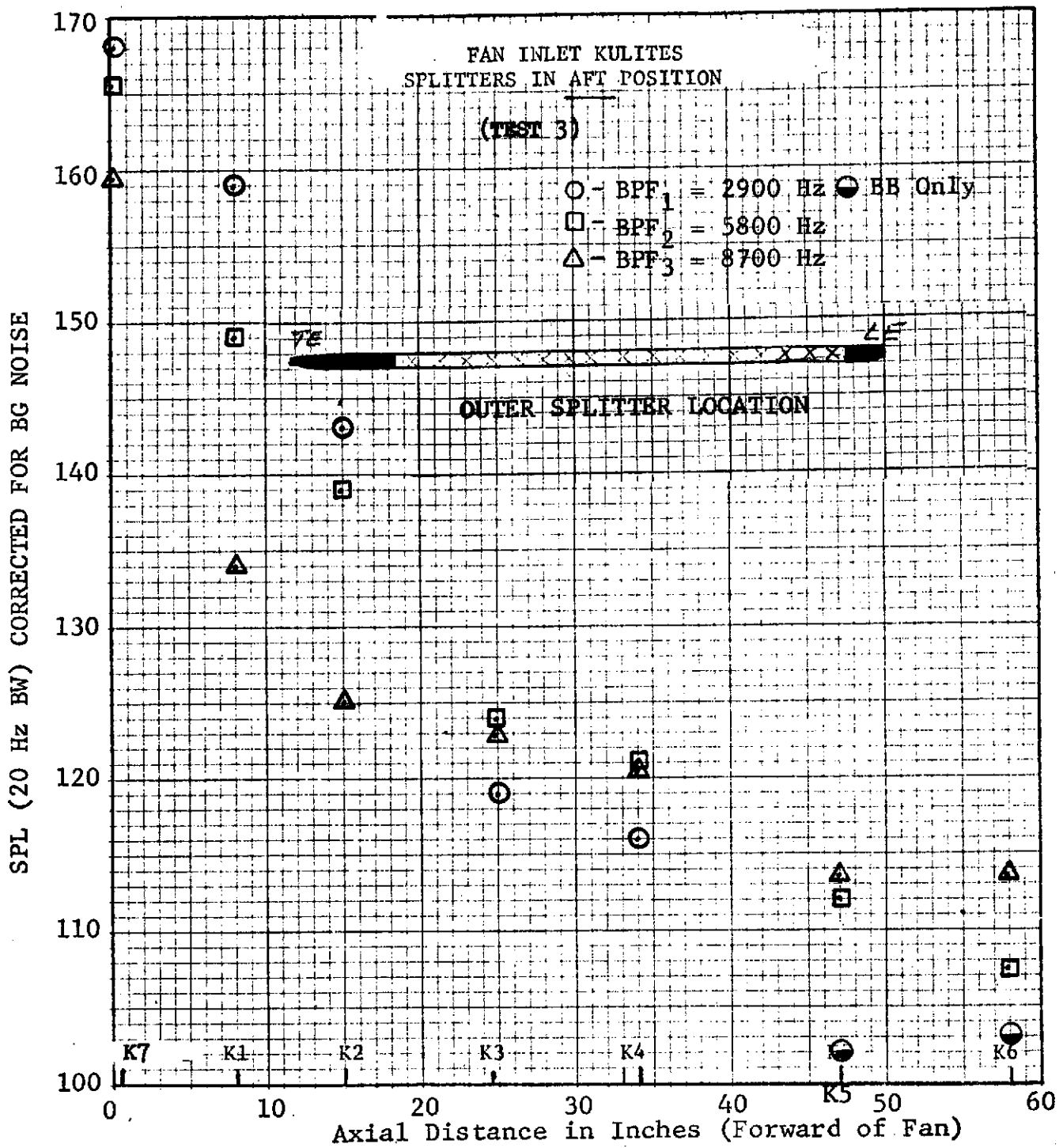

FIGURE IV B-5

FUNDAMENTAL, SECOND HARMONIC, AND THIRD HARMONIC DECAY IN THE FAN INLET WITH AXIAL DISTANCE

NF = 6200 RPM

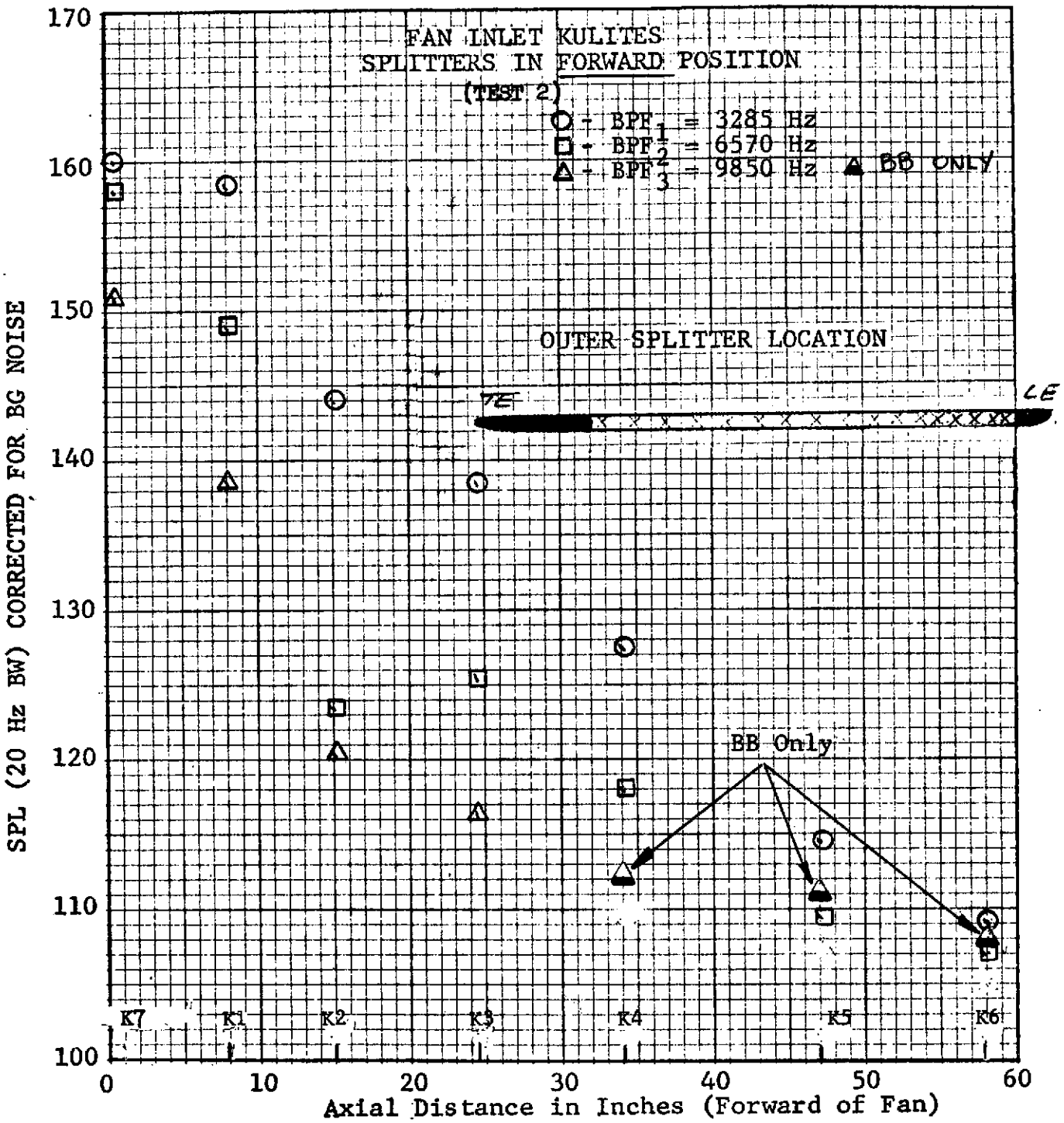

FIGURE IV B-6

FUNDAMENTAL, SECOND HARMONIC, AND THIRD HARMONIC DECAY IN THE FAN INLET WITH AXIAL DISTANCE

NF = 7040 RPM

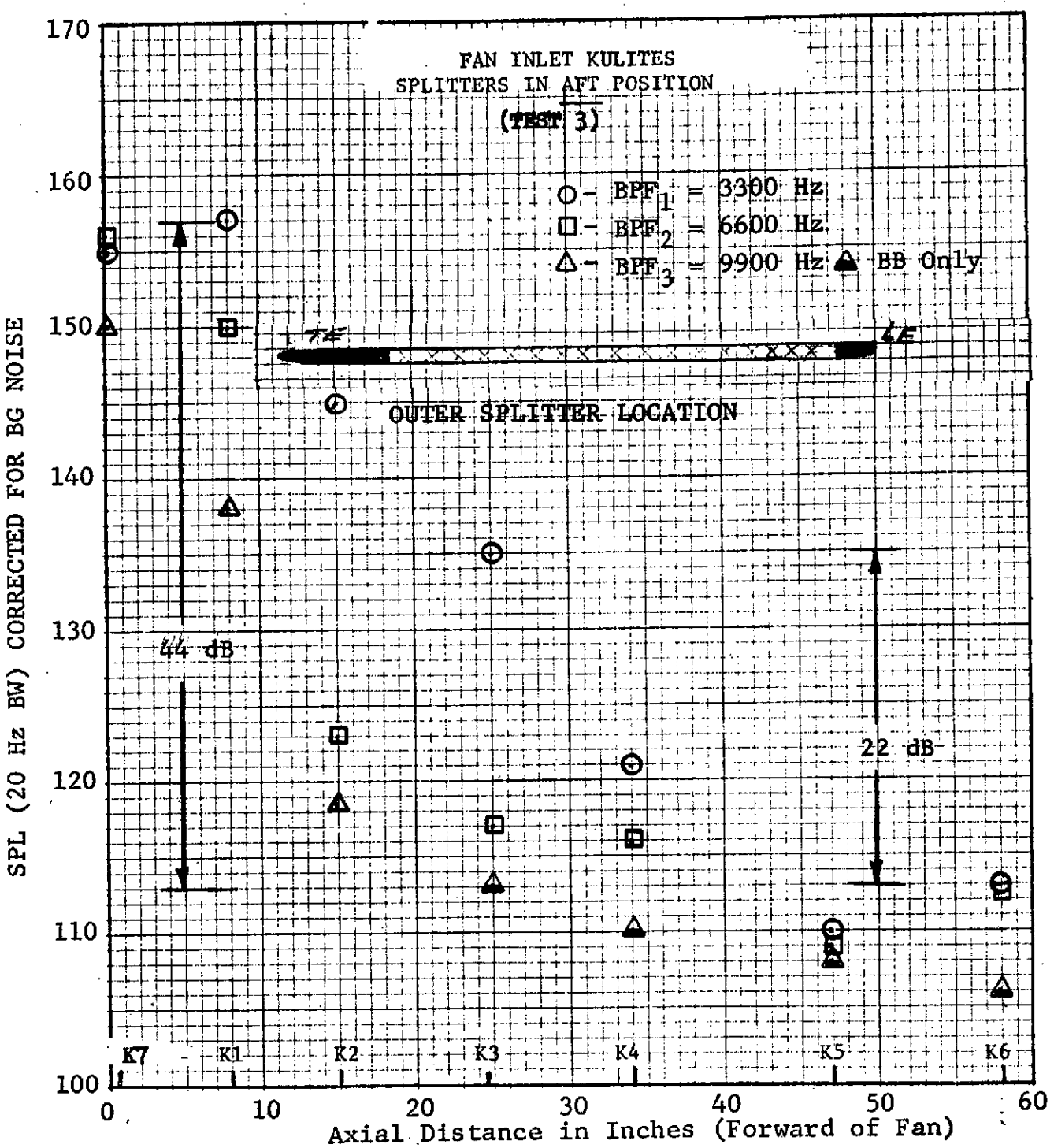

FIGURE IV B-7

FUNDAMENTAL, SECOND HARMONIC, AND THIRD HARMONIC DECAY IN THE FAN INLET WITH AXIAL DISTANCE

NF = 7030 RPM

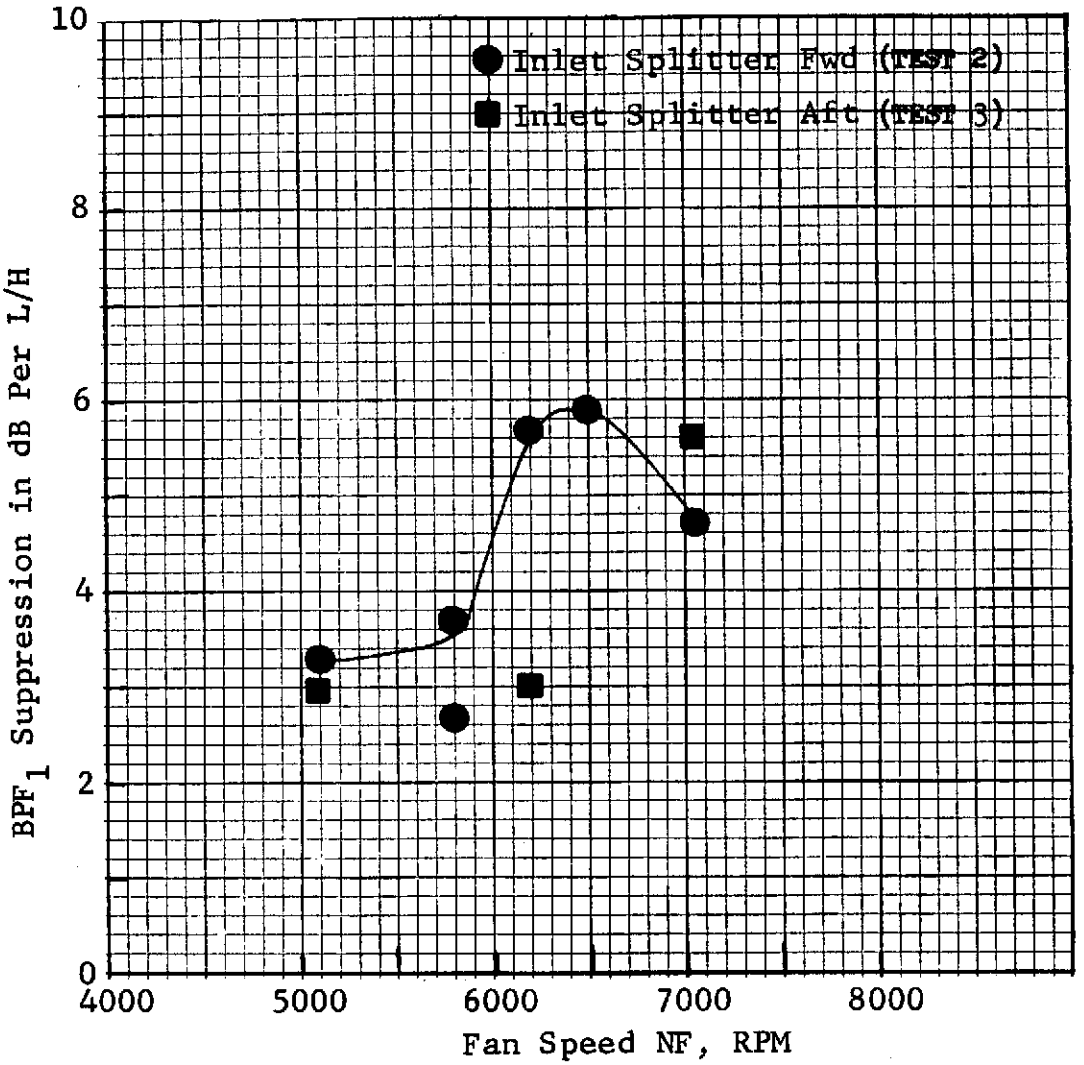

FIGURE IV B-8

FAN INLET BPF_1 SUPPRESSION PER L/H (FROM KULITES #3 & 6) AS A FUNCTION OF FAN SPEED.

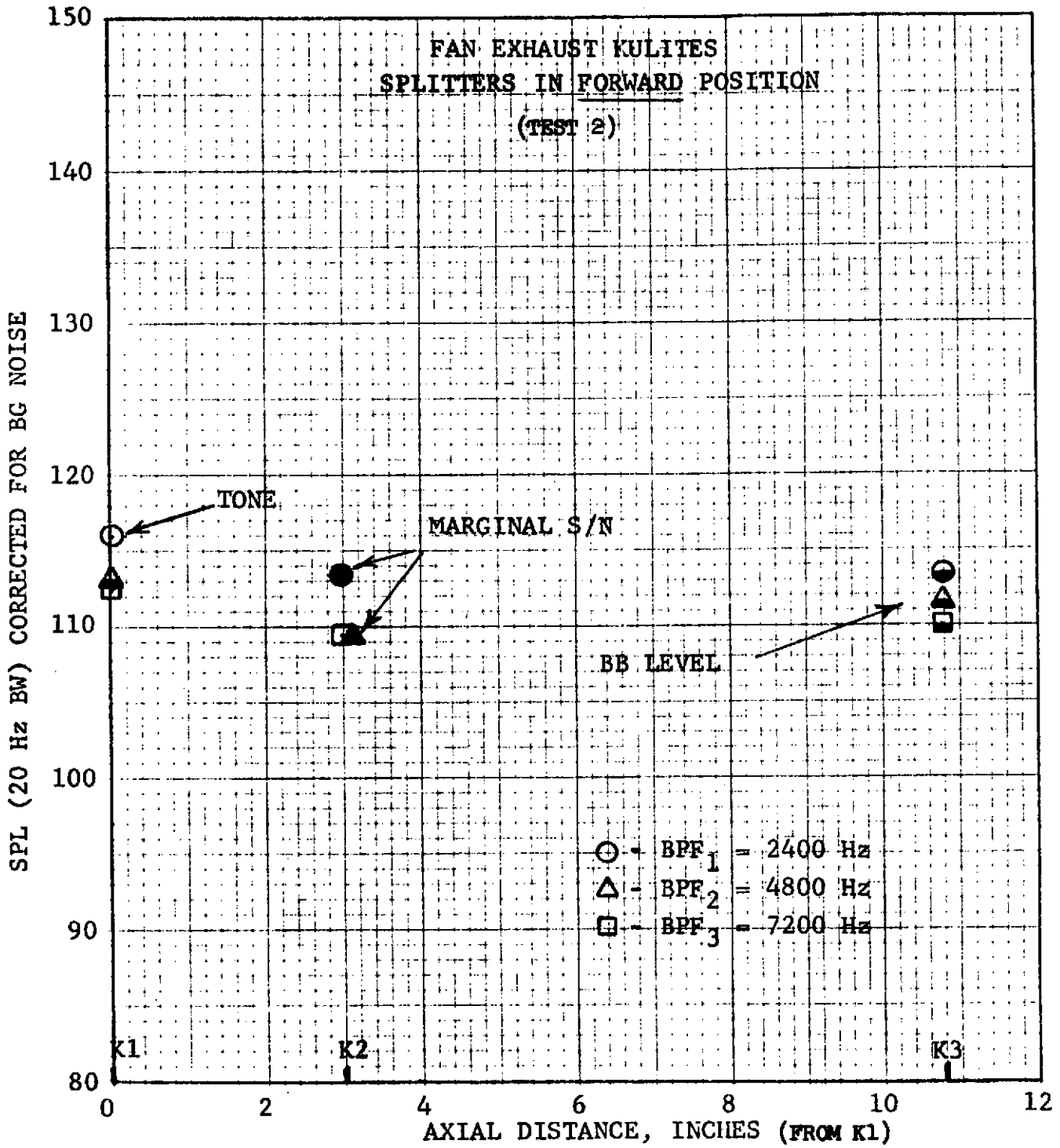

FIGURE IV B-9

FUNDAMENTAL, SECOND HARMONIC, AND THIRD HARMONIC DECAY IN FAN EXHAUST WITH AXIAL DISTANCE.

NF = 5100 RPM

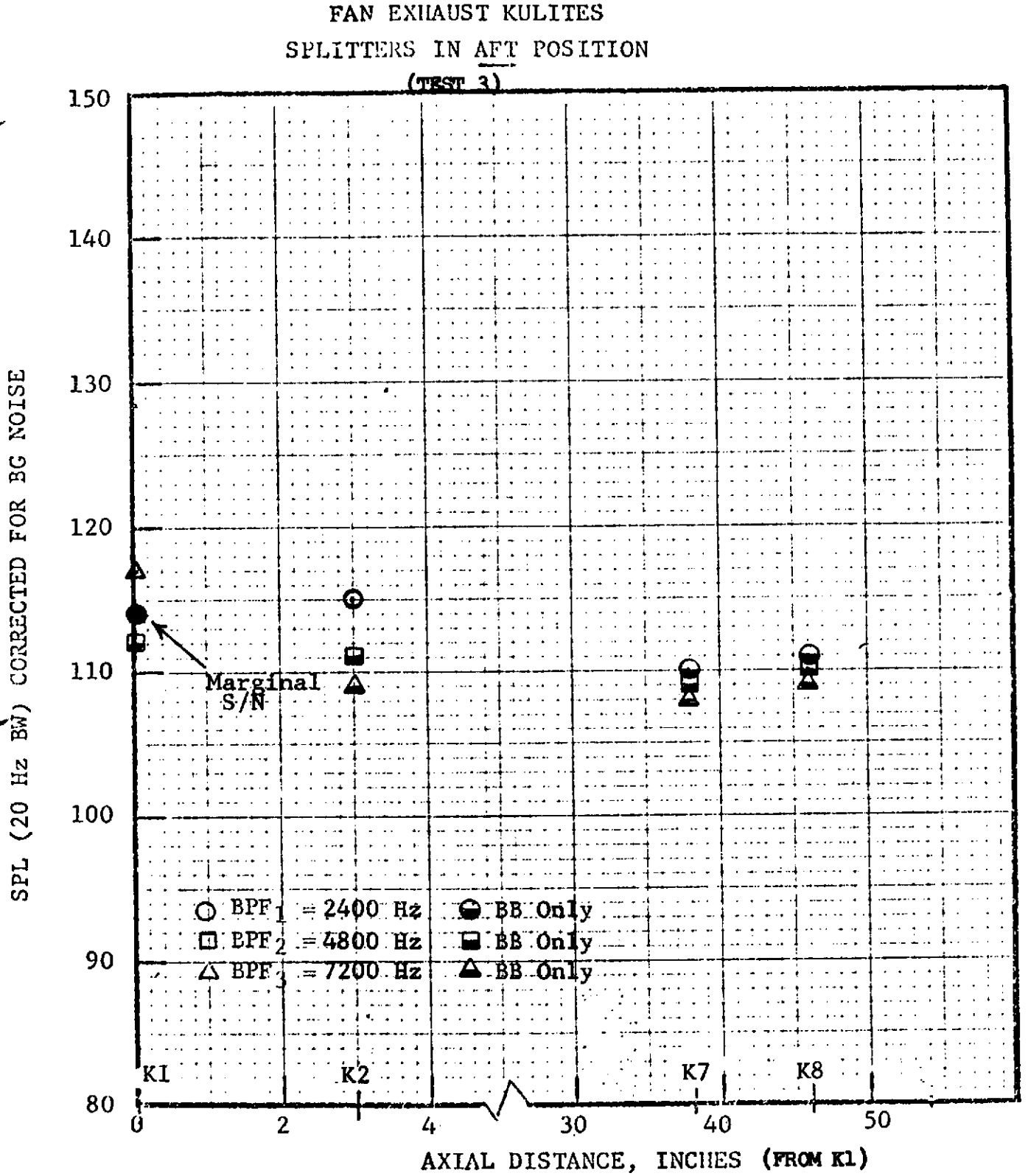

FUNDAMENTAL, SECOND HARMONIC, AND THIRD HARMONIC DECAY IN FAN EXHAUST WITH AXIAL DISTANCE.

NF = 5100 RPM

FIGURE IV B-10

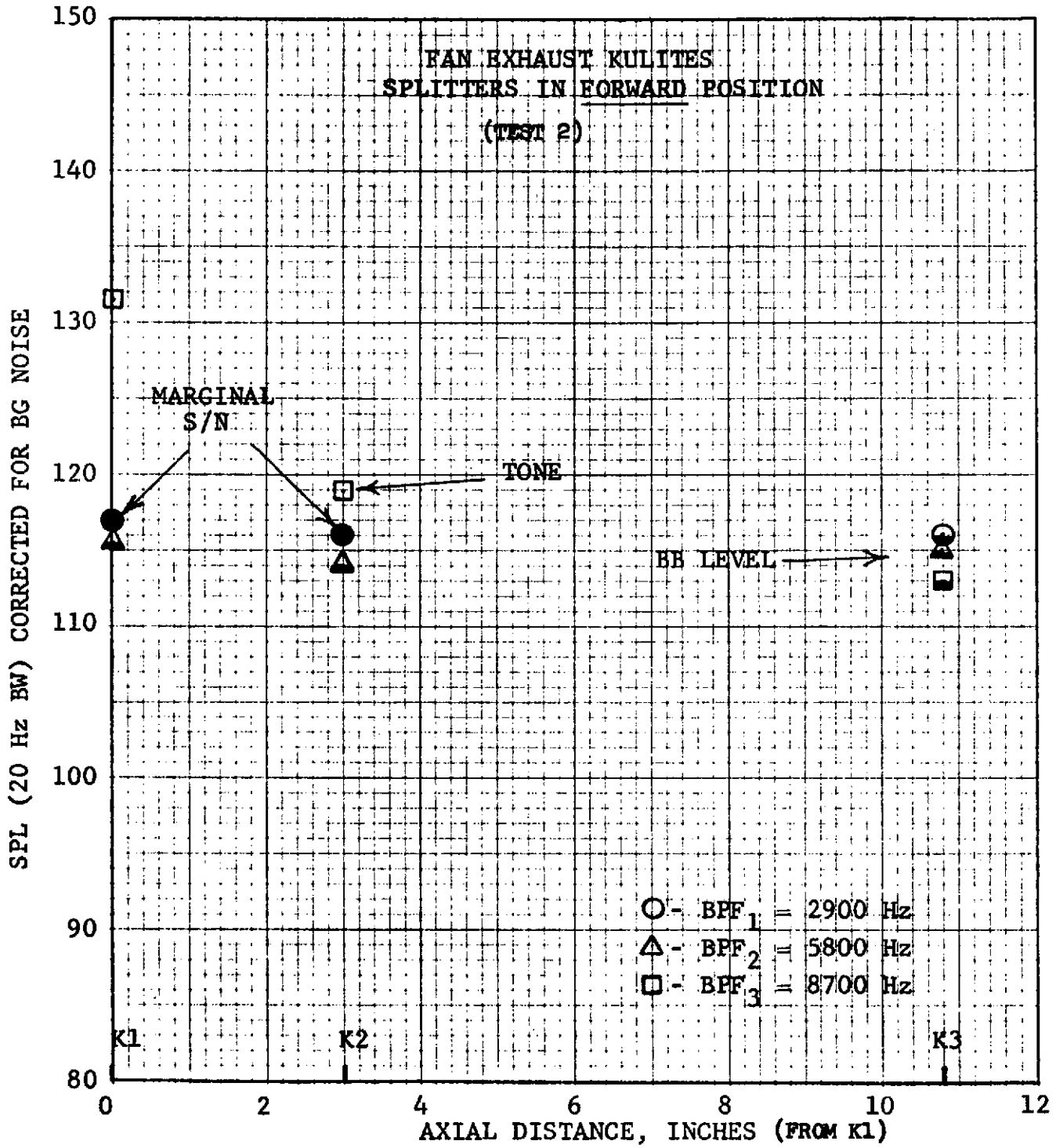

FIGURE IV B-11

FUNDAMENTAL, SECOND HARMONIC, AND THIRD HARMONIC DECAY IN FAN EXHAUST WITH AXIAL DISTANCE.
NF =6200 RPM

FAN EXHAUST KULITES

SPLITTERS IN AFT POSITION

(TEST 3)

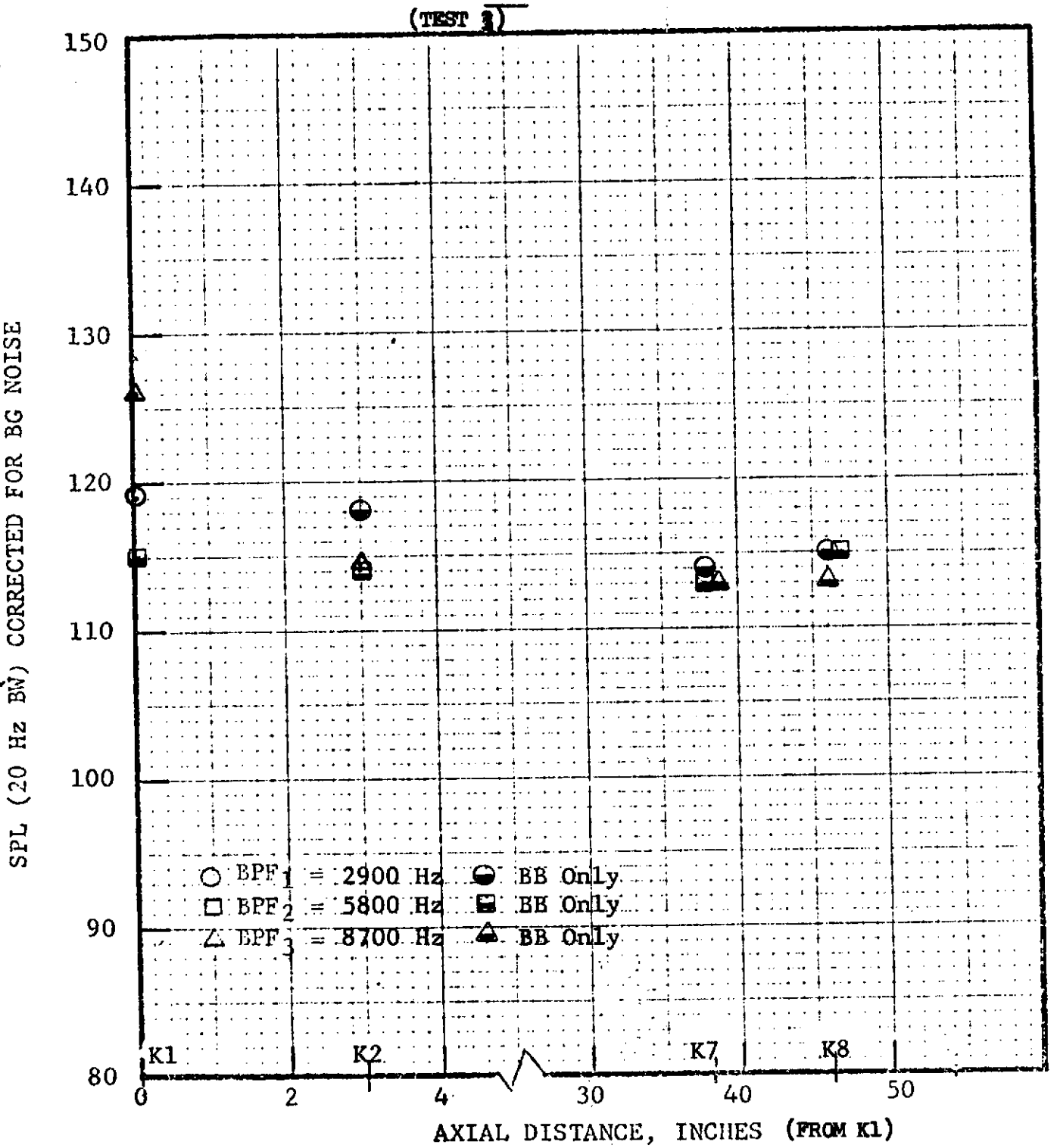

FUNDAMENTAL, SECOND HARMONIC, AND THIRD HARMONIC DECAY IN FAN EXHAUST WITH AXIAL DISTANCE.

NF = 6200 RPM

FIGURE IV B-12

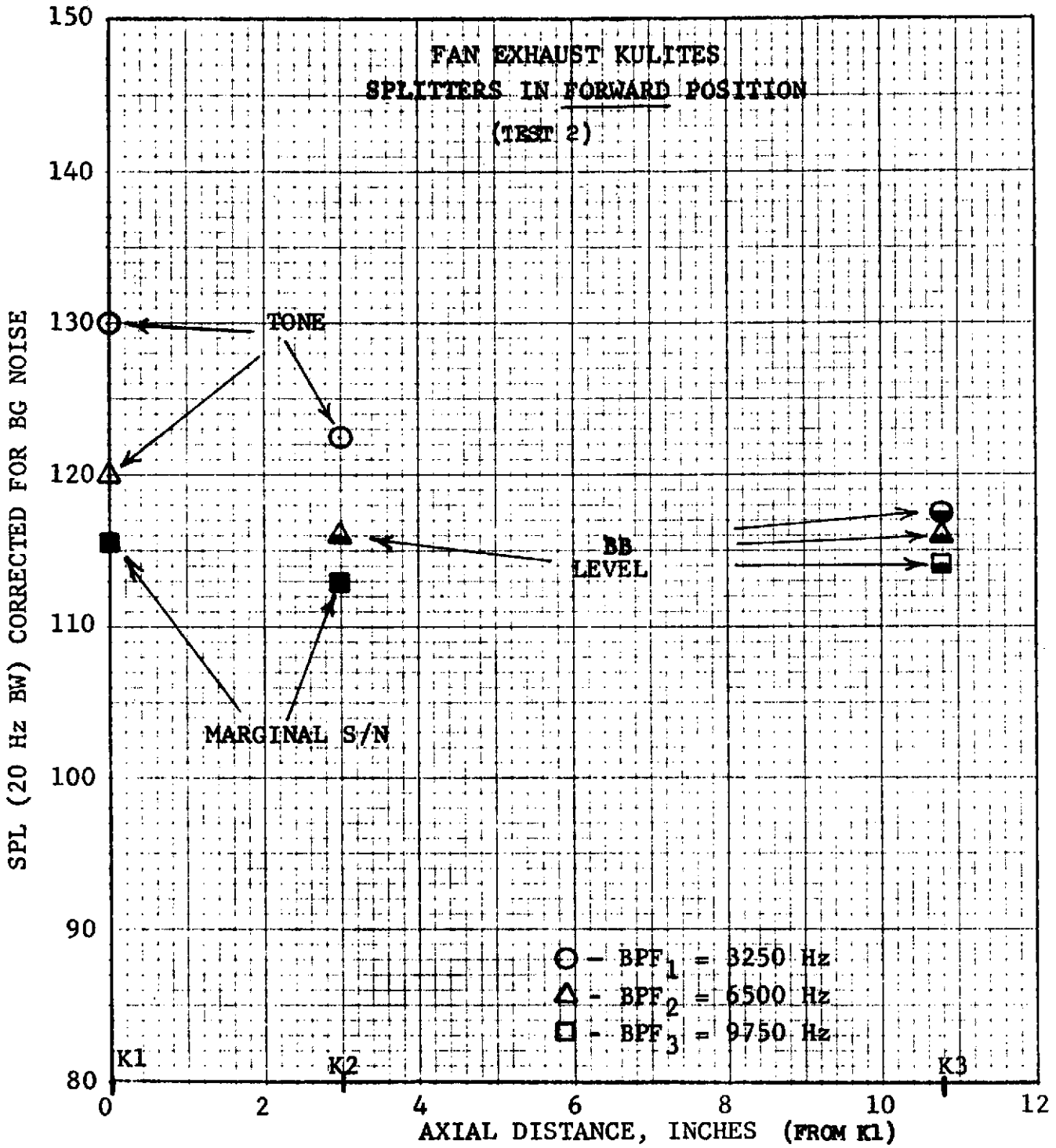

FIGURE IV B-13

FUNDAMENTAL, SECOND HARMONIC, AND THIRD HARMONIC DECAY IN FAN EXHAUST WITH AXIAL DISTANCE.

NF = MAX

FAN EXHAUST KULITES

SPLITTERS IN AFT POSITION

(TEST 3)

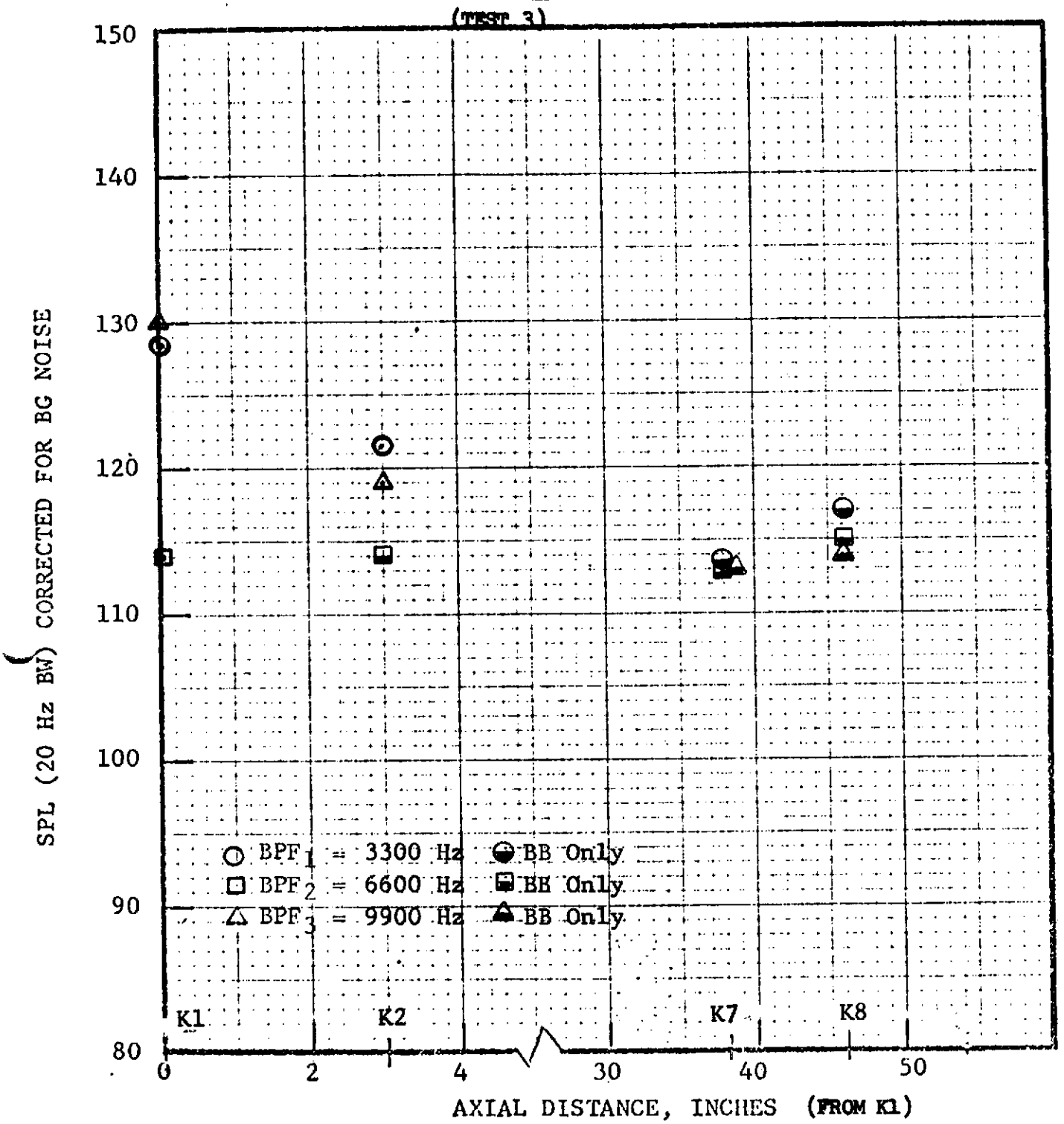

FUNDAMENTAL, SECOND HARMONIC, AND THIRD HARMONIC DECAY IN FAN EXHAUST WITH AXIAL DISTANCE.

NF = 7030 RPM

FIGURE IV B-14

FIGURE IV B-15

TF34 QUIET NACELLE

- MEASURED AFT SUPPRESSION
- 3150 Hz FUNDAMENTAL
- MAX POWER
- INLET SPLIITERS FORWARD (TEST 2)

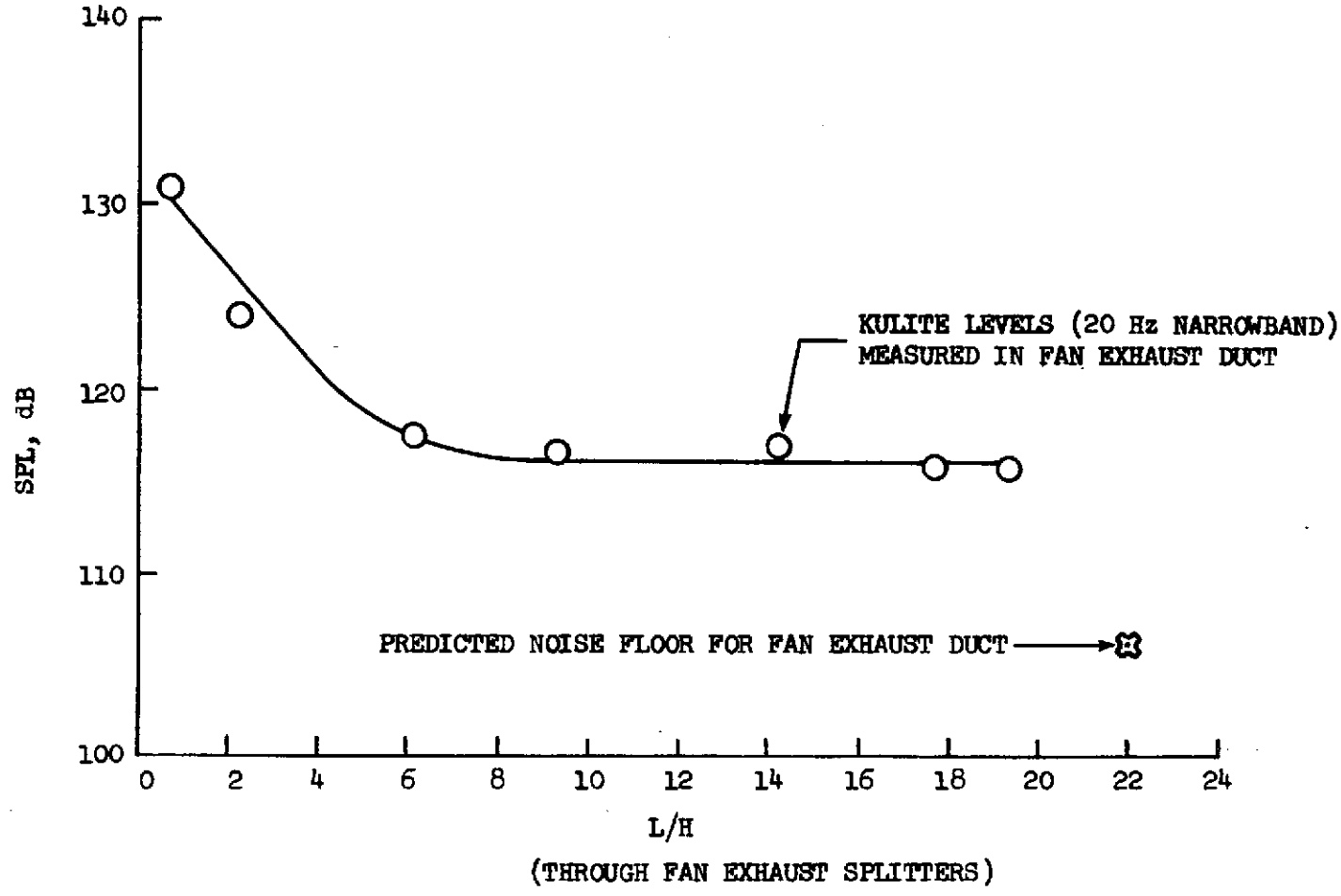

FIGURE IV B-16

TF34 FULLY SUPPRESSED NACELLE

CROSS-CORRELATION ANALYSIS OF FAN EXHAUST DUCT KULITE PRESSURE TRANSDUCERS, KULITE #2 TO KULITE #3 (TEST 2)

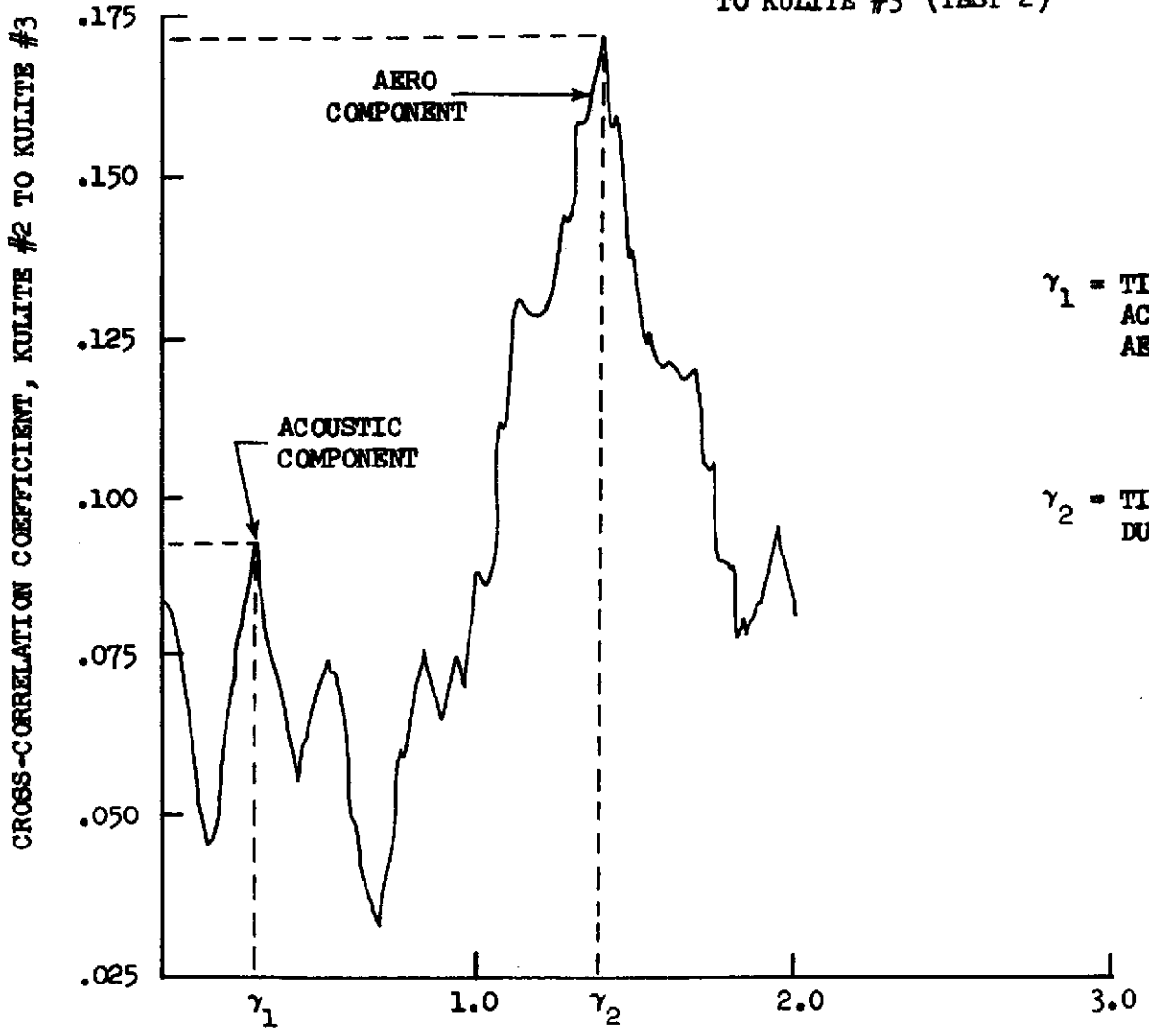

γ_1 = TIME DELAY CORRESPONDING TO ACOUSTIC VELOCITY PLUS DUCT AERODYNAMIC FLOW VELOCITY

γ_2 = TIME DELAY CORRESPONDING TO DUCT AERODYNAMIC FLOW VELOCITY

FIGURE IV B-17

RATIO OF MEASURED KULITE SIGNAL TO ACTUAL ACOUSTIC FLOOR

- TF34 QUIET NACELLE FAN EXHAUST DUCT
- MAX POWER
- o INLET SPLITTERS FORWARD (TEST 2)

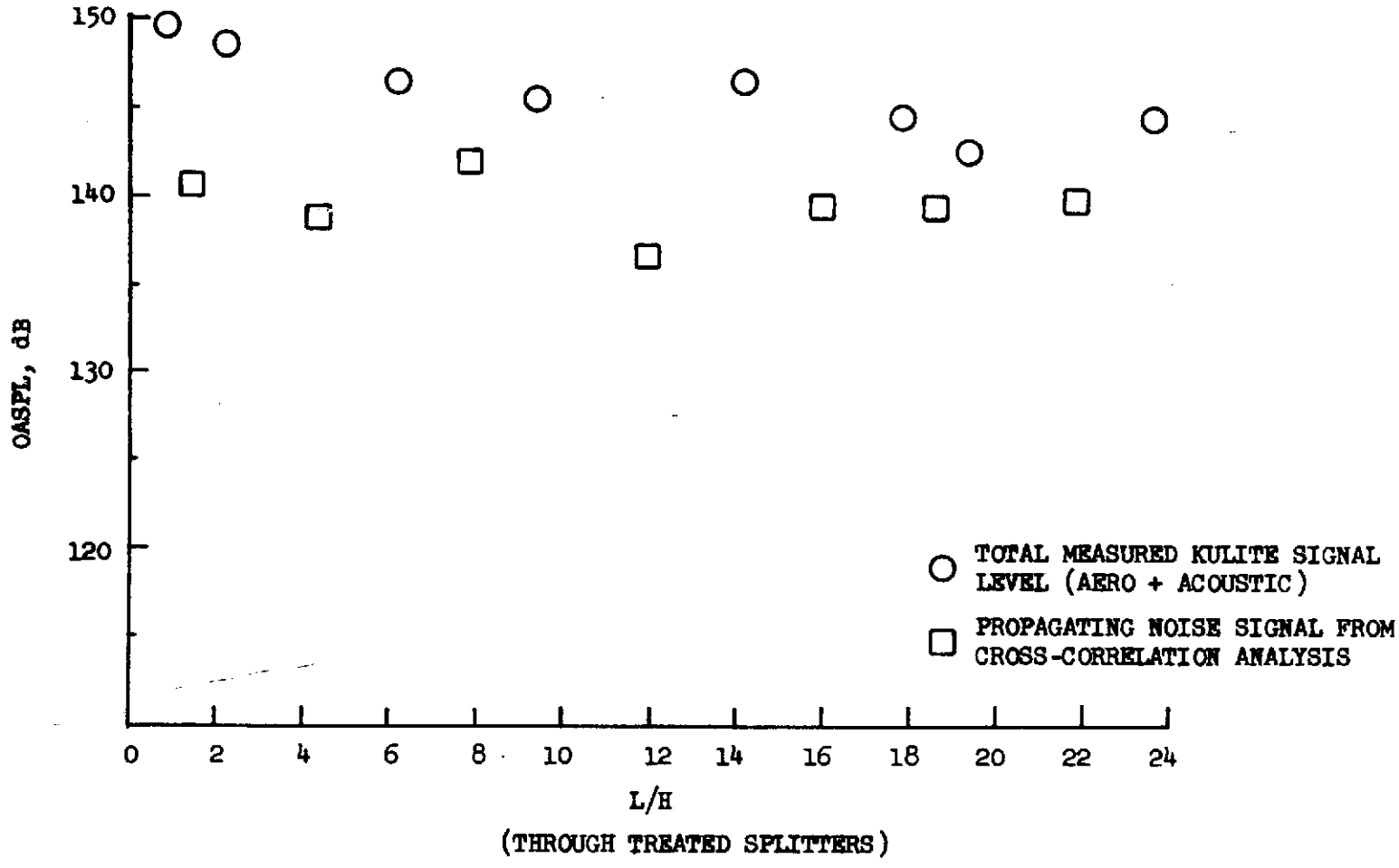

FIGURE IV C-1

TF34 FULLY SUPPRESSED NACELLE

UNCORRECTED ARRAY DATA

- MEASURING ANGLE = 50°
- ARRAY POINTED AT INLET
- 5100 RPM
- 20 Hz BANDWIDTH

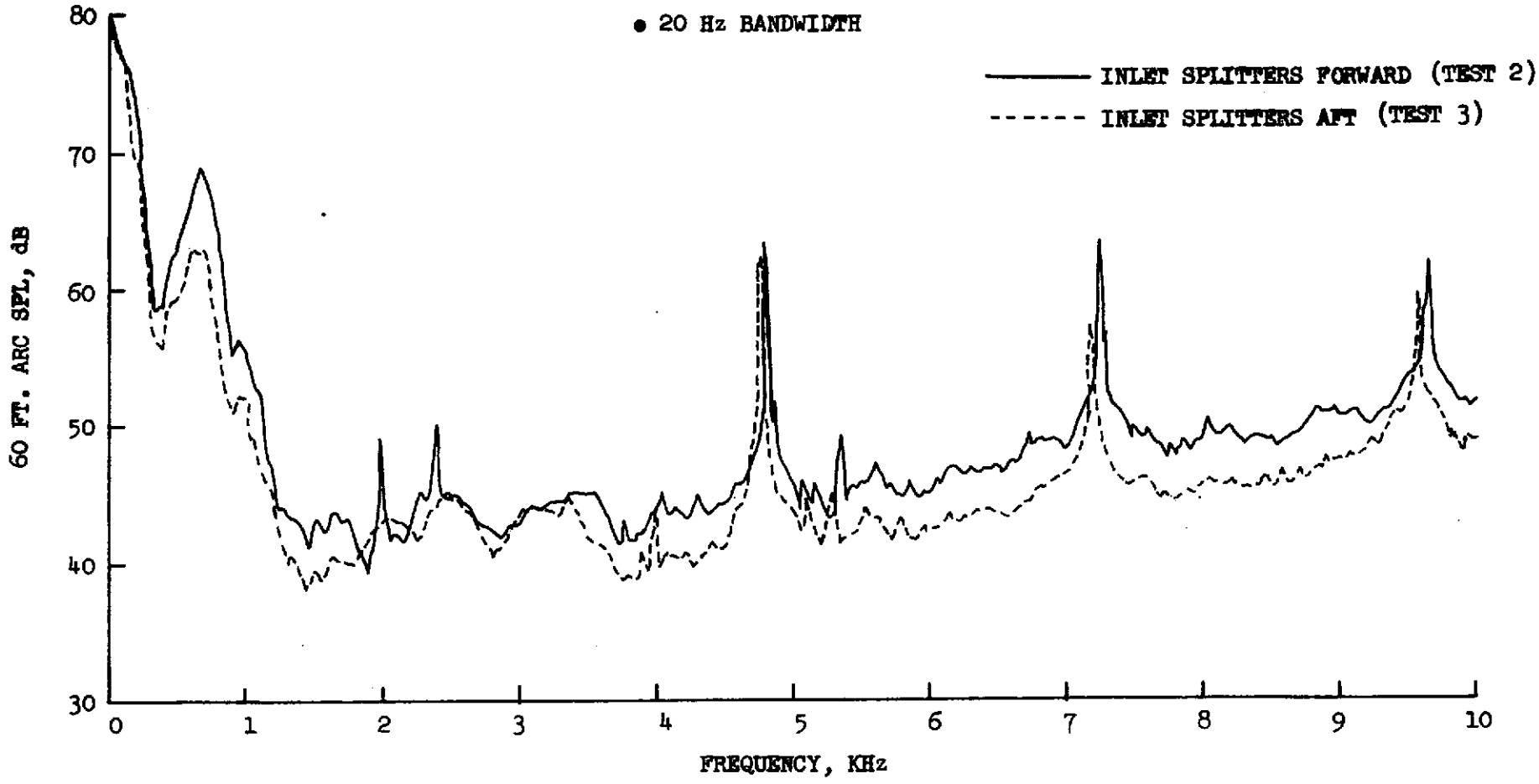

FIGURE IV C-2

TF34 FULLY SUPPRESSED NACELLE

UNCORRECTED ARRAY DATA

- MEASURING ANGLE = 110°
- ARRAY POINTED AT FAN EXHAUST
- 5100 RPM
- 20 Hz BANDWIDTH

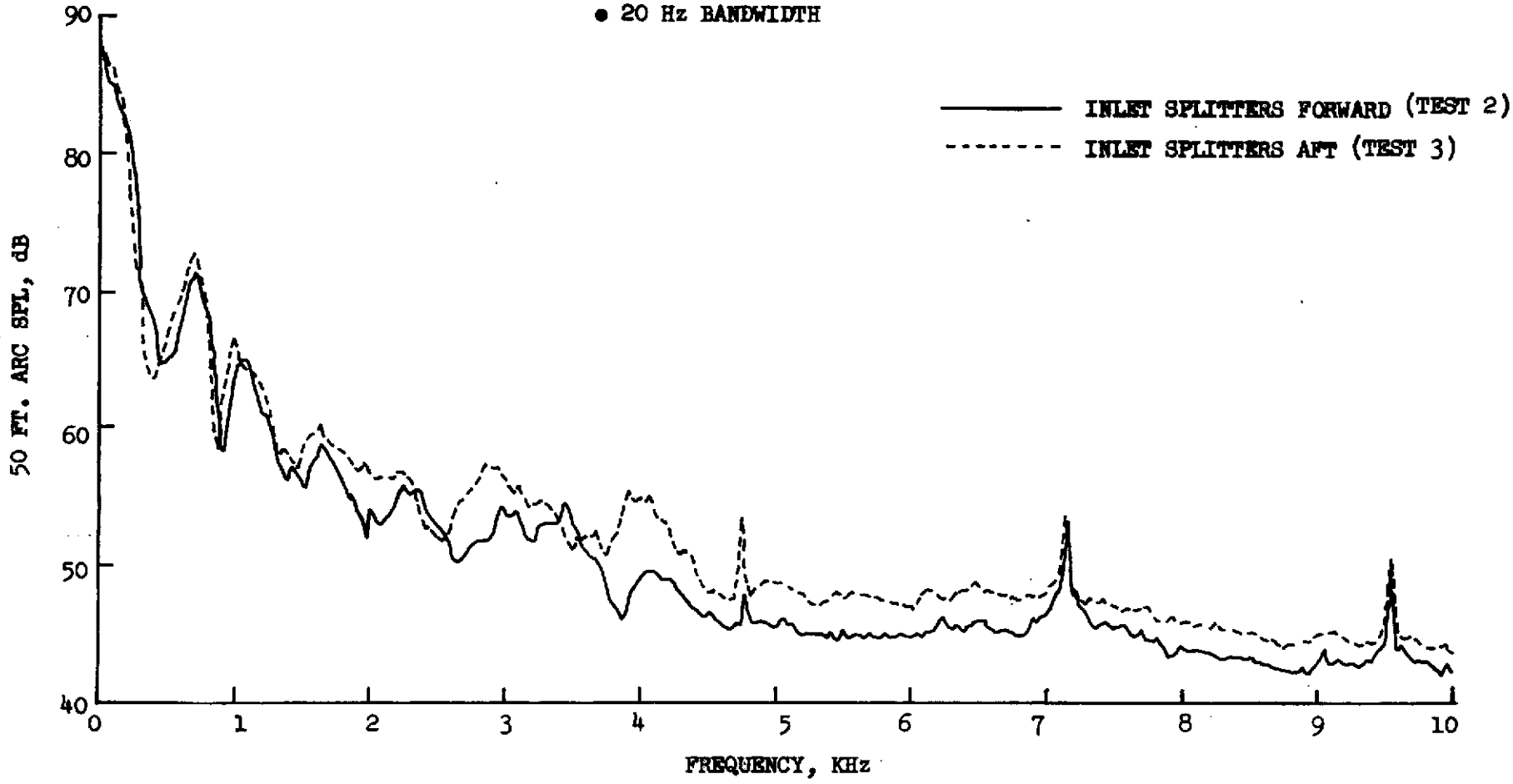

FIGURE IV C-3

TF34 FULLY SUPPRESSED NACELLE

UNCORRECTED ARRAY DATA

- MEASURING ANGLE = 50°
- ARRAY POINTED AT INLET
- MAX POWER
- 20 Hz BANDWIDTH

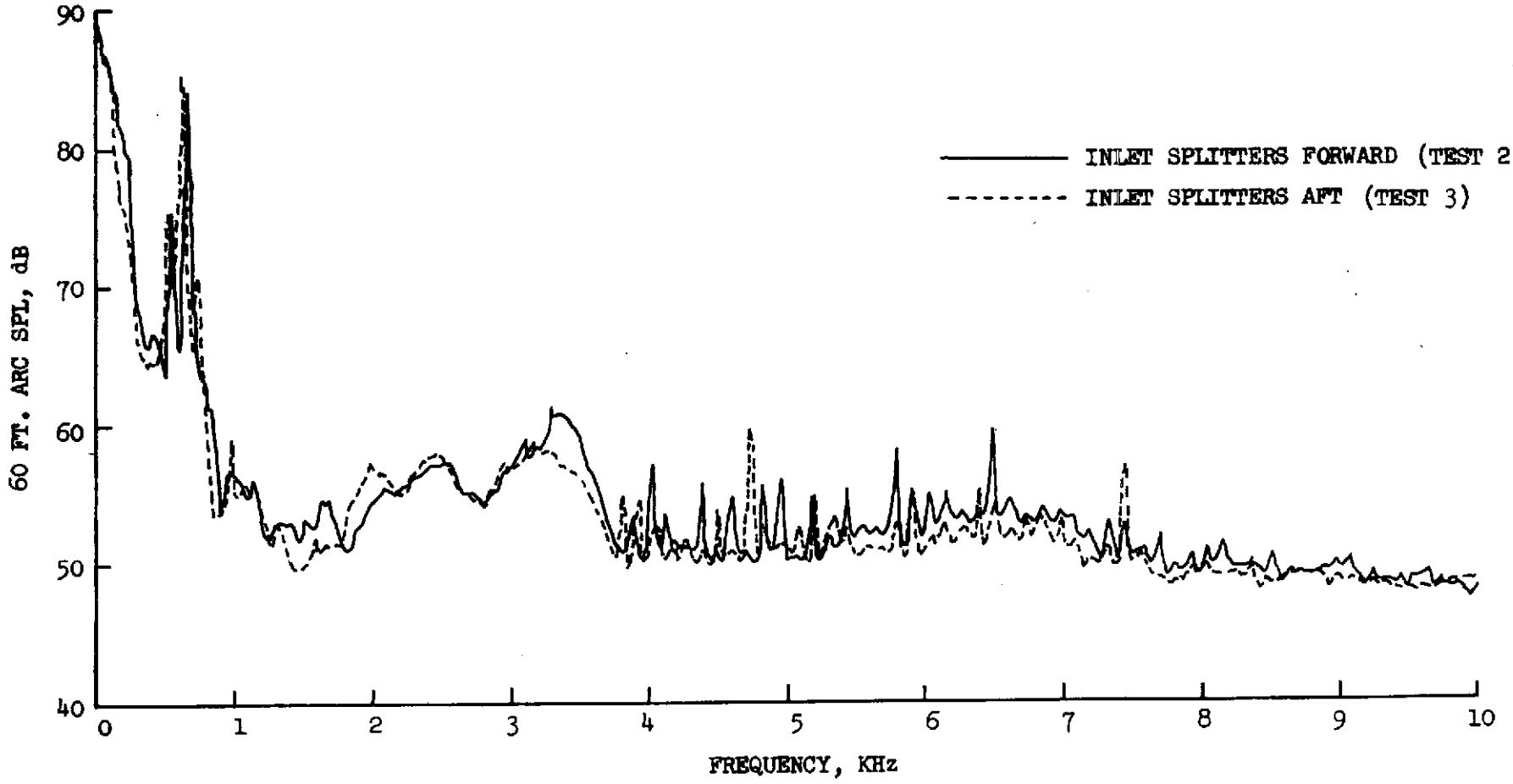

FIGURE IV C-4

TF34 FULLY SUPPRESSED NACELLE

UNCORRECTED ARRAY DATA

- MEASURING ANGLE = 110°
- ARRAY POINTED AT FAN EXHAUST
- MAX POWER
- 20 Hz BANDWIDTH

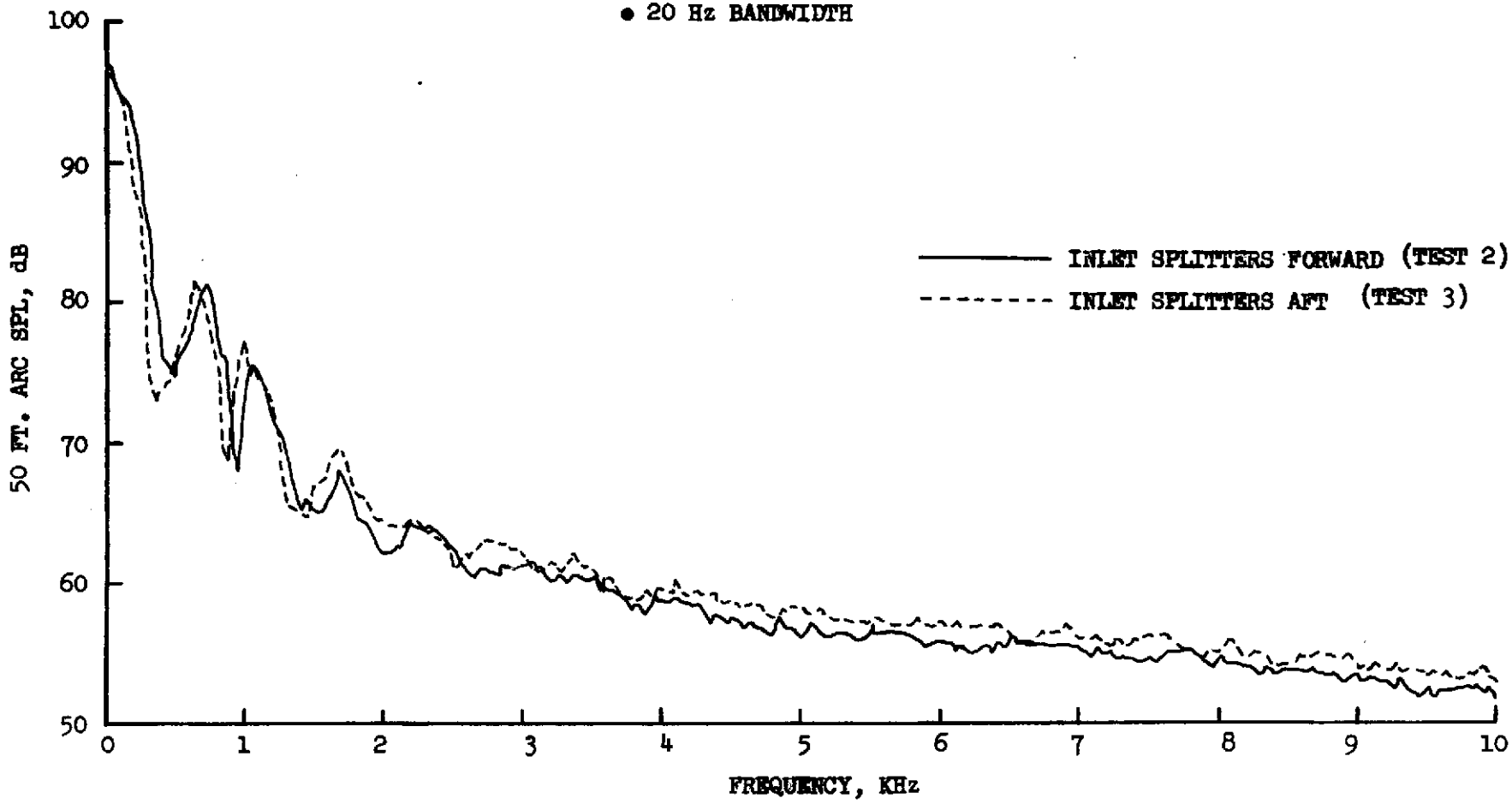

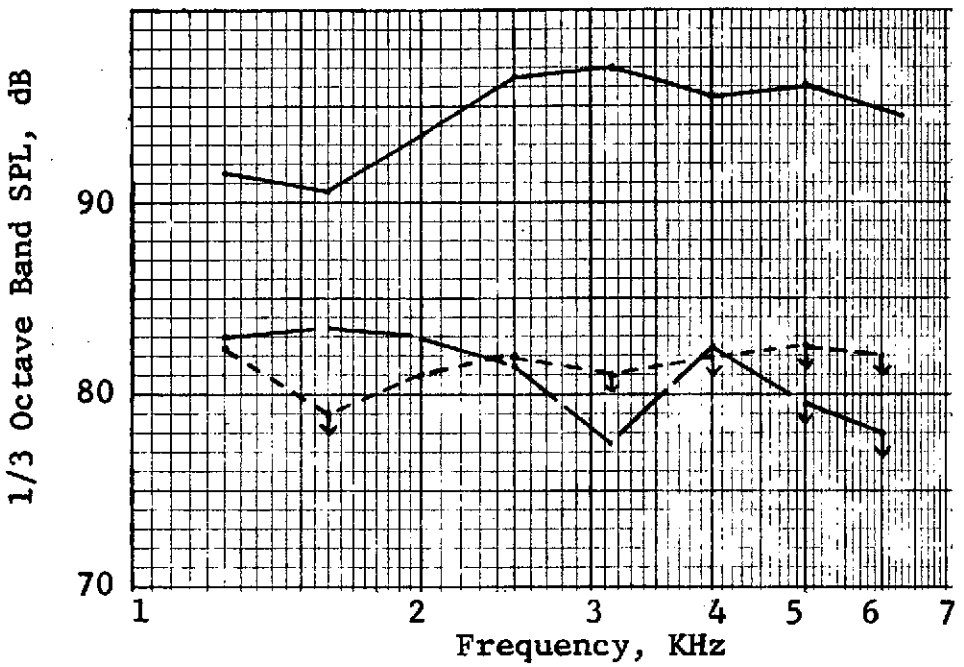

BASELINE CONFIGURATION
(120° Referenced to Fan Discharge Plane)

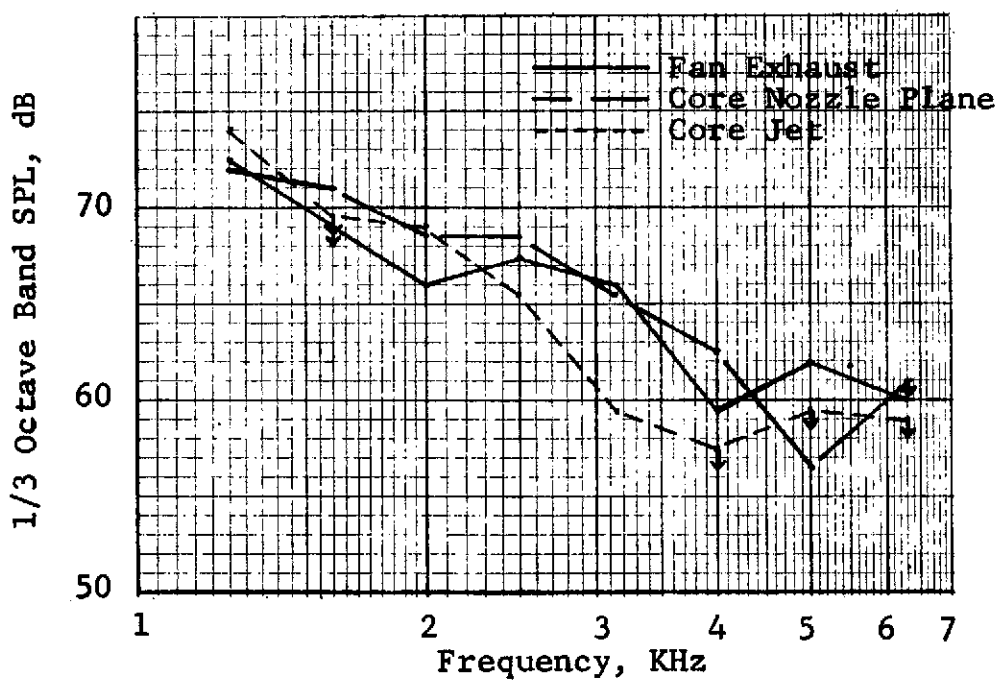

FULLY SUPPRESSED CONFIGURATION
(110° Referenced to Core Discharge Plane)
(TEST 2)

FIGURE IV C-5

TF34 ENGINE COMPONENT SPECTRA AT MAX AFT ANGLE
APPROACH (5100 RPM)

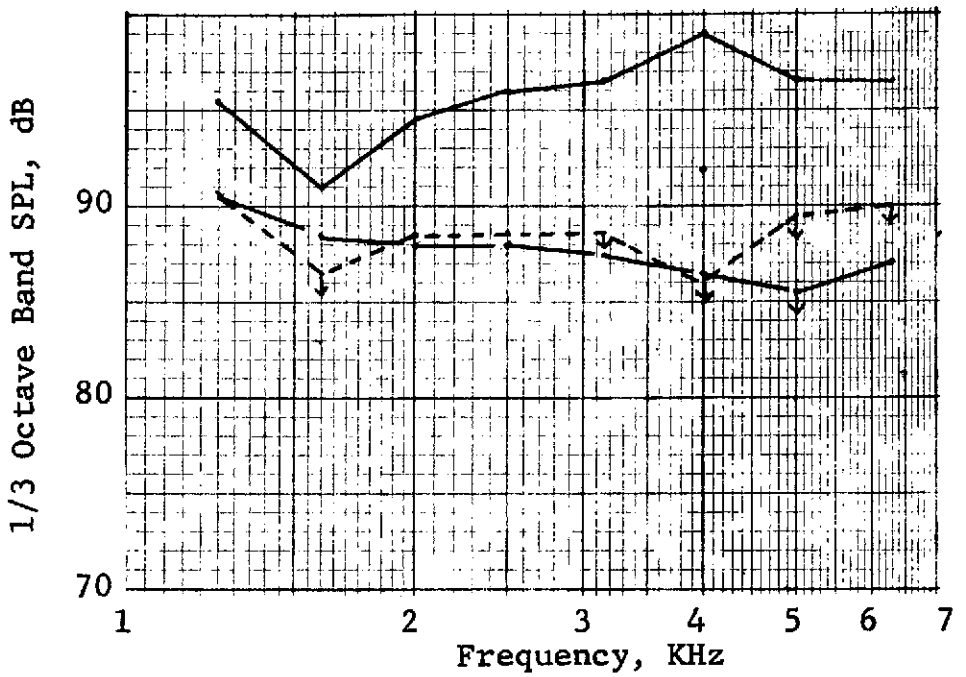

BASELINE CONFIGURATION
(120° Referenced to Fan Discharge Plane)

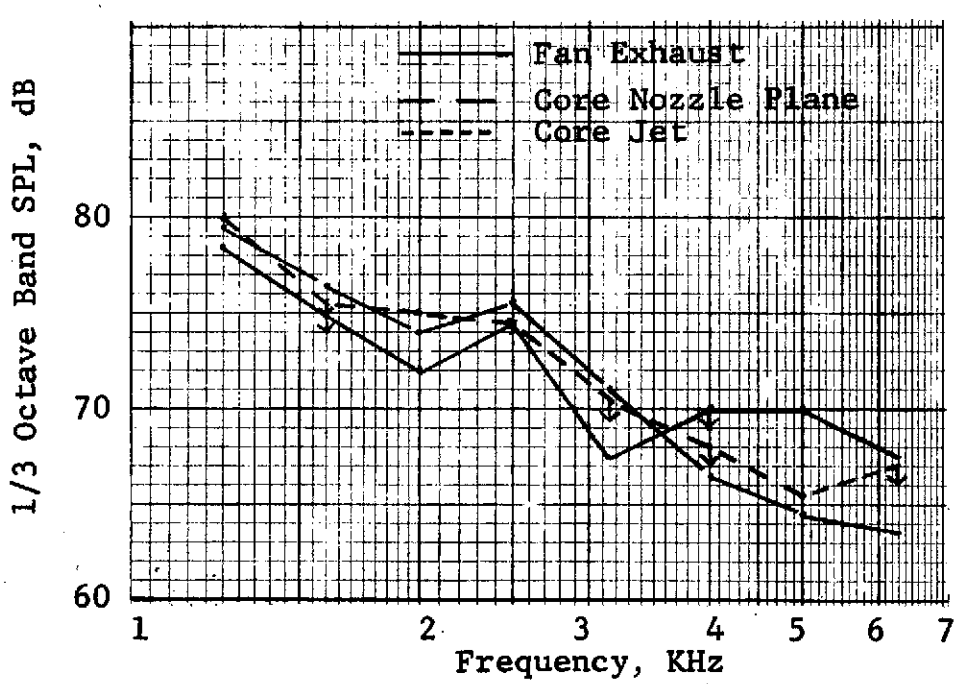

FULLY SUPPRESSED CONFIGURATION
(110° Referenced to Core Discharge Plane)

(TEST 2)

TF34 ENGINE COMPONENT SPECTRA AT MAX AFT ANGLE
(6200 RPM)

FIGURE IV C-6

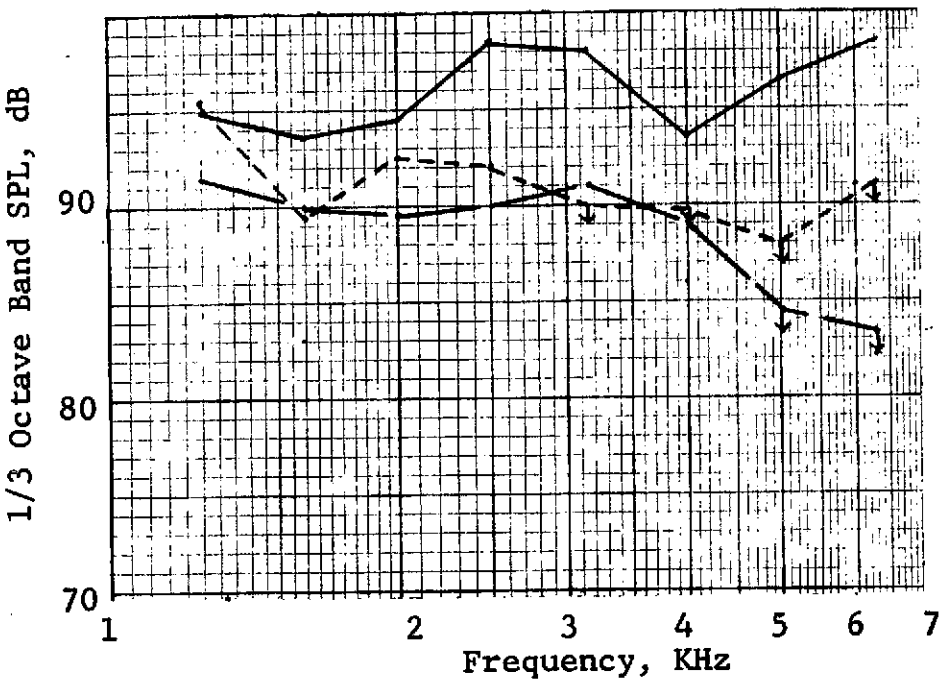

BASELINE CONFIGURATION
(120° Referenced to Fan Discharge Plane)

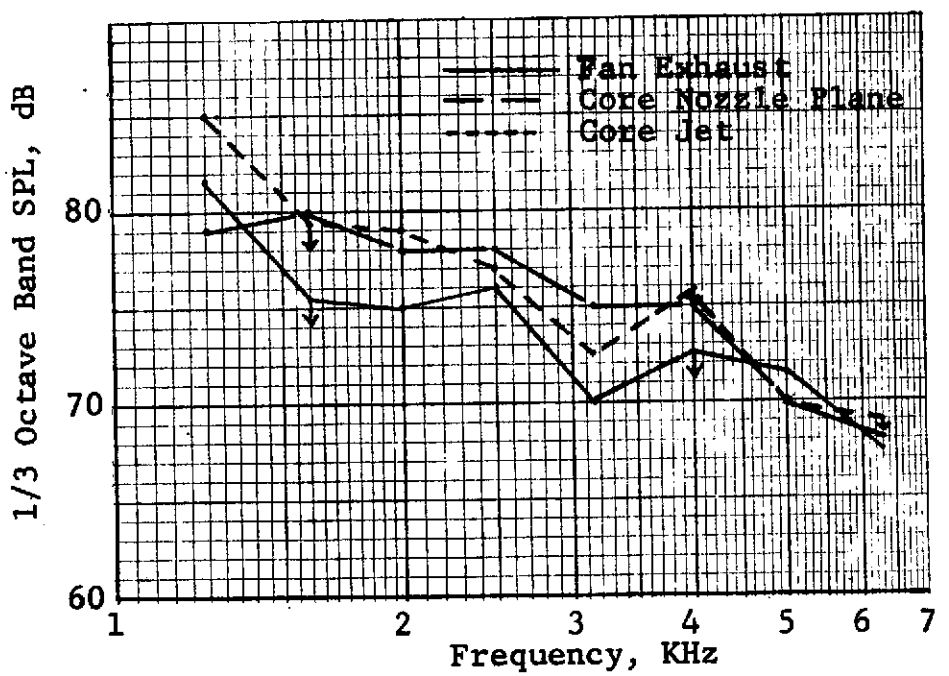

FULLY SUPPRESSED CONFIGURATION
(110° Referenced to Core Discharge Plane)

(TEST 2)

. TF34 ENGINE COMPONENT SPECTRA AT MAX AFT ANGLE
(7100 RPM)

FIGURE IV C-7

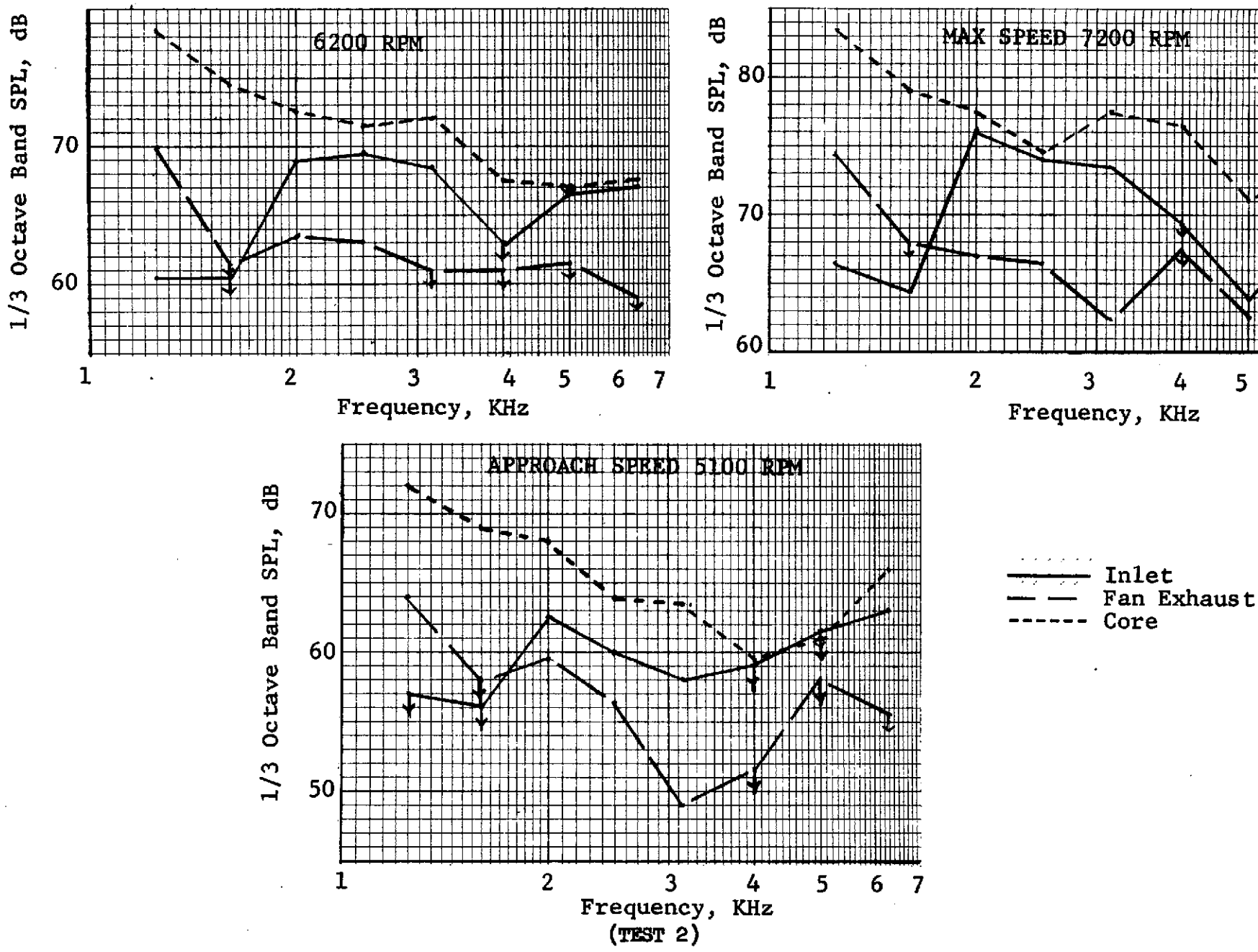

FULLY SUPPRESSED TF34 ENGINE COMPONENT SPECTRA AT MAX FWD ANGLE (50°)

FIGURE IV C-8

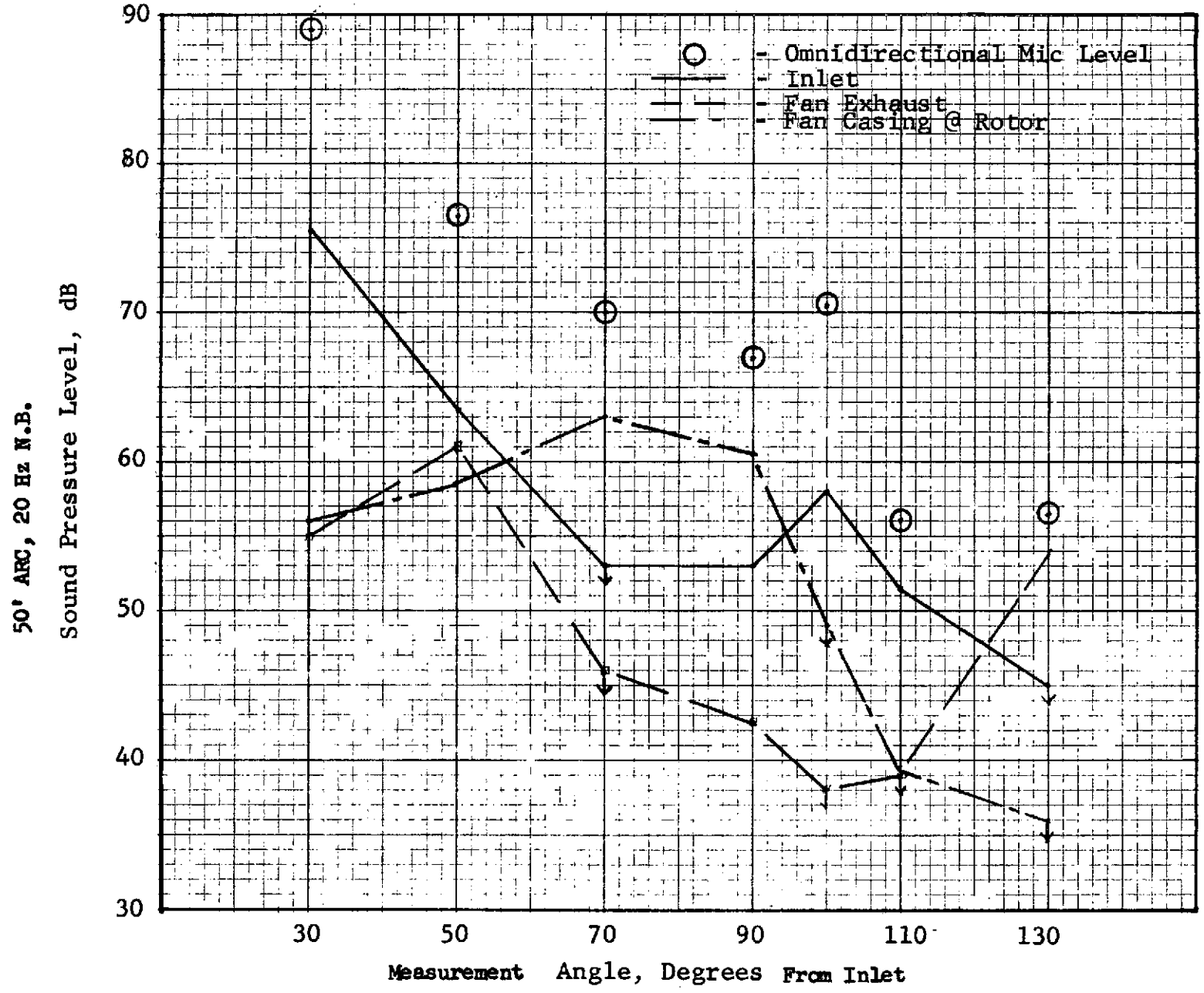

FULLY SUPPRESSED TF34 FAN DIRECTIVITY FOR 2ND HARMONIC (4780 HZ) AT 5100 RPM (TEST 2)

FIGURE IV C-9

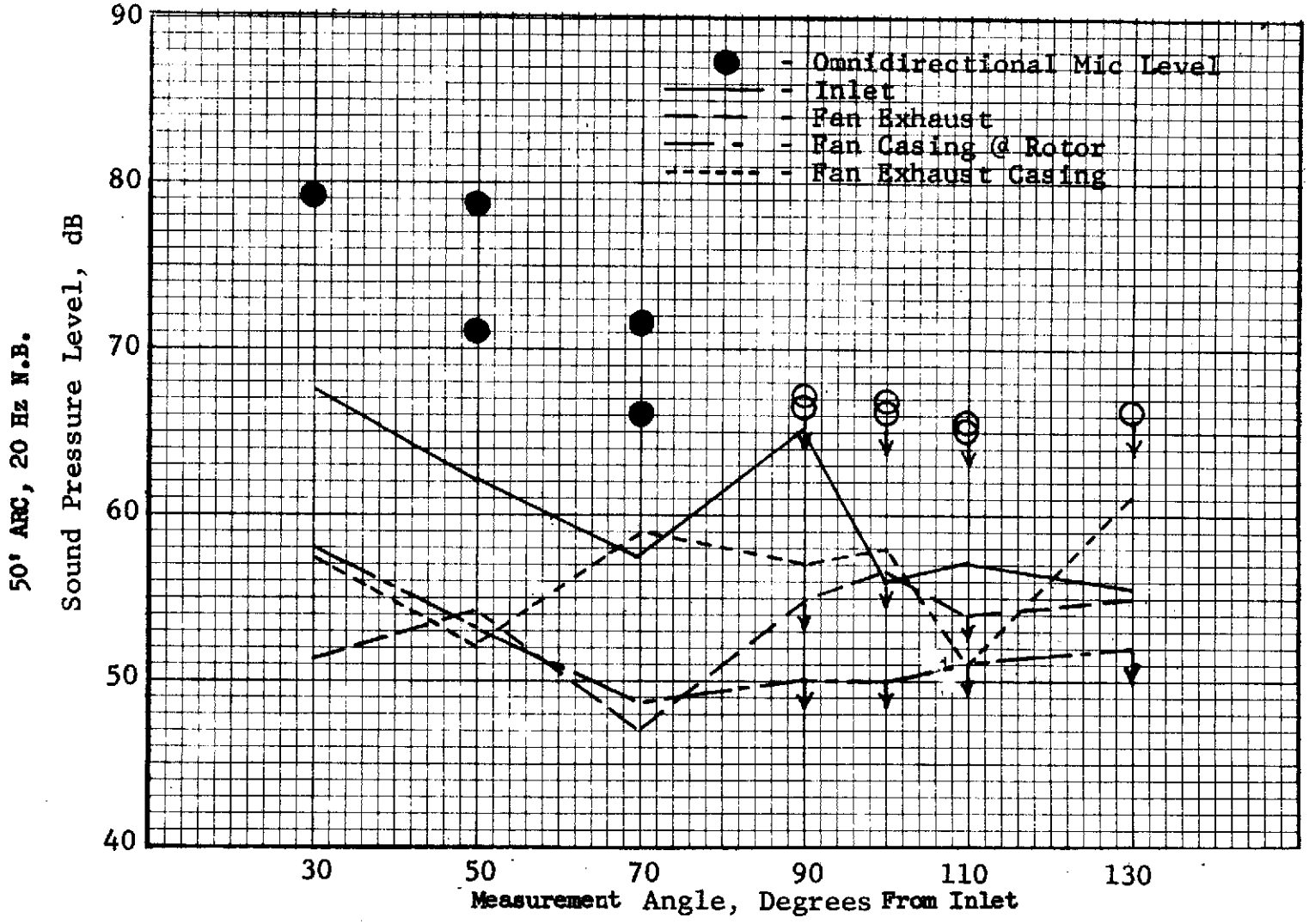

FULLY SUPPRESSED TF34 FAN DIRECTIVITY FOR FUNDAMENTAL (3300 Hz)
AT 7100 RPM (TEST 2)

FIGURE IV C-10

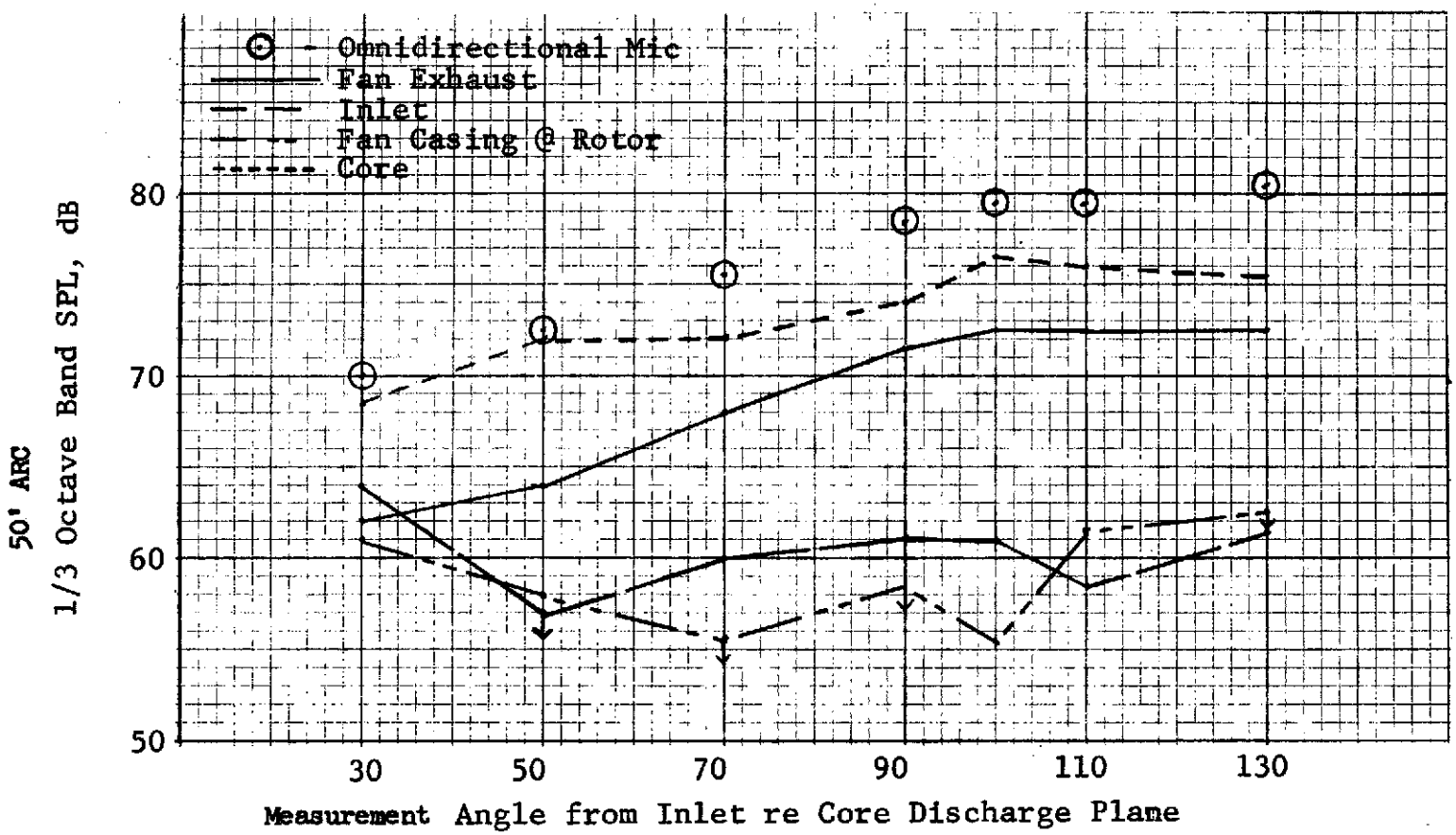

FIGURE IV C-11

TF34 BROADBAND SOURCE DIRECTIVITY AT APPROACH POWER (5100 RPM) AT 1.25 KHz (FULLY SUPPRESSED CONFIG.)

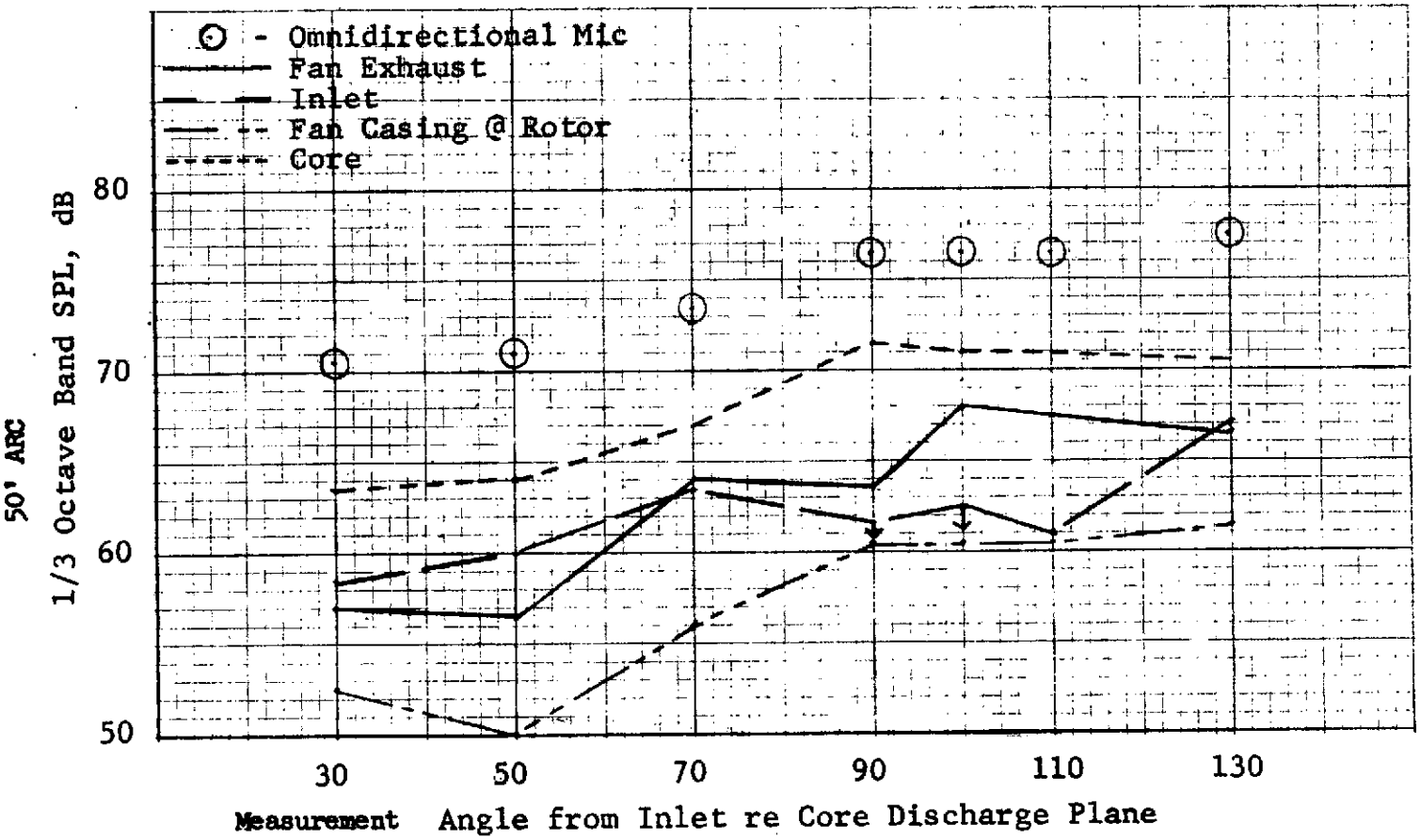

FIGURE IV C-12

TF34 BROADBAND SOURCE DIRECTIVITY AT APPROACH POWER (5100 RPM)
AT 2.5 KHz (FULLY SUPPRESSED CONFIG.)

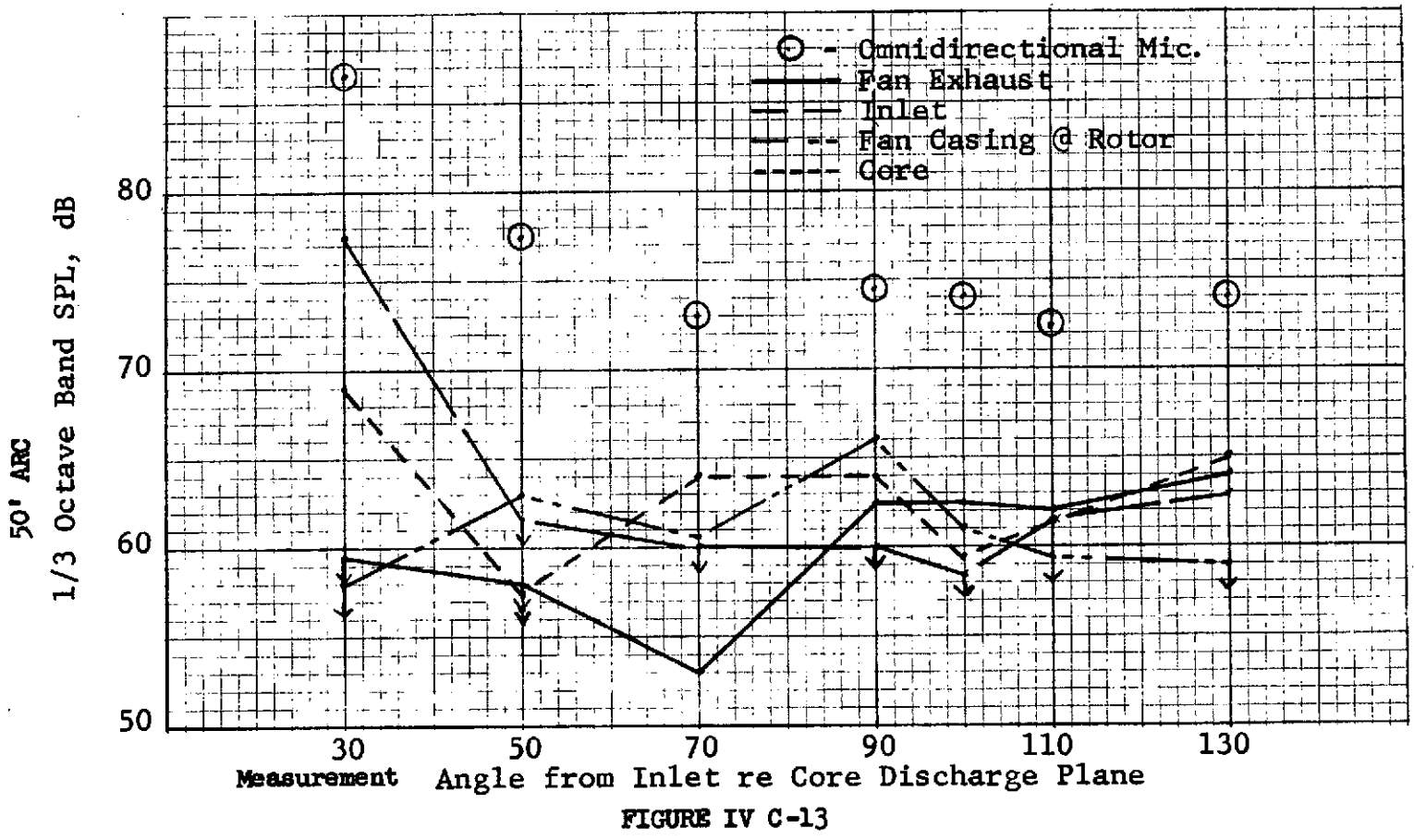

FIGURE IV C-13

TF34 BROADBAND SOURCE DIRECTIVITY AT APPROACH POWER (5100 RPM)
AT 5.0 KHz (FULLY SUPPRESSED CONFIG.)

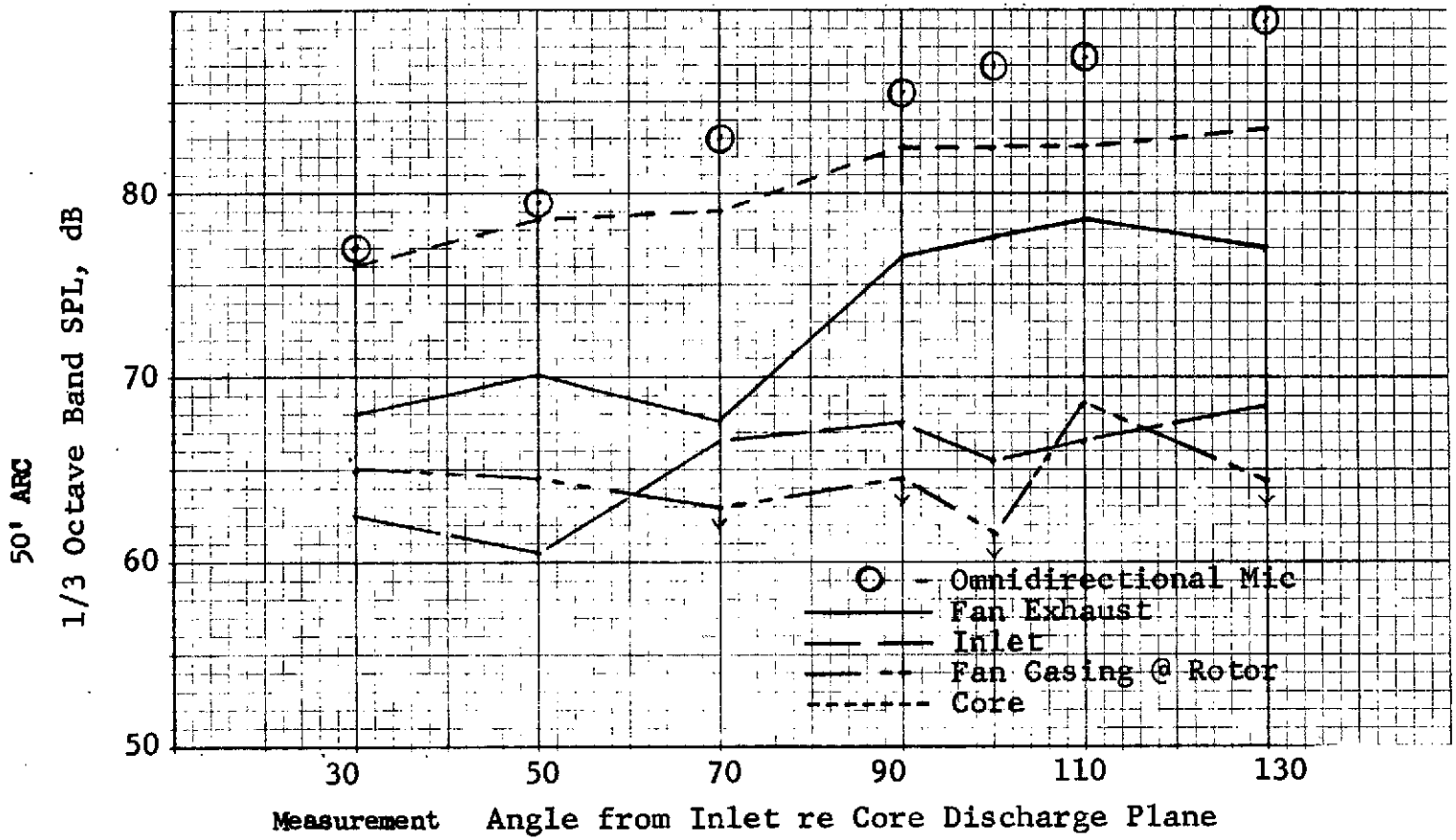

FIGURE IV C-14

TF34 BROADBAND SOURCE DIRECTIVITY AT 6200 RPM, 1.25 KHz
(FULLY SUPPRESSED CONFIGURATION - TEST 2)

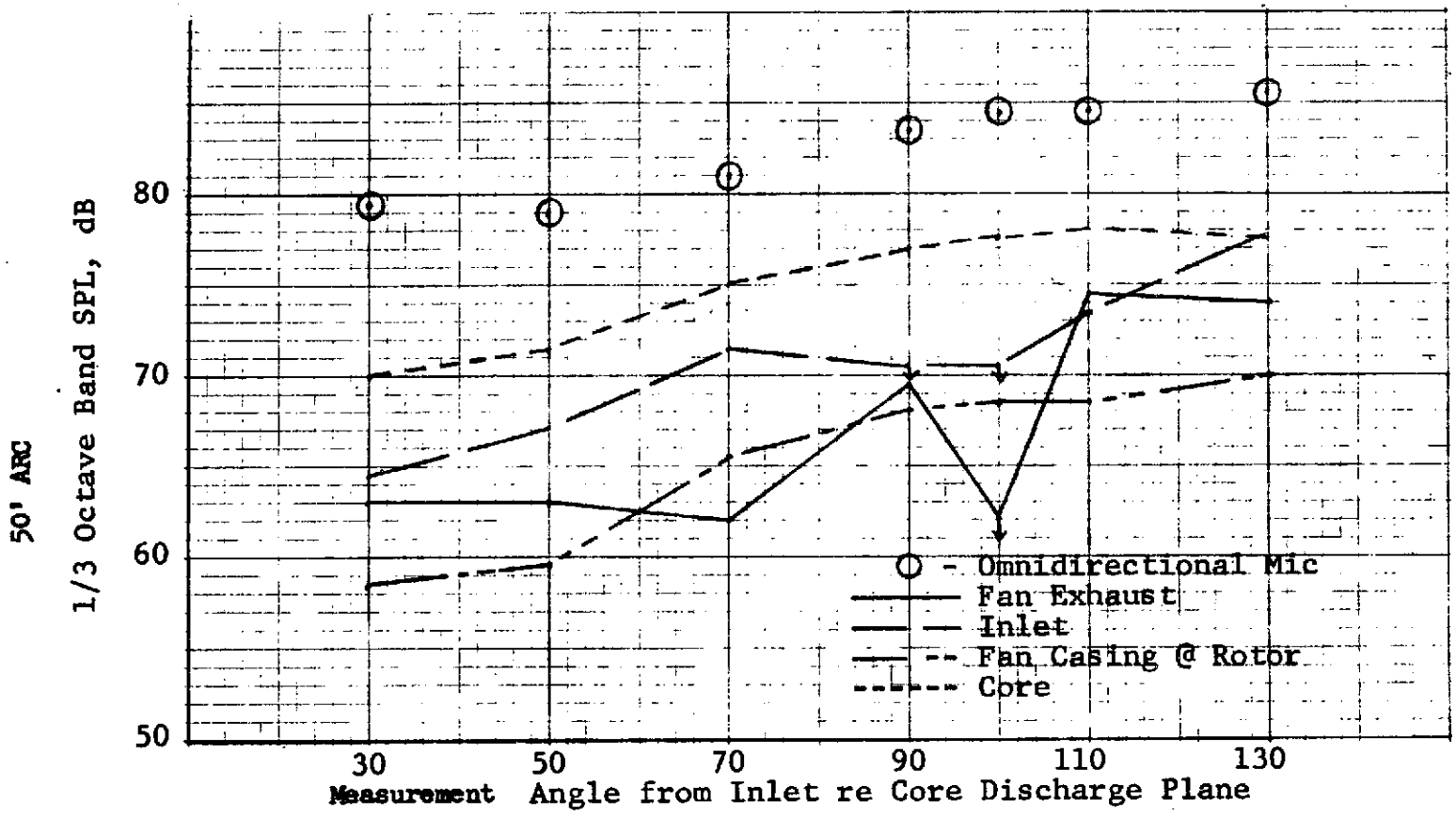

FIGURE IV C-15

TF34 BROADBAND SOURCE DIRECTIVITY AT 6200 RPM, 2.5 KHz
(FULLY SUPPRESSED CONFIGURATION

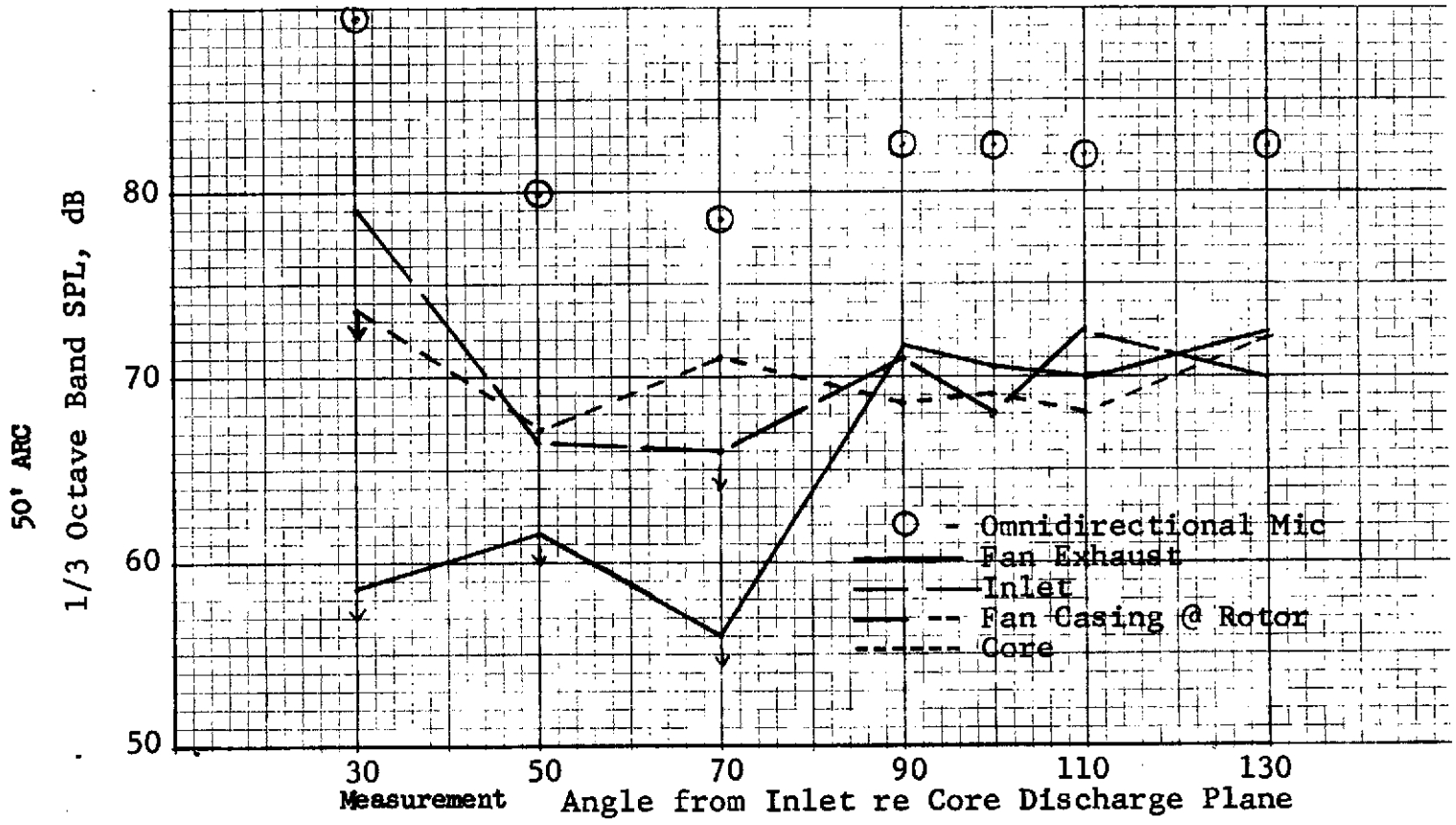

FIGURE IV C-16

TF34 BROADBAND SOURCE DIRECTIVITY AT 6200 RPM, 5.0 KHz
(FULLY SUPPRESSED CONFIGURATION

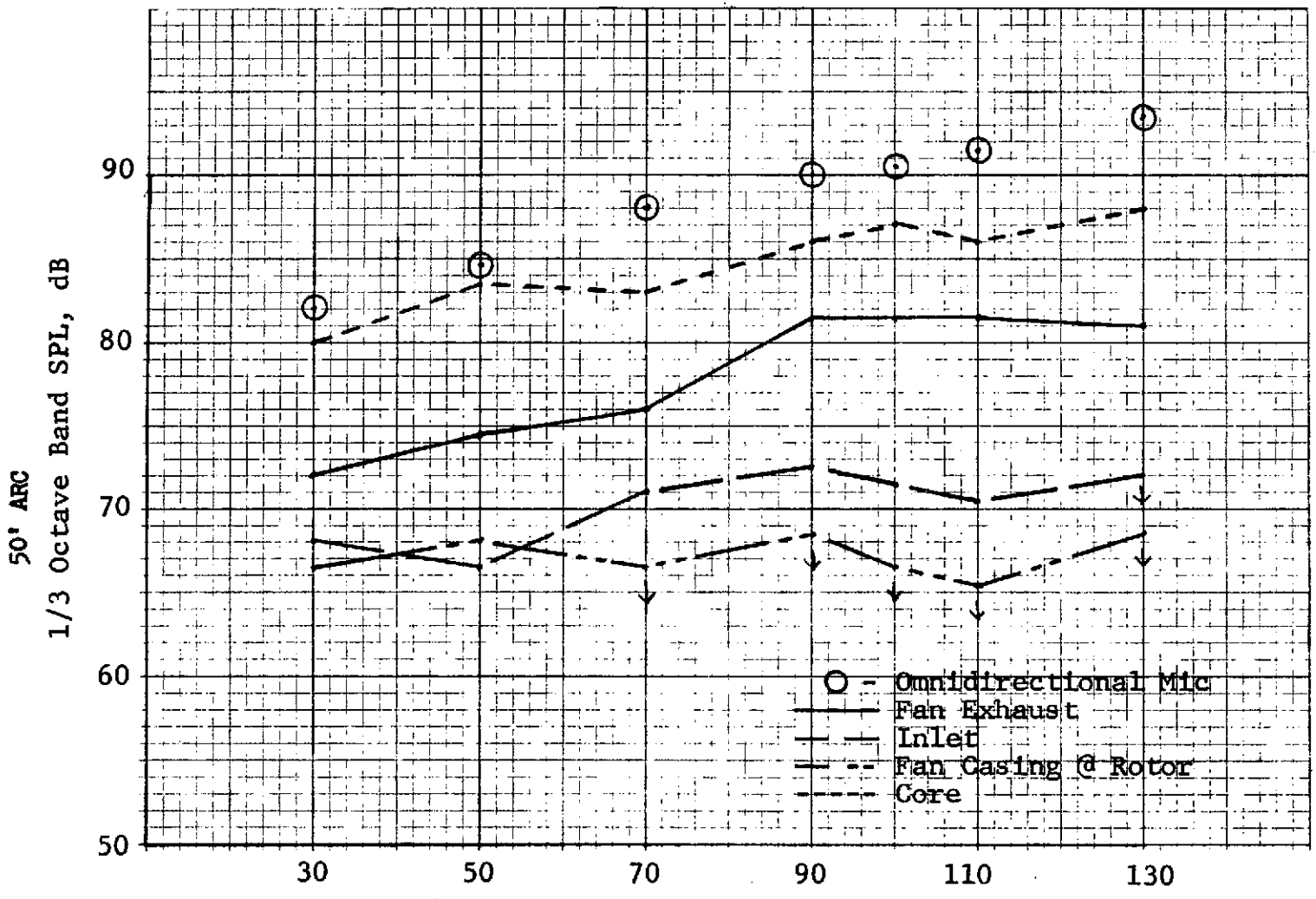

FIGURE IV C-17

TF34 BROADBAND SOURCE DIRECTIVITY AT MAX SPEED (~7100 RPM)
AT 1.25 KHz (FULLY SUPPRESSED CONFIGURATION - TEST 2)

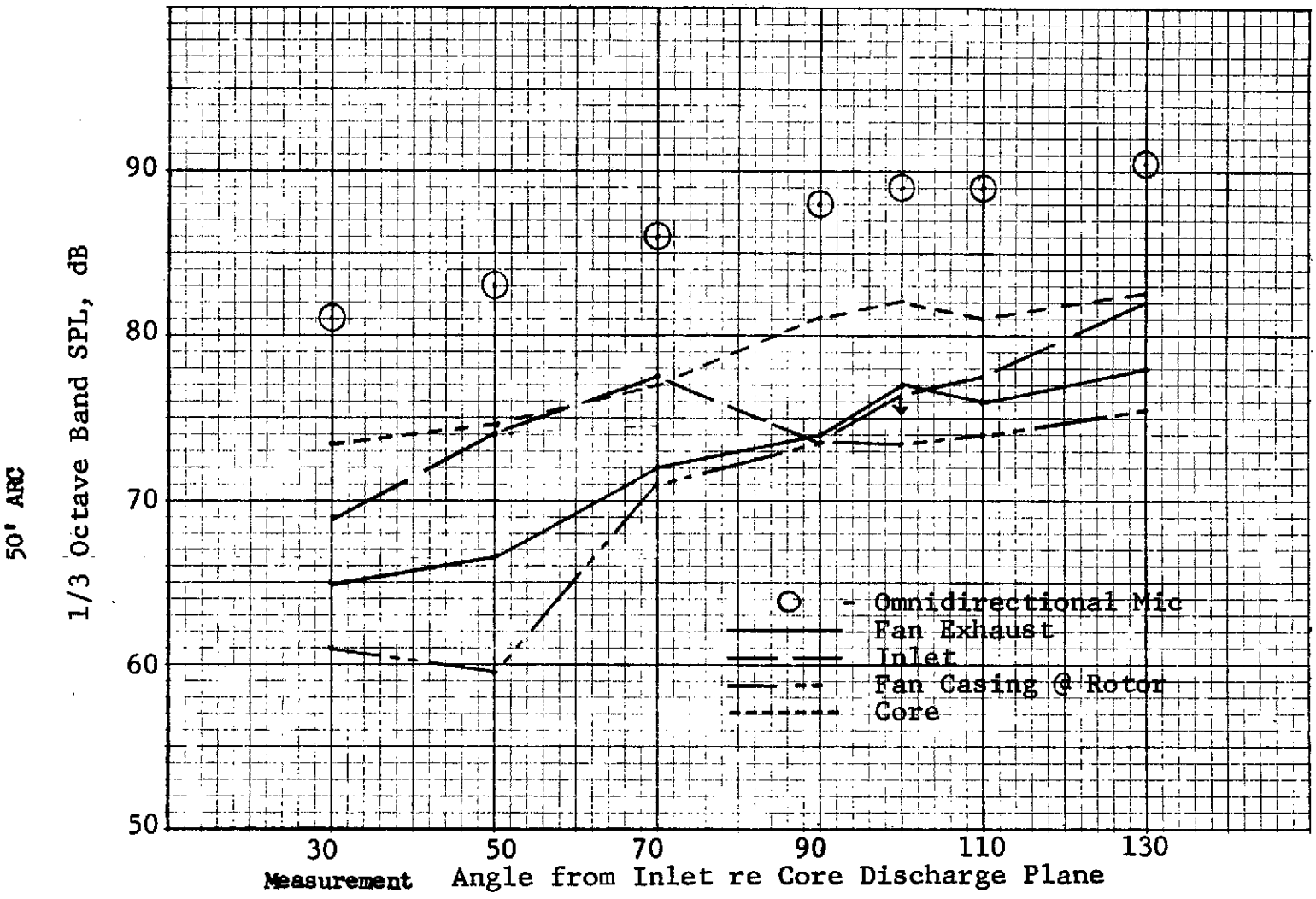

FIGURE IV C-18

TF34 BROADBAND SOURCE DIRECTIVITY AT MAX SPEED (~7100 RPM)
AT 2.5 KHz (FULLY SUPPRESSED CONFIGURATION - TEST 2)

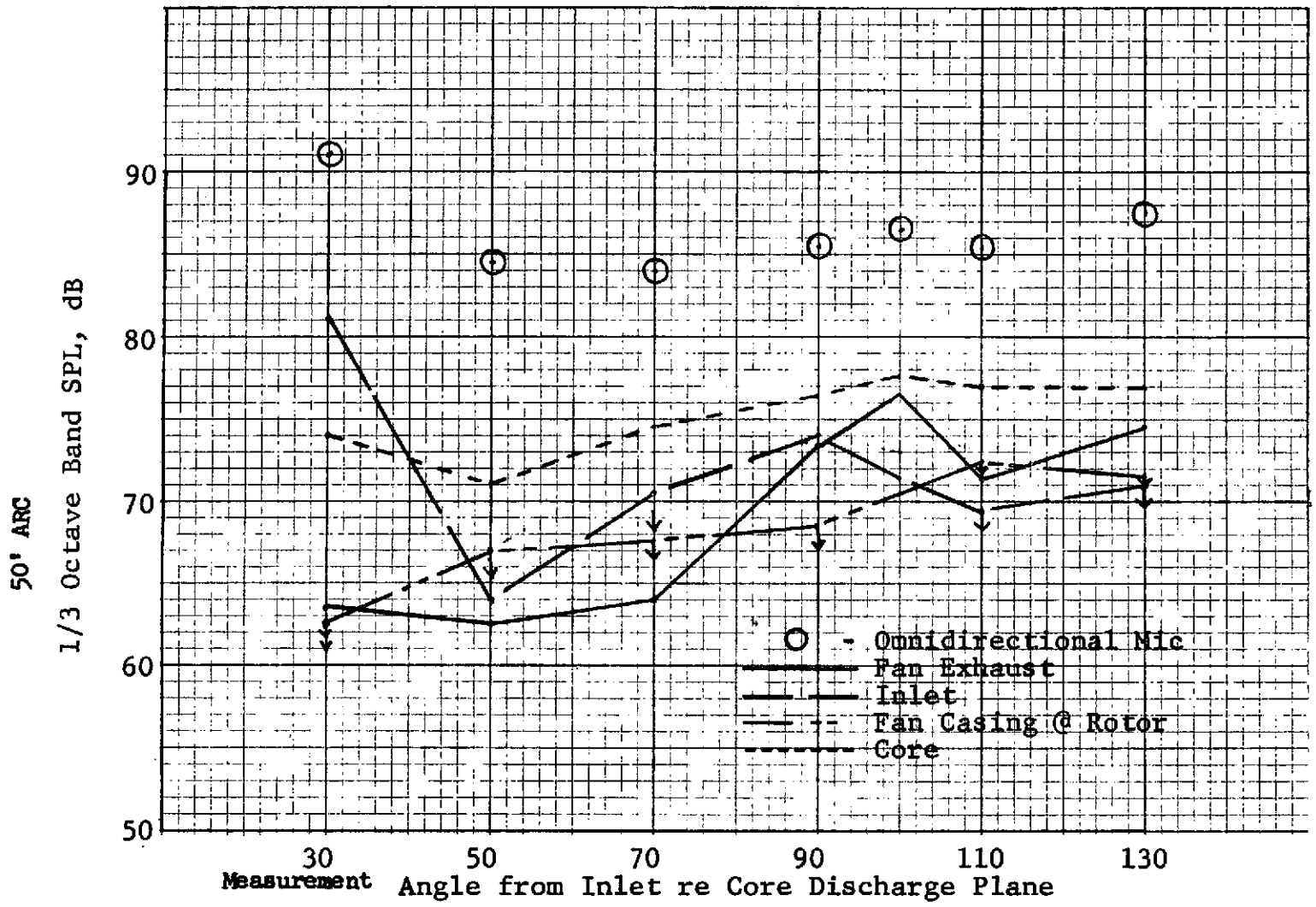

FIGURE IV C-19

TF34 BROADBAND SOURCE DIRECTIVITY AT MAX SPEED (~ 7100 RPM)
AT 5.0 KHz (FULLY SUPPRESSED CONFIGURATION - TEST 2)

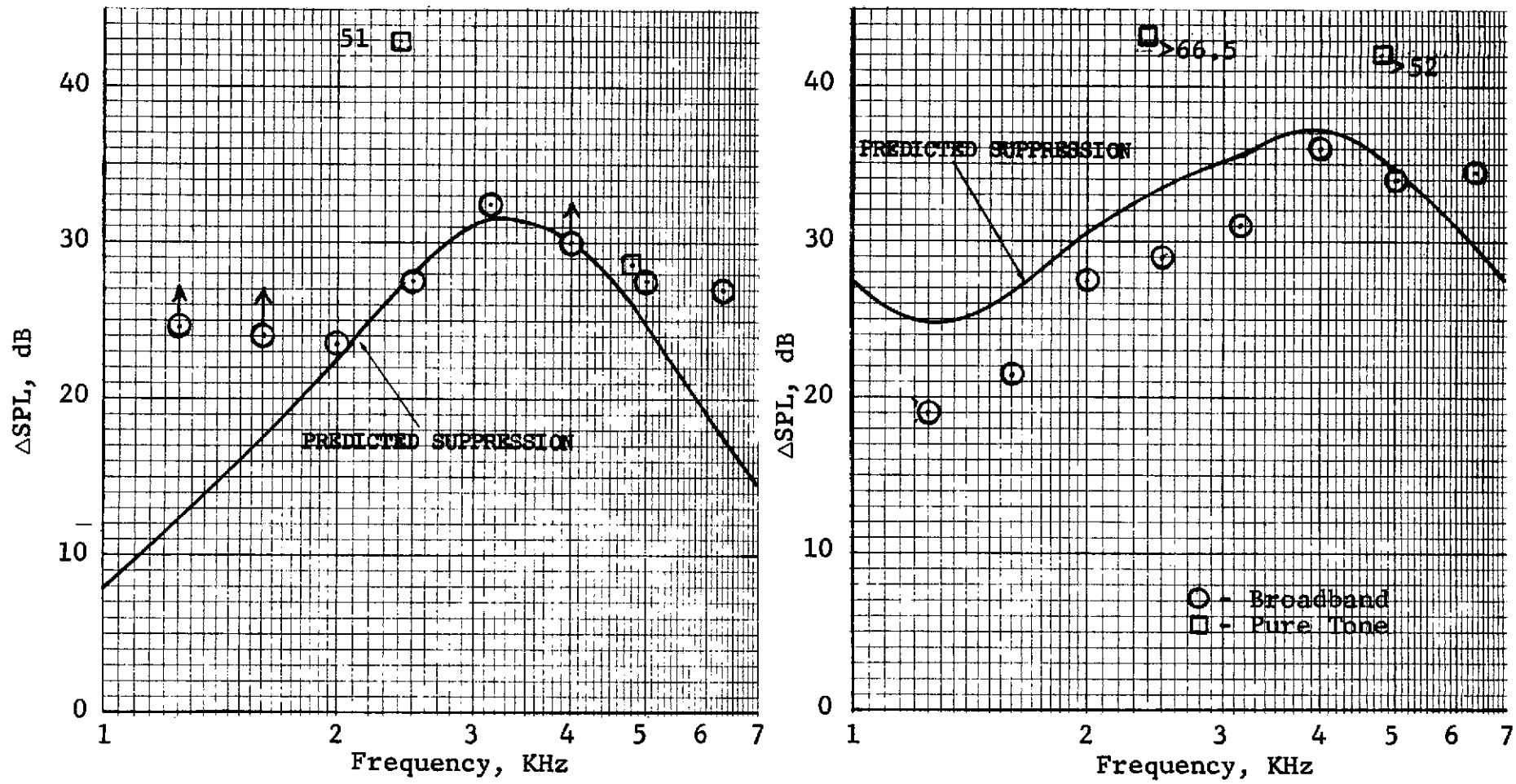

INLET SUPPRESSION AT MAX FWD ANGLE (50°)

FAN EXHAUST SUPPRESSION AT MAX AFT ANGLE (110°)

FIGURE IV C-20

TF34 FAN TREATMENT SUPPRESSION FROM DIRECTIONAL ACOUSTIC ARRAY

NF = 5100 RPM (APPROACH)

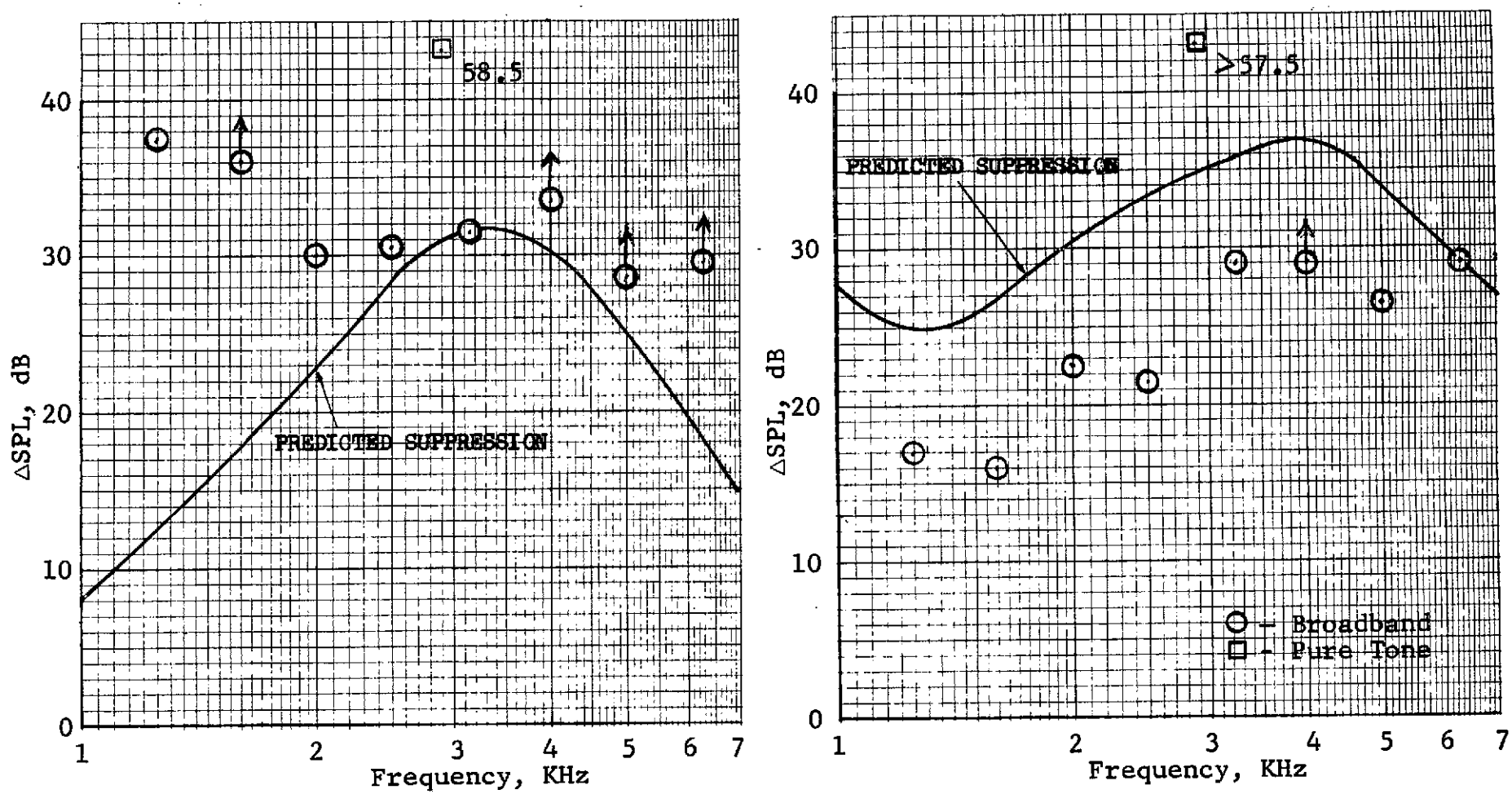

FIGURE IV C-21

TF34 FAN TREATMENT SUPPRESSION FROM DIRECTIONAL ACOUSTIC ARRAY

NF = 6200 RPM

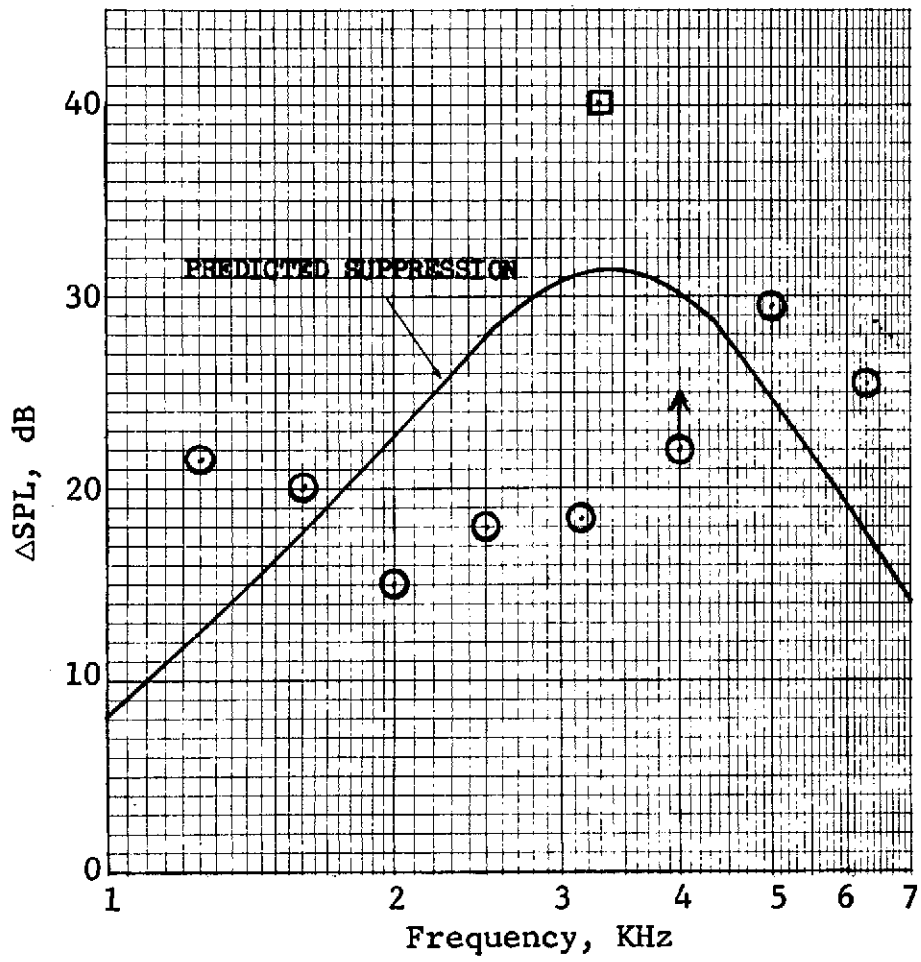

INLET SUPPRESSION AT MAX FWD ANGLE (50°)

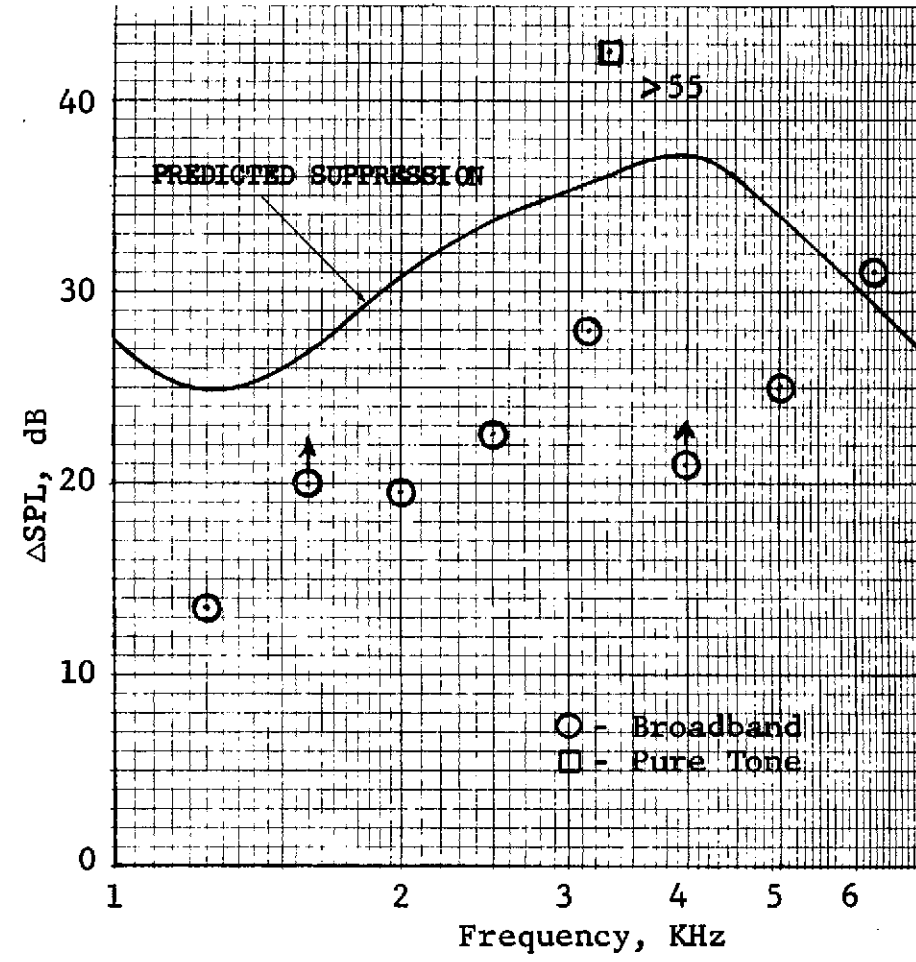

FAN EXHAUST SUPPRESSION AT MAX AFT ANGLE (110°)

FIGURE IV C-22

TF34 FAN TREATMENT SUPPRESSION FROM DIRECTIONAL ACOUSTIC ARRAY
NF = 7100 RPM (MAX)

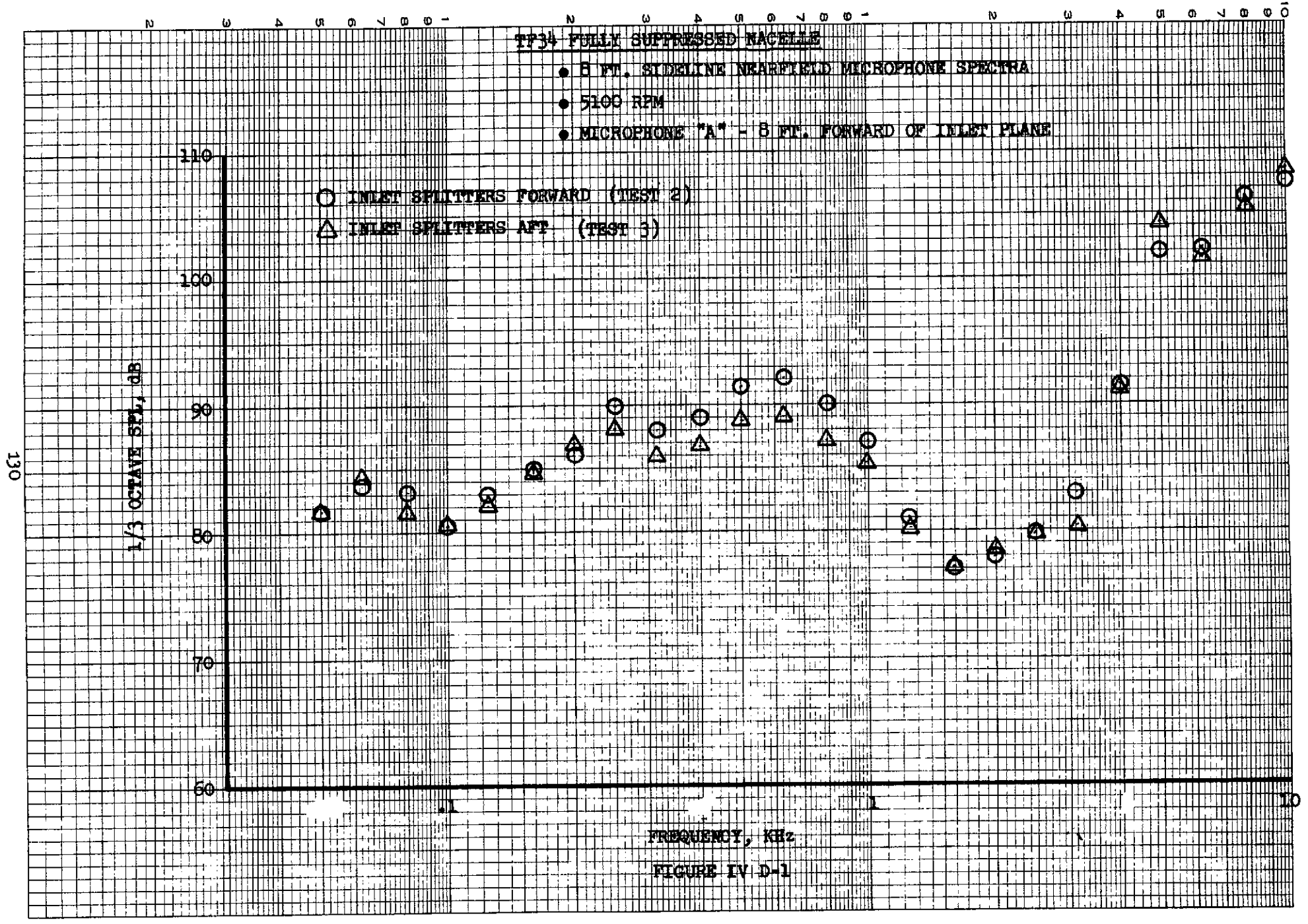

FIGURE IV D-1

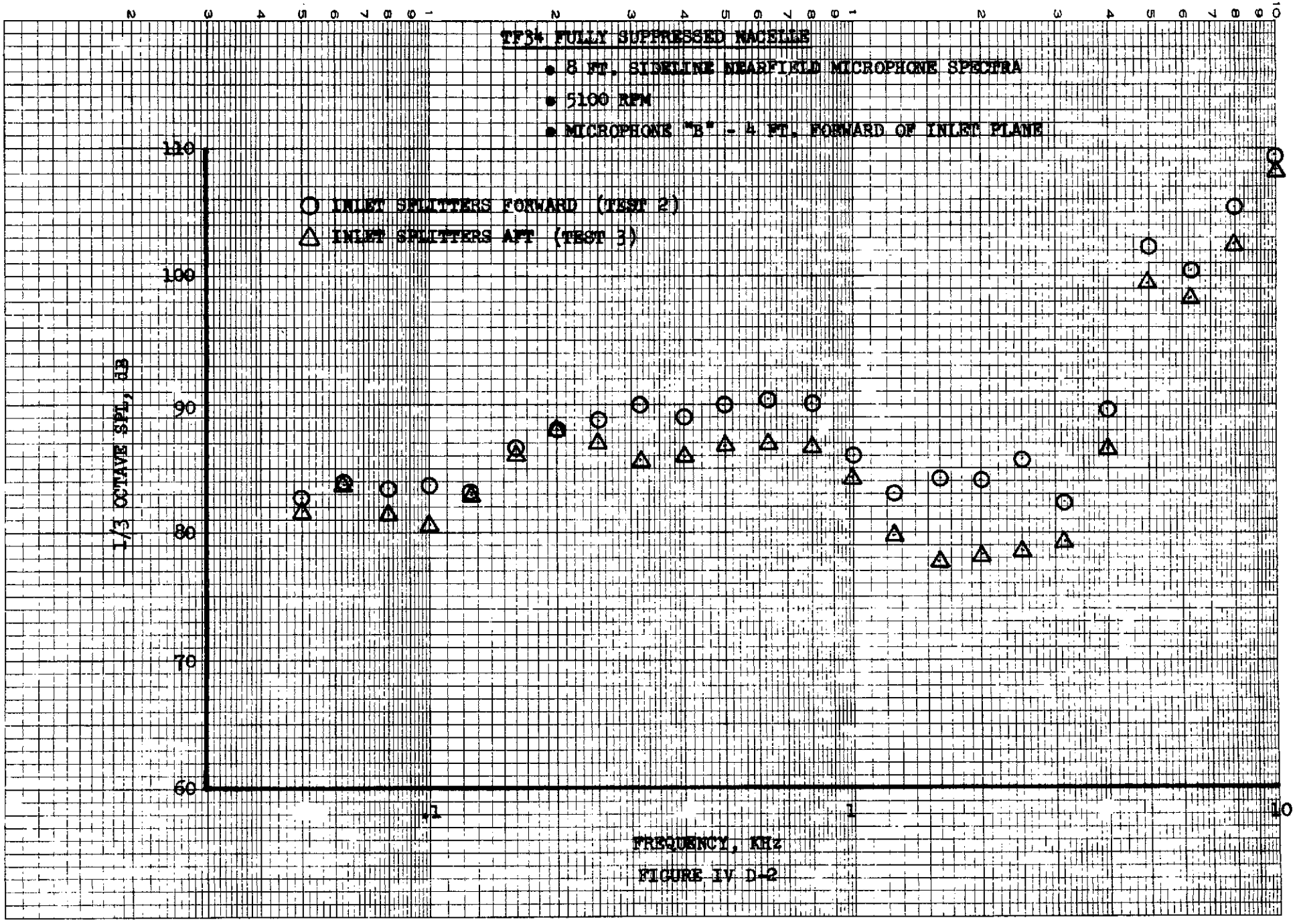

FIGURE IV D-2

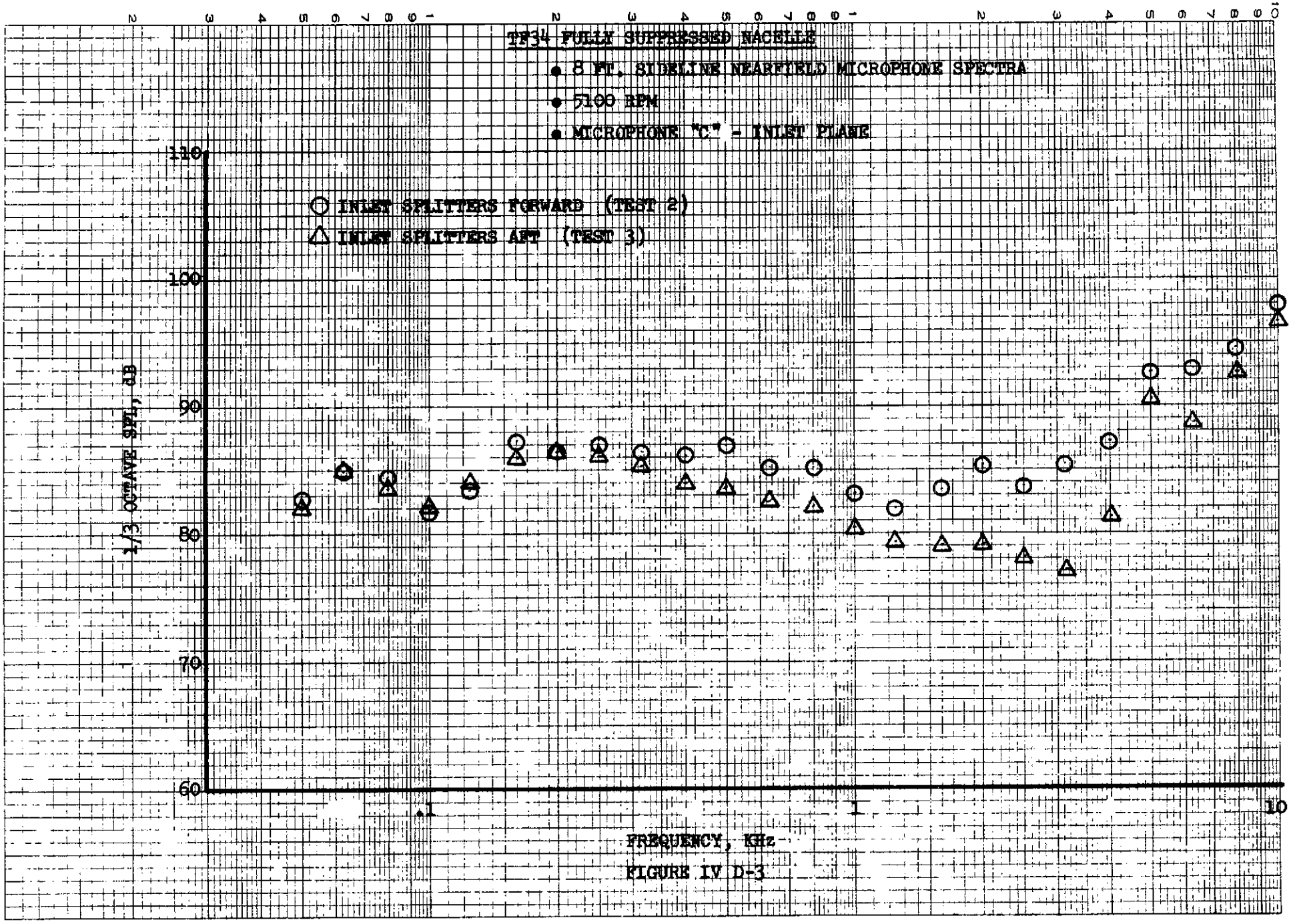

FIGURE IV D-3

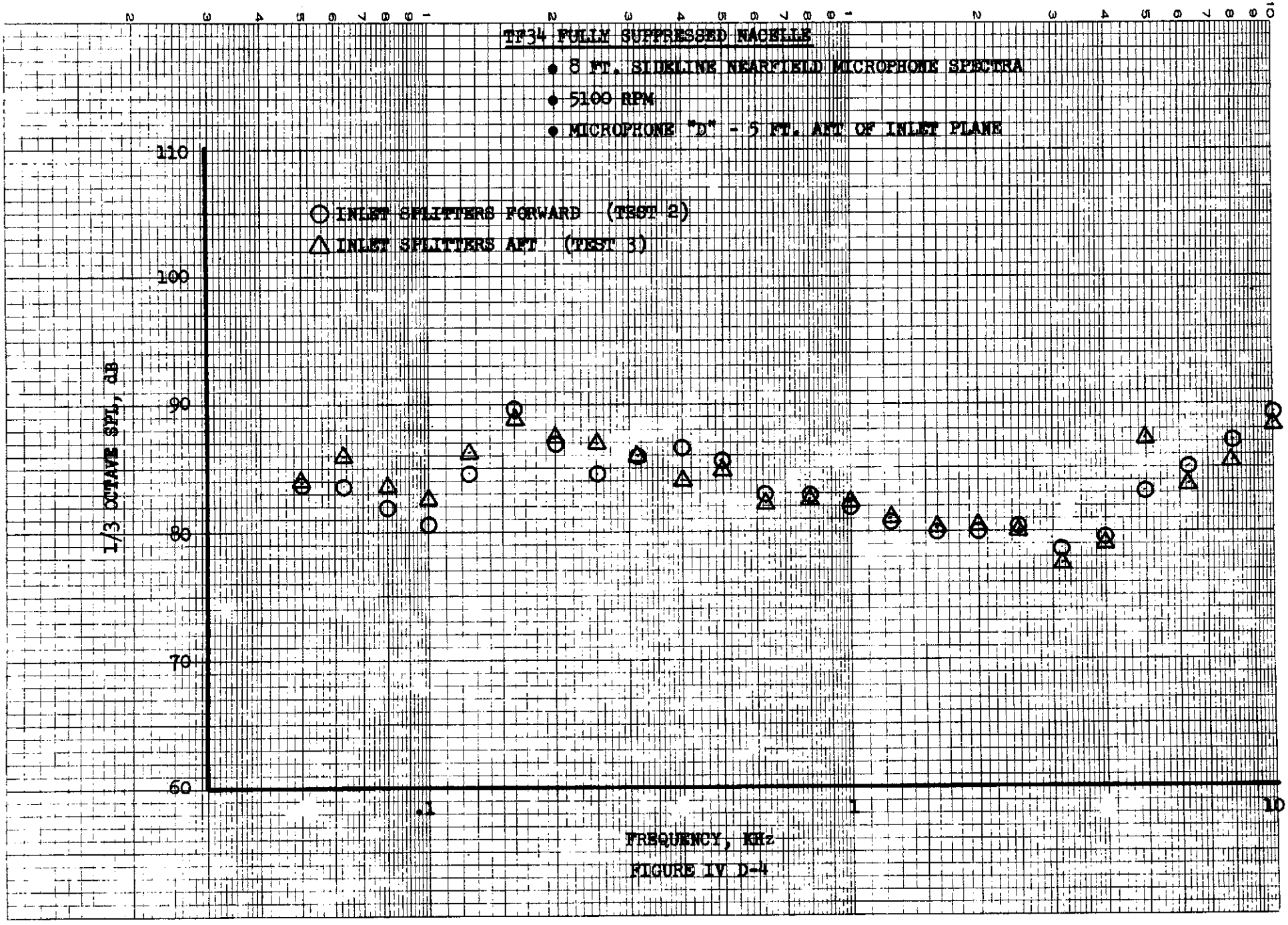

FIGURE IV D-4

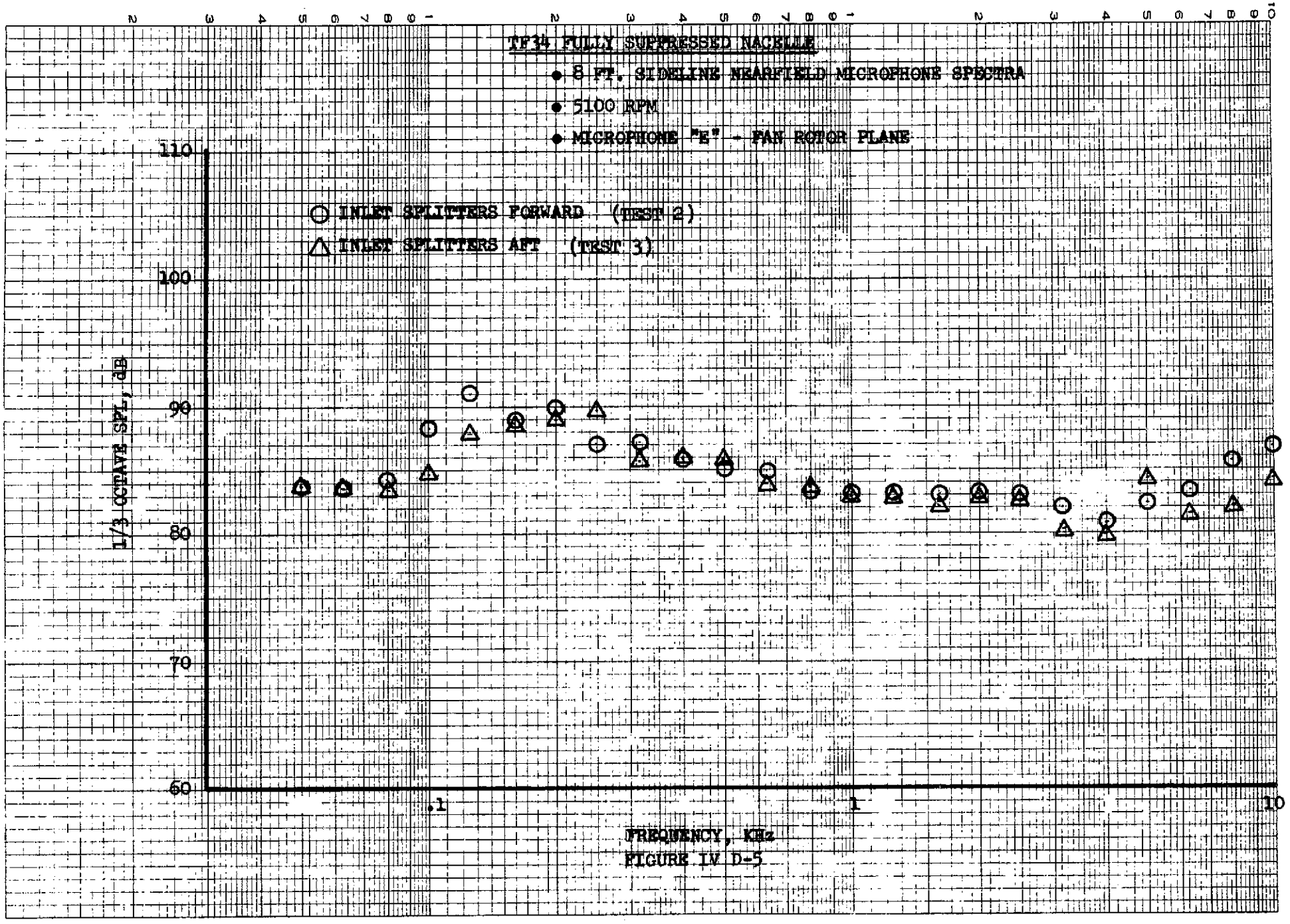

FIGURE IV D-5

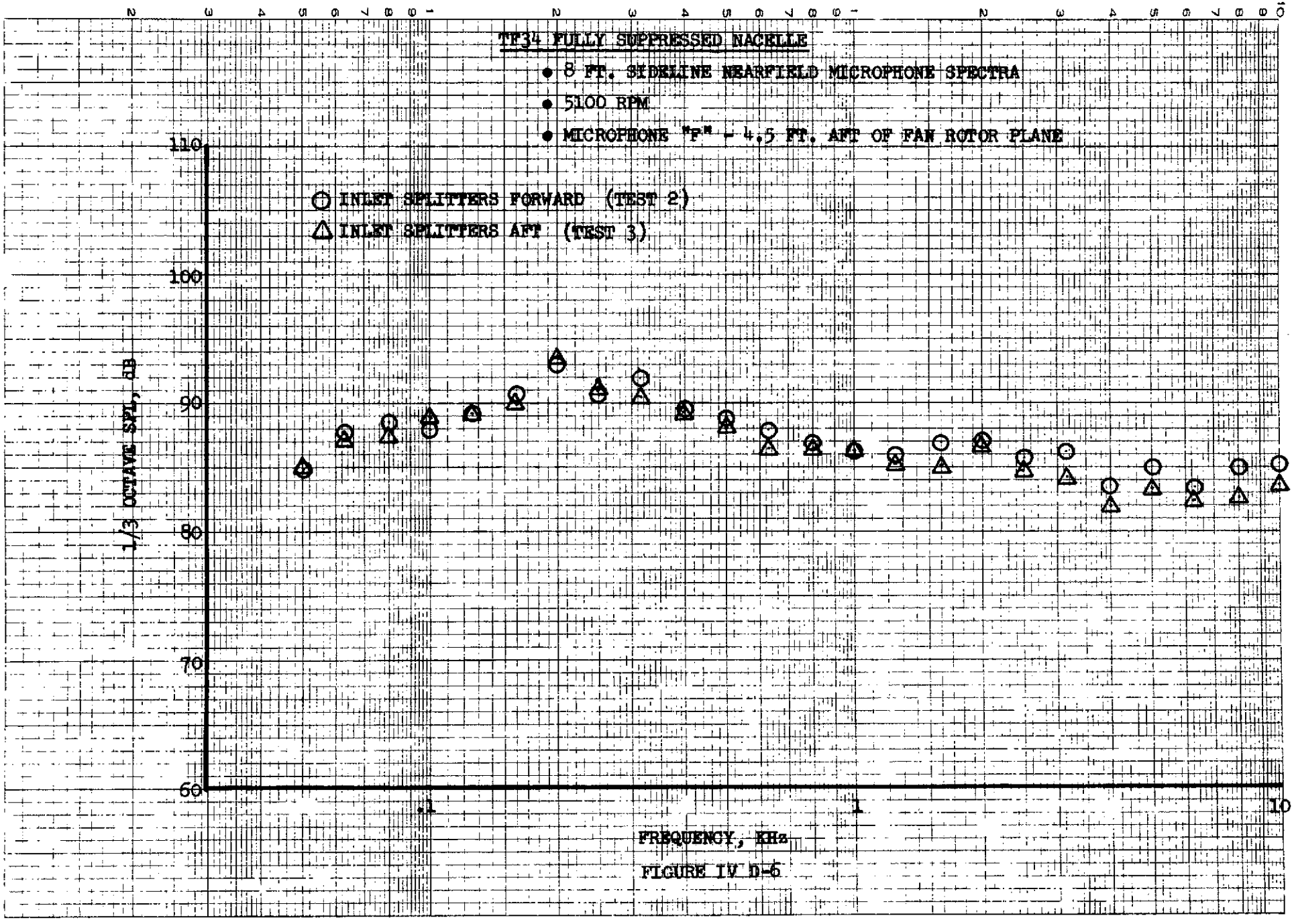
TF34 FULLY SUPPRESSED NACELLE
● 8 FT. SIDELINE NEARFIELD MICROPHONE SPECTRA
● 5100 RPM
● MICROPHONE "F" - 4.5 FT. AFT OF FAN ROTOR PLANE
○ INLET SPLITTERS FORWARD (TEST 2)
△ INLET SPLITTERS AFT (TEST 3)
1/3 OCTAVE SPL, dB
110
100
90
80
70
60
.1
1
10
FREQUENCY, KHz

FIGURE IV D-6

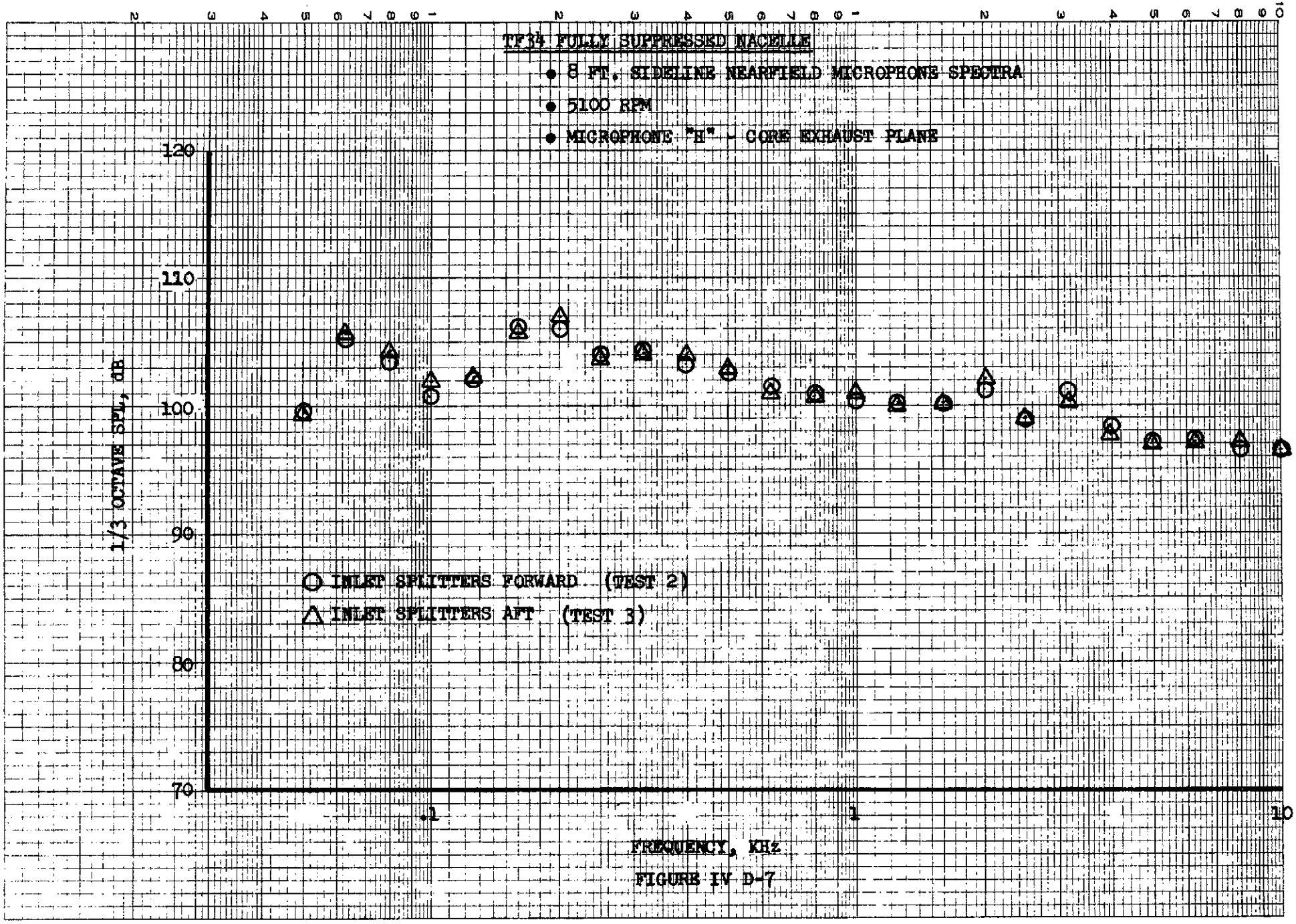

FIGURE IV D-7

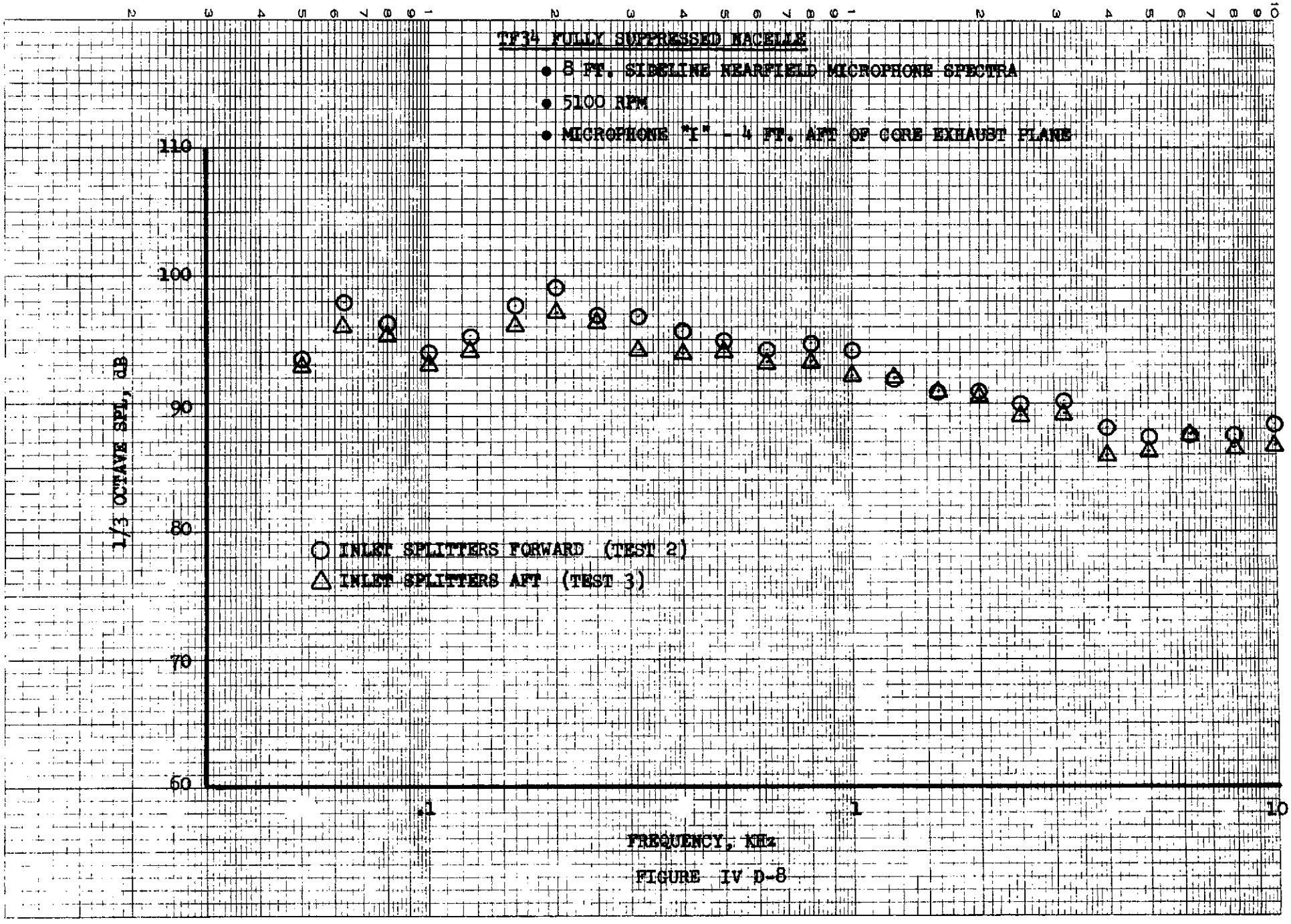

FIGURE IV D-8

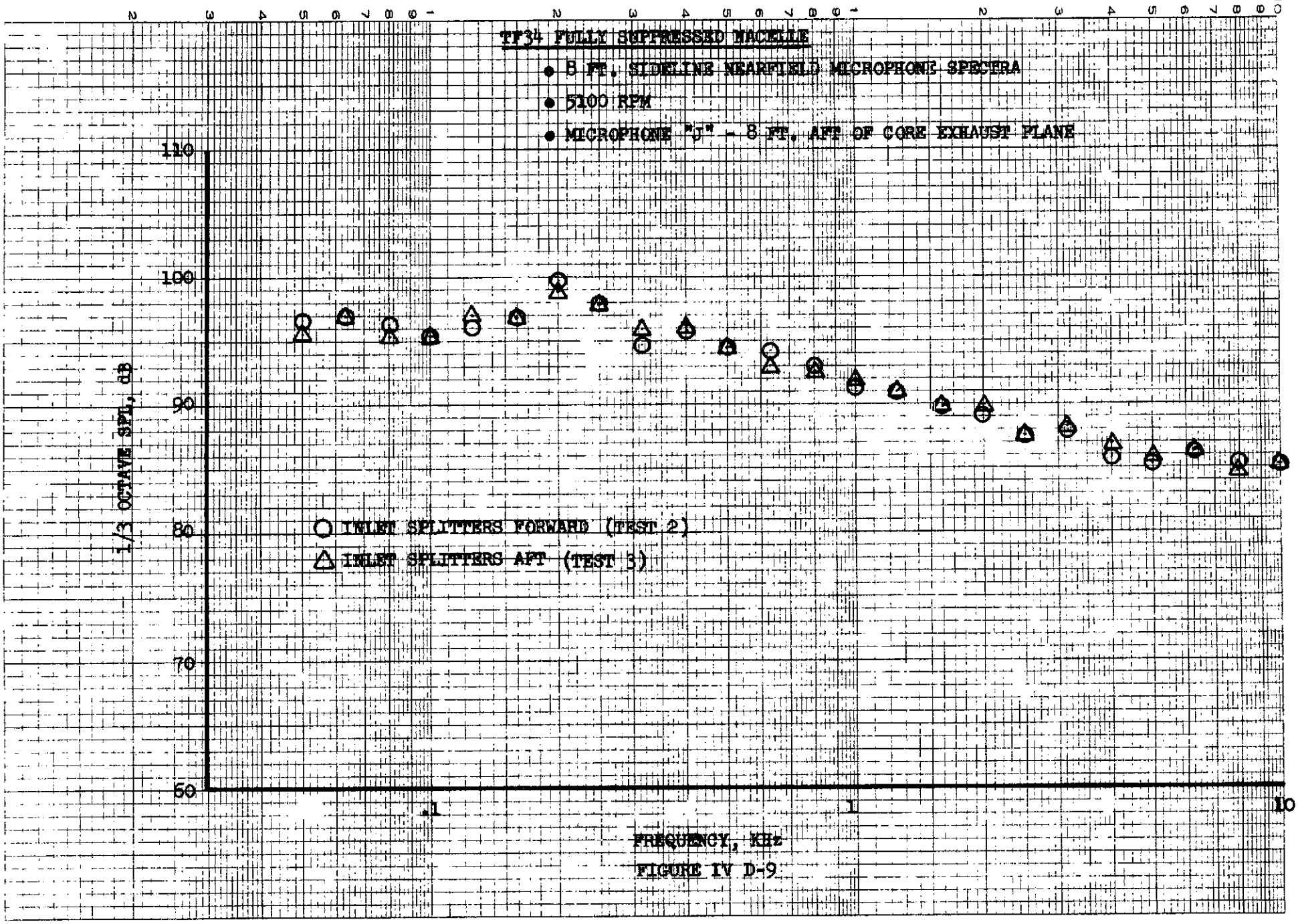

FIGURE IV D-9

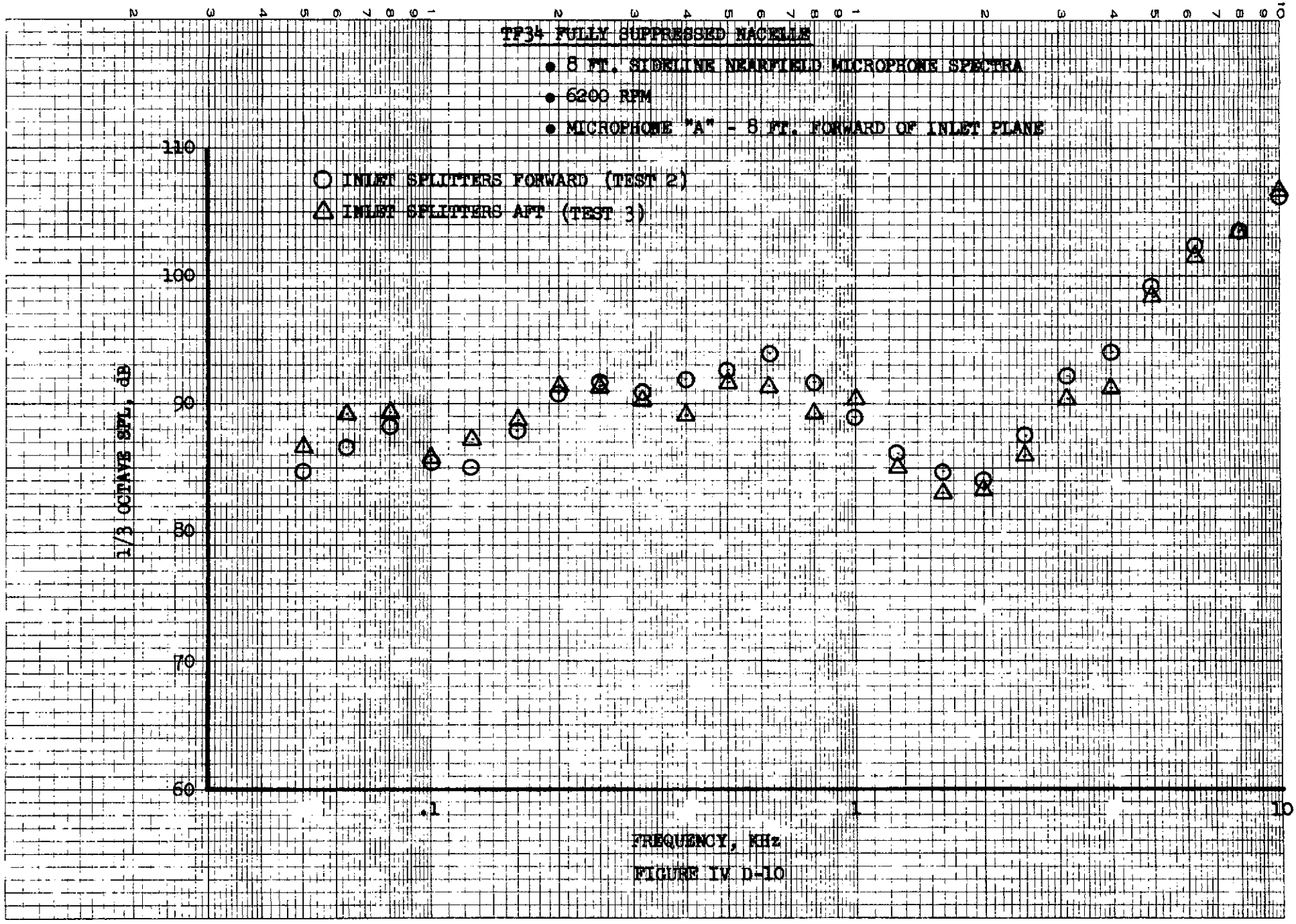

FIGURE IV D-10

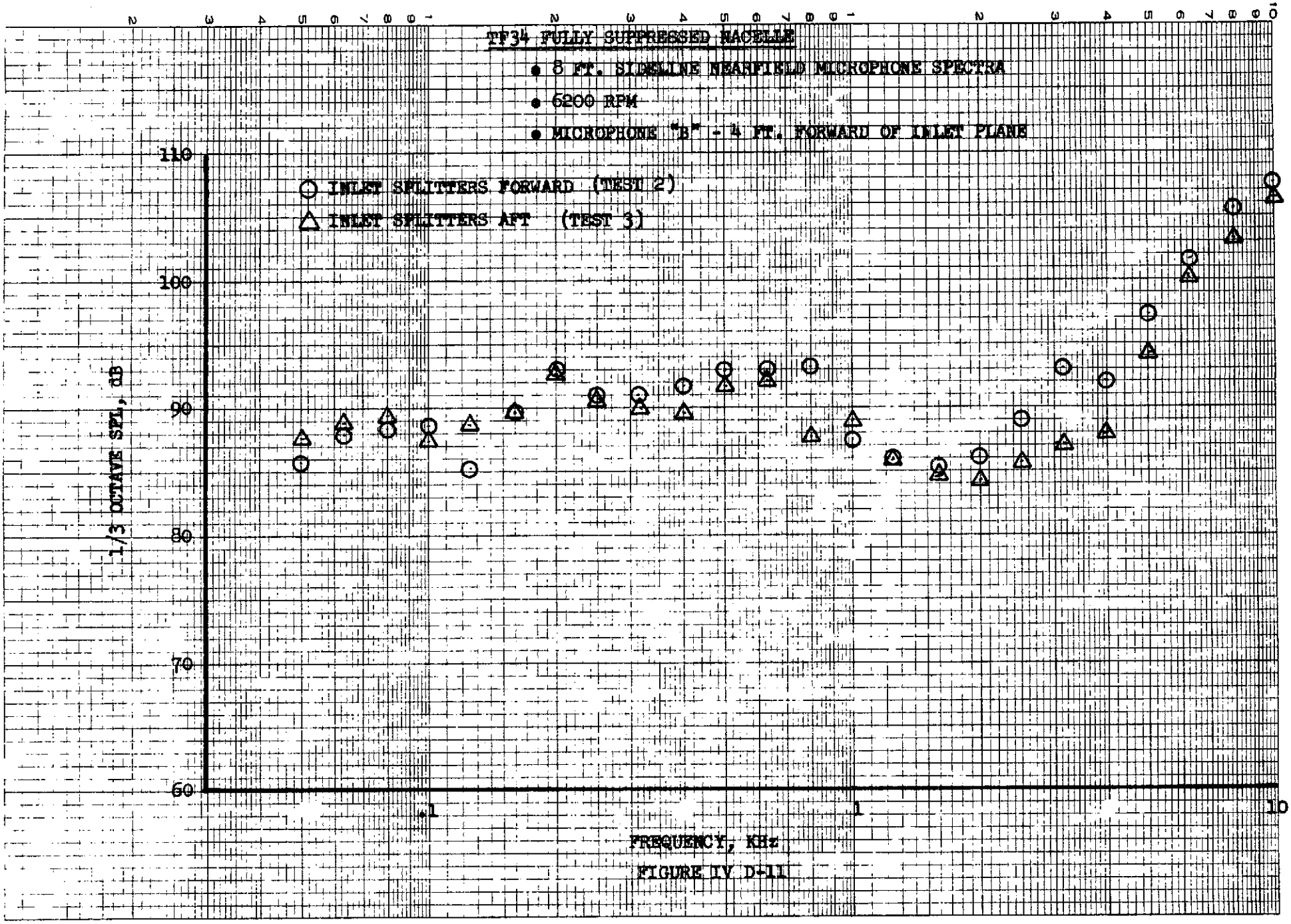

FIGURE IV D-11

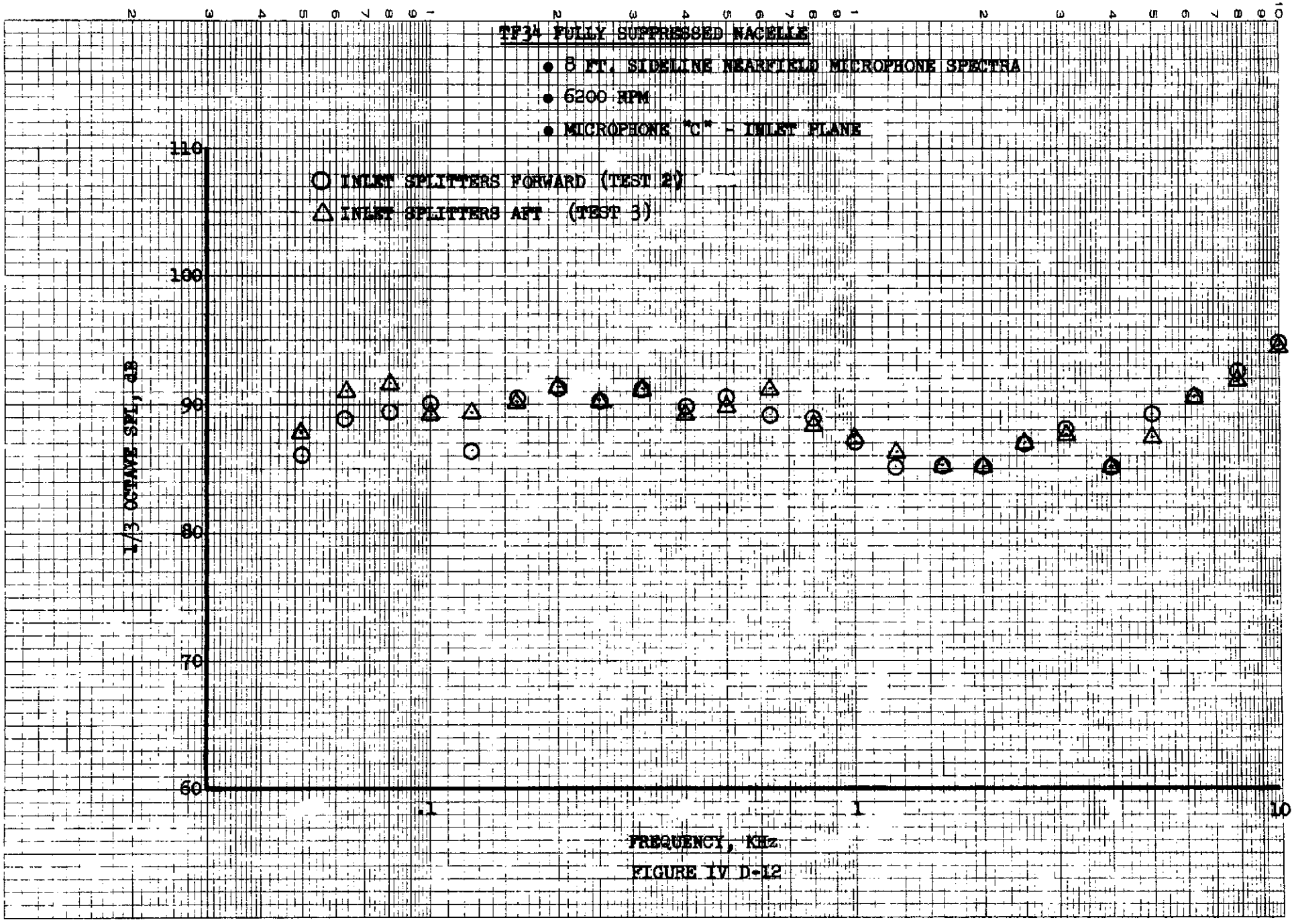

FIGURE IV D-12

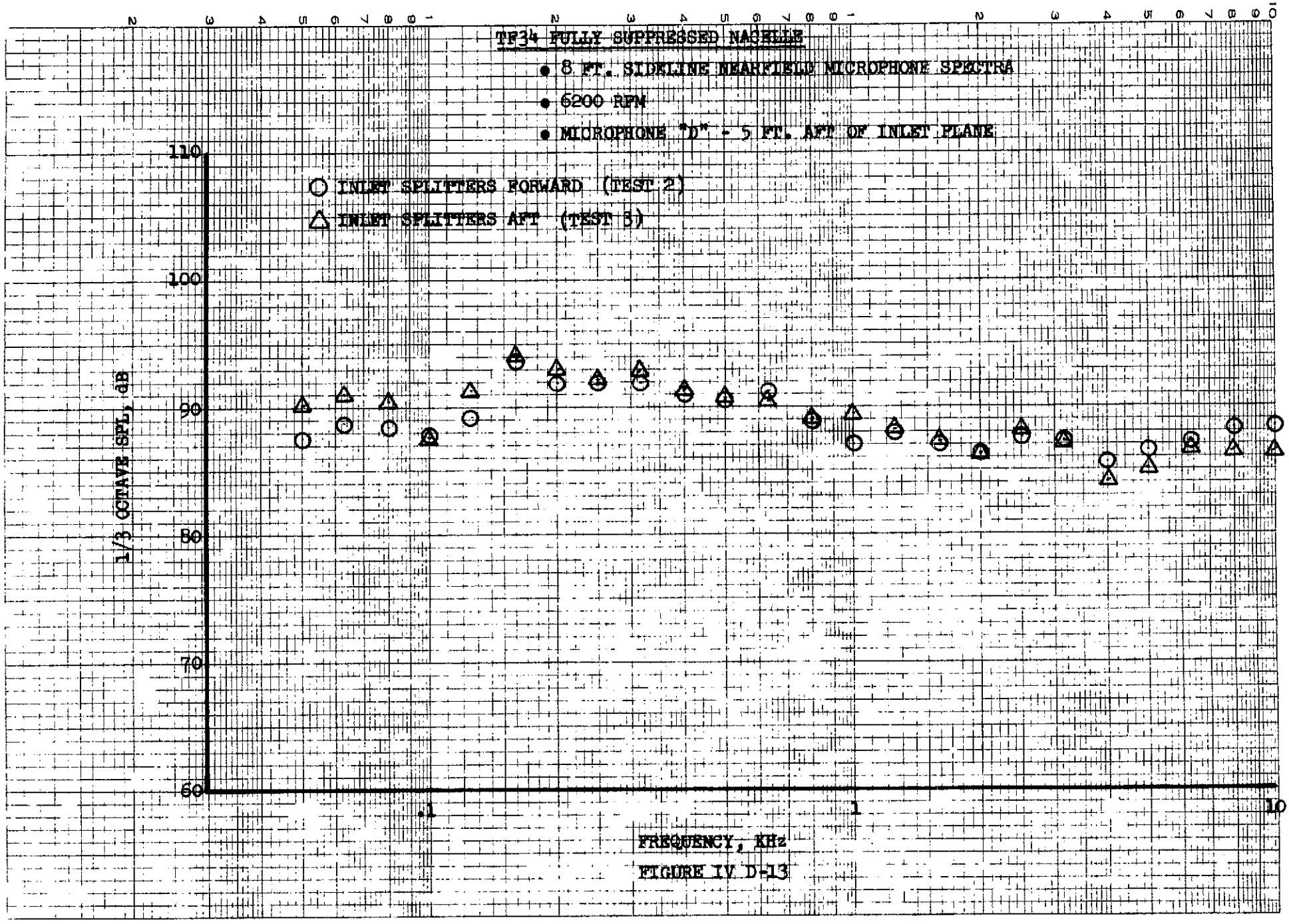

FIGURE IV D-13

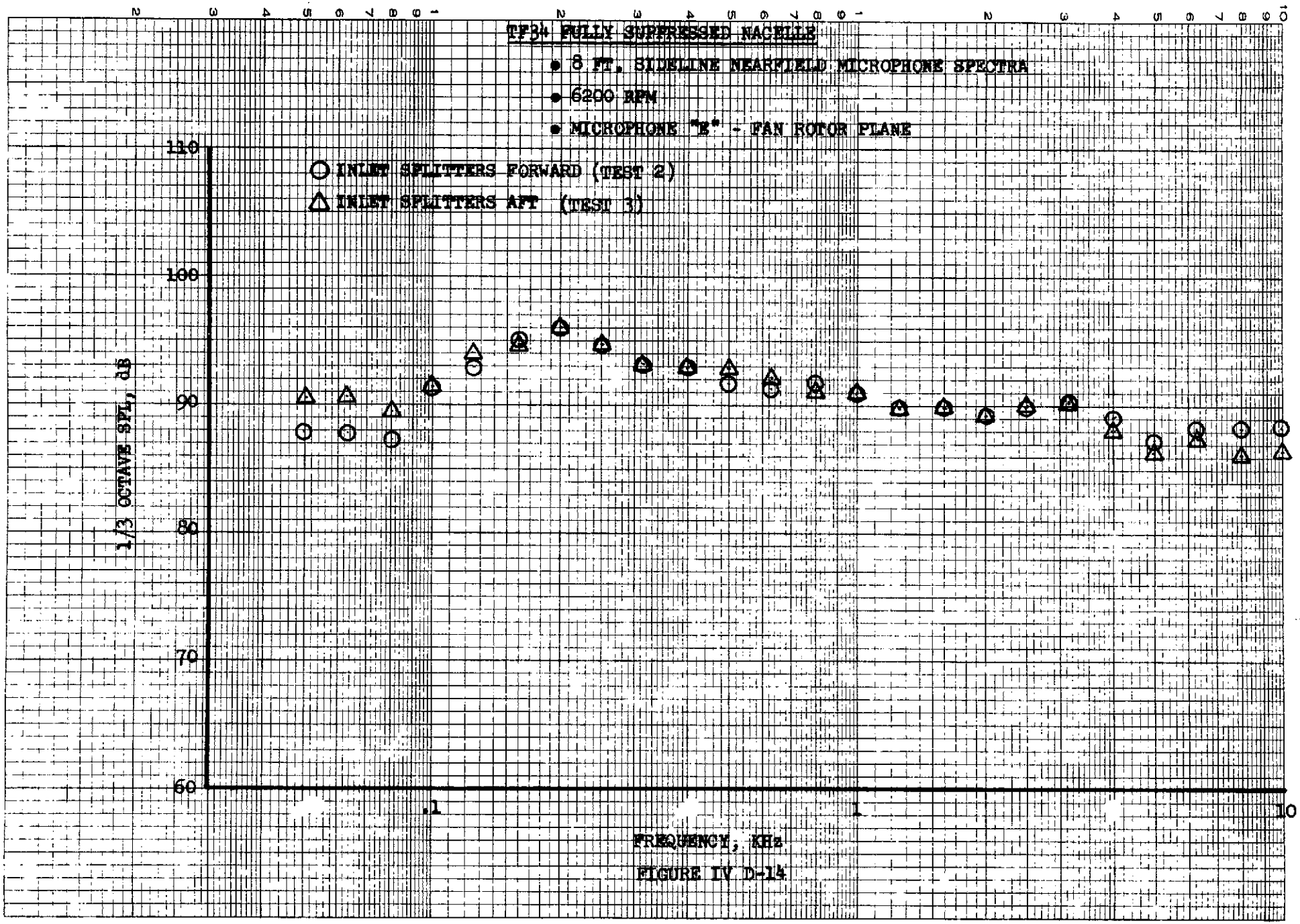

FIGURE IV D-14

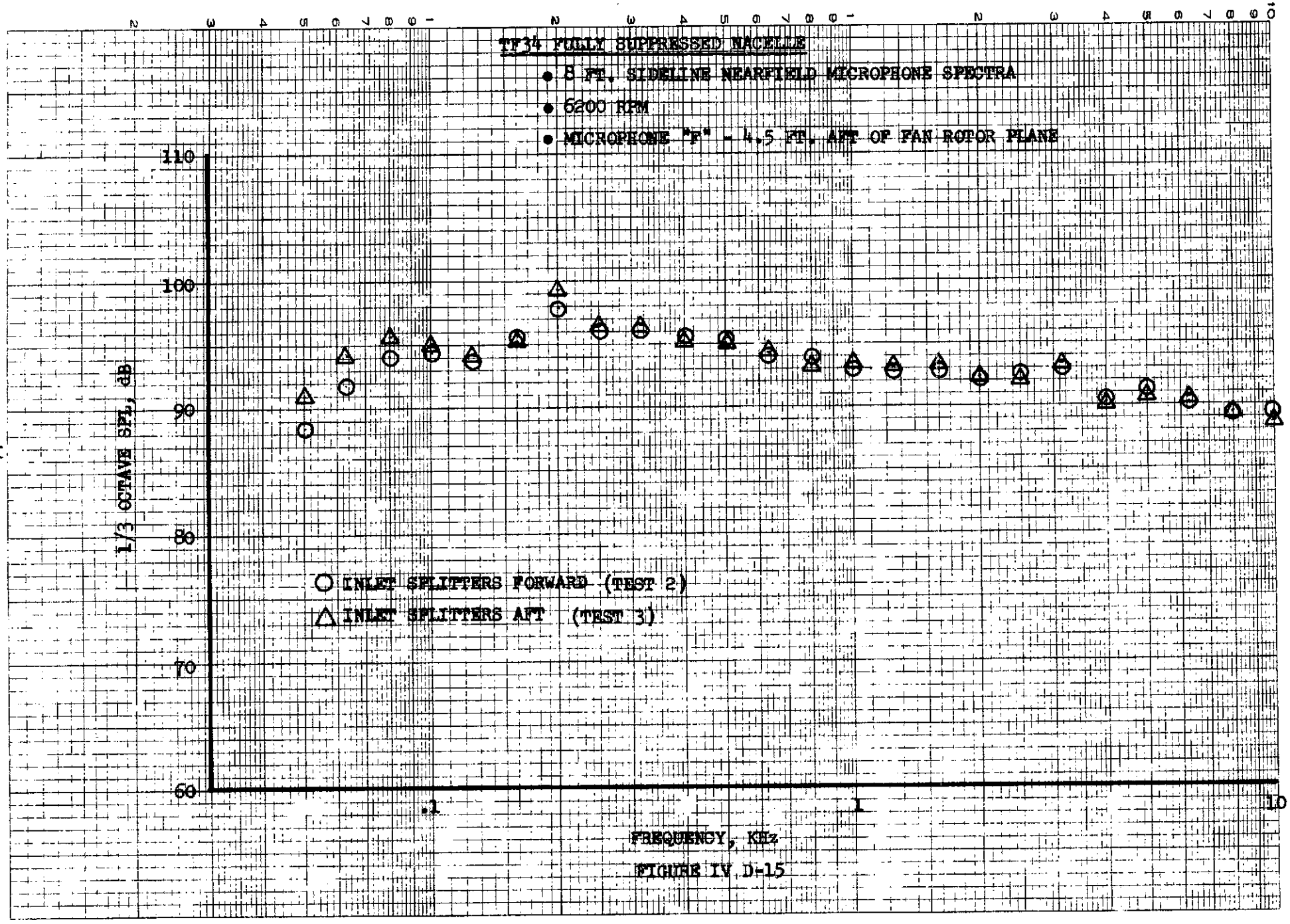

FIGURE IV D-15

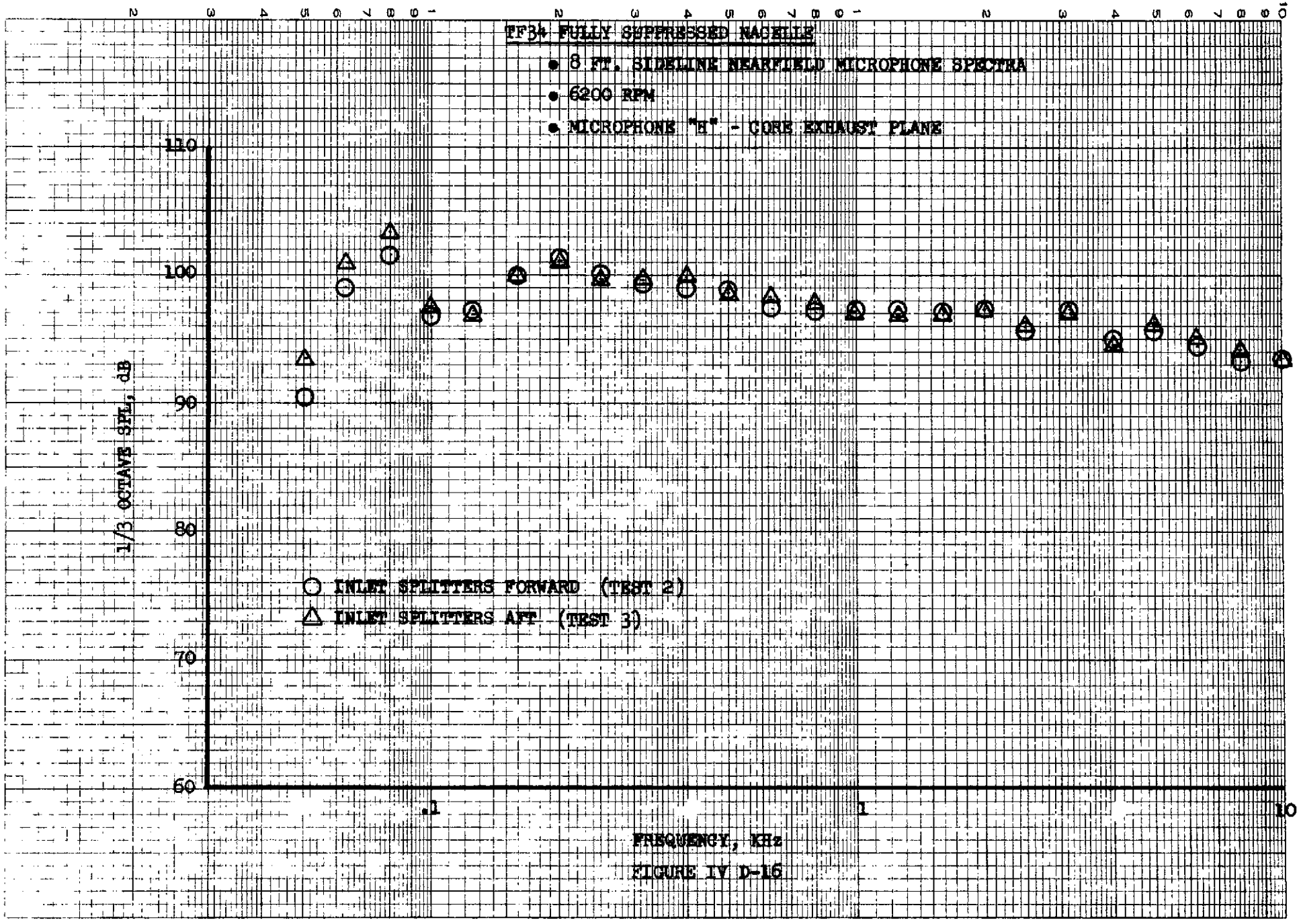

FIGURE IV D-16

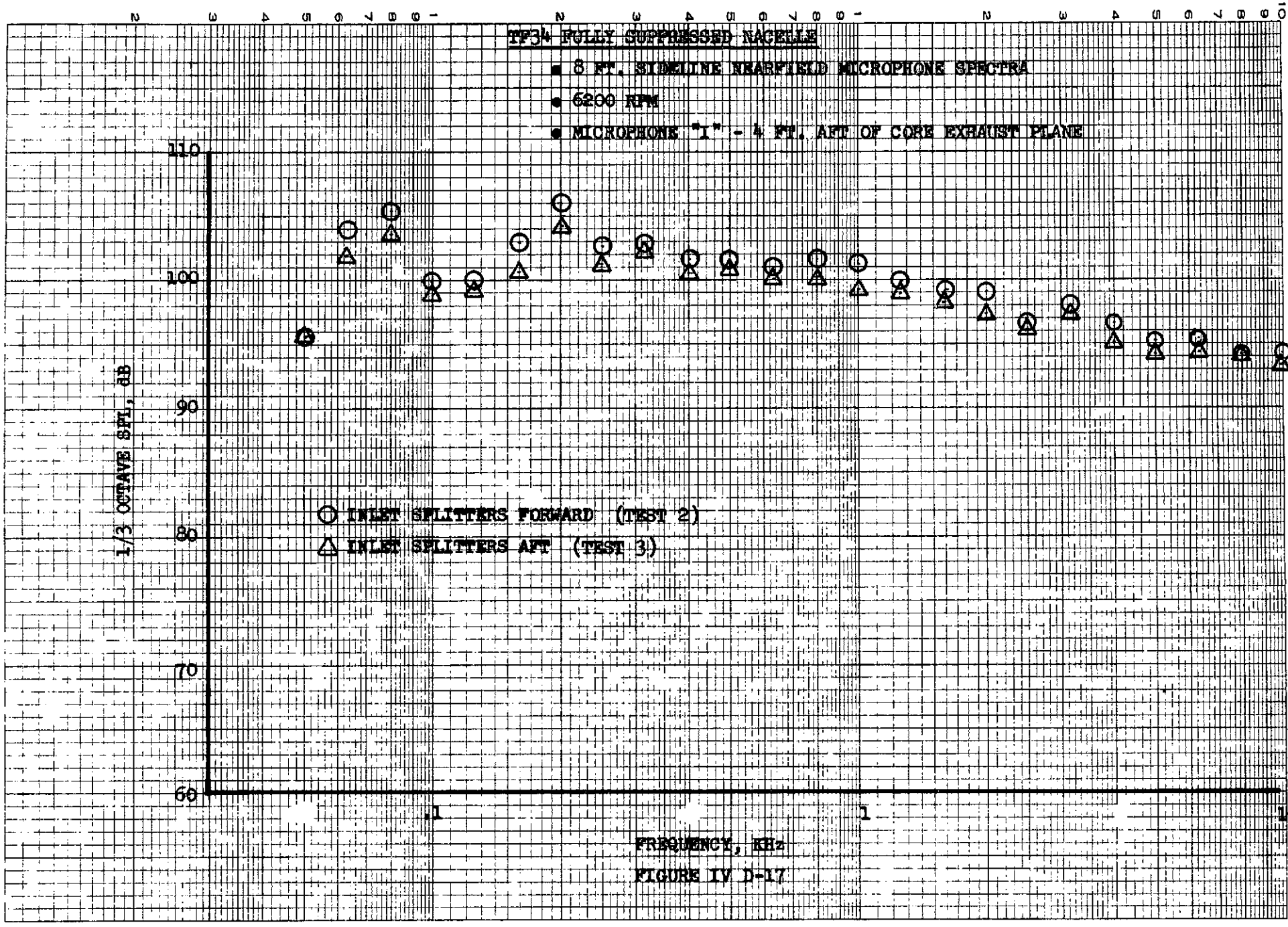

FIGURE IV D-17

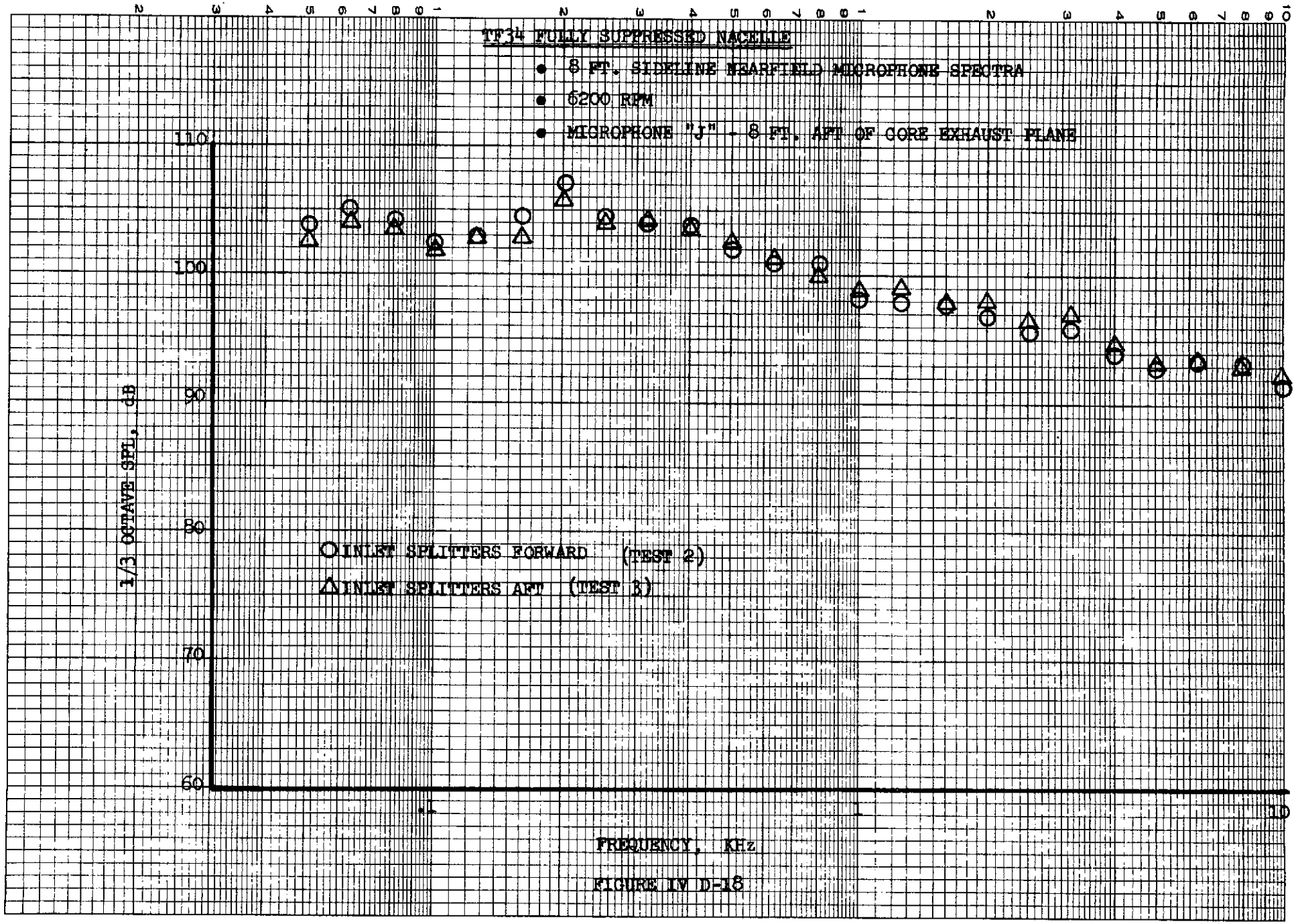

FIGURE IV D-18

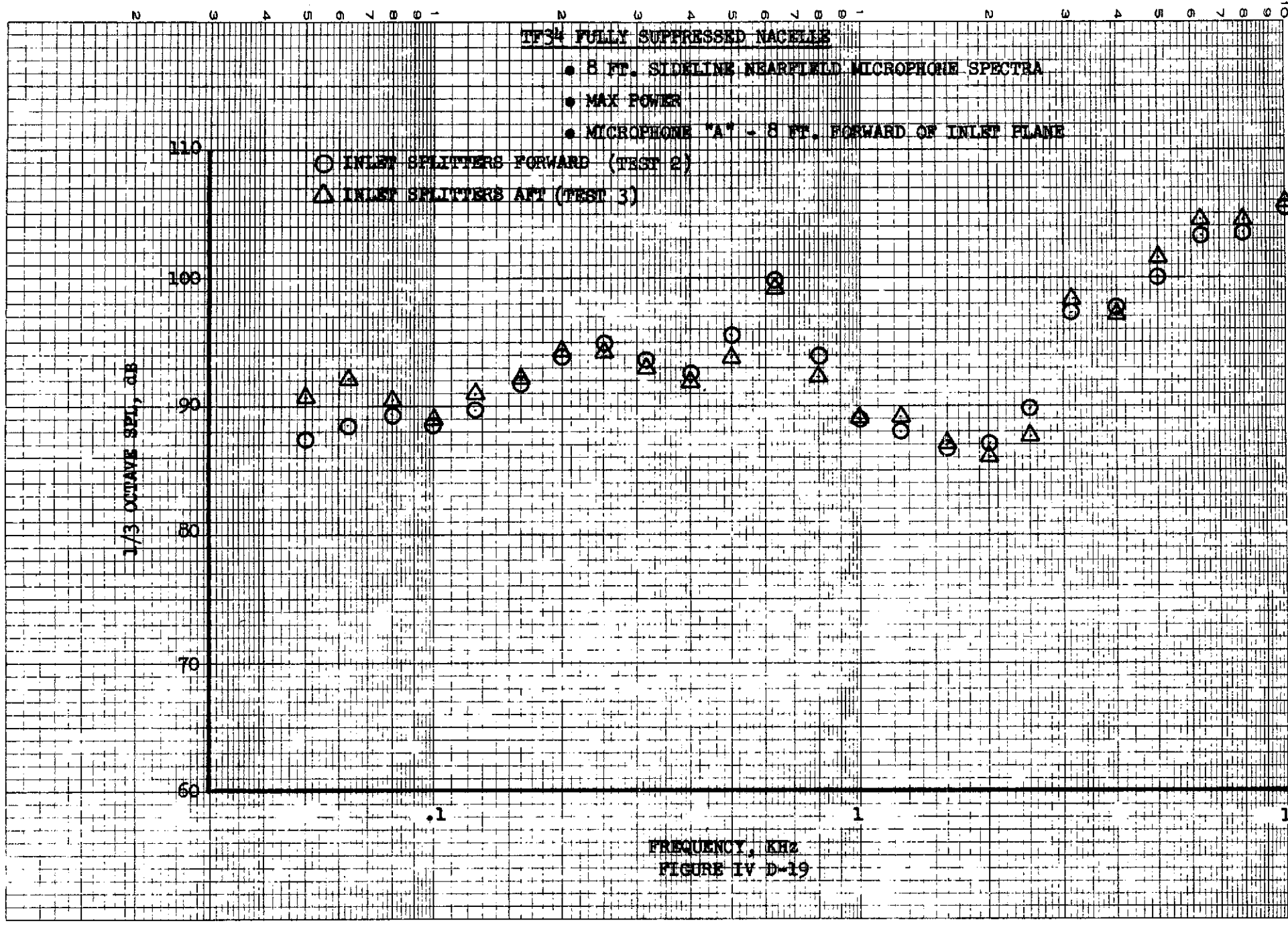

FIGURE IV D-19

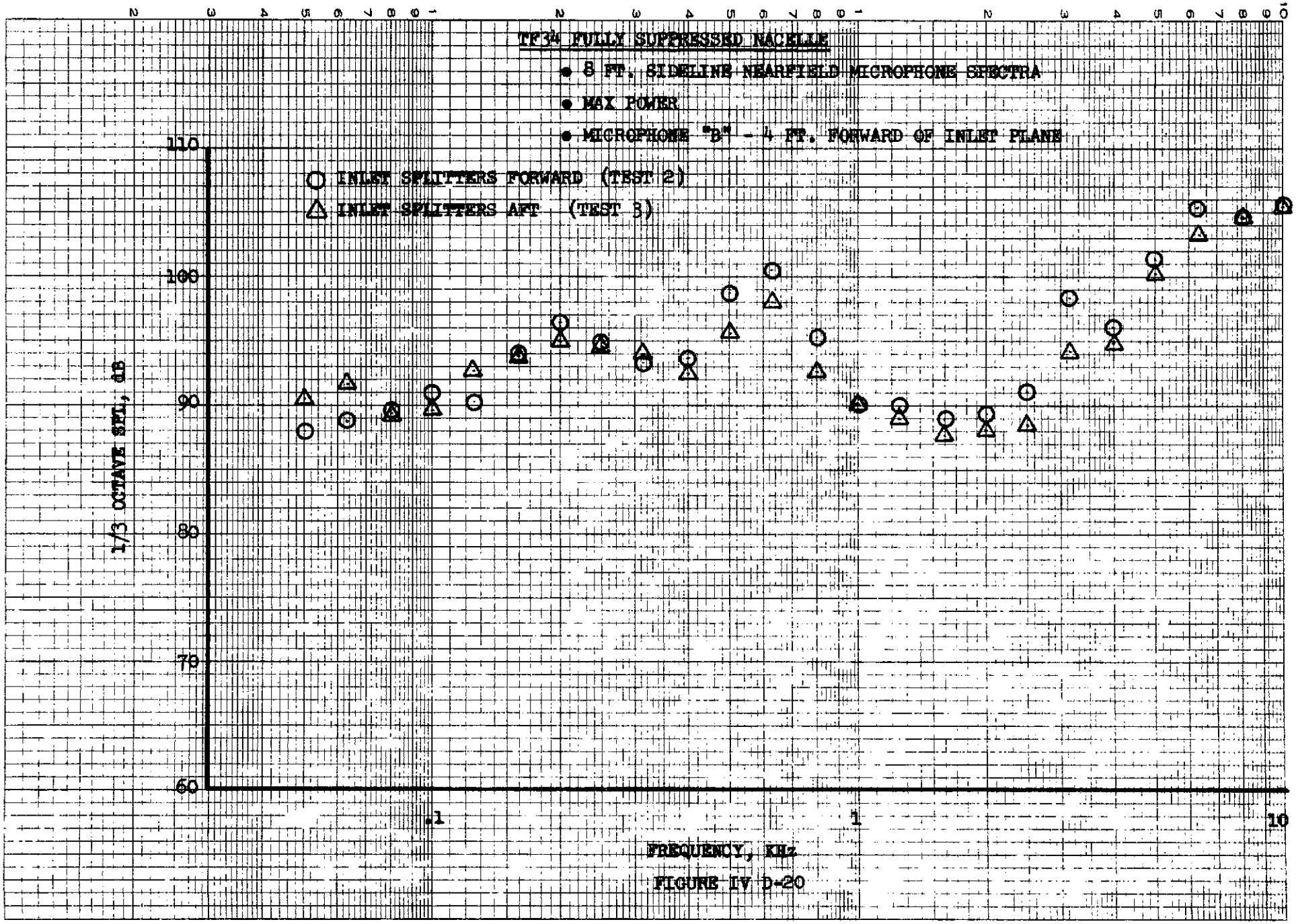

FIGURE IV D-20

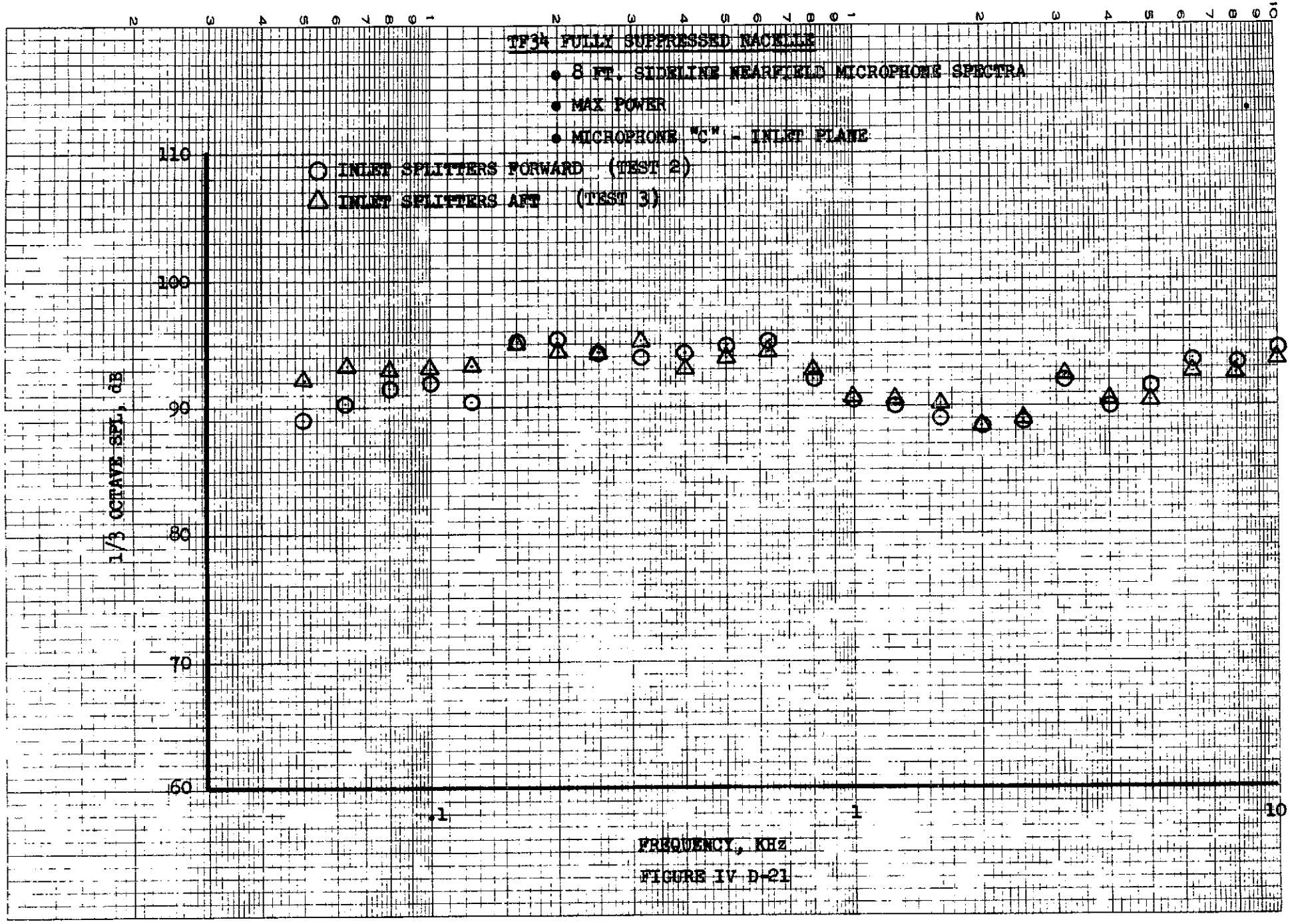

FIGURE IV D-21

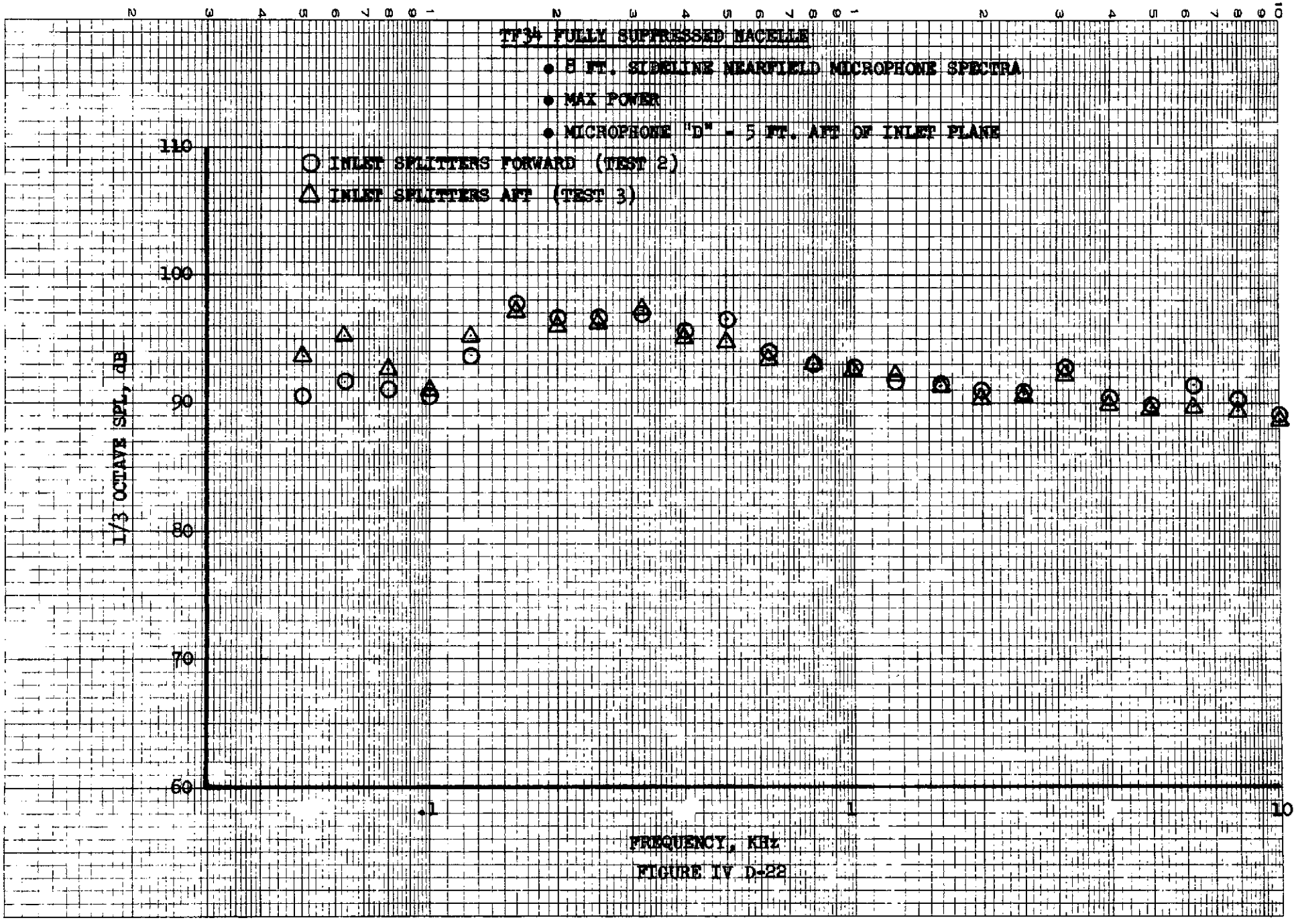

FIGURE IV D-22

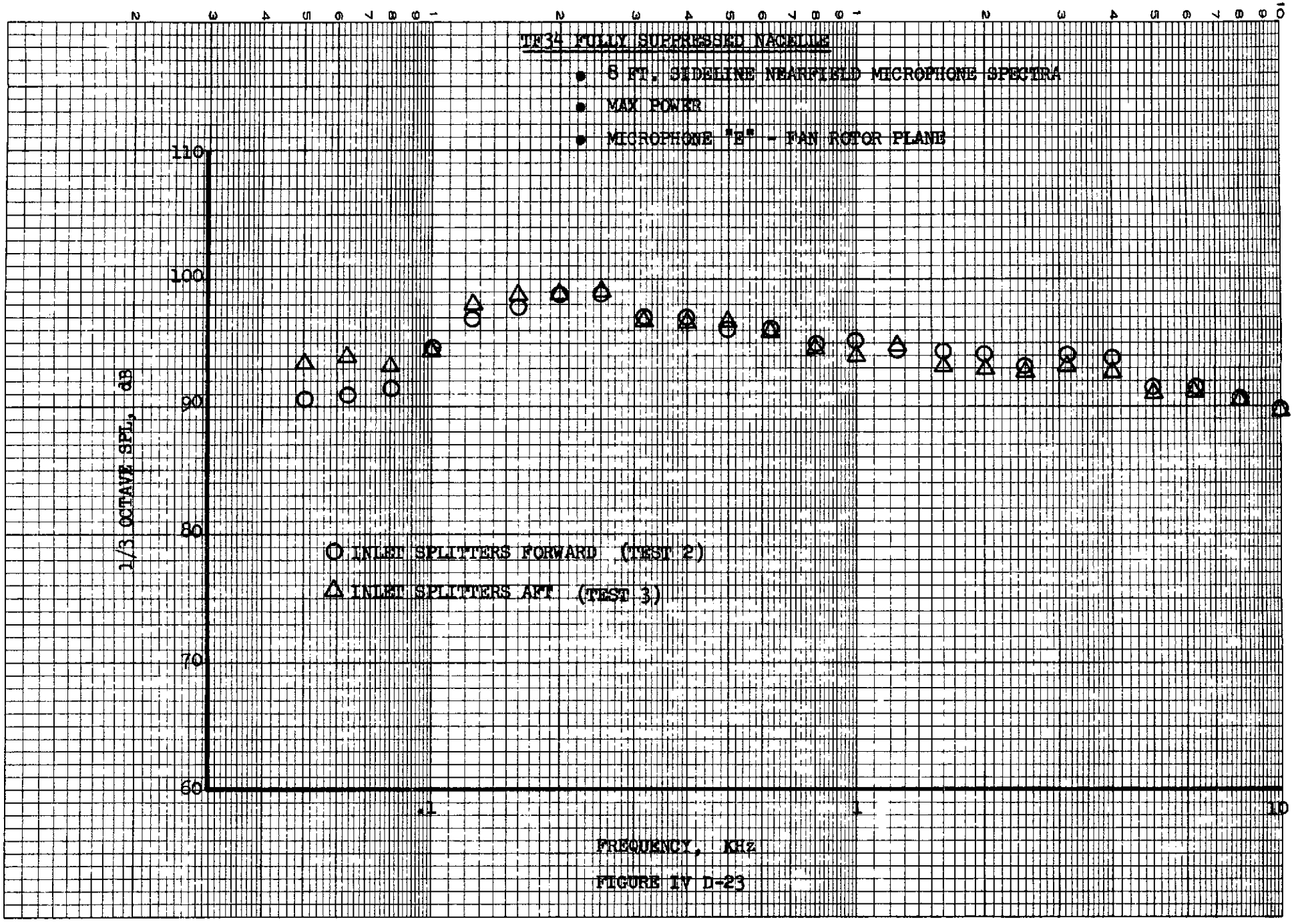

FIGURE IV D-23

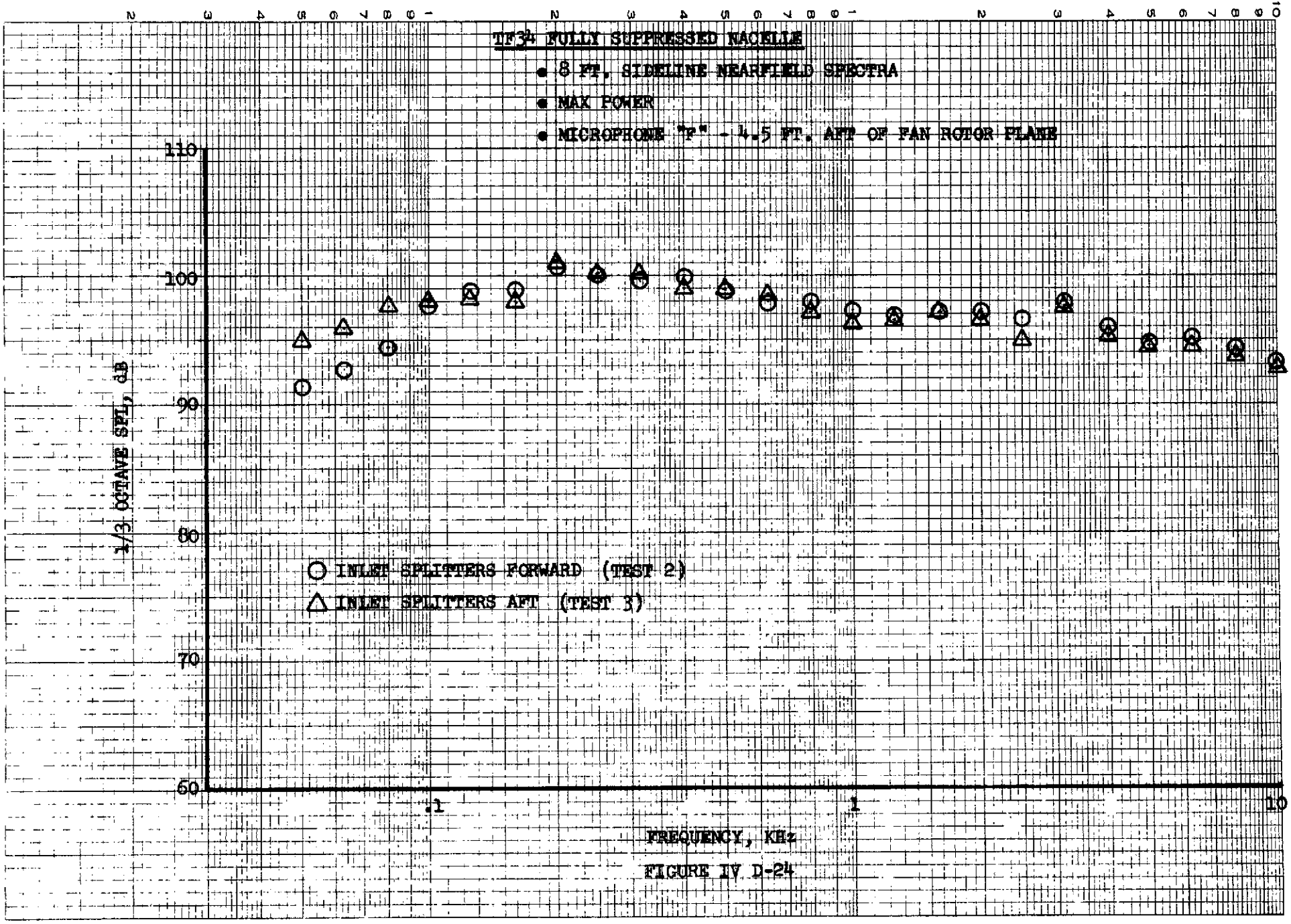

FIGURE IV D-24

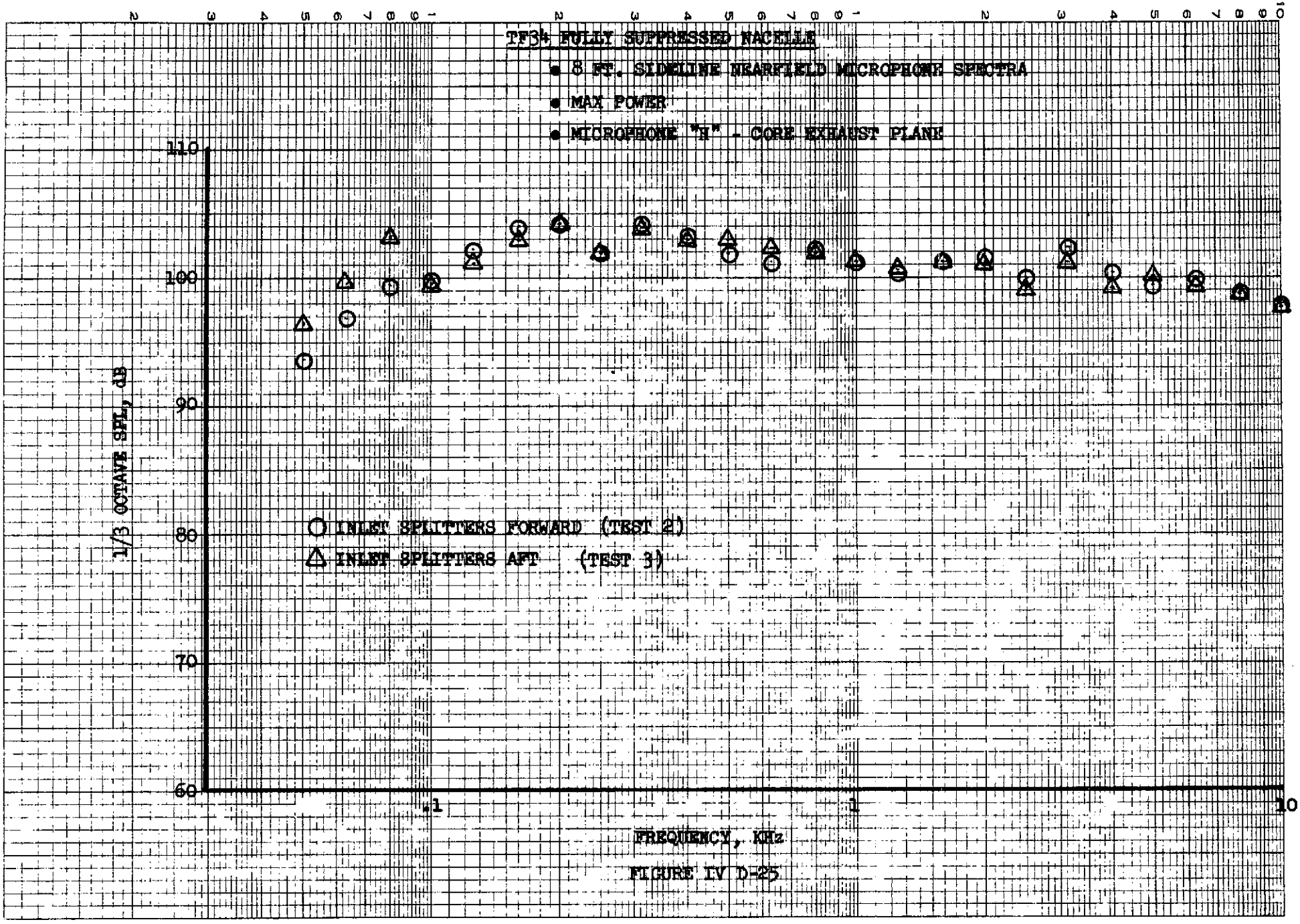

FIGURE IV D-25

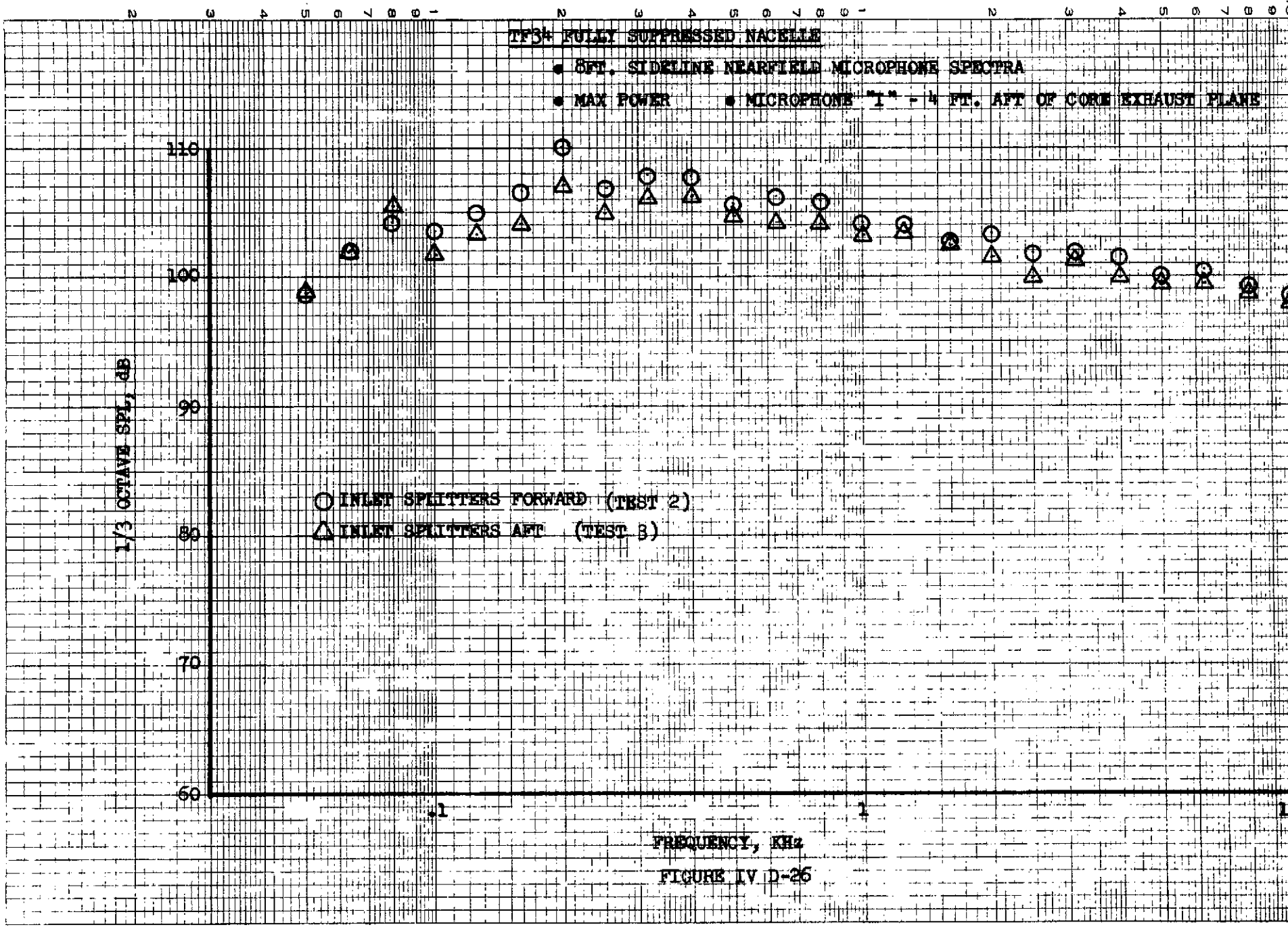

FIGURE IV D-26

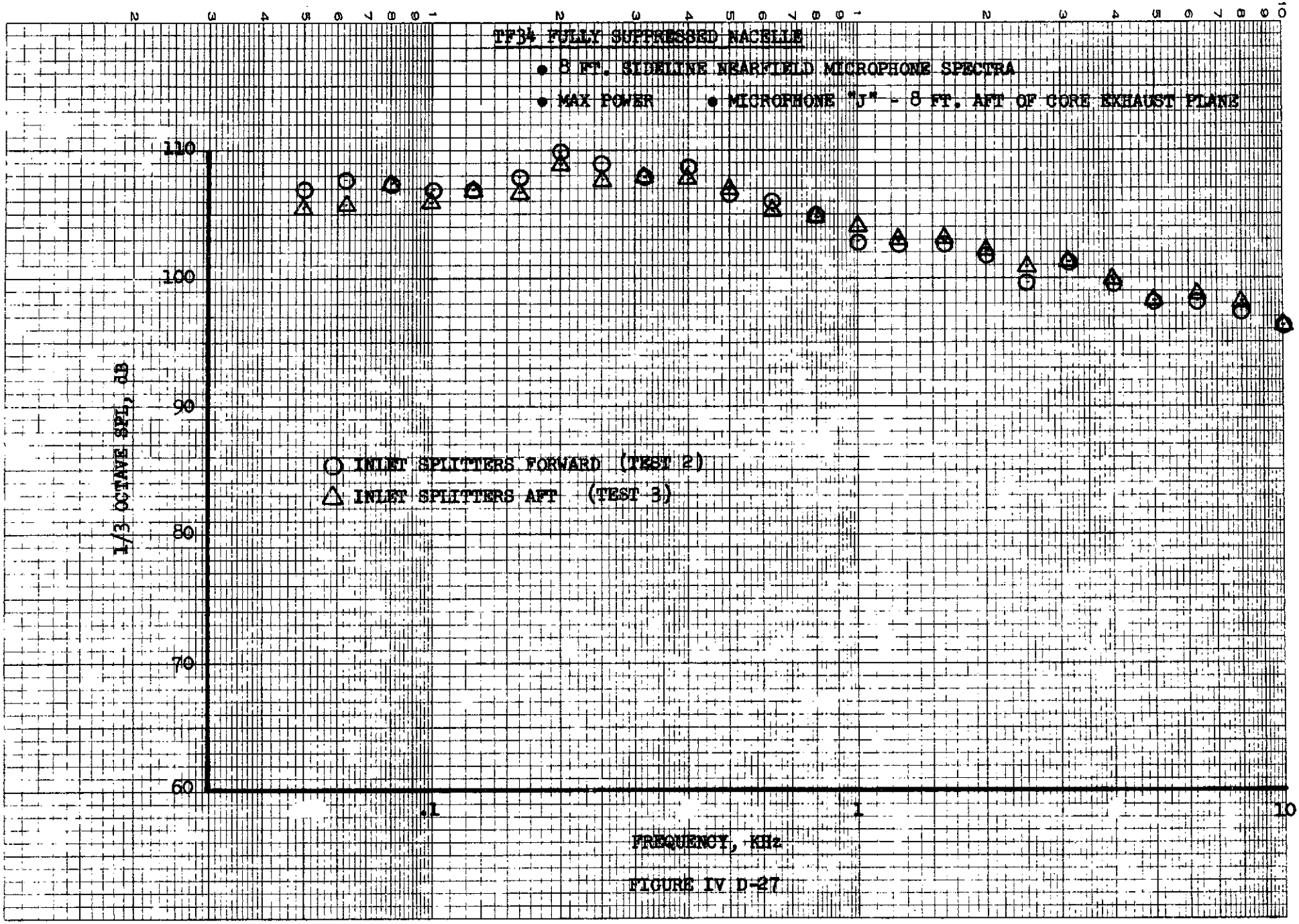

FIGURE IV D-27

TF34 FULLY SUPPRESSED NACELLE

- 8 FT. SIDELINE NEARFIELD MICROPHONE SPECTRA
- 20 Hz NARROWBAND
- 5100 RPM
- MICROPHONE "B" - 4 FT. FORWARD OF INLET PLANE

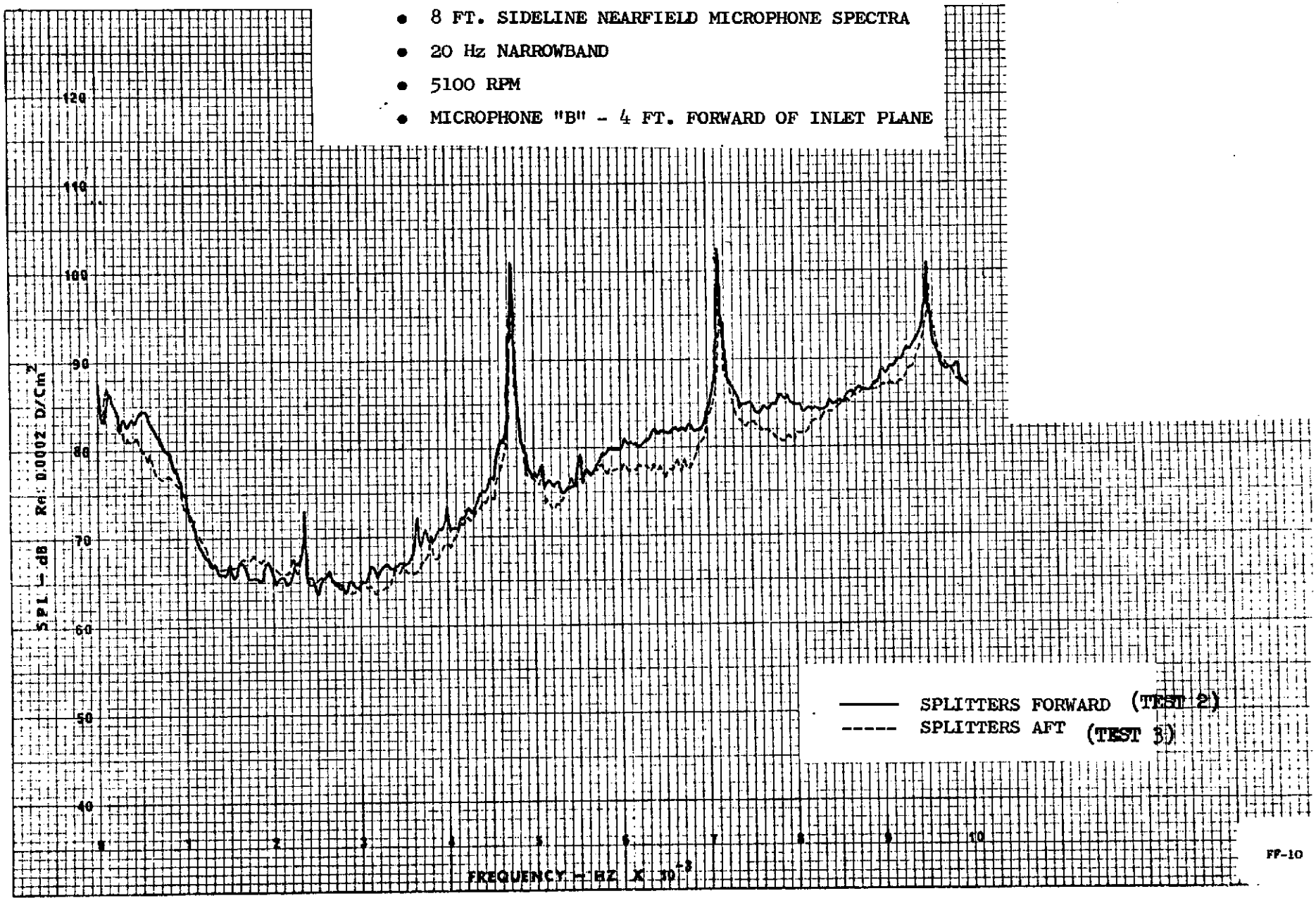

FIGURE IV D-28

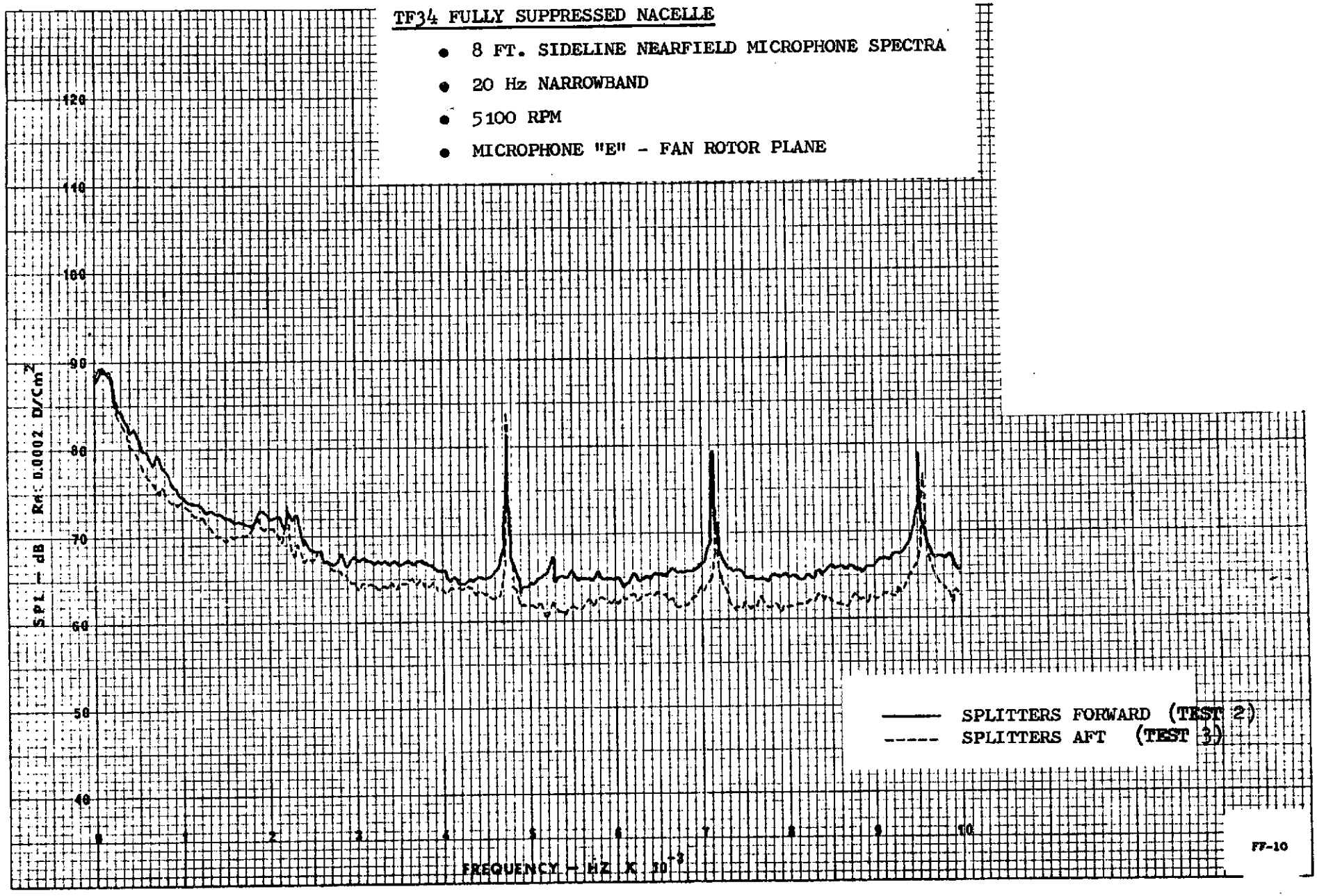

FIGURE IV D-29

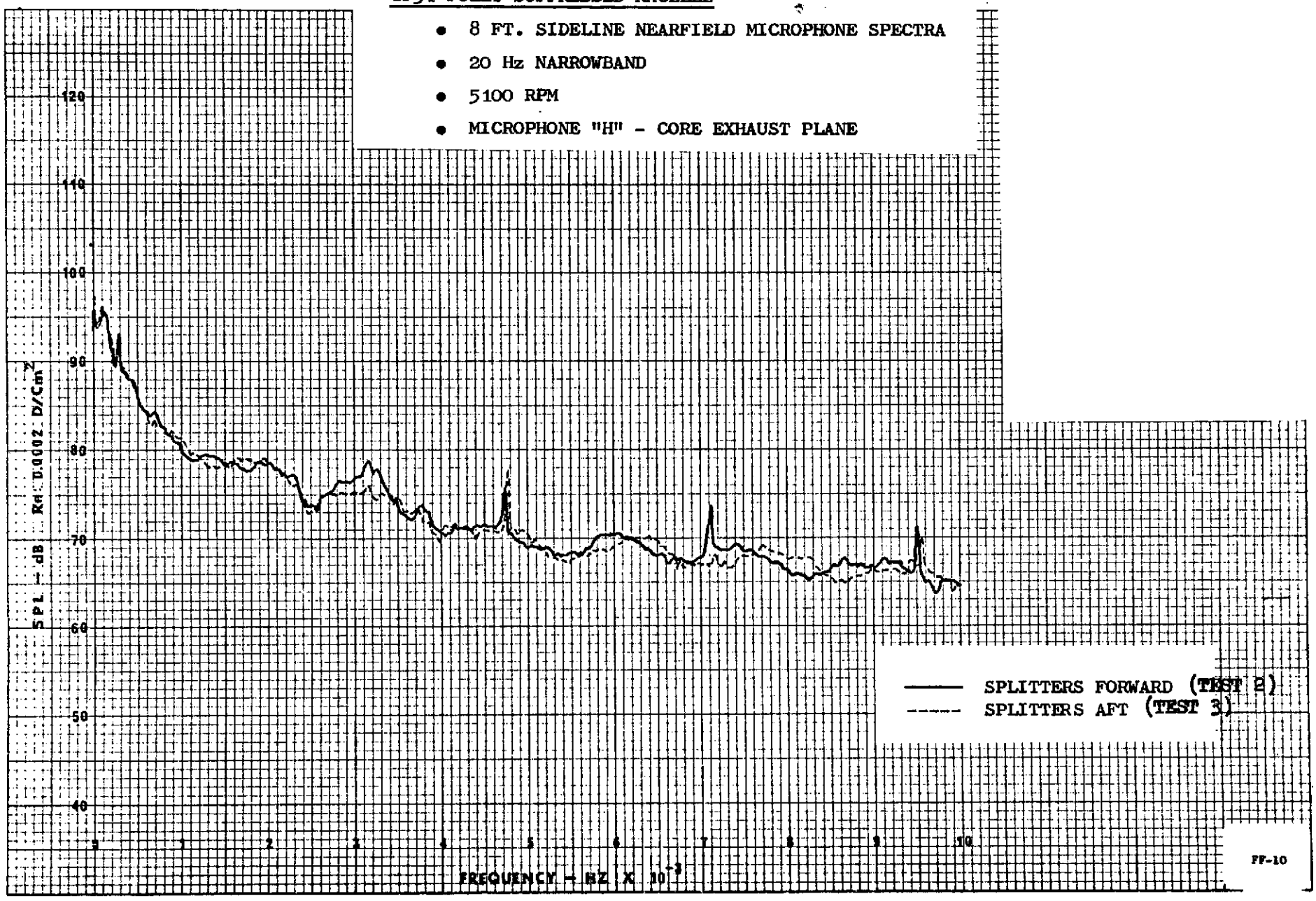

FIGURE IV D-30

TF34 FULLY SUPPRESSED NACELLE

- 8 FT. SIDELINE NEARFIELD MICROPHONE SPECTRA
- 20 Hz NARROWBAND
- 6200 RPM
- MICROPHONE "B" - 4 FT. FORWARD OF INLET PLANE

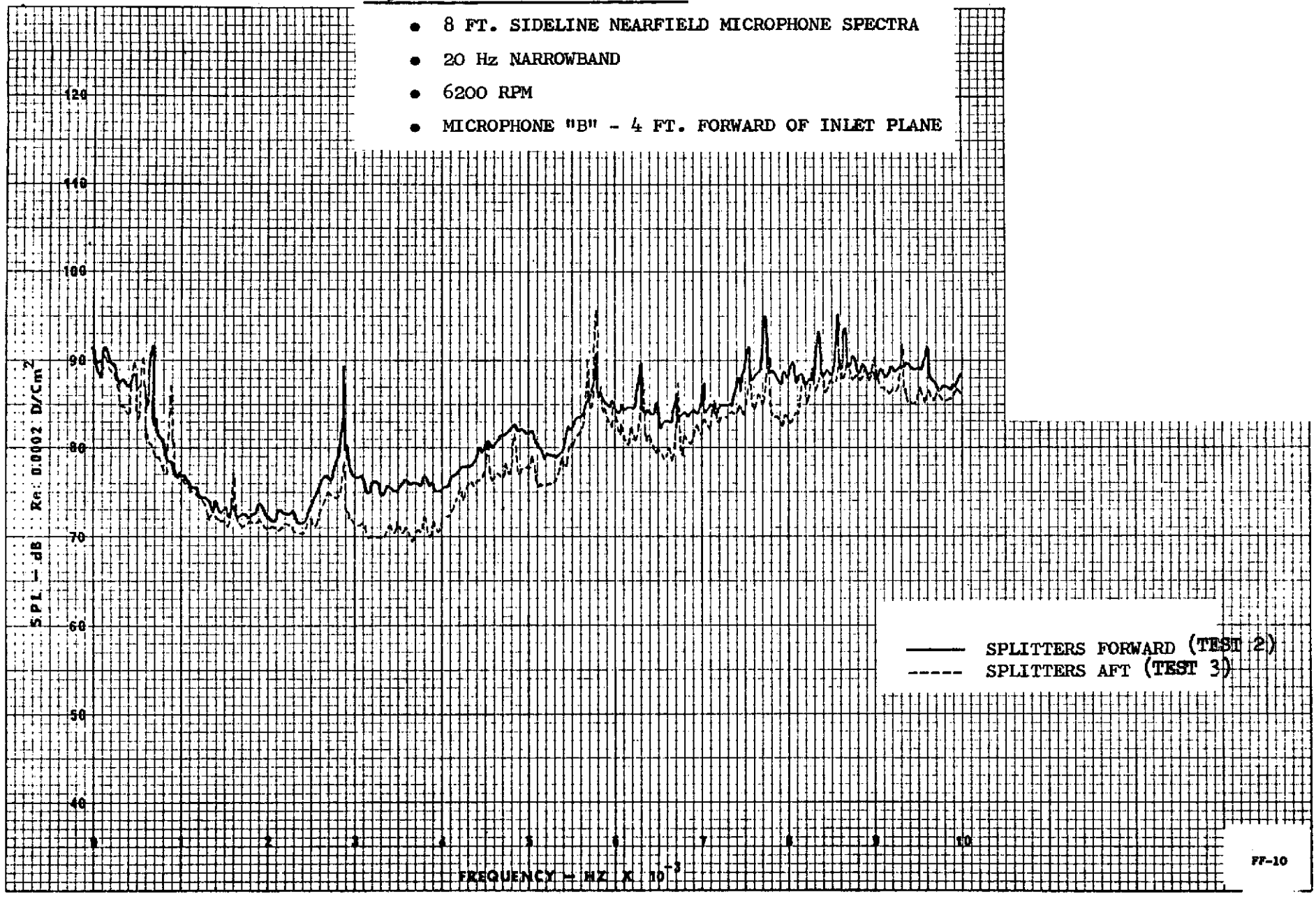

FIGURE IV D-31

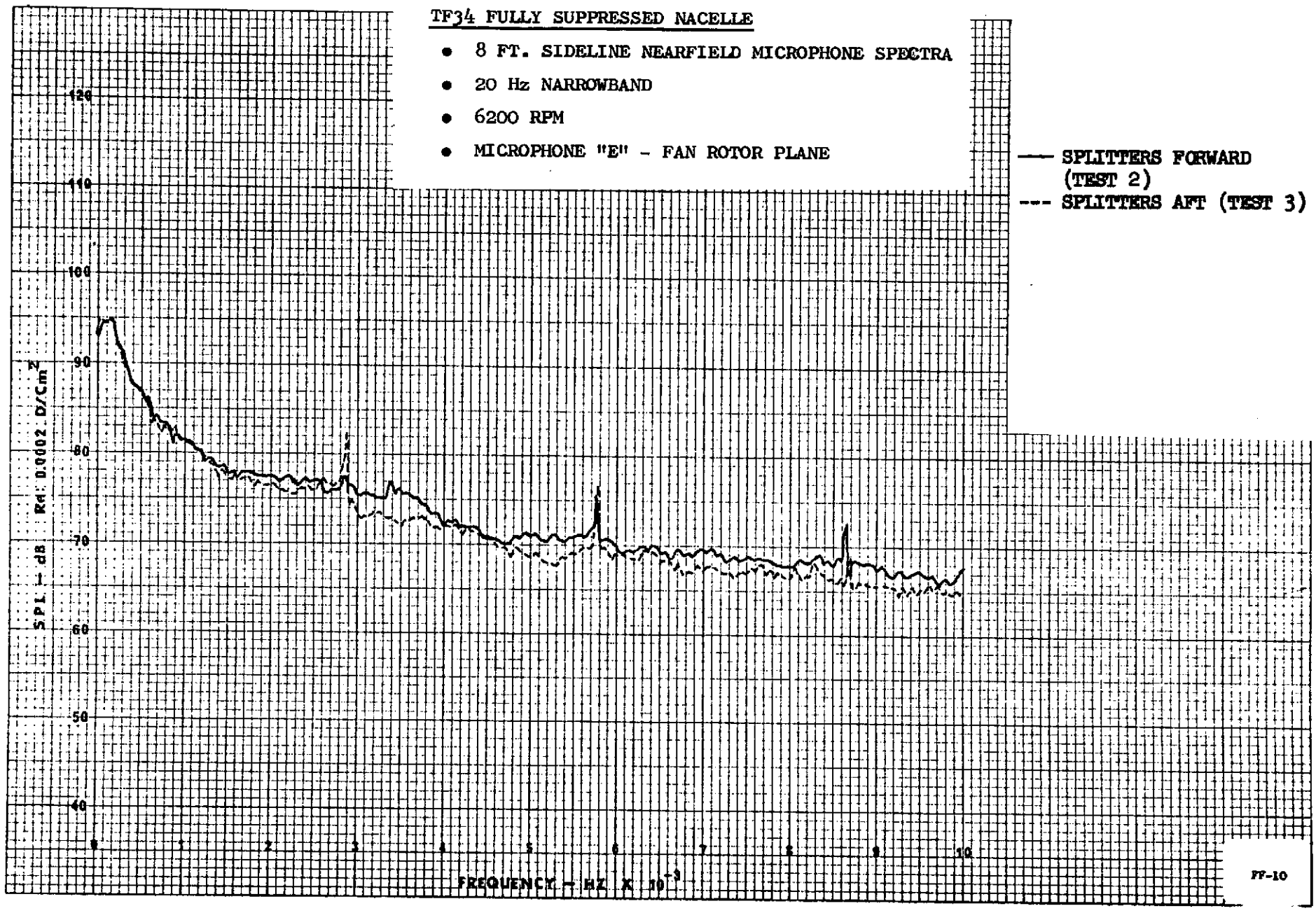

FIGURE IV D-32

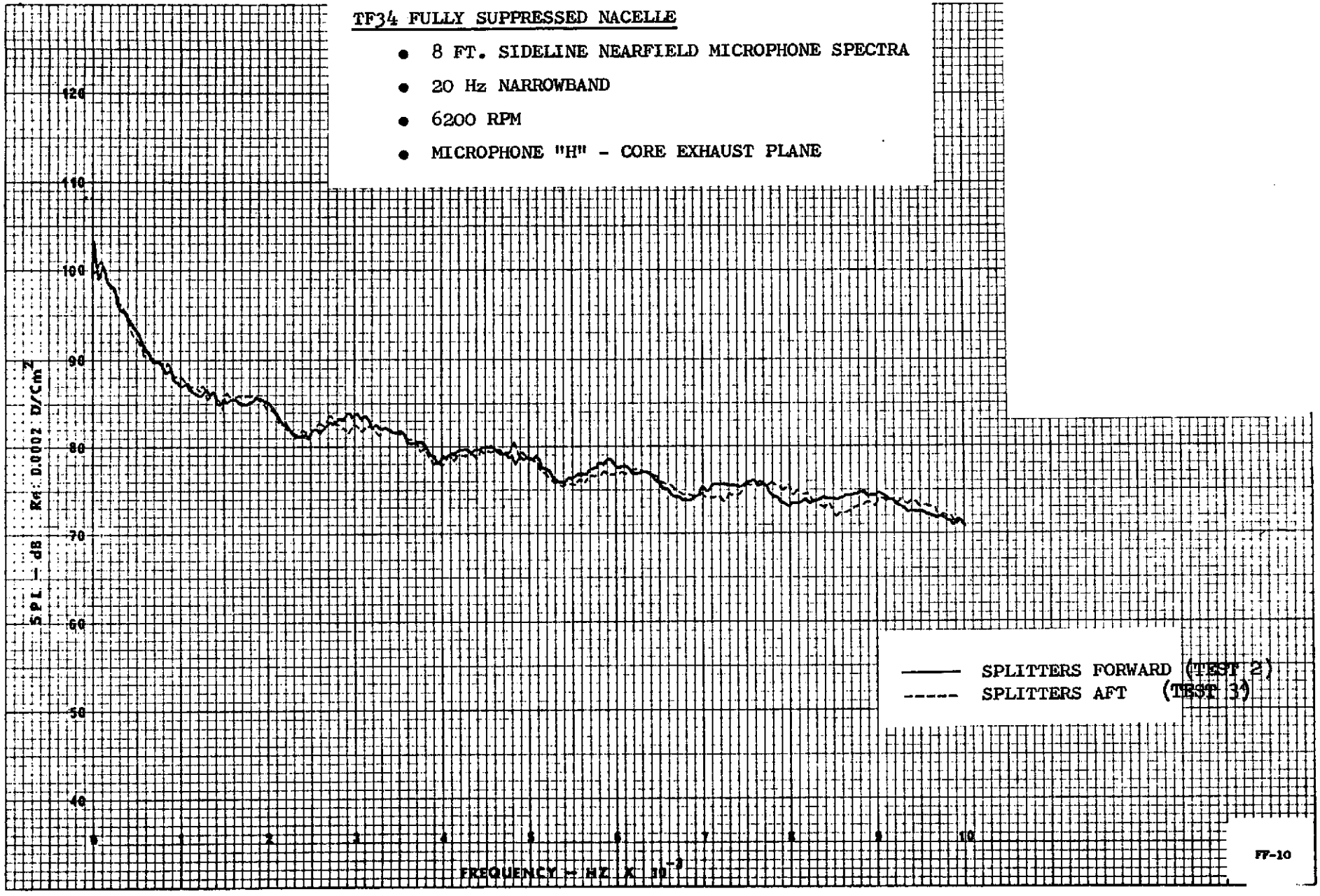

FIGURE IV D-33

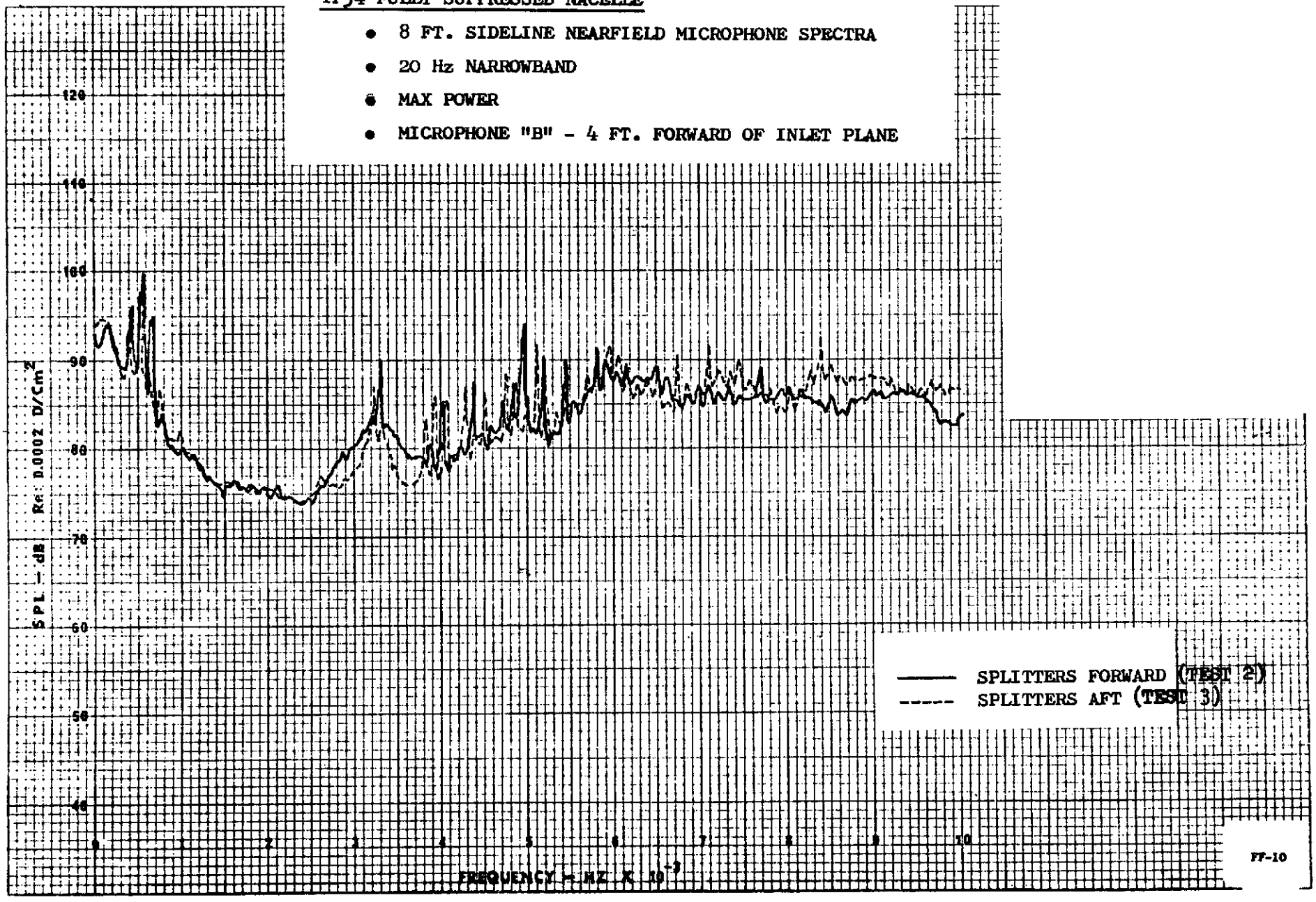

FIGURE IV D-34

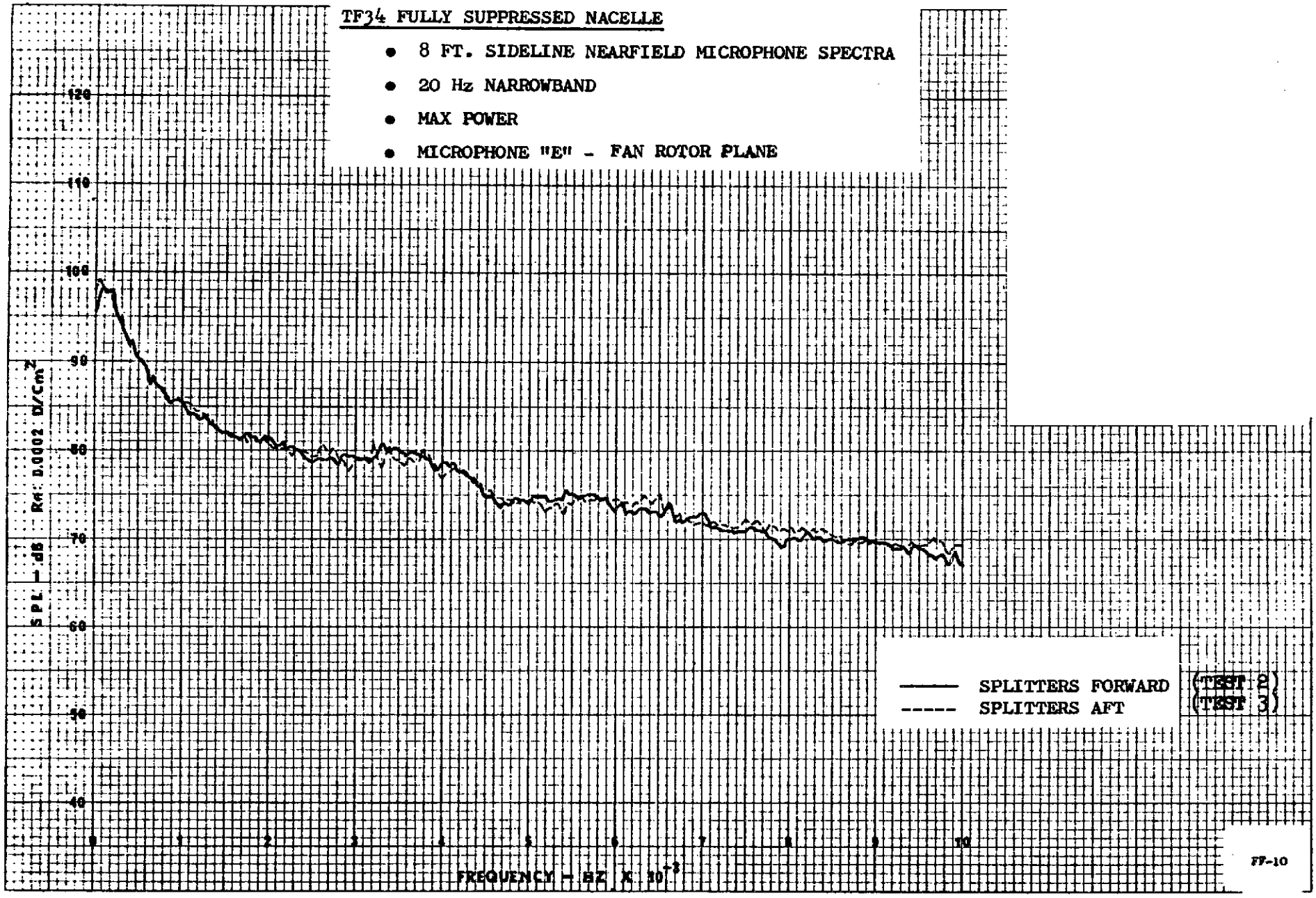

FIGURE IV D-35

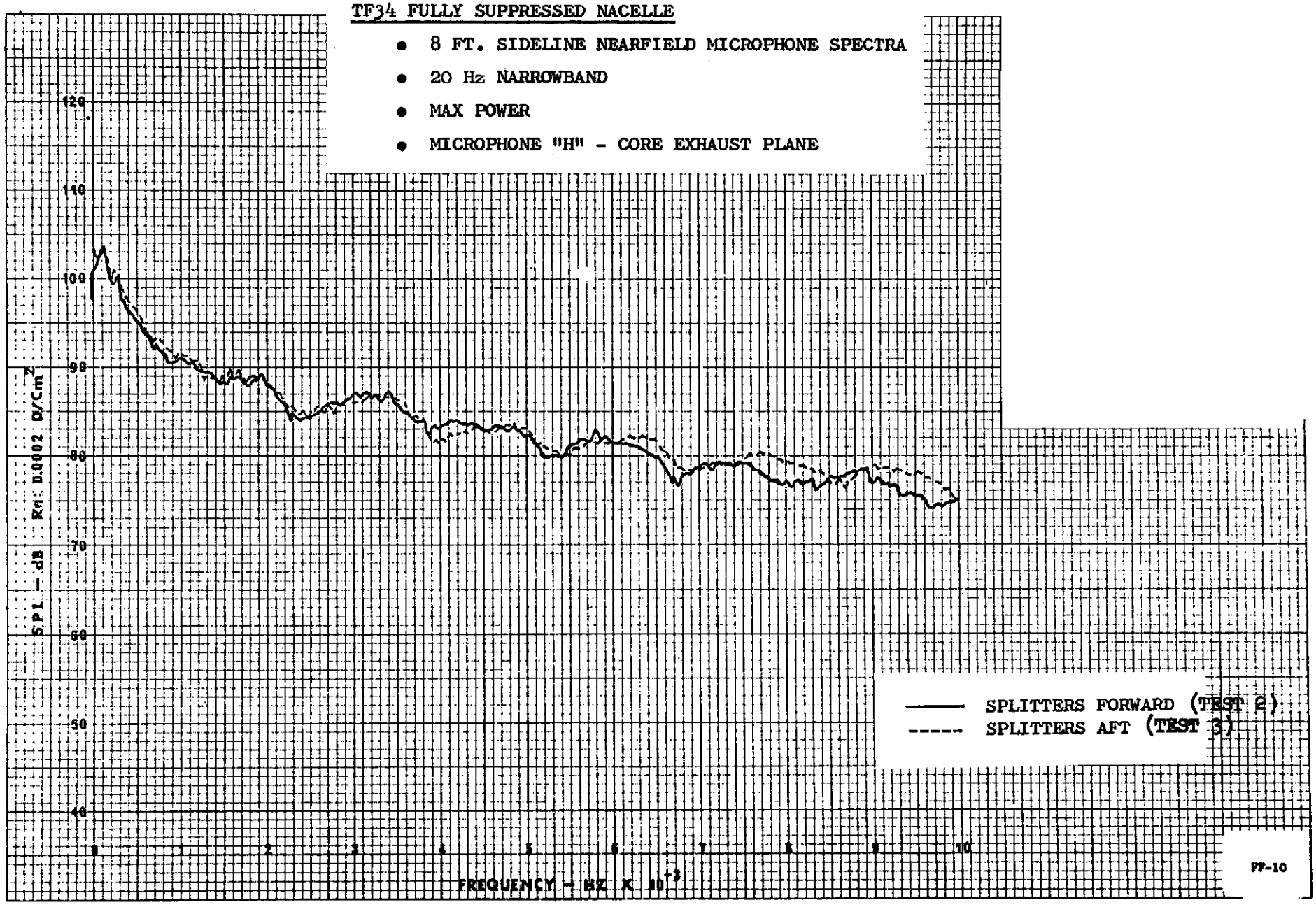

FIGURE IV D-36

V. DISCUSSION OF RESULTS

The "near field" acoustic instrumentation as described in previous sections was used on the TF34 Quiet Nacelle Program for two reasons. First, for purposes of "diagnostic analysis" in the event that the suppressed system noise levels were not obtained, and second, to determine the noise constituents produced by the fully suppressed nacelle. Fortunately, the success of the Quiet Nacelle made the diagnostic analysis unnecessary, but the data produced by the probes, directional array, and the Kulites was used extensively in a number of ways in pursuit of the second objective.

The noise produced by a turbofan engine, measured at a far field location is composed of many separate sources, some with multiple propagation paths. All of the major sources have either complex spectrum characteristics or are primarily broadband in character. Since the SPL spectrum measured at any particular point is the sum of these separate sources, it is very difficult to determine which source makes the major contribution to a given portion of the spectrum. The problems which result from this multiplicity-of-broadband-sources are many but include:

- the identification and ordering of controlling noise sources and propagation paths;
- the evaluation of component suppression; and
- the identification of "new" noise sources.

These problems are discussed in this section by presenting examples of the use of data from the "near field instrumentation."

A. Identification of Noise Constituents

In designing and evaluating suppressed nacelles for turbofan engines, there is always the problem of "overdesigning" in terms of suppressing a particular noise constituent, either through poor design or because of the existence of a noise floor not considered in the initial design. The directional array is a particularly useful tool in this area. For example, in Figure V A-1, the directivity characteristics in terms of 500 foot sideline PNdB are shown for the fully suppressed nacelle. The lines through these data points have been drawn to indicate what might be the first cut approximation of aft radiated and forward radiated noise. One would assume normally, that noise from the inlet would show a peak in the forward quadrant while the aft noise sources would peak in the aft quadrant and decay at forward angles. Additionally, the reasoning would go, that if further reduction were needed at an angle of 50°, then treatment should be added in the inlet. The fallacy of this line of reasoning is illustrated in Figure IV C-8 where the noise consitutents as measured by the directional array (at 50°) are shown for three engine power settings. In the plot at the bottom of the figure (5100 RPM), the inlet radiated noise is seen to be lower than the "core noise" over the frequency range important to the PNdB calculations. The same trend is observed at the other engine power settings. Consequently, if noise reduction at 50° was attempted with additional inlet treatment, total failure would have resulted leaving the treatment designer wondering why his treatment did not work. As a matter of fact, the data on Figure IV C-8 shows that if anything the inlet suppression is too large for a well balanced design and treatment could be removed with very little noise increase.

In a turbofan (both suppressed and unsuppressed), it is difficult to determine the difference between jet noise and fan noise in the frequency region where they cross, e.g., 500 - 1000 Hz. The acoustic probe data, both inlet and exhaust, can be used to calculate the fan power level spectra independent of the jet noise. Comparison of the farfield and probe-determined PWL spectra (or SPL spectra if fan noise directivity is sufficiently known) can help define the low frequency fan noise spectra. Figure IV A-13 through 15 are examples of this use of probe data. The farfield determined spectra is distorted by the ground reflection nulls but the crossover point is seen to be 400 - 800 Hz depending on the power setting. The probe-measured low frequency fan noise in these figures has large tones which occur at the fan once-per-rev and harmonics. (These strong tones do not appear in the probe measured spectra with the suppressed nacelle. Figure IV A-5 shows, for example, a comparison of the baseline and the two suppressed nacelle exhaust probe spectra). The value of determining the low frequency fan noise is obvious when a system suppression design utilizes jet noise and fan noise suppression simultaneously, as discussed in Section V.B.

One final example of the use of two supplementary measurements together is in separating high frequency core noise and jet noise. When two sources appear to emanate from the same point on the engine then the directional array is incapable of distinguishing between the two. When the array is pointed toward the core exhaust, the noise source detected could be either the jet noise generated in the vicinity of the core nozzle or noise generated in the core engine propagated out the core nozzle. Figure V A-2 shows, for two power settings, a method for separating core noise from jet noise. The calculated jet

noise for the baseline engine and the suppressed nacelle (fully treated) are shown on each plot. Opening up the nozzle areas dropped the fan and core velocity enough to produce an expected jet noise reduction. The directional array, when pointed at the core nozzle, produced a spectrum in agreement with the predicted spectrum at maximum power but substantially higher at 5100 RPM. In order to confirm that at the 5100 RPM power setting the array was detecting core noise and not jet noise, the probe determined core noise power spectrum was extrapolated to the 50' radius and plotted as the line on Figure V A-2. Although a little higher than the array would indicate, this probe data provided additional evidence that the core generated noise was indeed the predominant source at 5100 RPM.

B. Evaluation of Fan Noise Suppression

The fan noise suppression system on the Quiet Nacelle Program was designed to achieve a fan noise suppression level of 26 PNdB, taking the fan noise below the jet noise floor at the maximum power, static, condition. (In flight with a relative velocity reduction on jet noise, the full fan suppression would be needed in order to achieve a low system noise level). Since it was expected that the static jet noise would mask the suppressed turbomachinery noise, the directional array was utilized to determine if the design fan noise suppression was achieved.

Figure V B-1 shows the narrowband spectrum of the noise measured at the maximum aft angle with and without the suppressed nacelle in place. There is no evidence of fan noise in terms of blade passing frequency tones, with the suppressed nacelle. Fan noise suppression at the tones is large but the

difference between the two spectra was 20 PNdB. Again, directional array measurements were used to determine the suppressed fan noise level. Figure V B-2 shows the results of the array measurements at 110° in the aft quadrant, defining fan exhaust noise, core noise, and jet noise. In the top of the figure, the three constituent spectra are plotted. Since the farfield microphone measures the sum of all the sources, the spectra have been added logarithmically and plotted along with the "fan noise alone" spectrum. This procedure gives a measure of how far the "fan spectrum" lies below the total system noise. The fan noise measured by the array is plotted in Figure V B-3 with the maximum aft baseline spectra and the measured system noise all extrapolated to a 500 ft. sideline. The low frequency suppressed fan noise (below 1250 Hz) has been estimated (conservatively) based on the probe data discussed in the previous section. A table at the bottom of this figure tabulates the PNL values for these spectra. The maximum unsuppressed noise compared to the maximum suppressed fan noise is seen to yield a difference of 27 PNdB, confirming the design values.

Use of the near field instrumentation in identifying and analyzing a new noise source is discussed in the following section.

C. Flow Noise

An example of the application of special acoustic instrumentation to the definition of new noise sources is the use of Kulite, probe and mic array results of evaluate flow noise. On highly suppressed fan exhaust configurations, a broadband noise floor is reached which limits the observable suppression in the farfield. A potential source for this floor is the flow noise generated by the high velocity exhaust duct air passing over the perforated surfaces covering the acoustic treatment on the duct walls and the acoustic splitters.

This is shown schematically by Figure V C-1. A similar discrepancy between predicted and measured suppression was shown in Figures IV C-20 through IV C-22.

Since the flow noise is broadband in nature, farfield microphone results cannot be used to define its contribution to farfield levels, due to masking by the jet, core and other potential noise sources with similar broadband characteristics. Kulite, probe and mic array results, however, can be used to provide an analysis of the noise without these external noise sources. Figure IV B-15 presented wall Kulite measurements that had a noise level decay similar to that shown on Figure V C-1. Using cross-correlation techniques, these measurements were isolated into "pseudo" sound and acoustic signal, as shown on Figure IV B-17. The measured levels at 3150 Hz from Figure IV B-15 were corrected to represent acoustic signal levels using the ΔOASPL of Figure IV B-17. These are shown on Figure V C-2 and compared to the level measured by the acoustic probe. The two sets of data show good agreement and would indicate a true acoustic floor exists in the duct. Also shown on Figure V C-2 is the predicted flow noise level using the procedure described in Section IV.B. These results would lead to the conclusion that the Kulite and probe measured levels have confirmed the theoretical prediction of flow noise and thus established a modification to the current procedure for designing fan exhaust suppressors. Comparison of the data with the acoustic directional array results, however, shows that further modifications to the theoretical analysis may be required. Figure V C-3 shows the measured max aft angle farfield levels (extrapolated to a 500 foot sideline), the measured Kulite and probe results extrapolated to the farfield, and the measured acoustic

directional array fan exhaust noise. The duct data and predicted level agree well with the measured farfield floor. In contrast, the directional array fan exhaust noise is 12 to 16 dB below the floor level defined by the probes, prediction, and omni-directional microphone.

Although the comparison prevents a definite conclusion from being drawn regarding flow noise, it does provide a direction for continued analysis. In order to establish a lower measured acoustic signal from the Kulite and probe data, the cross-correlation analysis should be made with a filtered signal at 3150 Hz. This could result in a significant difference relative to the results of Figure IV B-17 which was obtained from an OASPL cross-correlation. The filtered acoustic signal could be 10 or 15 dB below the pseudo sound, and would then agree with the directional array data. The theoretical predictions could then be modified to represent a lower noise generation process, as a function of the flow Mach number, by matching the measured levels.

This comparison of farfield, duct and directional array levels has demonstrated the usefulness of detailed acoustic instrumentation in establishing new noise sources that are possibly limiting the attainment of even higher levels of suppression.

FIGURE V A-1

DIRECTIVITY PATTERN OF FULLY SUPPRESSED NACELLE

- 5100 RPM
- 500 FT. SIDELINE

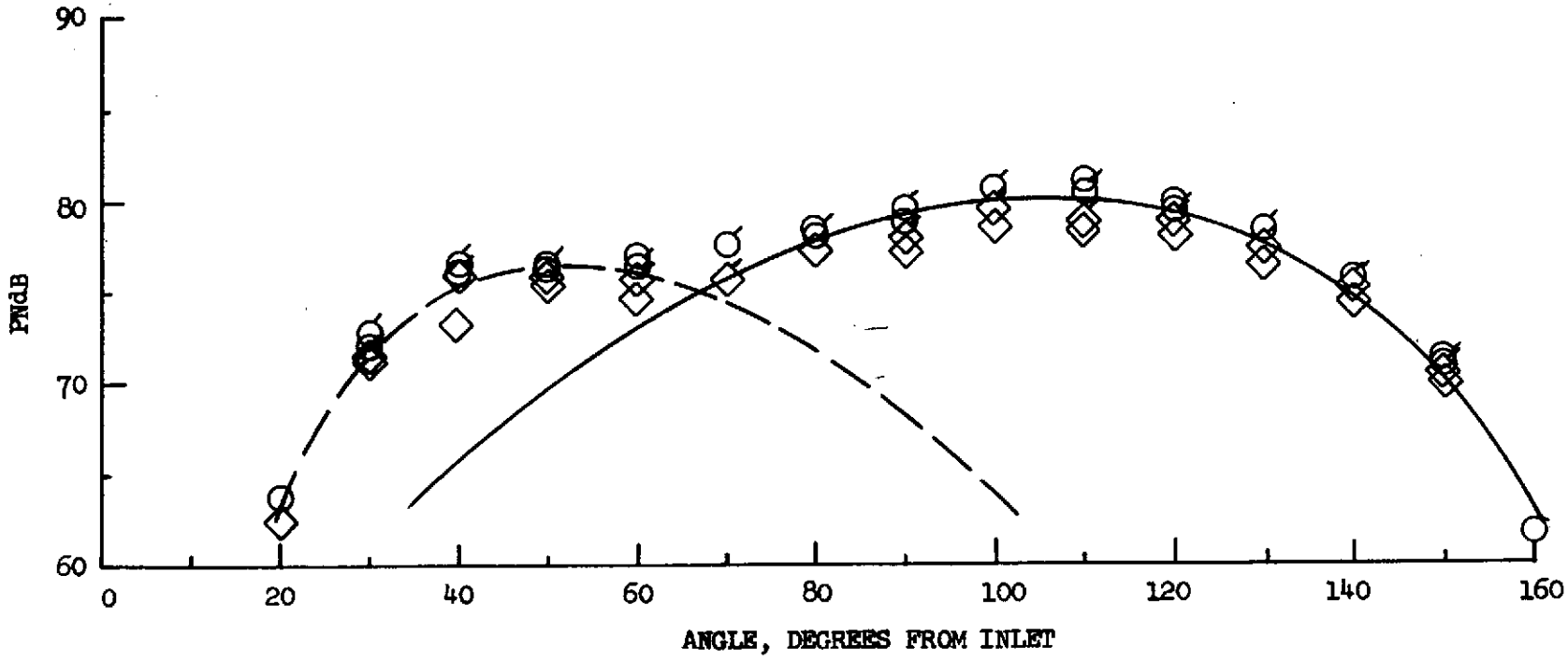

FIGURE V A-2

TF34 PREDICTED JET AND MEASURED CORE RADIATED NOISE AT APPROACH POWER (5100 RPM) AND MAX POWER (7100 RPM), ACOUSTIC ANGLE = 110°

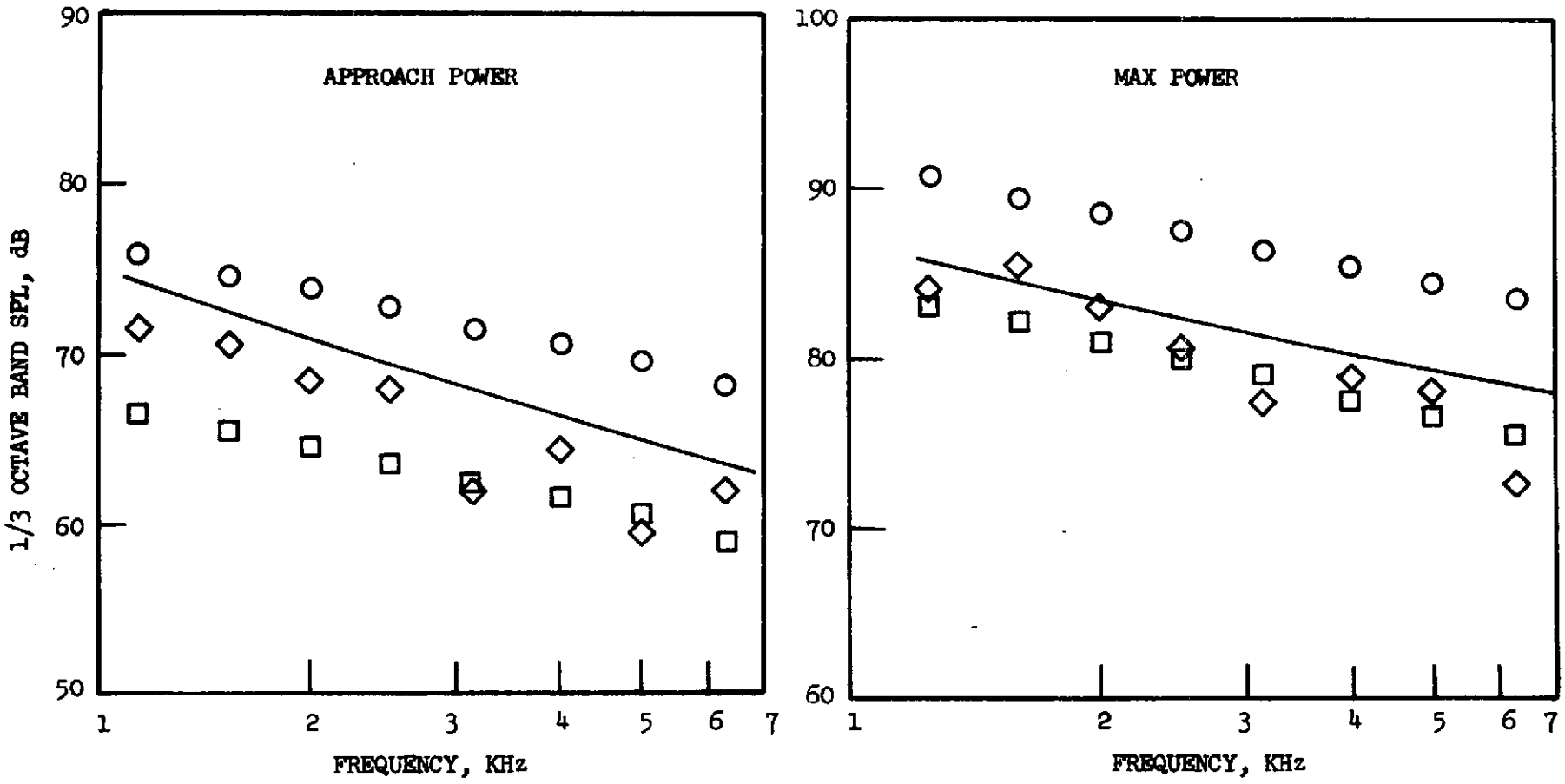

FIGURE V B-1

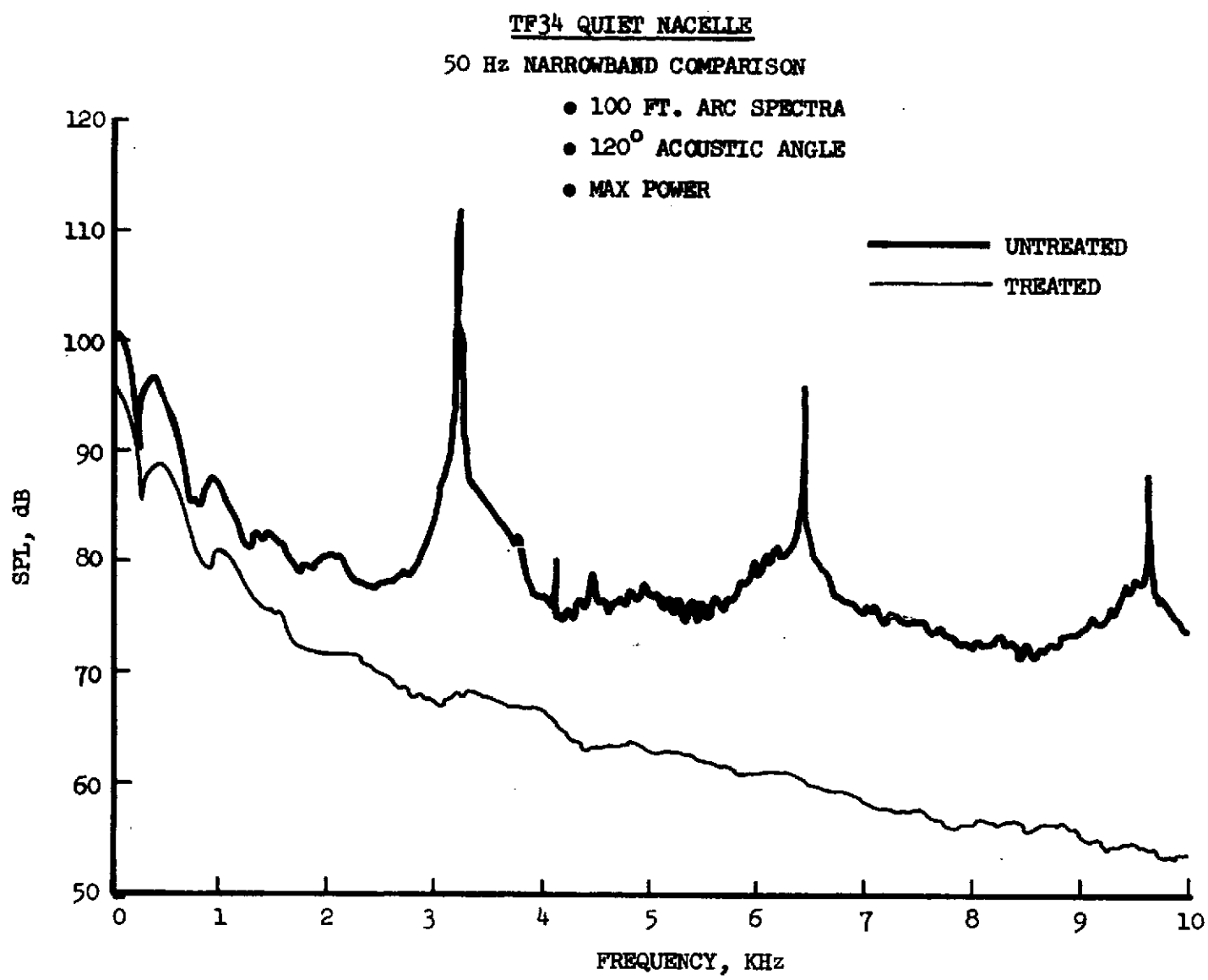
TF34 QUIET NACELLE
50 Hz NARROWBAND COMPARISON
• 100 FT. ARC SPECTRA
• 120° ACOUSTIC ANGLE
• MAX POWER
UNTREATED
TREATED
SPL, dB
120
110
100
90
80
70
60
50
0
1
2
3
4
5
6
7
8
9
10
FREQUENCY, KHz

FIGURE V B-2

DIRECTIONAL ARRAY MEASUREMENTS

- 50 FT. ARC
- 110° ACOUSTIC ANGLE
- FULLY SUPPRESSED
- MAX POWER

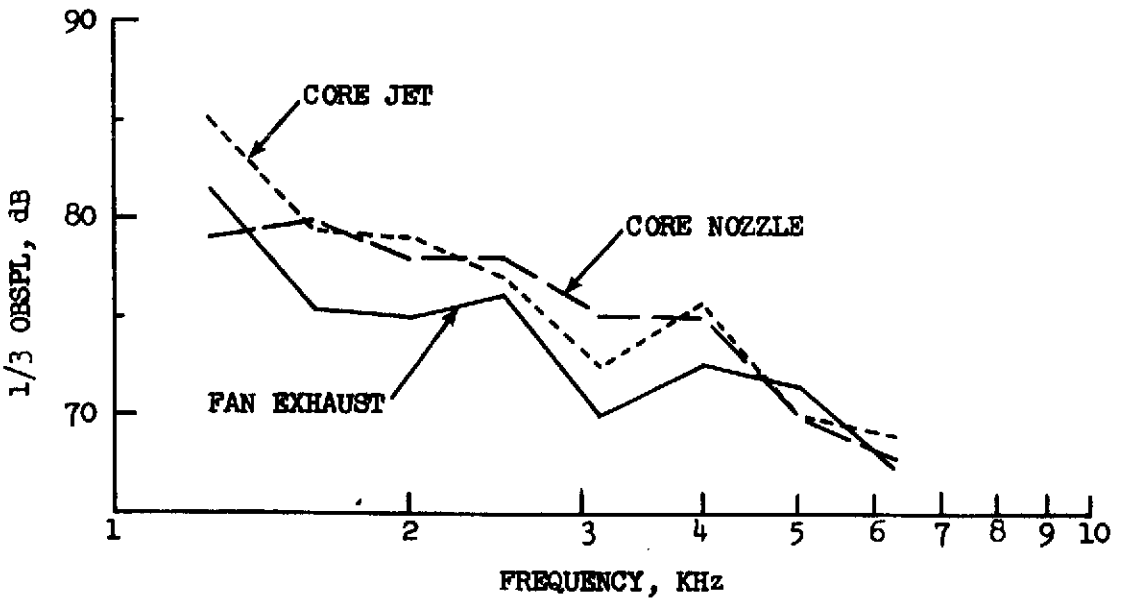

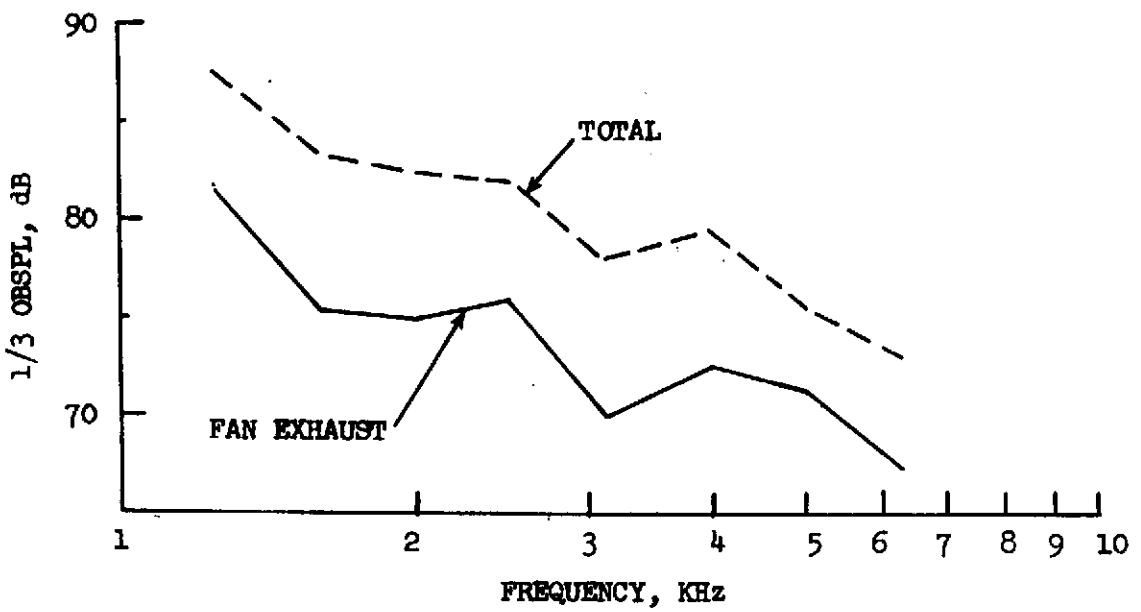

FIGURE V B-3

TF34 FAN NOISE SUPPRESSION

- MAX POWER
- 120° ACOUSTIC ANGLE

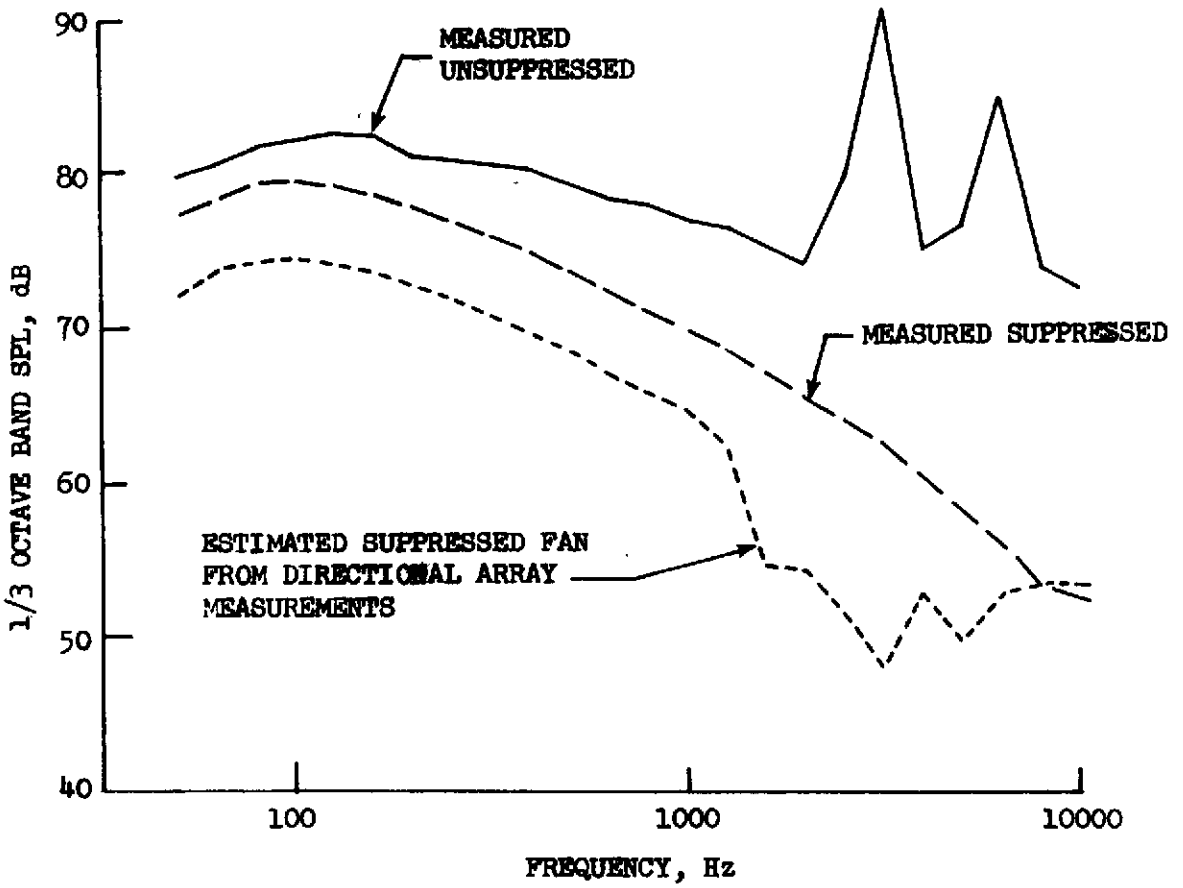

	MAX 500 FT. SL PNdB	ΔPNL re UNSUPP.
MEASURED UNSUPPRESSED (MAX ANGLE 90°)	113.0	-
MEASURED SUPPRESSED (TOTAL SYSTEM)(120°)	92.5	20.5
ESTIMATED SUPPRESSED (FAN ONLY)(120°)	86.0	27.0

FIGURE V C-1

EFFECT OF FLOW NOISE ON APPARENT PERFORMANCE OF ACOUSTIC TREATMENT

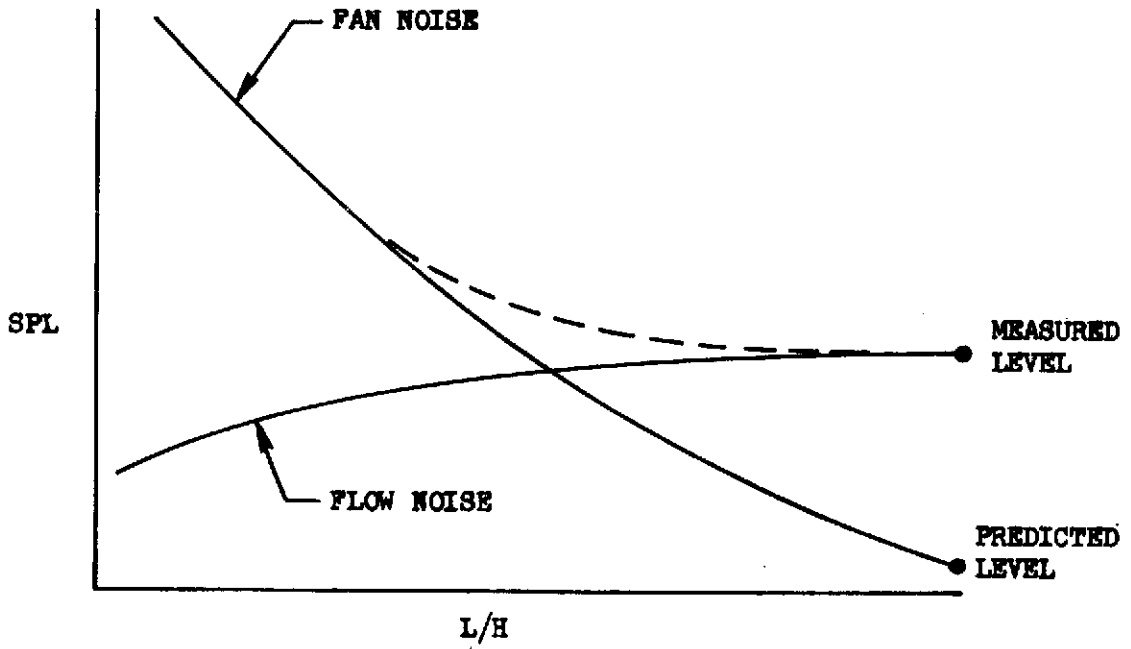

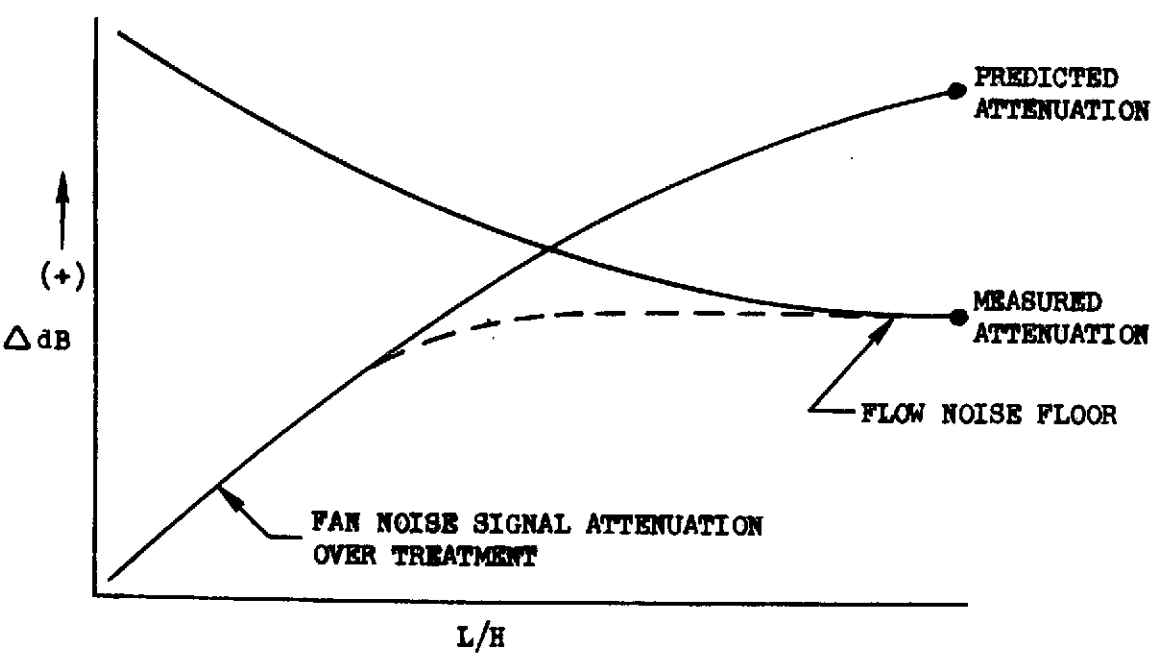

FIGURE V C-2

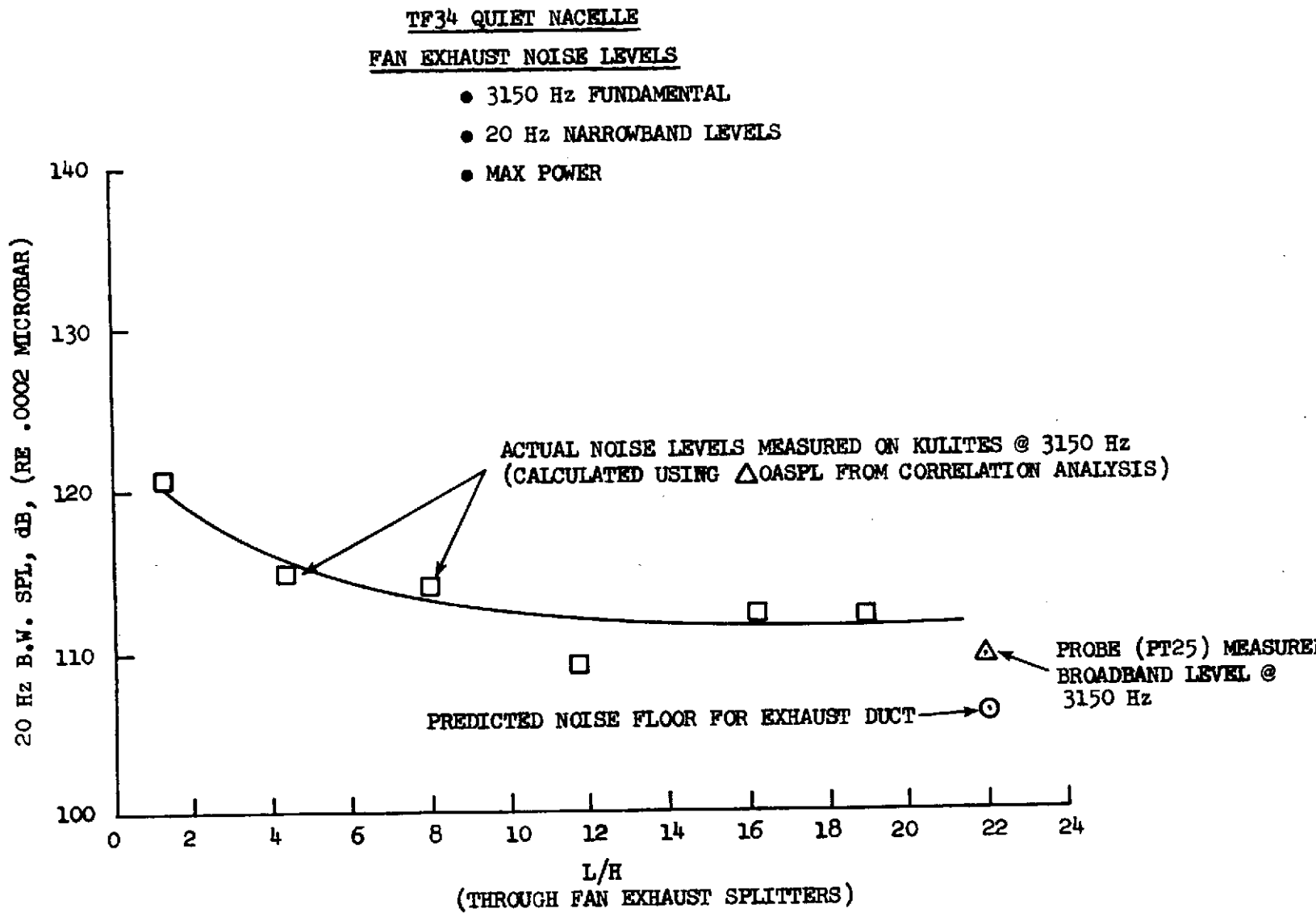
TF34 QUIET NACELLE
FAN EXHAUST NOISE LEVELS
• 3150 Hz FUNDAMENTAL
• 20 Hz NARROWBAND LEVELS
• MAX POWER
20 Hz B.W. SPL, dB, (RE .0002 MICROBAR)
140
130
120
110
100
ACTUAL NOISE LEVELS MEASURED ON KULITES @ 3150 Hz
(CALCULATED USING ΔOASPL FROM CORRELATION ANALYSIS)
PROBE (PT25) MEASURED
BROADBAND LEVEL @
3150 Hz
PREDICTED NOISE FLOOR FOR EXHAUST DUCT
0
2
4
6
8
10
12
14
16
18
20
22
24
L/H
(THROUGH FAN EXHAUST SPLITTERS)

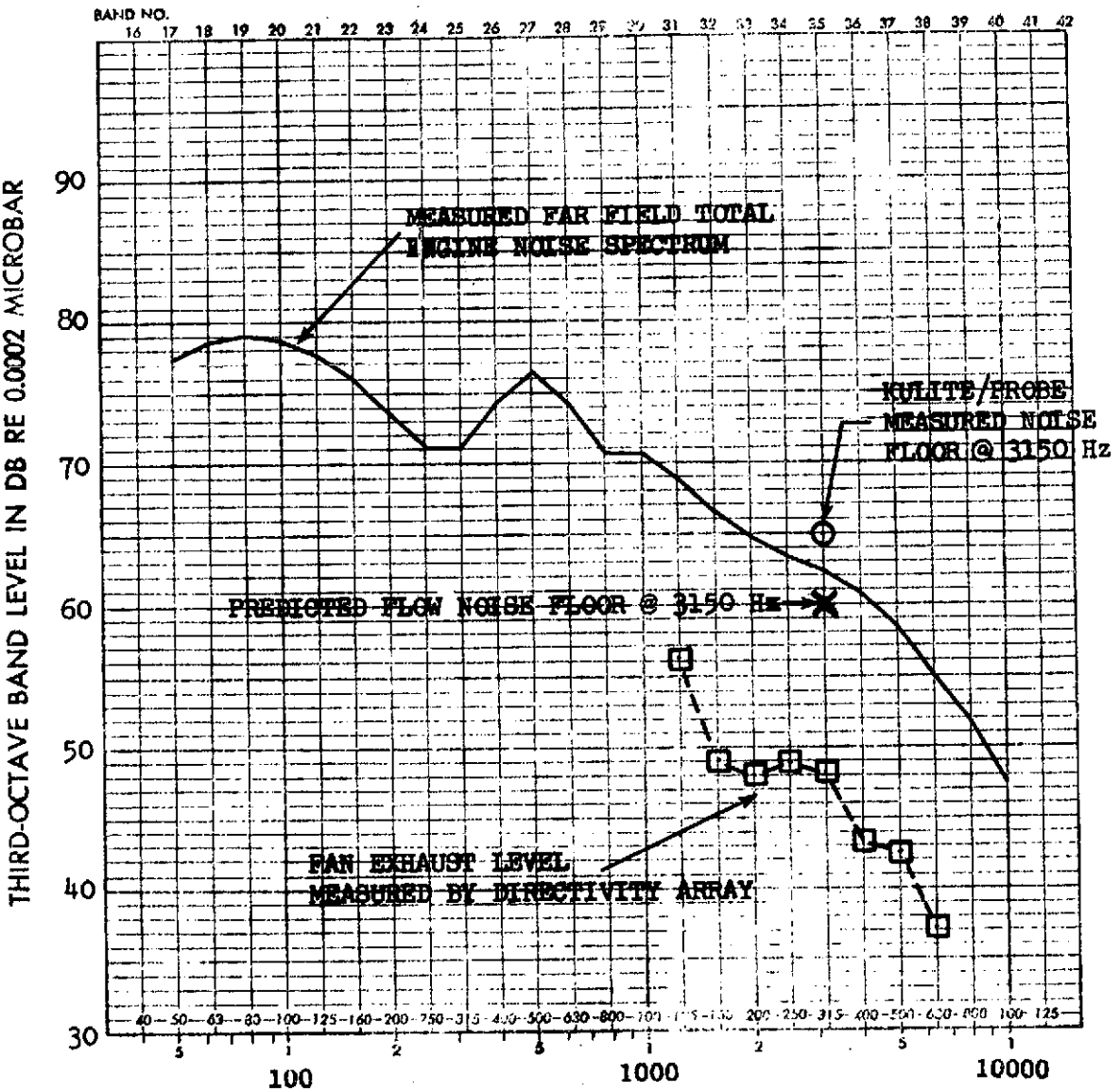

FIGURE V C-3

TF34 QUIET NACELLE TESTS

COMPARISON OF PREDICTED AND MEASURED NOISE FLOORS IN THE FAR FIELD

- FULLY SUPPRESSED NACELLE
- 500 FT. SIDELINE
- MAX AFT ANGLE
- MAX POWER

VI. CONCLUSIONS

The following are the most important conclusions to be drawn from the nearfield acoustic test results:

1. The nearfield acoustic instrumentation system made possible the accurate determination of achieved component suppression levels; this could not have been done using only the farfield microphones. As an example, Figure VB-3 is a comparison of the measured unsuppressed and suppressed engine noise on a 500 ft. sideline (max. aft angle); also compared is the suppressed fan noise, estimated from the directional array measurements. The ΔPNL measured on the farfield microphones was 20.5 PNdB for the total system; however, the array measurements indicate that the max. aft fan noise suppression was 27 PNdB, or one PNdB better than the goal.

2. The baseline engine is fan noise dominated as regards the frequencies important to PNL calculation.

3. The suppressed nacelle configuration is "core" (core + core jet) noise dominated at all angles, even those in the forward quadrant.

4. No significant differences in noise generation or suppression were incurred due to the closer inlet splitter spacing employed in this test series.

5. A "noise floor" exists in the treated fan exhaust duct, and is limiting achievable fan exhaust suppression. This floor is probably due to noise generated by flow over the treatment.

6. Further testing and analyses employing the nearfield instrumentation system is necessary for a more complete understanding of phenomena such as treatment-generated noise.

VII. REFERENCES

1. Jones, W.L., Heidelberg, L.J., and Goldman, R.G., "Highly Noise Suppressed Bypass 6 Engine for STOL Application", AIAA Paper No. 73-1031, October 15, 1973.

2. Latham, D., McCann, E.O., and Radecki, K.P., "TF34 Engine Detail Noise Data and Analysis", Report for NASA Contract NAS3-15545, July 8, 1971.

3. Edkins, D.P., "Acoustically Treated Ground Test Nacelle for the General Electric TF34 Turbofan Engine", NASA CR-120915.

4. Ffowcs-Williams, J.E., "The Acoustics of Turbulence Near Sound Absorbent Liners", Journal of Fluid Mechanics, Volume 51, Part 4, February 1972.

THE FOLLOWING PAGES ARE DUPLICATES OF ILLUSTRATIONS APPEARING ELSEWHERE IN THIS REPORT. THEY HAVE BEEN REPRODUCED HERE BY A DIFFERENT METHOD TO PROVIDE BETTER DETAIL